Jaime Bibiloni-Isaksson

Biogeography of photoheterotrophic microbes in coastal waters of Australia

C02031 Research Thesis

Spring 2016

Submitted in fulfilment of the requirements for C02031

Doctor of Philosophy, Spring Semester 2016

at the University of Technology Sydney

Supervisor: Ass/Prof Justin Seymour

Faculty of Science

University of Technology Sydney

TABLE OF CONTENTS

CERTIFICATE OF ORIGINAL AUTHORSHIP

CERTIFICATE OF ORIGINAL AUTHORSHIP

I certify that the work in this thesis has not previously been submitted for a degree nor has it been submitted as part of requirements for a degree except as part of the collaborative doctoral degree and/or fully acknowledged within the text.

I also certify that the thesis has been written by me. Any help that I have received in my research work and the preparation of the thesis itself has been acknowledged. In addition, I certify that all information sources and literature used are indicated in the thesis.

Signature of Student:

Date: 19/07/2017

ACKNOWLEDGMENTS

Foremost I would like to thank my main advisor, Justin Seymour, for his constant guidance, encouragement and patience throughout the entirety of my research. I would also like to thank my main co-advisor, Mark Brown, for their support and direction, which this research would not have been possible without the help and input of him, particularly with the bioinformatics and statistical analysis. You both are a very nice people. I would like to thank the crew of the R/V Southern Surveyor and staff from CSIRO for providing samples for this thesis. Also I would like to express my gratitude to the Graduate Research School for help in administrative matters. Finally I would like to acknowledge my family and friends that have been with me through this adventure.

ABSTRACT (general)

Marine microbes control the flux of energy and chemicals in the ocean and therefore mediate ocean productivity and biogeochemistry, which ultimately sustains marine life and controls global climate. A numerically and functionally important group of marine microbes, for which there is currently a significant gap in knowledge regarding their ecology and biogeography, are the photoheterotrophic bacteria. These microbes, including both Aerobic Anoxygenic Phototrophic Bacteria (AAnPB) and proteorhodopsin based phototrophic bacteria and Archaea (PRBA) comprise up to 70% of microbial communities within surface waters of the ocean. Capable of gaining energy from light-induced proton translocation and from the oxidation of organic material, these often highly abundant bacteria have been proposed to significantly influence marine biogeochemistry and trophodynamics. However, the environmental (i.e. physicochemical, seasonal, oceanographic) factors influencing the abundance and diversity of these organisms are currently poorly defined, particularly within the often highly productive waters of the Southern Hemisphere. The aim of this thesis was to examine changes in photoheterotrophic community abundance and composition in coastal waters of Australia and identify the key environmental influences on the ecology of these microbes. Samples collected from a combination of oceanographic research voyages and time-series sampling regimes were analysed using both amplicon sequencing approaches and quantitative PCR targeting *pufM* and proteorhodopsin genes to characterise AAnPB and PRBA populations respectively.

High temporal resolution analysis of photohetetrophic bacterial population dynamics in the coastal waters of Australia indicated seasonality in the abundance and diversity of these groups. Along the eastern coast of Australia, AAnPB abundance was highly variable, with *pufM* gene copies ranging from 1.1×10^2 to 1.4×10^5 mL^{-1}, and positively correlated with day length and solar radiation. *pufM* gene amplicon sequencing revealed that the majority of sequences were closely related to those obtained previously in other environments, suggesting that key AAnPB groups are widely distributed across similar environments globally. Temperature was a major structuring factor for AAnPB assemblages across large spatial scales, correlating positively with richness and *Gammaproteobacteria* (phylogroup K) abundance, but negatively with Roseobacter-clade (phylogroup E) abundance, with temperatures between 16-18 °C identified as a potential transition zone between these groups. Coastal PRBA assemblages were also dynamic in both space and time, with diversity correlated to indicators of waterbody oligotrophy including positively to temperature, Secchi depth and *Prochlorococcus* cell abundance and negatively to phosphate concentration. Shifts in taxonomic composition were best explained by temperature and day length. Seasonality in taxonomic structure was accompanied by temporal variability in proteorhodopsin spectral tuning. Finally, we provide evidence for spatial transitions in the abundance and diversity of key photoheterotrophic bacterial groups between different oceanographic provinces within northern Australian waters, indicating that shifts in physical and biotic characteristics can lead to sharp changes in the importance of these important marine microbial assemblages across

water masses. Total bacterial abundance was higher in ATS waters, which was reflected by higher AAnPB abundance in this region, whereas the major proteorhodopsin containing clade, SAR11, displayed the opposite trend, with higher abundances in the Coral Sea. Among the AAnPB, the Gammaproteobacterial phylogroup K dominated the community in both regions, with relatively stable composition of AAnPB across regions. Conversely, the PRBA community displayed clear differences between the two regions, with the Arafura Timor Sea (ATS) dominated by SAR11-like and Betaproteobacterial sequences, while the Coral Sea was dominated by Archaea group IIb and members of SAR11 clade A and B. In conclusion, this thesis has demonstrated how dynamic these populations are and that each of these two groups should not be treated as single population, but one that is comprised of many interacting and potentially competing units, that are each governed by different environmental factors and thereby fill discrete niches.

Key words: microbial oceanography, next-generation sequencing, photoheterotrophs, community composition, diversity, seasonality, biogeography, proteorhodopsin bacteria, aerobic anoxygenic phototrophic bacteria, East Australian current

THESIS FORMAT

This thesis has been formatted according to publication styles, with each of the three experimental chapters corresponding to manuscripts submitted, or in final preparation for submission, to international research journals. The research chapters correspond to the following manuscripts.

I. **Bibiloni-Isaksson J**, Seymour JR, Ingleton T, van de Kamp J, Levente Bodrossy L, and Brown MV. (2016) Spatial and temporal variability of aerobic anoxygenic photoheterotrophic bacterial along the east coast of Australia. (*Accepted to Environmental Microbiology on the 28-Jun-2016)*

II. **Bibiloni-Isaksson J**, Seymour JR, , Ingleton T, van de Kamp J, Levente Bodrossy L, and Brown MV (2016) Diversity patterns of proteorhodopsin containing bacteria along the east coast of Australia. *(Submitted to Environmental Microbiology Reports)*

III. **Bibiloni-Isaksson J**, Brown MV, Seymour JR (2016) Photoheterotrophic microbial community structure along the North coast of Australia. (In preparation for submission)

LIST OF ABBREVIATIONS

AAnPB	Aerobic Anoxygenic Photosynthetic bacteria
PRBA	Proteorhodopsin-containing Bacteria and Archaea
BCP	Biological carbon pump
bp	Base pairs
DOC	Dissolved organic carbon
DOM	Dissolved organic matter
EAC	East Australian Current
ENSO	El Niño-Southern Oscillation
IMOS	Integrated Marine Observing System
OM	Organic matter
OTU	Operational taxonomic unit
PCR	Polymerase chain reaction
perMANOVA	Permutation-based analysis of variance
PR	Protein Proteorhodopsin
qPCR	Quantitative Polymerase chain reaction
rRNA	Ribosomal ribonucleic acid
SAR11	A lineage of bacteria that was original discovery in the Sargasso Sea

"There is only one corner of the universe you can be certain of improving, and that's your own self"

Aldous Huxley

To my family

Chapter 1

General introduction of the study

INTRODUCTION

Microbes in the Ocean

Since Pomeroy (1970) first described the numerical and metabolic significance of microorganisms in the ocean, there have been significant conceptual and technological advances, which have revealed the fundamentally important roles that microbes play in ocean ecosystems (Fuhrman, 2015). It is now well known that a litre of seawater may contain hundreds of millions of microbes (Whitman *et al.,* 1998), including different communities of bacteria, archaea, protists, and unicellular fungi, and that these account for most of the oceanic biomass, metabolic activity and diversity (Pomeroy *et al.,* 2007). These microbes control the flux of energy and biologically important chemical elements in the ocean and therefore mediate ocean productivity and biogeochemistry (Azam et al. 1983; Falkowski et al. 2008).

In contrast to the primary producers on land, which are mostly large plants, microorganisms are responsible for 98% of primary production in the ocean (Atlas and Bartha, 1993; Whitman *et al.,* 1998), which ultimately accounts for approximately 50% of the total oxygen derived from photosynthesis globally. Heterotrophic bacteria are generally considered as secondary producers that carry out more that 95 % of the respiration in the ocean (del Giorgio & Duarte 2002), half of which occurs in the photic zone (del Giorgio & Williams 2005). In addition, bacteria and archaea are essential to the maintenance of ocean productivity, not only through recycling carbon but also by

recycling other essential nutrients, such as phosphorous, nitrogen, sulphur, iron and silica (Falkowski *et al.*, 2008). Ocean productivity thus depends on a range of microbial species, the true diversity of which has only recently become clear through the lens of molecular biology (e.g. Sogin *et al.,* 2012).

Microbial Metabolism in the Ocean

It is not surprising that during billions of years of evolution, microorganisms have developed a high metabolic diversity and a wide range of ecological niche associations and life styles (Madigan *et al.,* 2012). However, every organism on Earth requires carbon for either synthesis of cellular material or energy, or often both. The versatility of microorganisms in employing different respiratory metabolisms is based on specialisation through exploitation of different substrates. Carbon can be sourced from a range of simple "one carbon" molecules (e.g. CO_2, CO and CH_4) through to more complex organic molecules (e.g. proteins, nucleic acids, and polysaccharides).

Carbon is principally needed for biomass production, and microbes can obtain it by using either inorganic carbon (autotrophy) or organic substances (heterotrophy). Generally, depending on their energy requirements, microbes are classified into two major groups: autotrophs, which rely on light or inorganic substrates for energy and CO_2 for carbon, and heterotrophs, which are generally reliant on the assimilation of organic compounds for energy and carbon. Primary producers, such as micro-algae and cyanobacteria, are considered photoautotrophs since they use light energy,

whereas organoheterotrophic bacteria are secondary producers (e.g., Azam *et al.*, 1983; Sherr and Sherr, 1988). However, some marine microorganisms have the capacity to simultaneously display many different metabolic pathways and combine or switch styles of metabolism depending on the situation (see review by Eiler, 2006).

Examples of different microbial metabolisms include mixotrophy, which is common amongst protists, (e.g. Stoecker *et al.*, 1987; Fabricious and Klumpp, 1995; Stoecker, 1998) and certain bacteria. These organisms can generate energy from light, but in the dark assimilate organic carbon for energy (Yurkov and Beatty, 1998). Marine picocyanobacteria such as *Prochlorococcus* (Rocap *et al.*, 2003) and *Synechococcus* (Palenik *et al*., 2003) are the most abundant photosynthetic organisms in the world's oceans and until recently were considered purely photoautotrophs; however several studies have now shown that they are able to assimilate organic compounds such as amino acids or dimethylsulfoniopropionate (DMSP) (Malmstrom *et al.*, 2005; Zubkov, 2003; Zubkov and Tarran, 2005). These organisms can thus be classified as photoheterotrophs.

Photoheterotrophy

It has become apparent only relatively recently that aside from *Cyanobacteria* and eukaryotic phototrophs, other types of bacteria are able to harvest light energy. Two groups of bacteria, known commonly as photohetrotrophs are able to synthesise ATP through light absorption (Figure 1). These include (i) Aerobic Anoxygenic

Photosynthetic Bacteria (AAnPB), which use a unique form of chlorophyll called bacteriochlorophyll *a* for photosynthesis (Shiba *et al.,* 1979 and Yurkov and Beatty, 1998), and (ii) bacteria that use proteorhodopsin, a light-driven proton pump, which allows for energy acquisition (Beja *et al.,* 2001; Dioumanev *et al.,* 2002; Giovanni *et al.,* 2005). However, unlike eukaryotic phototrophs and cyanobacteria, these photoheterotrophic bacteria do not produce O_2 as a by-product of their photochemical reactions. These two groups use light as an energy source, but require sources of organic carbon for cell synthesis (Yurkov and Beatty, 1998; Rappe *et al.,* 2002; Giovanni *et al.,* 2005). These organisms have been shown to be very abundant (up to 70% of total bacterial community) in many oceanic regions (Beja and Suzuki, 2008), indicating that may play an important role in carbon and energy cycling and in the microbial loop (Jiao *et al*., 2010; Karl, 2014).

Proteorhodopsin Containing Marine Bacteria

The existence and potential physiological importance of rhodopsin in microorganisms was first discovered in the halophile archaeon *Halobacterium salinarum* (Oesterhelt & Stoeckenius, 1971). It was referred to as bacteriorhodopsin, and was initially thought to be unique to *H. salinarum*. In *H. salinarum*, light is not used for photosynthesis, but it provides enough energy for the proton pump to pump Na^+ ions out and K^+ ions into the cell (an important physiological process in hypersaline environments) and support a low metabolic activity when organic nutrients are limited (Oesterhelt & Stoeckenius, 1971).

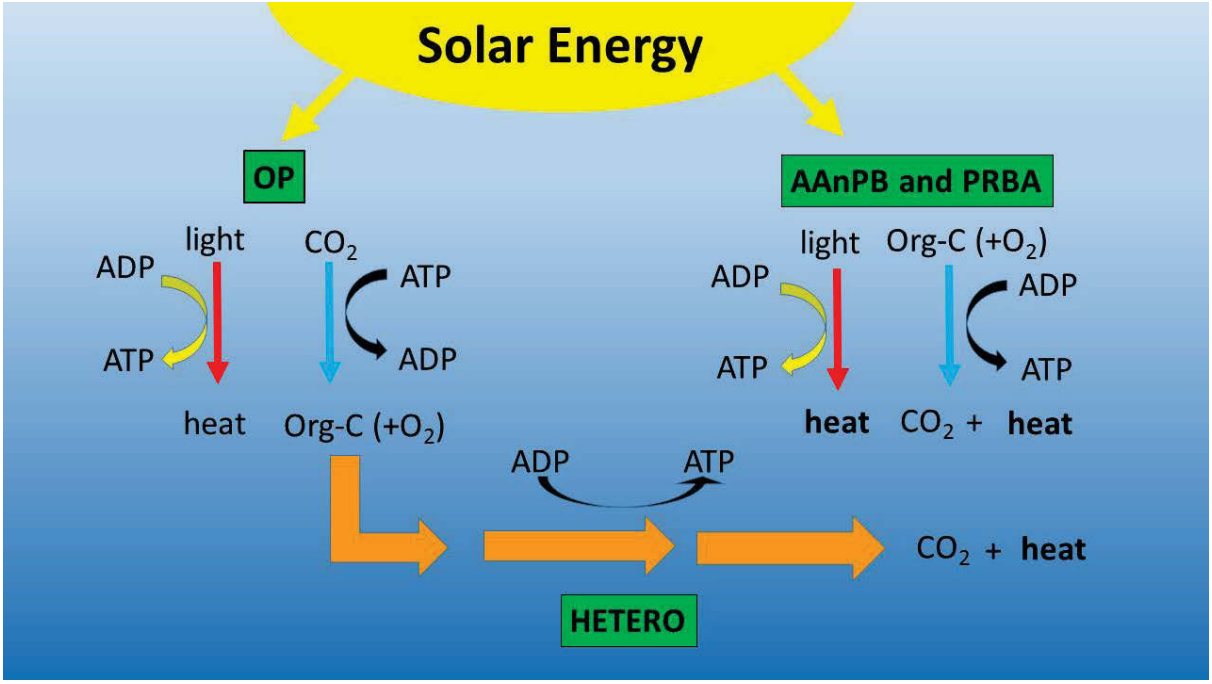

Figure 1: A current view of the complex relationships between the flow of energy (red arrows), carbon (blue arrows), or energy plus carbon (orange arrows) through a hypothetical marine system. Solar energy capture processes all three modes of phototrophy: oxygenic phototrophy (OP), aerobic anoxygenic phototrophy (AAnPB) and rhodopsin-based (PRBA). All these strategies convert solar energy into chemical bond energy as ATP plus heat, and in the case of OP a portion of the energy gain is used to reduce carbon dioxide (CO_2) to organic carbon (Org-C). The light-independent heterotrophic (HETERO) flow of carbon and energy ultimately dissipates the potential energy in Org-C to heat. Modified from Karl (2014)

In 2000, proteorhodopsin (PR) was discovered in a metagenomic fosmid library derived from a seawater sample collected in Monterey Bay, California (Béjà *et al*. 2000). A gene with high homology with bacteriorhodopsins of Archaea and other rhodopsins was found to be co-localised with an rRNA gene of a member of the SAR86 group of *Gammaproteobacteria* (Béjà *et al*., 2000). The name proteorhodopsin (PR) was subsequently coined as reference to the organism it was first associated with, but it has since been found in other bacterial phyla. PR is a transmembrane 34-36 kilodalton protein, typically possessing seven transmembrane helix domains (Béjà *et al*., 2001). A retinal light harvesting cofactor derived from carotenoid is required for the PR to be functional (Béjà *et al*., 2000; Andersson *et al*., 2009). PR is a light-driven proton pump that may enhance ATP production in heterotrophic bacteria (Figure 1 & 2) that

normally rely on the oxidation of organic material for energy (Béjà *et al.*, 2000a; 2001; Martinez *et al*., 2007). Since the discovery of PR (Beja *et al*., 2000b), a diverse range of PR variants have been identified (Beja *et al*., 2001; de la Torre *et al*., Sabehi *et al*.,2003;2004;2005:Venter *et al*., 2004: Frigaard *et al* 2006; McCarren and DeLong, 2007).

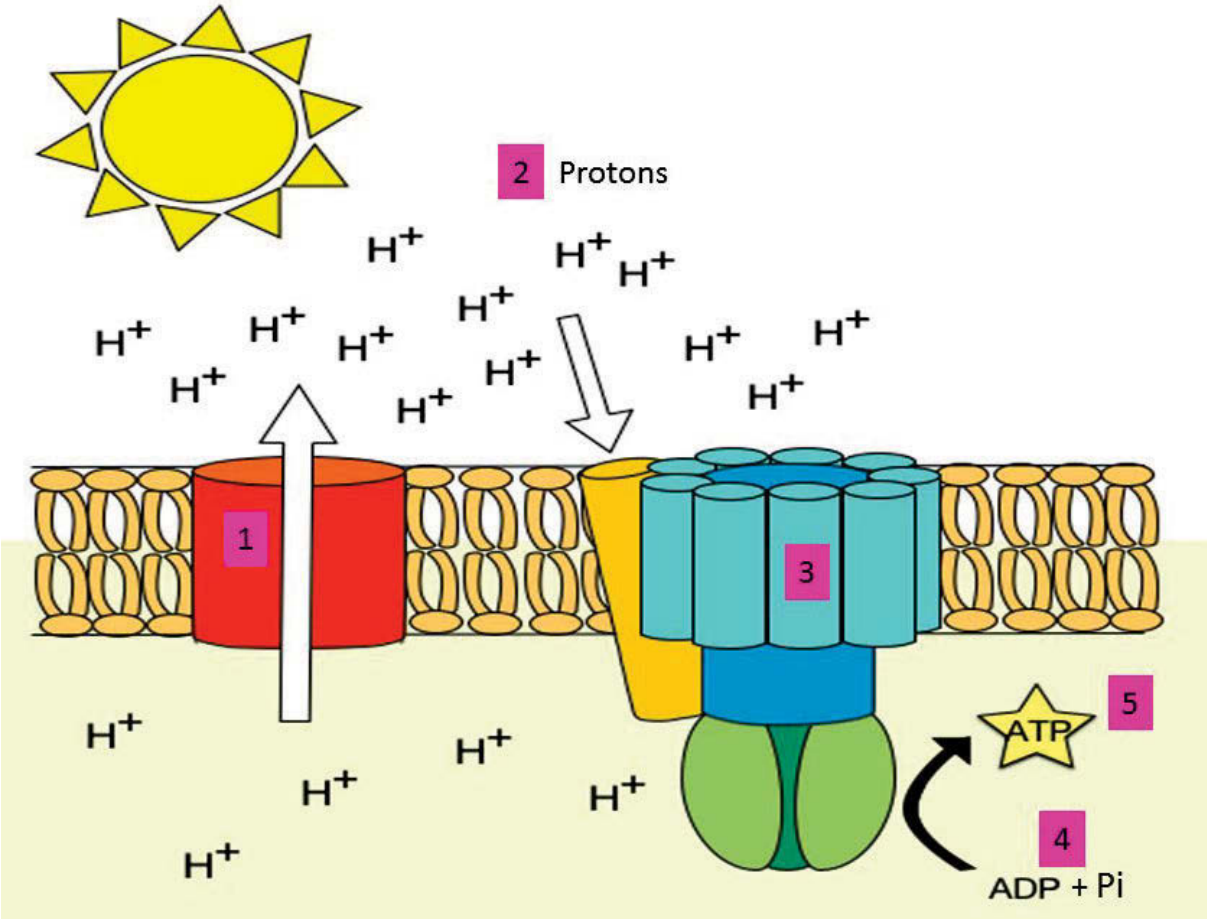

Figure 2: Model of the energy generating mechanism in proteorhodopsin containing marine bacteria. When sunlight strikes a rhodopsin molecule (1), it changes its configuration such that a proton is expelled from the cell (2). The chemical potential causes the proton to flow back into the cell (3), thus generating energy (4) in the form of adenosine triphosphate (5). Modified from Walter et al. (2007).

Proteorhodopsin are known to have different absorption spectra including green and blue visible light. It has been suggested PRs in surface seawater organisms mainly possess a leucine (L) amino acid position 105 and maximally absorb green light

(maximum 530 nm). Organisms adapted to deeper waters have PRs that contain a glutamine (Q) and absorb maximally blue light (near 490 nm) (Béjà et al., 2001; Man et al., 2003; Wang et al., 2003). In addition, Gomez-Casarnau et al., (2007) revealed that Bacteroidetes living surface seawater have PRs that have methionine (M) at position 105, which results in the PR with an absorption maximum at 535 nm. Grouping of PR by sequence alignment reveals distinct clades (Sabehi *et al* 2003; 2005, McCarren and DeLong, 2007). Divergence of these sequences seems potentially related to geographical isolation, speciation and gene transfer processes (de la Torre, 2003; Sabehi *et al*, 2003; McCarren and DeLong, 2007).

Proteorhodopsin (PR) containing microbes are widespread in oceanic surface waters, especially in oligotrophic areas where they can comprise more than 50% of microbial assemblages (e.g. Béjà *et al.*, 2001; Venter *et al.*, 2004; Campbell *et al.*, 2008, Evans *et al.*, 2015). Microbial groups possessing PR include ubiquitous marine bacterial clades such as the Gammaproteobacteria SAR86 (Sabehi *et al.*, 2005) and SAR92 (Venter *et al.*, 2004; Stingl *et al.*, 2007), the Alphaproteobacteria SAR11 (Giovannoni *et al.*, 2005; Lami and Kirchman, 2014; Evans *et al.*, 2015) and SAR116 (Dong Han Cho *et al.*, 2015) as well as members of the Flavobacteriaceae (Gomez-Consarnau *et al.*, 2007; Yoshizawa *et al.*, 2012) and Archaea (Philosof and Béjà, 2013). The widespread occurrence of proteorhodopsin in marine surface waters of oligotrophic oceans is changing our understanding of carbon fluxes and life within low nutrient environments.

An understanding of the biogeography of PRBA is emerging (Finkel *et al*., 2013), but little is currently known about the oceanographic properties (i.e. biological-physical-chemical) that influence the spatiotemporal dynamics of PRBA communities. Evidence exists that the composition of PRBA communities may be explained by specific oceanographic conditions, with differences in communities observed between oligotrophic and eutrophic systems (Venter *et al*., 2004) and coastal and open ocean environments (Campbell *et al*., 2008). For instance, in eutrophic coastal environments PRBA taxa belonging to Flavobacteria, Archaea group II and Gammaproteobacteria are often more dominant, while in deprived nutrient environments PRBA populations are typically dominated by SAR11, SAR92, SAR116 (Venter *et al*., 2004; Campbell *et al*., 2008; Zhao *et al*., 2009; Riedel *et al*., 2010; Evans *et al*., 2015).

Aerobic anoxygenic phototrophic bacteria

In addition to PR-containing bacteria, a second group of photoheterotrophic bacteria have been shown to play an important role in the global ocean. The aerobic anoxygenic phototrophic bacteria (AAnPB) were first discovered by Shiba *et al.* (1979), but it was not until more recently that it was shown that these bacteria represent an important new functional group in the ocean that may constitute up to 10% of the total bacterial population in ocean surface waters (Kolber *et al.,* 2000). These bacteria are related to anaerobic anoxygenic phototrophs (Pfennig, 1978), and possess a fully functional photosynthetic apparatus, which includes the molecule bacteriochlorophyll a (Bchl*a*) (van Neil, 1932). Whereas AAnPB are incapable of photoautotrophy and rely on

heterotrophy for 80% or more of their cellular energetics, sunlight can double organic carbon assimilatory efficiency over that of strict non-photoheterotrophs, making AAnPB key players in the marine carbon cycle (Jiao *et al.,* 2010). AAnPB have been shown to be widely distributed, with populations observed in rivers, freshwater and saline lakes, sediments, soils, sea ice and deep-ocean hydrothermal vents (Shiba *et al*. 1979, Yurkov and Beatty 1998, Jiang *et al*. 2009, Csotonyi *et al*. 2010, Martinez-Garcia *et al*. 2012, Feng *et al*. 2013).

The AAnPB are primarily chemoheterotrophic bacteria that produce a functional purple bacterial photosynthetic reaction center (RC) and one or more peripheral light-harvesting (LH) complexes that can amend heterotrophic energy generation by up to 20% (Kolber *et al.,* 2001; Madigan *et al.,* 2012) (Figure 1 & 3). One of the main characteristics of AAnPB is the possession of BChl*a*, a bacterial pigment capable of absorbing the electromagnetic energy of light. All known AAnPB are able to synthesize BChl*a* (Yurkov and Beatty, 1998). As their name indicates, they do not produce O_2 photosynthetically, principally because they do not use H_2O as an electron donor. Several important characteristics differentiate AAnPB from traditional anoxygenic phototrophs, including: (i) a requirement of O_2 for photosynthesis, excluding their existence in anaerobic irradiated environments, (ii) synthesis of Bchl*a* is inhibited by light, (iii) they lack the enzyme Rubisco, thus they are unable to assimilate CO_2, (iv) generally, they possess a very low number of photosynthetic units

per cell, which can absorb light energy and transmit it to the bacteriochlorophyll. (Yurkov and Csotonyi, 2003; Rathgeber et al., 2004).

Metabolic diversity in AAnPB is exceptionally large, perhaps as expected for a functional group relying exclusively on heterotrophy for carbon needs. Several AAnPB taxonomic groups including *Erythrobacter, Erythromicrobium, Porphyrobacter, Roseicyclus, Roseobacter* and *Sandaracinobacter* are able to metabolise numerous organic compounds such as carbohydrates, organic acids, alcohols and complex organics (Yurkov and Csotonyi, 2003). Some of these compounds used by AAnPB have attracted substantial attention for their ecological significance. One example is the case of dimethylsulfoniopropionate (DMSP), an osmolyte produced by phytoplankton and an important marine source of sulfur. The prominent role of *Roseobacters* in DMSP consumption by cleavage or demethylation and dethiolation, and the resulting liberation of sulfide or dimethyl sulphide (DMS) compounds ultimately influences climate, and implicates this important group of AAnPB as key modulators of the marine sulfur cycle and regional climate control (Wagner-Döbler and Biebl, 2006; Moran *et al*., 2007).

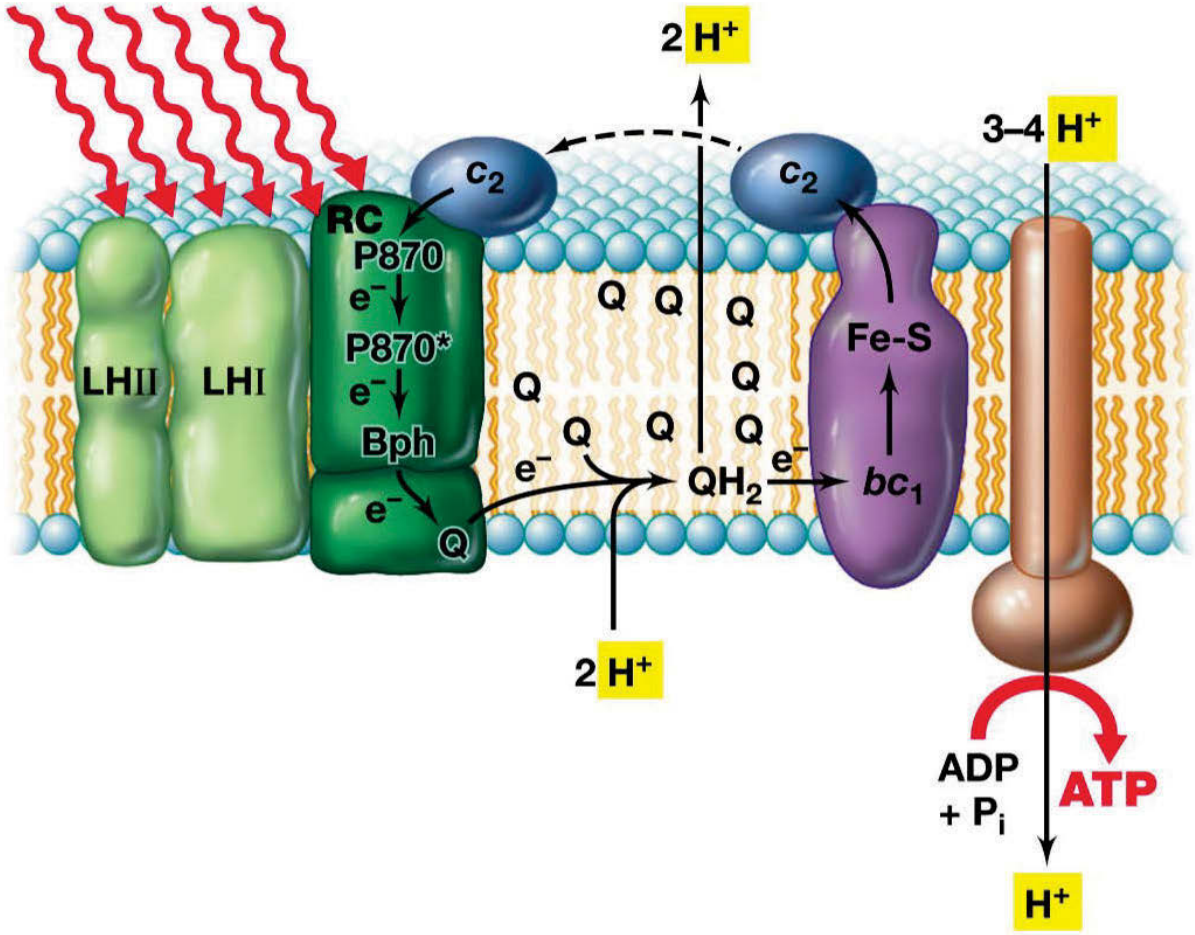

Figure 3: Reaction center of purple phototrophic bacterium: Arrangement of protein complexes in the photosynthetic membrane of a purple phototrophic bacterium. The light-generated proton gradient is used in the synthesis of ATP by the ATP synthase (ATPase) (Madigan *et al.*, 2012). (LH=light harvesting, RC=reaction center, Bph=bacteriophaeophytin b, ADP=Adenosine diphosphate)

In marine ecosystems, the abundance and distribution of AAnPB differs between oceanographic provinces, indicating niche separation driven by different physical and chemical parameters. Most AAnPB are members of the Alpha-, Beta- and Gammaproteobacteria. Yutin *et al*. (2007) proposed a phylogenetic framework for assigning AAnPB into 12 phylogroups (labelled phylogroups A through L), defined according to the structure of the puf operon and the phylogeny of the *pufM* gene. Different phylogroups have been shown to be abundant in different marine environments. For example, Alphaproteobacterial phylogroups E and F, which

contain Rhodobacter-like bacteria, and G, which contains Roseobacter-like bacteria, are common in nutrient rich coastal waters (Lehours *et al*., 2010, Salka *et al*., 2008), whereas phylogroups C and D have been mostly observed in offshore waters (Ritchie and Johnson, 2012). Phylogroup K, which contains members of the Gammaproteobacteria, also has a widespread distribution, and has been demonstrated to dominate AAnPB composition in samples from the Atlantic and Pacific Oceans (Hu *et al*. 2006, Mašín *et al*. 2006, Yutin *et al*. 2007, Ritchie and Johnson 2012, Boeuf *et al*. 2013a) as well as the Arctic (Lehours and Jeanthon 2015) and Mediterranean Seas during summer (Lehours *et al*. 2010, Ferrera *et al*. 2014). Although the diversity of AAnPB is becoming clearer, there is still a lack of data concerning their distribution and activity in different aquatic environments.

With some exceptions (Lami *et al*., 2007), AAnPB on average constitute typically 1–7% of total prokaryotes in the oligotrophic areas of the oceans, while in estuaries shelf or seas they can comprise up to 15% of the community (Cottrell *et al*. 2006; Du et al. 2006; Mašín *et al*. 2006, Sieracki *et al*. 2006, Jiao et al. 2007Yutin *et al*. 2007, Waidner and Kirchman 2007, Cottrell et al. 2010, Lehours *et al*. 2010; Ritchie and Johnson 2012; Ritchie and Johnson 2012; Stegman *et al*. 2014). In estuaries, light attenuation, nitrate, and ammonium have all been shown to be positively correlated with AAnPB, further suggesting an ecological association with productivity or organic particles (Waidner and Kirchman, 2007).

Ecological theory towards understanding microbial oceanography

By definition, biogeography is the study of species distributions over space and time (Fierer, 2008). Traditionally, due to their size, dispersion capabilities, rapid reproductive rates and dormant stages, constraint by geographical barriers or distances have not been considered significant drivers of microbial biogeography (Hanson *et al.,* 2012). Indeed observed patterns on both small scales and larger scales indicate that many marine bacterial clades are widespread across the global ocean (Venter *et al.,* 2004; Rusch *et al.,* 2007). However, the majority of these clades display biogeographic patterns when examined using higher resolution molecular markers, although the specific biological and/or physical barriers driving this separation are often unclear (i.e. Barberan and Casamayor 2010;, Ghiglione *et al*., 2012; Sul *et al*., 2013; Brown et al., 2014). A number of mechanisms have been suggested to account for these contrasting patterns in marine microbial distribution, ranging from selection, drift, dispersal and mutation mechanisms (Hanson *et al*., 2012). However, efforts to investigate species abundance patterns over relevant spatial and temporal scales remain critical (McGeoch and Gaston, 2002; Prosser *et al.,* 2007). To this end, assessing seasonal and spatial patterns in photoheterotrophic microbial community abundance and diversity is critical when attempting to resolve potential drivers of large-scale spatial patterns of these important microbes. Initial attempts to integrate such spatial and temporal patterns on a global scale are promising, and predict diversity peaks in temperate latitudes across the world's oceans (Ladau et al., 2013).

Most natural environments harbour a stunningly diverse collection of microbial species (i.e. Sogin *et al.,* 2006). In these communities, bacteria compete with their neighbours for space and resources. Despite recent efforts, studies related to intra and inter species relationships among specific bacterial groups (i.e. competition vs. mutualism) are rare. This shortage of knowledge has been due to difficulties in obtaining robust data at suitable scales using traditional microbial approaches (Fuhrman *el al.,* 2006). Advances in high-throughput sequencing technology and new analytical software have provided an unprecedented new knowledge on intra- and inter-species interactions in microbial communities. For instance, network analysis has recently been applied in microbial ecology to examine spatial and temporal associations between discrete microbial operational taxonomic units (OTUs) and their environment (Steele *et al.,* 2011; Zhou *et al.,* 2011). Co-occurrence patterns among microorganisms may indicate ecological relationships between the members of a community and biogeochemical properties (Barberan et al., 2012; Eiler, Heinrich & Bertilsson, 2012; Faust & Raes, 2012; Gilbert et al., 2012). Association networks are built from co-occurrence data to capture relationships among individual microorganisms (OTUs) and environmental parameters. For example, if two organisms are frequently present together, and absent together, across multiple environments or samples, this can be interpreted as evidence that they occupy similar ecological niches (Horner-Devine et al., 2007; Faust & Raes, 2012). This clustering of organisms into larger modules or "guilds" that share related ecology, regardless of their phylogeny, may

allow detection of novel ecological associations among important and abundant photoheterotrophic microbial groups.

Australian Marine Ecosystems

One of the principal goals of this thesis is to provide the first insights into the abundance and diversity of photoheterotrophic microbes in the Australian marine environment. Until now, there have been no examinations of photoheterotrophic bacteria within Australian aquatic ecosystems, despite these organisms comprising a significant fraction of the microbial communities inhabiting the euphotic zone of world's oceans. The Australian maritime estate, bordered by the Indian Ocean in the west, the Pacific Ocean in the east, and Southern Ocean in the south, and also encompassing the Arafura, Timor, Coral and Tasman Seas, is large and characterised by particularly complex oceanography. The west and east coasts are bounded by two major warm, nutrient-poor, poleward flowing currents, the East Australian Current (EAC) and Leeuwin Current (Figure 4). These currents exert substantial influence on marine biota, along with the Australian climate (Hobday *et al.*, 2006, Feng *et al.*, 2009, Polozanska *et al.*, 2007). One of the main characteristics of Australian marine ecosystems is that they are generally oligotrophic (nutrient poor), principally experiencing nitrate and phosphate limitation and low productivity (Ridway, 2007; Thompson *et al.*, 2011).

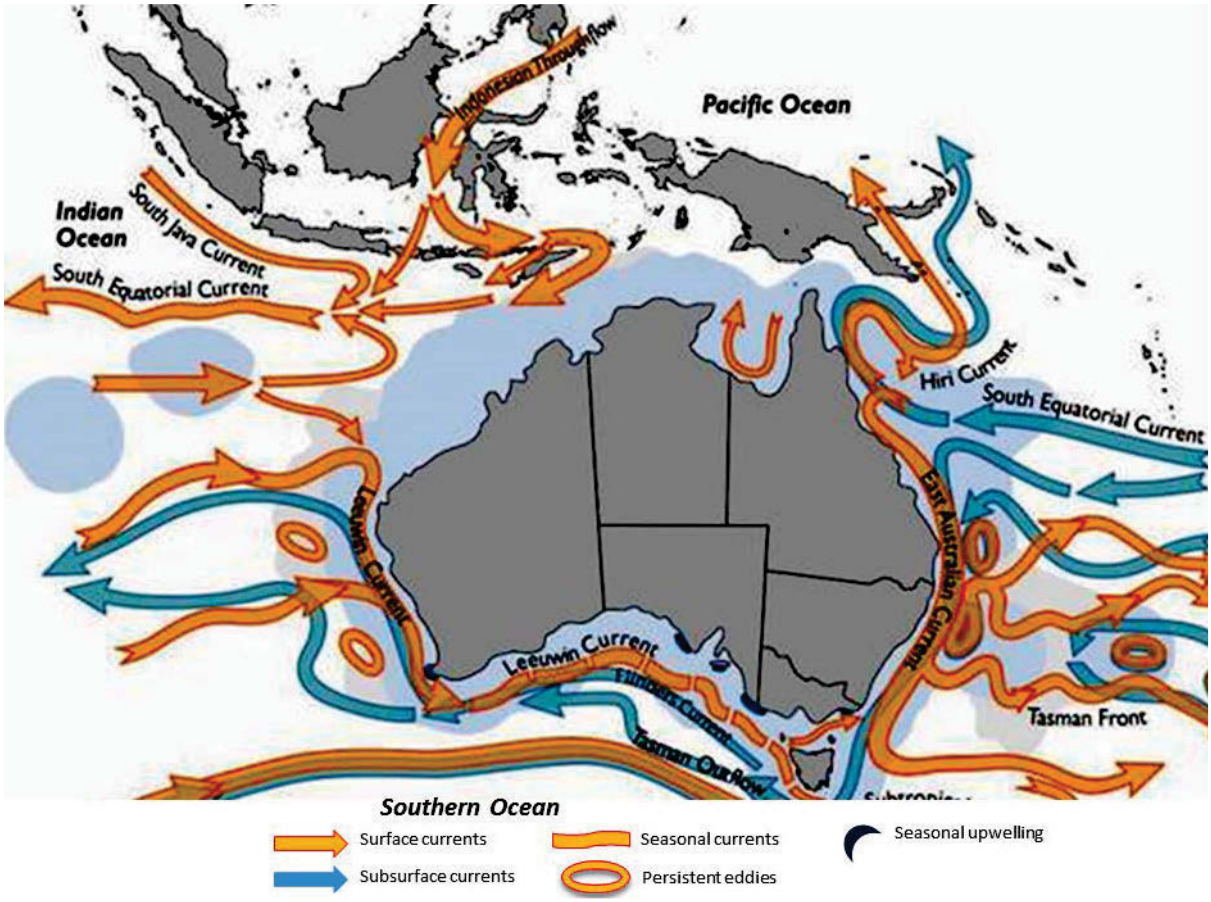

Figure 4. Major currents and circulation patterns around Australia. The continent is bounded by the Pacific Ocean to the east, the Indian Ocean to the west and the Southern Ocean to the south. Image modified. Source http://www.oceanclimatechange.org.au/.

The primary study region for the research included in this thesis encompasses the coastal waters of northern and eastern Australia. These regions have been sampled during research voyages and as well as through the Australian Marine Microbial Biodiversity Initiative (AMMBI), which operates a sustained marine microbial sampling program at the numerous marine National Reference Stations around Australia established by the federally funded agency the Integrated Marine Observing System (IMOS). These stations are located at coastal sites around Australia and comprise both moored sensors and routine vessel-based sampling. The stations are designed to provide multi-decadal time series of the physical and biogeochemical properties of Australia's coastal oceans. In this thesis I aim to investigate for first time

in Australian coastal waters, the spatial and temporal patterns in the abundance and diversity of photoheterotrophic microorganisms. It is predicted that key ecosystem processes are likely to shift due to climate change (Ducklow *et al.*, 2010), so it is important that we examine the role of environmental parameters (e.g., nutrients, chlorophyll, pH, salinity, temperature), that are predicted to shift in the future, on the dynamics of abundant and ecologically important microbial groups. Given the potential biogeochemical significance of photoheterotrophic bacteria in the ocean (Eiler, 2006, Moran and Miller, 2007), it is particularly essential that we understand how environmental variability influences the dynamics of this microbes.

AIMS

The overall objective of this PhD was to investigate patterns in the abundance and diversity of photoheterotrophic bacterial communities over space and time within the oceanographically complex Australian marine environment, and to identify the environmental factors responsible for seasonal and biogeographic shifts in these important groups of marine microorganisms. The specific aims of the thesis are to:

1. Determine whether photoheterotrophic microbes constitute a numerically and functionally significant element within Australian ocean waters.
2. Identify the environmental factors influencing photoheterotrophic community composition and diversity within Australian marine waters.
3. Determine whether distinct photoheterotrophic populations fill specific environmental niches within marine ecosystems.

Chapter 2

Spatial and temporal variability of aerobic anoxygenic photoheterotrophic bacteria along the east coast of Australia

Spatial and temporal variability of aerobic anoxygenic photoheterotrophic bacteria along the east coast of Australia

Jaime Bibiloni-Isaksson[1], Justin Seymour[1], Tim Ingleton[2], Jodie van de Kamp[3], Levente Bodrossy[3], Mark Brown[4]

Author Contributions

Conceived and designed the experiments: JBI, JS, MVB. Performed the experiments: JBI, TI, JV, LB. Analysed the data: JBI, JS, MVB. Wrote the paper: JBI, JS, MVB.

1. Plant Functional Biology and Climate Change Cluster, University of Technology, Sydney

2. Waters and Coastal Science Section, Department of Environment, Climate Change and Water, PO Box A290, Sydney South NSW 1232, Australia.

3. CSIRO Oceans and Atmosphere, Castray Esplanade, Hobart, Tasmania, Australia 7000

4. School of Biotechnology and Biomolecular Science, UNSW Australia, Sydney, Australia 2052

Running title: AAnPB variability in coastal waters of Australia

Originality-Significance Statement

Using comparative time-series data from three marine stations spanning 15° latitude along the east coast of Australia, we reveal the environmental parameters structuring aerobic anoxygenic photoheterotrophic bacteria (AAnPB) over large spatial scales and seasonal cycles. The patterns observed indicate that different members of the AAnPB community exhibit markedly different associations with environmental factors, indicative of niche diversity among this important group of marine bacteria.

Abstract

Aerobic Anoxygenic phototrophic bacteria (AAnPB) are ecologically important microorganisms, widespread in oceanic photic zones. However, the key environmental drivers underpinning AAnPB abundance and diversity are still largely undefined. We examined temporal patterns in AAnPB dynamics at three oceanographic reference stations spanning ~15° latitude along the Australian east coast. AAnPB abundance was highly variable, with *pufM* gene copies ranging from 1.1 x 10^2 to 1.4 x 10^5 mL^{-1} and positively correlated with day length and solar radiation. *pufM* gene Miseq sequencing revealed that the majority of sequences were closely related to those obtained previously, suggesting that key AAnPB groups are widely distributed across similar environments globally. Temperature was a major structuring factor for AAnPB assemblages across large spatial scales, correlating positively with richness and *Gammaproteobacteria* (phylogroup K) abundance but

negatively with Roseobacter-clade (phylogroup E) abundance, with temperatures between 16-18 °C identified as a potential transition zone between these groups. Network analysis revealed that discrete AAnPB populations exploit specific niches defined by varying temperature, light and nutrient conditions in the Tasman Sea system, with evidence for both niche sharing and partitioning amongst closely related OTUs.

Supplementary material

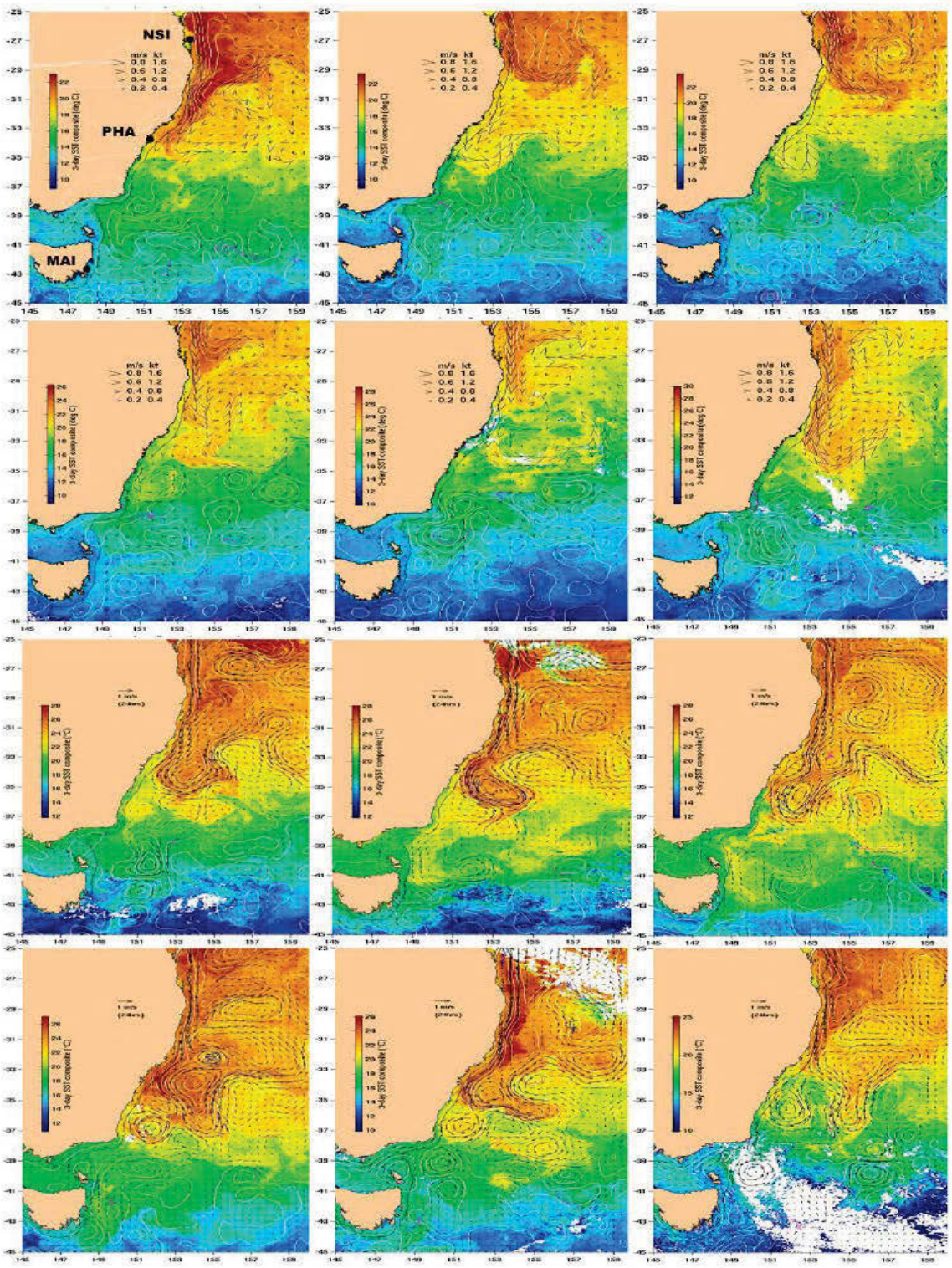

Figure S1: Sea Surface Temperature maps highlight the complex oceanography of the eastern Australian coastline where our samples were collected. Each image was taken from the 15th day of the month, beginning with 15-Jul-2012 in the upper left-hand corner and continuing to the right with 15-Jun-2013 in the bottom right-hand corner. The East Australian Current (EAC) can be seen travelling south, indicated by the warm sea surface temperature, and separating into eddies near the Port Hacking region. Images source: IMOS (http://oceancurrent.imos.org.au/). North Stradboke Island station (NSI), Port Hacking station (PHA) and Maria Island station (MAI).

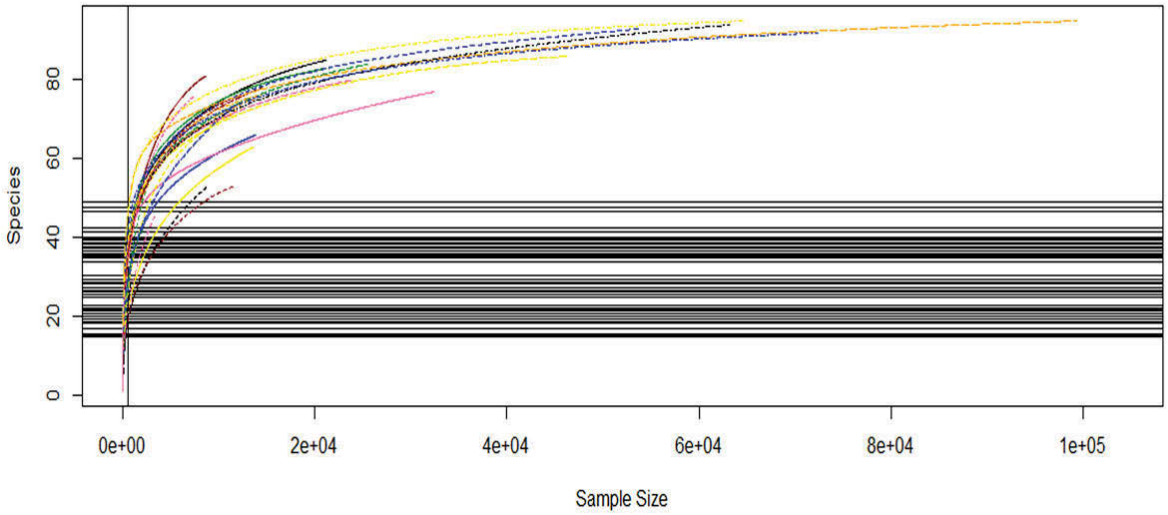

Figure S2: Rarefaction curve for all samples at all stations.

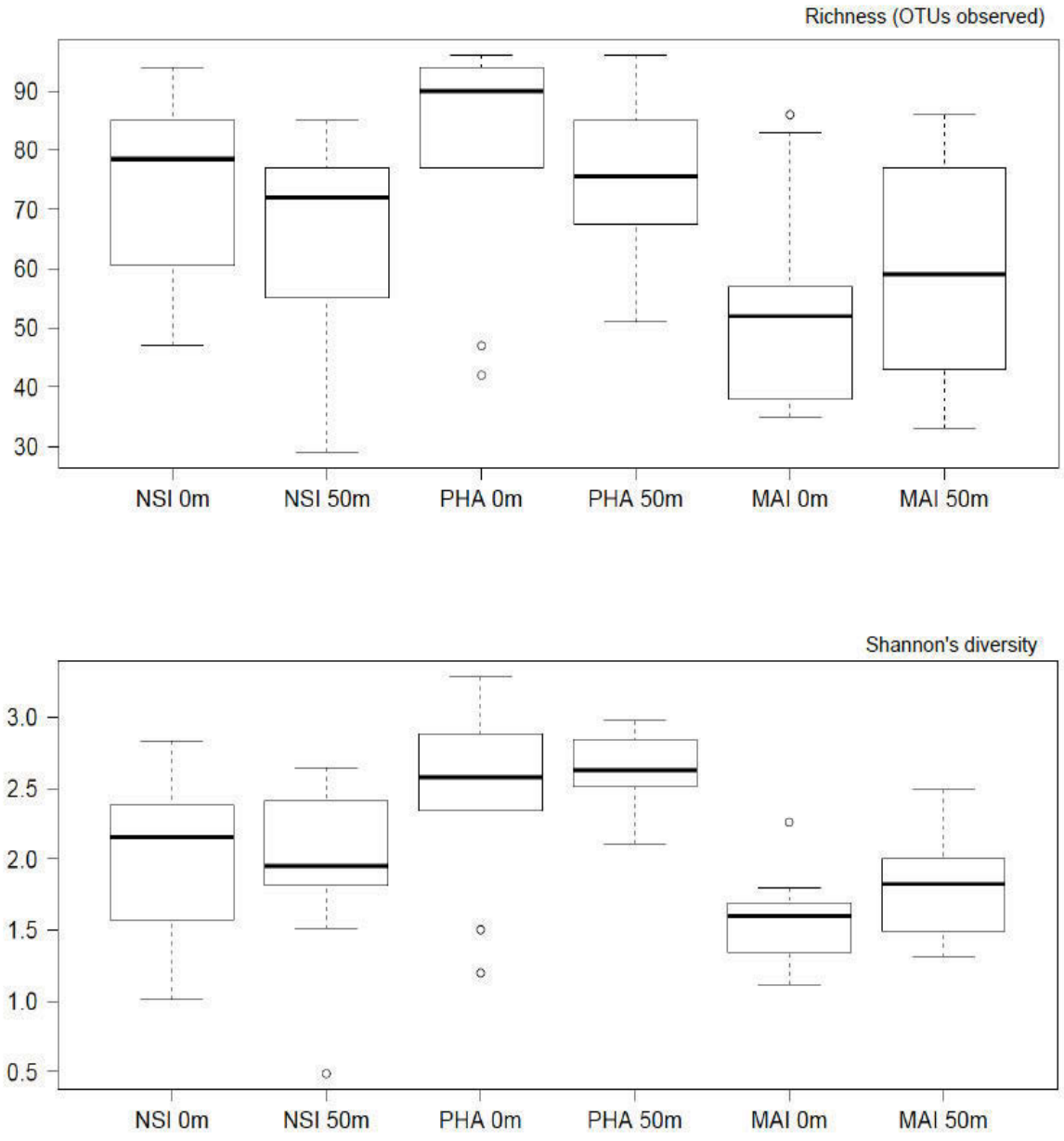

Figure S3: Box plots displaying richness (top) and Shannon's diversity index (bottom) at each site and depth sampled.

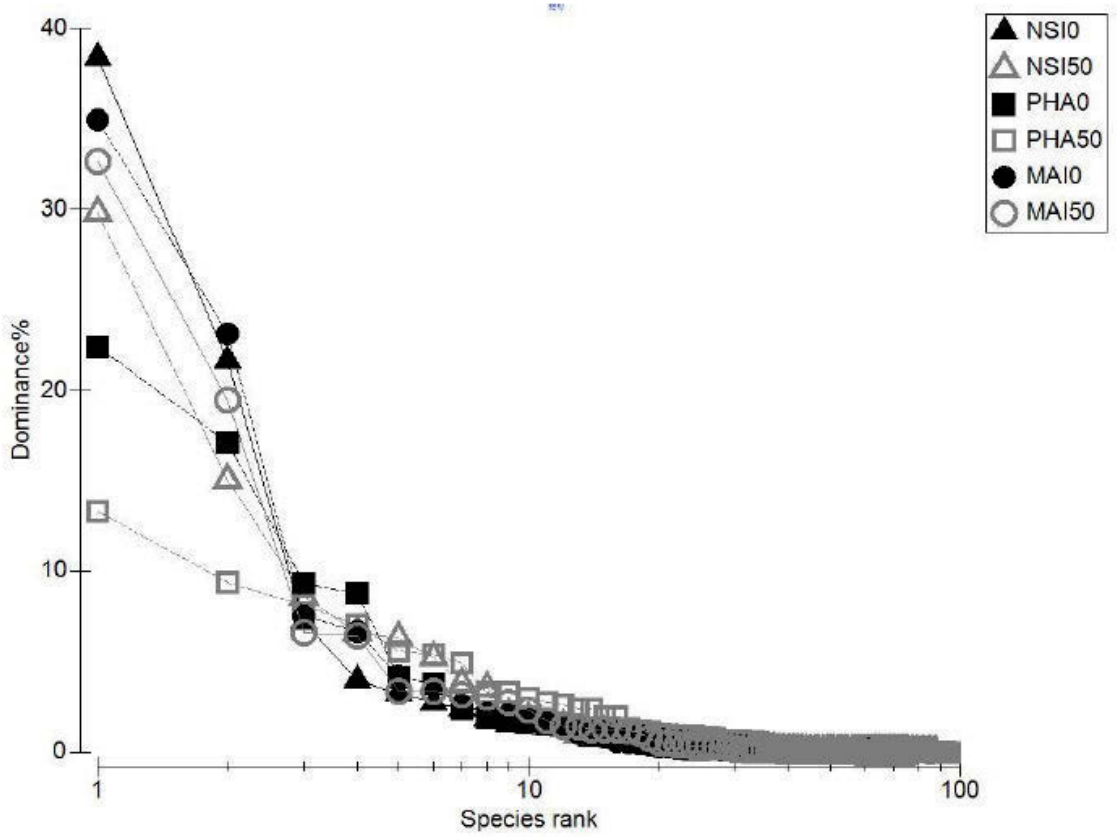

Figure S4: OTU rank abundance curves for each station and depth.

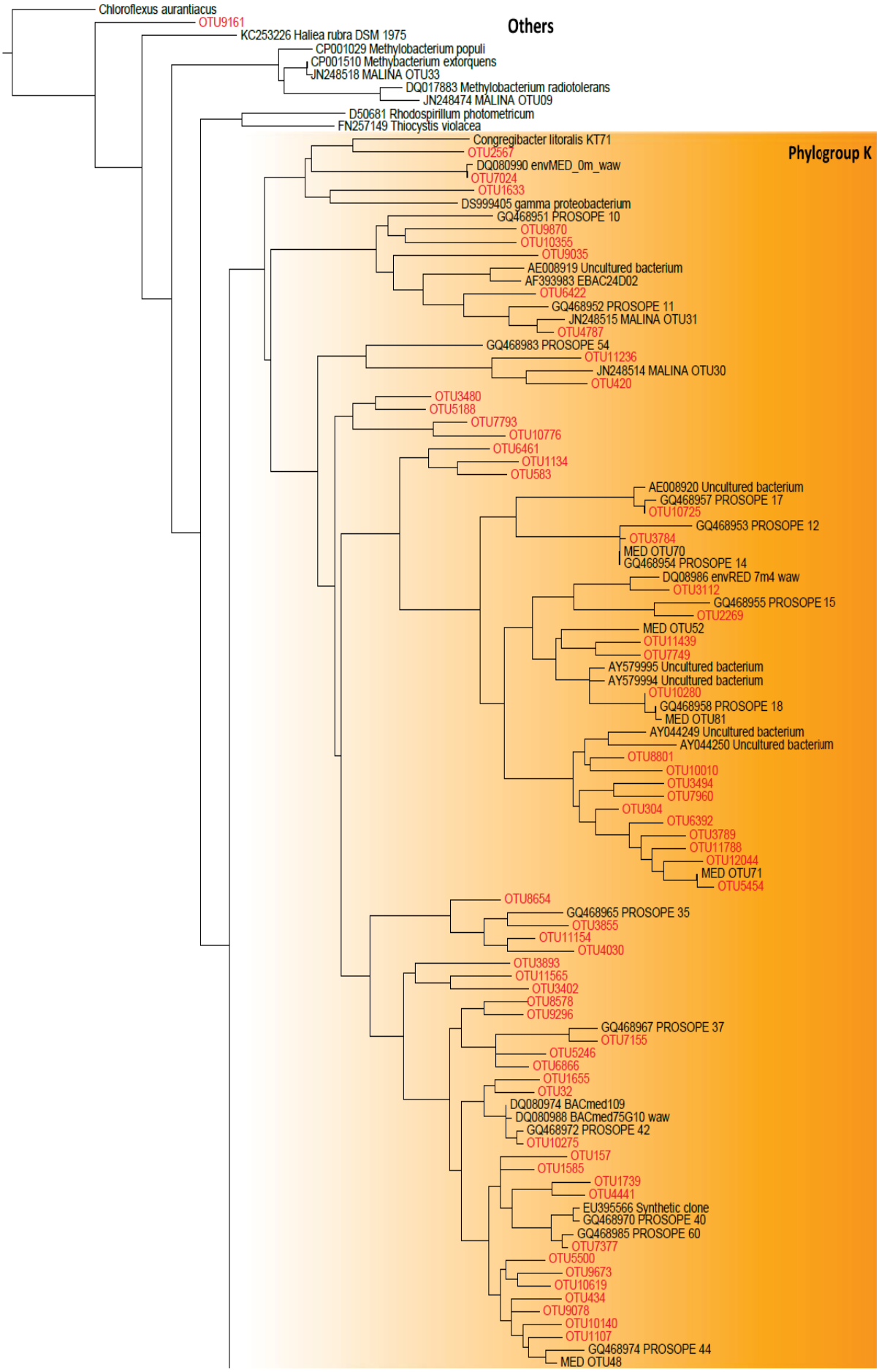
Chloroflexus aurantiacus
OTU9161
Others
KC253226 Haliea rubra DSM 1975
CP001029 Methylobacterium populi
CP001510 Methylobacterium extorquens
JN248518 MALINA OTU33
DQ017883 Methylobacterium radiotolerans
JN248474 MALINA OTU09
D50681 Rhodospirillum photometricum
FN257149 Thiocystis violacea
Congregibacter litoralis KT71
OTU2567
Phylogroup K
DQ080990 envMED_0m_waw
OTU7024
OTU1633
DS999405 gamma proteobacterium
GQ468951 PROSOPE 10
OTU9870
OTU10355
OTU9035
AE008919 Uncultured bacterium
AF393983 EBAC24D02
OTU6422
GQ468952 PROSOPE 11
JN248515 MALINA OTU31
OTU4787
GQ468983 PROSOPE 54
OTU11236
JN248514 MALINA OTU30
OTU420
OTU3480
OTU5188
OTU7793
OTU10776
OTU6461
OTU1134
OTU583
AE008920 Uncultured bacterium
GQ468957 PROSOPE 17
OTU10725
GQ468953 PROSOPE 12
OTU3784
MED OTU70
GQ468954 PROSOPE 14
DQ08986 envRED 7m4 waw
OTU3112
GQ468955 PROSOPE 15
OTU2269
MED OTU52
OTU11439
OTU7749
AY579995 Uncultured bacterium
AY579994 Uncultured bacterium
OTU10280
GQ468958 PROSOPE 18
MED OTU81
AY044249 Uncultured bacterium
AY044250 Uncultured bacterium
OTU8801
OTU10010
OTU3494
OTU7960
OTU304
OTU6392
OTU3789
OTU11788
OTU12044
MED OTU71
OTU5454
OTU8654
GQ468965 PROSOPE 35
OTU3855
OTU11154
OTU4030
OTU3893
OTU11565
OTU3402
OTU8578
OTU9296
GQ468967 PROSOPE 37
OTU7155
OTU5246
OTU6866
OTU1655
OTU32
DQ080974 BACmed109
DQ080988 BACmed75G10 waw
GQ468972 PROSOPE 42
OTU10275
OTU157
OTU1585
OTU1739
OTU4441
EU395566 Synthetic clone
GQ468970 PROSOPE 40
GQ468985 PROSOPE 60
OTU7377
OTU5500
OTU9673
OTU10619
OTU434
OTU9078
OTU10140
OTU1107
GQ468974 PROSOPE 44
MED OTU48

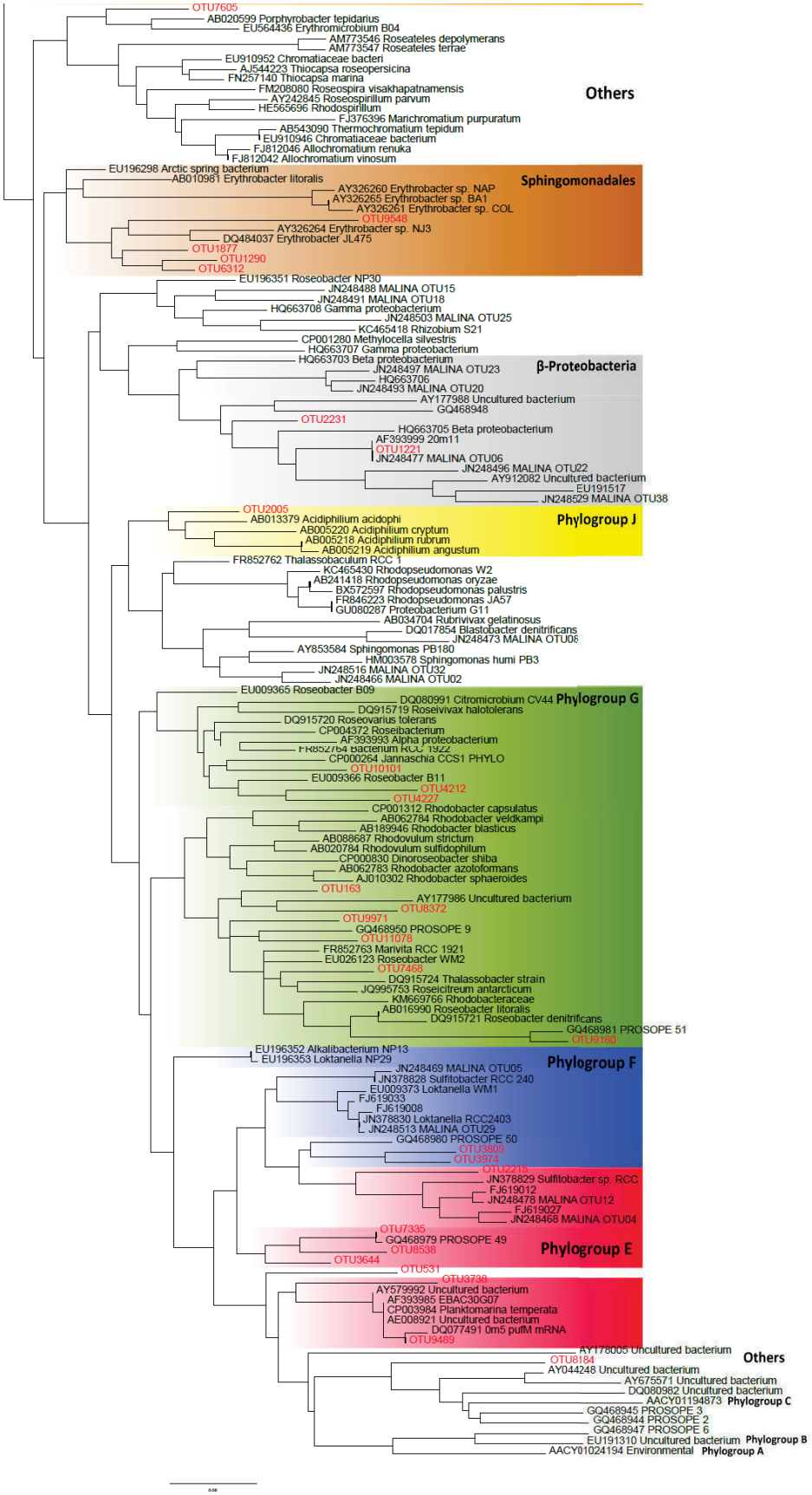

Figure S5: Phylogenetic tree showing the relationships between *pufM* gene sequences from this study and environmental samples and nearest relatives retrieved from GenBank. The tree is based on a Bayesian tree to which short sequences were added by ARB_PARSIMONY. Colours were included to indicate taxonomic groups defined by Yutin *et al.,* (2007).

Chapter 3

Regional heterogeneity and seasonal succession in proteorhodopsin containing microbial assemblages

Regional heterogeneity and seasonal succession in proteorhodopsin containing microbial assemblages

Jaime Bibiloni-Isaksson[1], Mark V. Brown[2], Tim Ingleton[3], Jodie van de Kamp[4], Levente Bodrossy[4], John P. Bowman[5], Justin R. Seymour[1]

Author Contributions

Conceived and designed the experiments: JBI, JS, MVB. Performed the experiments: JBI, TI, JV, LB. Analysed the data: JBI, JS, MVB. Wrote the paper: JBI, JS, MVB.

1. Plant Functional Biology and Climate Change Cluster, University of Technology, Sydney

2. School of Biotechnology and Biomolecular Science, UNSW Australia, Sydney, Australia 2052
3. Waters and Coastal Science Section, Department of Environment, Climate Change and Water, PO Box A290, Sydney South NSW 1232, Australia.

4. CSIRO Oceans and Atmosphere, Castray Esplanade, Hobart, Tasmania, Australia 7000

5. School of Land and Food, Tasmanian Institute of Agriculture, University of Tasmania, Hobart, Tasmania, Australia

Summary: A significant proportion of the marine prokaryote community is comprised of microbes that utilise proteorhodopsin (PR), a retinal based photoreceptor used for generating ATP from light. While these organisms have been shown to be ubiquitous across the marine environment, an understanding of the factors that structure the diversity and composition of this important group of marine microbes in space and time is lacking. Here we examined spatial and temporal patterns in the diversity of PR containing Bacteria and Archaea (PRBA) along the east coast of Australia. Surface seawater samples were collected at monthly intervals over a 12 month period from 3 oceanographic time-series sites spanning 15˚ of latitude. An amplicon sequencing approach was used to characterise and compare the composition and diversity of proteorhodopsin containing microbes. Coastal PRBA assemblages were dynamic in both space and time, with diversity linked to several environmental factors including positive correlations to temperature, Secchi depth and *Prochlorococcus* cell abundance and negative correlations to phosphate concentration. Shifts in the taxonomic composition of the PRBA assemblage were best explained by temperature and day length. Seasonality in taxonomic structure was accompanied by temporal variability in proteorhodopsin spectral tuning characteristics. The ratio of blue absorbing proteorhodopsin proteins (BPR) to green absorbing proteorhodopsin proteins (GPR) was strongly linearly correlated with day length, with levels GPR increasing with longer day lengths. These observations highlight the dynamic nature of proteorhodopsin containing marine assemblages, which exhibit substantial shifts in

both taxonomy and spectral tuning properties in response to seasonal and spatial variability in environmental conditions.

Introduction

Photoheterotrophic microbes are capable of harvesting light energy to supplement their metabolic requirements and represent a significant fraction of prokaryote communities in euphotic zones of the ocean (Béjà and Suzuki, 2008). A major group of marine photoheterotrophs are those that contain proteorhodopsin, a light-driven proton pump that enhances ATP production in heterotrophic organisms that would otherwise rely entirely on the oxidization of organic material for energy (Beja *et al.*, 2000; Martinez *et al.*, 2007; Lehours and Jeanthon, 2015). Proteorhodopsin containing bacteria and Archaea (PRBA) are widespread in oceanic surface waters, where they can comprise nearly 50% of the prokaryotic population and outnumber photosynthetic microbes by up to three orders of magnitude (Finkel *et al.*, 2013). Since their discovery less than 20 years ago (Beja *et al.*, 2000), the ubiquitous occurrence, and indeed often high abundance, of proteorhodopsin containing marine microbes has fundamentally shifted our perception of microbial metabolisms, and their influence on carbon and energy cycling in the surface ocean (Finkel *et al.*, 2013; Karl, 2014).

While initially identified in an uncultivated marine bacterium from within the SAR86clade (Beja *et al.*, 2000), it is now apparent that proteorhodopsin is widespread

among diverse groups of marine prokaryotes, including dominant bacterial clades such as *Gammaproteobacteria* SAR86 (Sabehi *et al.*, 2005) and SAR92 (Stingl *et al.*, 2007), the *Alphaproteobacteria* SAR11 (Giovannoni *et al.*, 2005; Lami and Kirchman, 2014; Evans *et al.*, 2015) and SAR116 (Choi *et al.*, 2015), as well as members of the *Flavobacteriaceae* (Gómez-Consarnau *et al.*, 2010; Yoshizawa *et al.*, 2012) and *Euryarchaeota* group IIa and IIb (Philosof and Béjà, 2013). However, while an understanding of the biogeography of PRBA is developing (Finkel *et al.*, 2013), little is currently known about the physical and chemical drivers and oceanographic properties that influence the composition and spatiotemporal dynamics of PRBA communities in the ocean.

There is evidence that the composition of the PRBA community may be defined by specific waters properties, with differences in PRBA assemblage structure observed between eutrophic and oligotrophic systems (Rusch *et al.*, 2007) and coastal and open ocean environments Evans *et al.,* 2015; Brindefalk *et al.,* 2016). In oligotrophic environments PRBA populations are typically dominated by SAR11, SAR92 and SAR116, while in more nutrient rich coastal environments PRBA taxa belonging to *Flavobacteria*, *Archaea* group IIb and *Gammaproteobacteria* are often more dominant (Venter *et al.*, 2004; Campbell *et al.*, 2008; Zhao *et al.*, 2009; Riedel *et al.*, 2010; Evans *et al.*, 2015).

In addition to the phylogenetic diversity among proteorhodopsin containing marine microbes, there is notable heterogeneity in the biophysical properties of the proteorhodopsins employed by different taxonomic groups. Since the discovery of PRBA (Beja *et al.*, 2000), a diverse range of proteorhodopsin variants have been identified (Béja *et al.*, 2001; De la Torre *et al.*, 2003; Sabehi *et al.*, 2003; Sabehi *et al.*, 2005; Frigaard *et al.*, 2006; Koh *et al.,* 2010; McCarren and DeLong, 2007; Sabehi *et al.*, 2007; Pushkarev and Beja, 2016) and categorized by the colour of light at the peak of their absorbance spectrum. Green light absorbing proteorhodopsins (GPRs) have a peak absorbance around 525 nm, while blue light absorbing proteorhodopsins (BPRs) have a peak absorbance near to 490 nm (Béja *et al.*, 2001). In addition, proteorhodopsins from members of the *Bacteriodetes* phylum have a slightly shifted green light absorption maximum at 535 nm (Gómez-Consarnau *et al.*, 2010). The spectral tuning of these different proteorhodopsin variants undoubtedly define, or are defined by, the distribution of different proteorhodopsin taxa across different light and water-body characteristics in the environment.

Here we examined patterns in PRBA community composition and diversity within the western Tasman Sea, in a region spanning the eastern coast of Australia, with the goal of identifying PRBA community seasonal and spatial patterns and revealing the key environmental drivers of community structure. The highly dynamic and complex physical oceanography of this region (Ridgway and Dunn, 2003; Ridgway, 2007) has been shown to influence the composition and function of zooplankton, phytoplankton,

and bacterial assemblages (Seymour *et al.,* 2012; Armbrecht *et al.,* 2014; Lynch *et al.,* 2014). Recently we demonstrated that another important group of marine photoheterotrophs, the aerobic anoxygenic phototrophic bacteria (AAnPB) display substantial seasonal and spatial variability in abundance and diversity in this region (Bibiloni-Isaksson *et al.,* 2016). Here we aimed to employ this dynamic oceanographic region as a model system to expand our understanding how PRBA diversity changes in space and time and reveal key physical, chemical and biological drivers of PRBA community structure.

Results & Discussion

Seawater samples were collected from three oceanographic time-series stations separated by ~ 15 ° latitude and situated along Australia's eastern coastline (Fig.1). These sites included the Australian Commonwealth Government's Integrated Marine Observatory System (IMOS) National Reference Stations (NRS) located at North Stradbroke Island (NSI) (27.35° S, 153.56° E), Port Hacking (PHA) (34.07° S, 151.12° E) and Maria Island (MAI) (42.59° S, 148.23° E). These sites vary considerably in their local oceanography and climatology as well as the timing and extent of impact of the southerly flowing East Australian Current (EAC) (Fig. S1; Table S1 as Appendix II) (Ridgway, 2007). The most northerly station at NSI is a subtropical site where seasonality principally extends to two seasons, with strong variations in water-body conditions such as temperature and solar radiation exposure. The mid-latitude site at PHA occupies a warm temperate region, which is strongly affected by

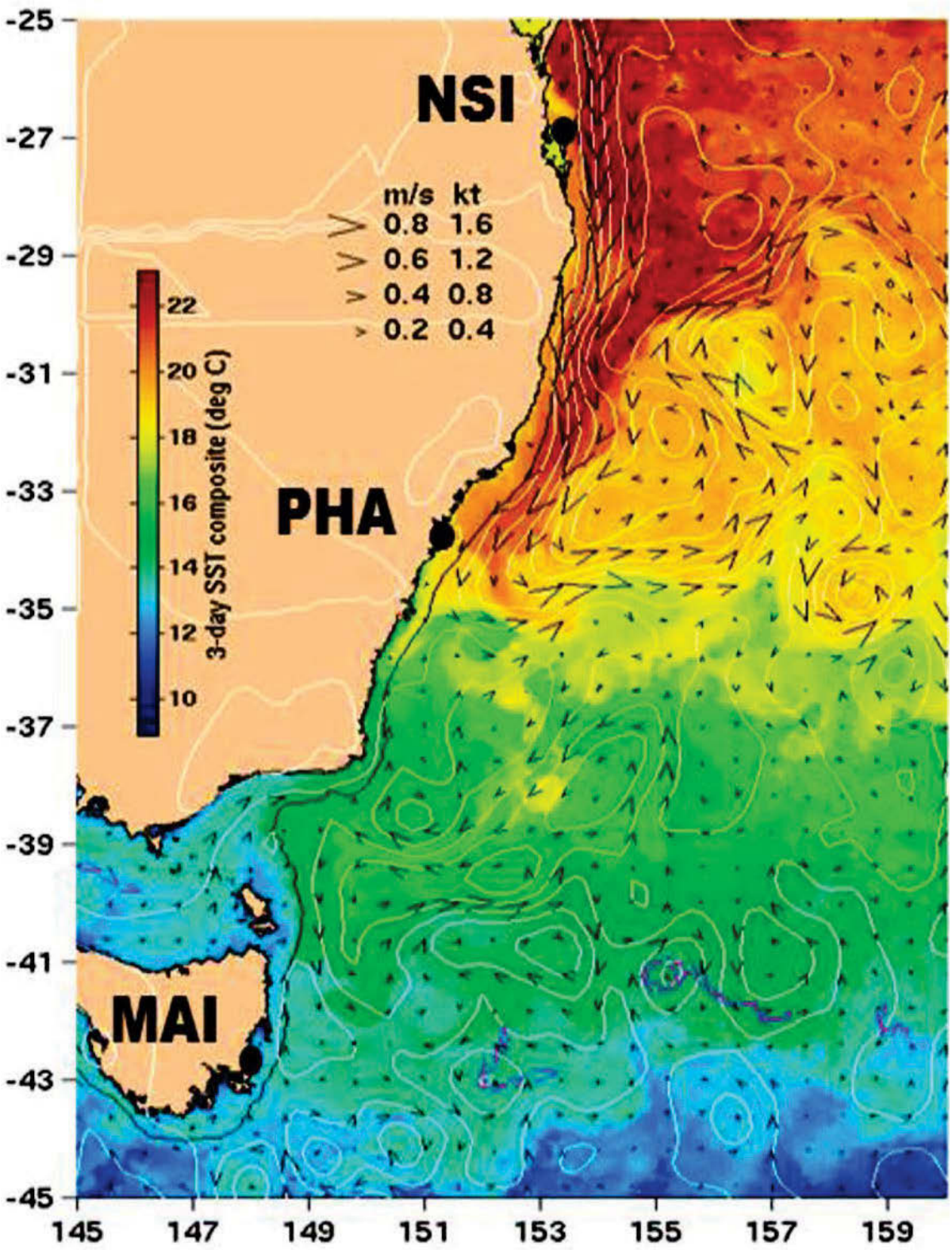

Figure 1: Sea Surface Temperature map of the eastern Australian coastline including the location of the three oceanographic reference stations where monthly seawater samples were collected. This image was compiled from July 15, 2012. The East Australian Current (EAC) can be seen travelling south, indicated by the warm sea surface temperature, and separating into eddies near the Port Hacking region (PHA). Images source: IMOS (http://oceancurrent.imos.org.au/). Sampling was conducted as part of the Australian Marine Microbial Biodiversity Initiative (AMMBI), which conducts standardised sampling for microbial community analysis, in conjunction with the Australian Commonwealth Government's Integrated Marine Observing System (IMOS), at multiple National Reference Stations (NRS) within the Australian marine environment. Samples were collected at 10m depth on a monthly basis during the period of July 2012 to June 2013 (Figure S1).

the EAC eddy field (Suthers *et al.*, 2011). In summer, during stratified periods at NSI and PHA the upper euphotic zone is characterised by higher temperatures, low nutrient (oligotrophic) concentrations and a high solar insolation level. The most southerly site at MAI is situated off the eastern coastline of Tasmania and experiences distinctive seasonal and inter-annual variability in temperature, salinity and nutrients (Harris *et al.*, 1987) and is also periodically influenced during the Austral summer/autumn by a residual EAC extension from the northeast (Ridgway and Godfrey, 1997)

Proteorhodopsin community structure was characterised using an Illumina Miseq amplicon sequencing approach targeting microbial rhodopsin genes (see Figure 2 caption and supplementary material for nucleic acid collection and extraction, amplification, sequencing and bioinformatics analysis). To ensure even sequencing effort, sequence data were subsampled to 1078 sequences per sample, and 134 PRBA operational taxonomic units (OTUs, sequences binned at a 97% sequence similarity) representing 99.99 % of all subsampled sequences were used for analysis. Rarefaction analysis revealed the level of subsampling was sufficient to retrieve the majority of the PRBA community diversity (Fig. S2), although additional PRBA taxa are likely to appear with deeper sequencing efforts for some samples. The obtained nucleotide sequences were translated into partial protein sequences and aligned against a custom alignment, which included several cultured representatives and environmental sequences extracted from NCBI, in addition to sequences obtained from other studies

conducted elsewhere in the Australian marine environment (Bibiloni-Isaksson, unpublished). All sequences were placed into a phylogenetic tree to discern different taxonomic groups (Fig. S3).

PRBA richness (observed OTUs) and Shannon's diversity were higher at NSI and PHA than the southernmost station at MAI (Fig. S4). Across the entire data-set, both richness and diversity were correlated (Pearson's correlation coefficient) with temperature ($R=0.759$, $p<0.0001$ and $R=0.723$, $p<0.0001$ respectively), and *Prochlorococcus* cell counts ($R=0.550$, $p=0.002$ and $R=0.485$, $p=0.009$), while richness was also positively correlated with Secchi depth ($R=0.379$, $p=0.047$) and negatively correlated with phosphate ($R=-0.385$, $p=0.043$) (Table S2). Variability in PRBA diversity was lower when considering each station separately, although there was a trend for both richness and diversity to be lower during the austral winter/spring months than during the summer/autumn at NSI and MAI ($P<0.05$, Student's t-test), but not at PHA ($P>0.05$, Student's t-test) (Fig. S5). PRBA diversity at MAI was positively correlated with temperature ($R=0.705$, $p=0.023$), but no significant correlations with local environmental conditions were identified at NSI or PHA (Table S2). Notably, this pattern is consistent with recent observations for aerobic anoxygenic phototrophic bacteria at these stations, whereby temperature was found to be a structuring factor across all stations (i.e. at a regional scale), but not within stations (Bibiloni-Isaksson *et al.*, 2016).

We retrieved proteorhodopsin sequences from a wide range of marine clades, including the SAR11, SAR116, SAR92 and SAR86 groups, *Flavobacteria*, several unclassified α-δ, and γ-*Proteobacteria* groups and the marine group IIa and IIb Euryarchaeota (Fig. 2; Fig. S3). Interestingly, some OTUs, including both abundant and rare organisms, clustered distantly from currently known groups, including a potential SAR11-like OTU (OTU27983), which was in the top 5 most abundant OTUs at all 3 sites. OTU281 and a potential SAR11-like OTU60167 (both only observed at MAI) and a potential SAR11-like OTU8912 (only observed at NSI and PHA) also clustered distantly from known PRBA groups (Fig. S3)

There was significant overlap between OTUs occurring at the three sites, with only ~10% of OTUs restricted in their distribution to just one site. Notably, the majority of these "endemic" PRBA (i.e. organism restricted to only one site) OTUs occurred at the MAI site (Figure S6). Unsurprisingly, the temperate PHA station, which was characterised by mid-range environmental conditions in our data set, displayed the most overlap in PRBA community structure with both the sub-tropical NSI and the cold-temperate MAI. Indeed, the NSI OTU dataset and the PHA dataset showed considerable overlap in PRBA community structure. Of the OTUs comprising more than 2.5% of the total proteorhodopsin sequences, all were observed at all three stations, suggesting that these abundant organisms have a cosmopolitan distribution within the western Tasman Sea. However, despite these consistent features across the three stations, differences in the relative abundance of OTUs resulted in

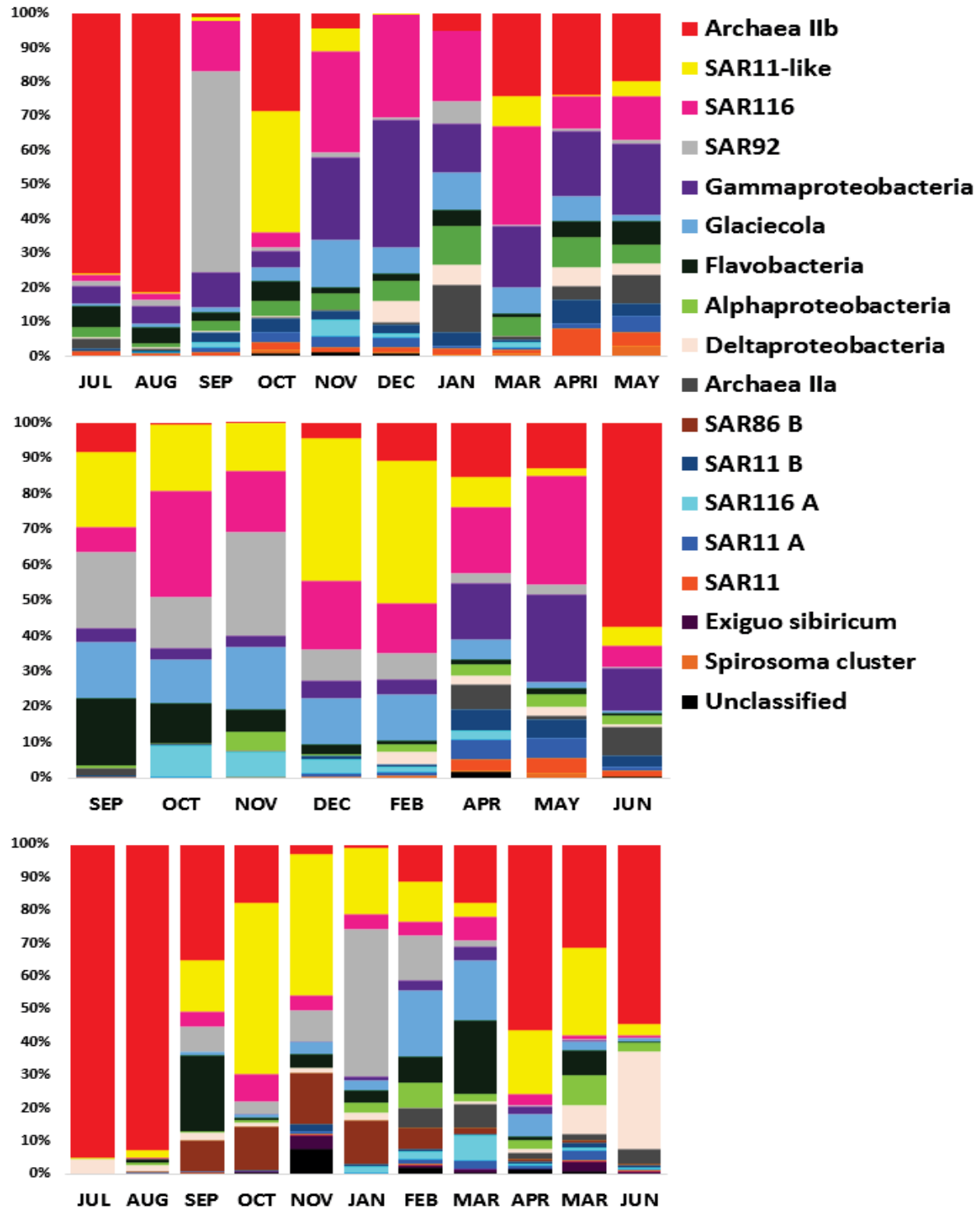

Figure 2: Comparison of the most abundant PRBA OTUs (> 1%) composition across all stations (OTUs=134). In order to detect coding genes for proteorhodopsin (PR), a set of degenerate multiplex PCR primers were used (PR1 MGN TAY ATH GAY TGG YT; PR2 WWN MGN TAY GTN GAY TGG; PR3 GGR TAD ATN GCC CAN CC, Sabehi *et al.*, 2005) to target a ~312 bp amplicon. Amplicon sequencing was performed using the Illumina MiSeq platform and sequence data were processed using the Quantitative Insights Into Microbial Ecology (QIIME) 1.8.0-dev pipeline (Caporaso *et al.*, 2010). Samples (n=30) were randomly resampled to 629 sequences. Sequences were binned into OTUs using de-novo uclust (Edgar, 2010) with a 97% identity threshold (Sabehi et al., 2003; Philosof and Béjà, 2013), and the most abundant sequence from each OTU was selected as a representative sequence for that OTU. Translated protein sequences were blasted to a curated database for the analysis of microbial rhodopsin diversity and evolution (MicRhoDE) (Boeuf et al. 2015). Representative sequences from each OTU were imported and aligned to a curated in-house database containing a custom reference collection of PR amino acids sequences compiled from cultured or otherwise well-characterized species in Genbank.

significantly different community compositions across the entire data with temperature and day length (P=0.001) identified as the environmental variables that explained the majority of this variability (Figure 3).

Within each station, a suite of variables linked to seasonal fluctuations in physical and biological factors statistically explained temporal shifts in PR community structure, including temperature (P=0.019) and solar radiation (P=0.043) at NSI; day length (P=0.05) at PHA and temperature and zooplankton (both P=0.001) at MAI (Fig. S7). Recently, Evans *et al.* (2015) showed evidence that photoheterotrophy is ubiquitous in ocean surface waters of the southern and consistent with other studies performed in the northern hemisphere (i.e. Michelou *et al.,* 2007; Gomez-Pereira *et al.,* 2013), demonstrated that light enhanced substrate uptake by PR. Our results also demonstrate the importance of light-associated environmental variables (solar irradiation, day length) and highlight the point that light should be considered as a key environmental factor involved not only in autotrophic metabolisms, but heterotrophy in the global ocean.

The seasonal and spatial shifts in phylogenetic structure of PRBA assemblages were mirrored by patterns in the biophysical properties of proteorhodopsin (Figure 4). Previous biophysical analysis of marine rhodopsin proteins has shown that the maximum absorbance of proteorhodopsin can be shifted from blue to green by substituting just one amino acid residue (owing to absorbance and the scattering of other wavelengths) (Man *et al.,* 2003). Therefore, spectral tuning by

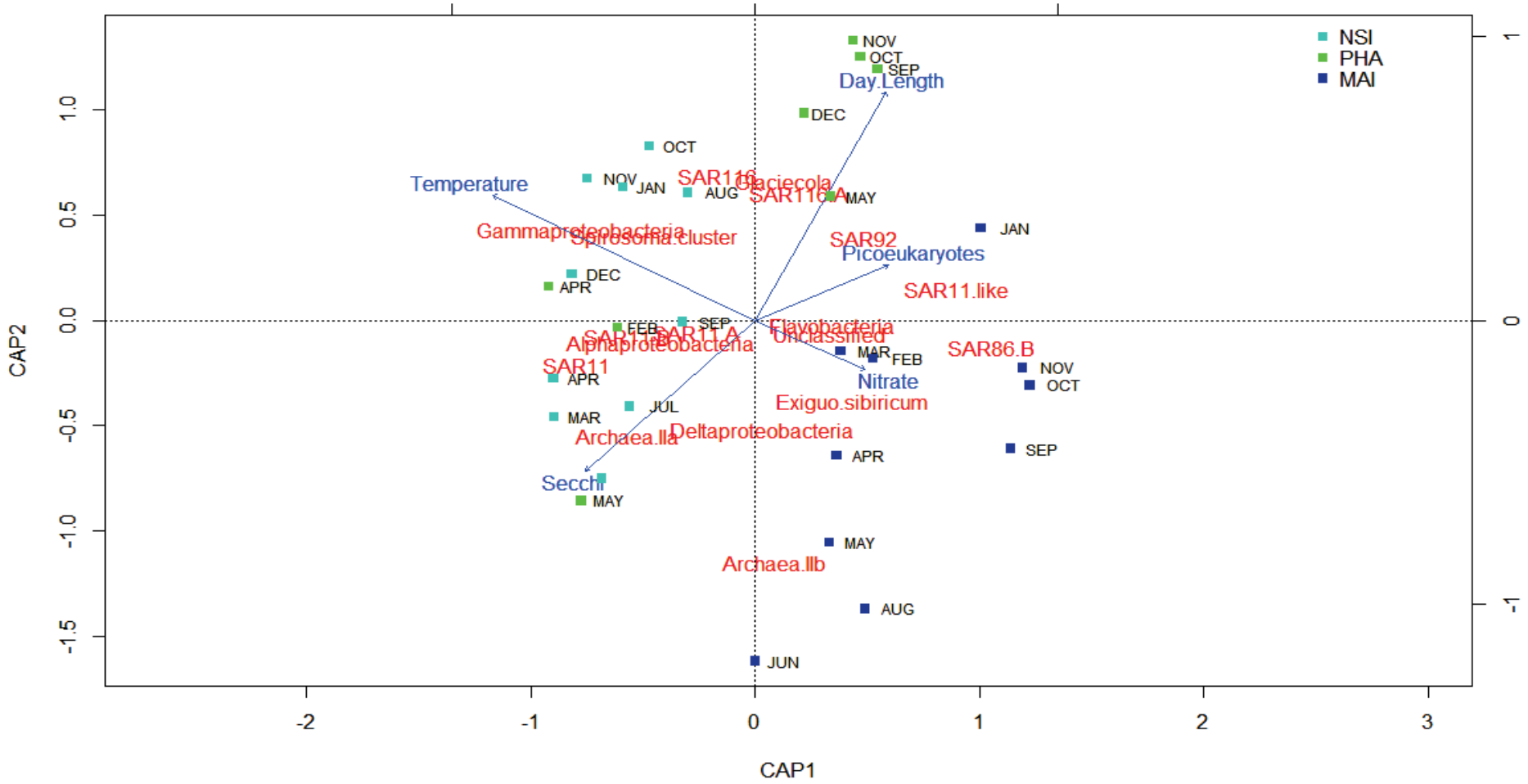

Figure 3: Distance based redundancy analysis of PRBA communities from the three time-series stations situated along Australia's east coast. Overlayed on the plot are the taxonomic affiliation of PRBA groups contributing to the positioning of samples, and vectors indicating significantly correlated environmental variables. The length and direction of each vector indicates the strength and sign of the relationship between the given variable and the dbRDA axes.

proteorhodopsins might maximize absorbance of the available light at different locations and depths (Man *et al.*, 2003; Sabehi *et al.*, 2007). Indeed a trend for a greater proportion of green- light absorbing proteorhodopsins (GPRs) has been detected in surface and coastal waters, whereas a trend for blue- light absorbing proteorhodopsins (BPRs) has been detected in the open ocean and deeper waters (Benjamini and Hochberg, 1995; Man *et al.*, 2003; Sabehi *et al.*, 2005; Rusch *et al.*, 2007; Sabehi *et al.*, 2007; Stingl *et al.*, 2007). Here we observed evidence for marked seasonality in the ratios of BPR to GPR (Figure 4), and, perhaps predictably, shifts in this spectral tuning were linked to light-associated environmental factors and included strong positive correlations to day length ($R= 0.660$, $p < 0.0001$) and solar radiation exposure ($R= 0.674$, $p = 0.033$), along with negative correlations to Secchi depth ($R= -0.774$, $p = 0.009$).

Overall, BPRs containing glutamine were mainly observed in OTUs affiliated with Marine group IIa and b Archaea, non-SAR86 *Gammaproteobacteria* including *Glaciecola* , Deltaproteobacteria and SAR11 clade B. GPRs containing leucine sequences were associated with SAR11 clade A (including a putative SAR11-like group of sequences), SAR86, SAR92 and SAR116. The proportion of GPRs containing methionine compared with leucine was low, but increased with latitude from NSI to MAI, with methionine peaking before and after summer (~22 %) at MAI. This pattern was related to an increased presence of *Flavobacteria* at MAI.

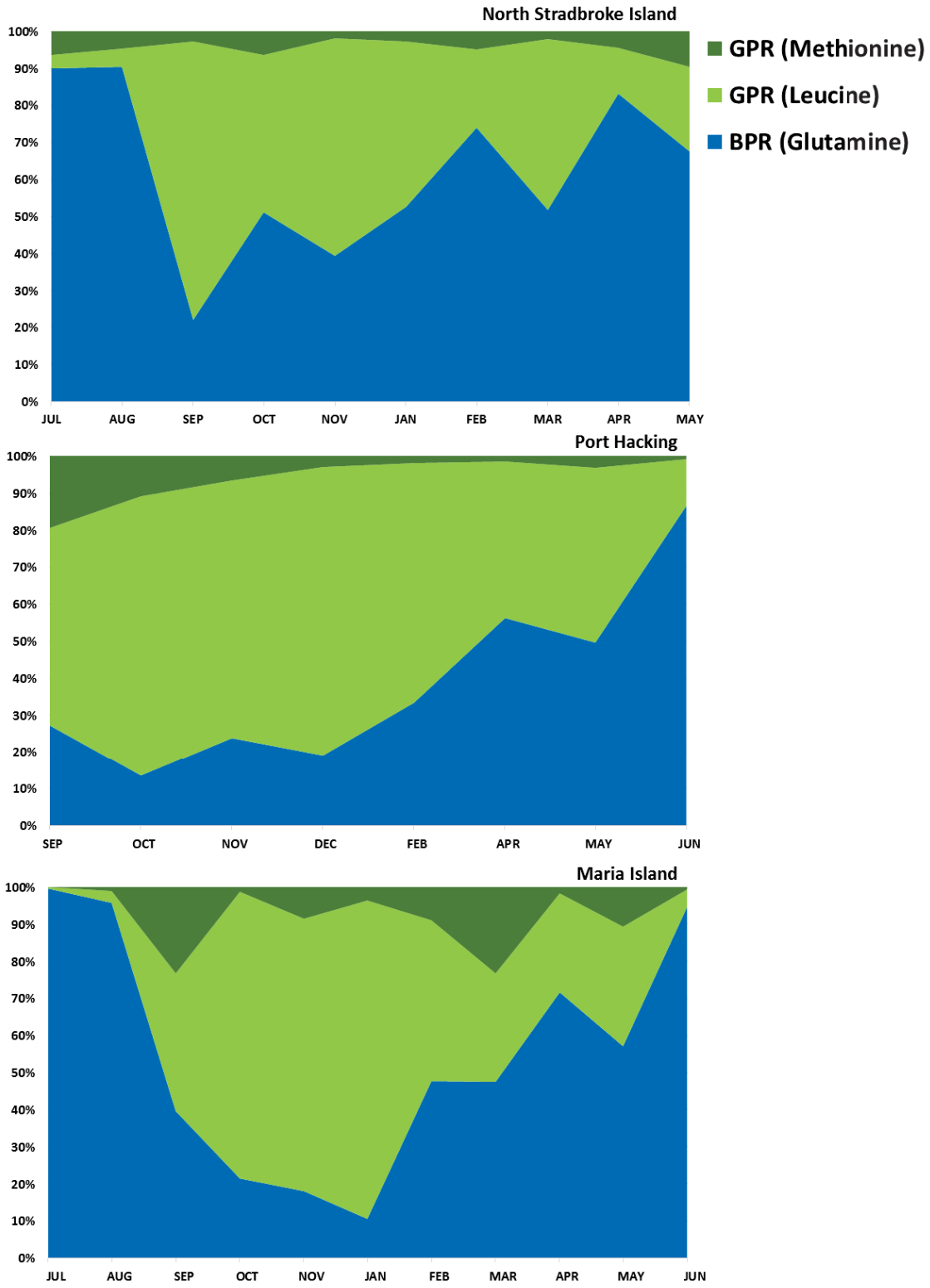

Figure 4: Green light absorbing proteorhodopsin (GPR) and blue light absorbing proteorhodopsin (BPR) distributions at the NSI, PHA and MAI time-series sites. All protein sequences were classified corresponding to their predicted spectral tuning switch, mainly a single amino-acid change at position 105, methionine (Consarnau *et al.*, 2007) and leucine (Man *et al.*, 2003) for green, and glutamine for blue (Man *et al.*, 2003). Shaded areas represent percentages of GPRs containing leucine (marked in green), BPRs containing glutamine (marked in blue) and GPRs containing methionine (marked in dark green) at the NSI, PHA and MAI sites during the sampling period.

The marine group IIb Archaea were the dominant taxonomic group during the austral winter months (June, July and August) at all three stations, where they at times comprised > 90% of all sequences (Figure 3). This resulted in the predominance of BPR during these times. We observed just one OTU related to marine group IIa Archaea, which occurred during the summer/ autumn at all three stations. These temporal dynamics among the Archaeal community are directly compatible with seasonal variability reported in the Mediterranean Sea, where MG IIb are more abundant during periods of winter mixing when nutrients concentrations increase, and MG IIa predominant in summer when nutrients become depleted (Galand *et al.*, 2010), and summer peaks in the abundance and activity of MG IIa in surface water of the Mediterranean Sea linked to the enhanced phototrophy in response to greater irradiance (Hugoni *et al*., 2013).

At all stations there was a transition away from a characteristic winter proteorhodopsin assemblage, dominated by *Archaea*, during September, when the BPR containing taxa *Glaciecola* and SAR11 B became more abundant along with a number of GBR containing taxa including SAR11 A (including SAR11-like sequences), SAR86, SAR116, SAR92 and *Flavobacteria*. By November at NSI, a relatively stable PRBA assemblage had formed, primarily consisting of *Gammaproteobacteria* (including *Glaciecola*), SAR11 and SAR116, which was maintained throughout the summer, with increases in archaeal abundance occurring again in late summer and autumn. At PHA, the spring assemblage was dominated by GPR taxa and this situation was maintained

throughout the summer, before an increase in BPR groups in autumn. The spring /summer assemblage consisted primarily of SAR92, SAR116, SAR11-like OTUs and *Glaciecola* , with *Flavobacteria* peaking at 20% of sequences in September and decreasing steadily thereafter. Both dbRDA (Fig.4) and nMDS (Fig. S8) analysis clustered assemblages retrieved from PHA during the austral autumn (April, May, June) with those from NSI. During these months there was an increase in the relative abundance of Archaea IIa and b, *Gammaproteobacteria*, SAR11b and a decrease in *Flavobacteria*, *Glaciecola* related sequences and SAR92 at PHA. (Fig. S3). Notably, this timing coincides with the penetration of warm EAC waters into the near-coastal region of PHA observed by SST (Fig. S1) and is in line with known seasonal dynamics of the EAC in this region (Ridgway and Godfrey, 1997). The MAI site was characterised by the strongest seasonality in both taxonomic transitions and spectral tuning. GPR were dominant during the start of spring (September) through to summer, with increases in SAR11, SAR92, and *Flavobacteria*. Late summer and autumn saw an increase in BPR containing *Archaea* and *Glaciecola* . Overall, GPRs particularly those containing leucine, were strongly positively correlated to day length and solar radiation (Table S2), along with indicators of water body productivity including picoeukaryotes and zooplankton abundances. Conversely, Secchi depth, was positively correlated to BPRs which is consistent with the previously demonstrated preferences of this group for clear water, low productivity, and oligotrophic conditions (Sabehi *et al.,* 2007). These patterns suggest that differential exploitation of the light spectrum via the use of variants of proteorhodopsin underpin a separation

of the proteorhodopsin community across different seasons, positions in the water column or different regions of the ocean. Thus the ecological significance of spectral tuning may be considered within the context of classical niche theory, whereby utilisation of different features of the light spectrum provide opportunities for niche differentiation and allows coexistence of PRBA species absorbing different colours of light (Stomp *et al.,* 2007).

Concluding remarks

By applying a high-throughput sequencing approach to assess the diversity of proteorhodopsin containing microbes at multiple time-series sites we have observed significant seasonal and spatial variability in the composition of PRBA along the eastern coast of Australia. Across the data-set, PRBA diversity, taxonomic composition and spectral tuning were governed by common environmental factors, in particular temperature and day length. At each site, winter-time communities were generally dominated by Marine Group IIb Archaea, while springtime saw the development of a new PRBA assemblage characterised by SAR92, Flavobacteria and SAR116. The subsequent stability of the springtime assemblage differed across sites, with evidence that summer stratification and the lack of nutrients in the upper water column provided a niche for more oligotrophic proteorhodopsin containing groups including SAR11 and SAR116. Generally, PRBA community diversity in the Tasman Sea appears to be greatest within warm oligotrophic conditions, which are more prevalent at the northern-most stations studied here. Within this context, it is notable

that diversity at our mid-latitude site at PHA was highest during the period when the influence of the southward flowing East Australian Current was strongest, leading to the southerly transport of warm oligotrophic waters (Feb and April). While the bulk of PRBA taxa identified in this study were observed at all 3 sites, indicative of a cosmopolitan distribution throughout the Tasman Sea, a few taxa were only detectable at only one station, particularly in the cold temperate waters of MAI, suggesting that regional endemism may sometimes be an additional factor in driving the diversity of PRBA communities. In addition to the phylogenetic shifts among the PRBA community, we also observed seasonal and spatial shifts in the biophysical properties of the dominant form of proteorhodopsin in these communities, manifested by shifts from blue light absorbing proteorhodopsins to green light absorbing proteorhodopsins that could also statistically be explained specific environmental factors. Divergent patterns in the occurrence of PRBA containing blue light absorbing proteorhodopsins and green light absorbing proteorhodopsins indicate that differential spectral tuning characteristics may underpin niche separation among microbes that use proteorhodopsin. Taken together, our observations suggest that both seasonal fluctuations in physical conditions and regional oceanographic processes govern the diversity, structure and biophysical properties of PRBA communities, and provide new insights into the seasonal and biogeographical dynamics of this important group of marine prokaryotes.

ACKNOWLEDGEMENTS

We gratefully thank Frank Coman, Claire Davies, Dion Frampton and Tim Moltmann at IMOS for assistance with sampling and biogeochemical sample analyses. Data were sourced as part of the Integrated Marine Observing System (IMOS) - IMOS is supported by the Australian Government through the National Collaborative Research Infrastructure Strategy and the Super Science Initiative. This research was supported by the Australian Research Council Discovery Grant DP120102764 to JRS and MVB. JRS was supported by ARC Future Fellowship FT130100218. MVB was supported by ARC QEII Fellowship DP0988002.

Supplementary material

Experimental procedures

Sampling, DNA extraction and chemical characterization

Sampling was conducted as part of the Australian Marine Microbial Biodiversity Initiative (AMMBI), which conducts standardised sampling for microbial community analysis, in conjunction with the Australian Commonwealth Government's Integrated Marine Observing System (IMOS), at multiple National Reference Stations (NRS) within the Australian marine environment. For this study we sampled at three NRS that span 15° latitude along Australia's eastern coastline, including the stations at North Stradbroke Island (27.345° S, 153.562° E), Port Hacking (34.1192° S, 151.2267° E) and Maria Island (42.5967° S, 148.2333° E). Samples were collected at 10m on a monthly basis during the period of July 2012 to June 2013. Water samples (2 L) were collected using niskin bottles, filtered through 0.2 μm Sterivex filters (Millipore, USA) and stored at -80° C until analysis. DNA was extracted and purified using the PowerWater® Sterivex™ DNA Isolation Kit (MOBIO laboratories, Carlsbad, CA), following a slightly modified version of the manufacturer's instructions. The quality and quantity of DNA was checked using a NanoDrop™ 8000 Spectrophotometer (Thermo Scientific™) and DNA archived at -80 °C.

Amplification, Sequencing and analysis

In order to detect coding genes for proteorhodopsin (PR), a set of degenerate multiplex PCR primers were used (PR1 MGN TAY ATH GAY TGG YT; PR2 WWN MGN TAY

GTN GAY TGG; PR3 GGR TAD ATN GCC CAN CC, Sabehi *et al.*, 2005) to target a ~312 bp amplicon. PCR reactions were performed in a 25 µl reaction mixture consisting of 12.5 µl ImmoMix (Bioline, NSW, Australia), 1 µl of each Primer (10 pmol/µl), and 9.5 µl of dH2O. Twenty-four µl of the "master mix" and 1µl of template DNA (10 ng final concentration) of each replicate were used. Amplification proceeded under the following thermo cycling conditions: an initial denaturation of 95°C for 10 minutes, followed by 34 cycles of denaturation at 95°C for 10 seconds, annealing at 47°C for 30 seconds, extension at 72°C for 1 minute, and a final extension at 72°C for 2 minutes. Each sample was purified using ISOLATE II PCR and Gel Kit (Bioline, Australia), and quantified using a Qubit fluorometer (Invitrogen). PCR products from all samples were normalized in equimolar amounts before sequencing.

Amplicon sequencing was performed using an Illumina MiSeq platform (Molecular Research LP, Shallowater, TX, www.mrdnalab.com) according to the manufacturer's directions. Resultant sequence data were processed using the Quantitative Insights Into Microbial Ecology (QIIME) 1.8.0-dev pipeline (Caporaso *et al.*, 2010; http://www.qiime.org/) using default parameters unless otherwise noted. For all 30 samples, the numbers of reads were 1,091,909. Sequences were quality trimmed, and assigned to samples based on unique 8-bp barcodes. Low quality fragments were removed before Chimera detection and removal using U-Chime (Edgar *et al.*, 2011). The number of reads ranged from 20 to 294933. Samples was randomly resampled to 629 sequences, resulting in 1 samples being removed due to low number of reads.

Sequences were binned into OTUs using de-novo uclust (Edgar, 2010) with a 97% identity threshold (Philosof and Béjà, 2013; Sabehi *et al*., 2003), and the most abundant sequence from each OTU was selected as a representative sequence for that OTU.

Phylogenetic analysis of PR genes

Translated protein sequences were blasted to a curated database for the analysis of microbial rhodopsin diversity and evolution (MicRhoDE) (Boeuf *et al.* 2015). The database currently covers 7857 aligned sequences. Representative sequences from each OTU were imported and aligned to a curated in-house database containing a custom reference collection of PR amino acids sequences compiled from cultured or otherwise well-characterized species in Genbank, supplemented with sequences reported from two environmental surveys, a study done in 2012 at coastal waters of Tasmania (Bibiloni-Isaksson *et al.,* unpublished) and a research voyage in August 2013 north tropical coast (Bibiloni-Isaksson *et al.,* unpublished), were aligned with ClustalW (Bioedit) and manually revised. Phylogenetic trees were plotted using FigTree software.

Statistical analysis

Pearson's correlation coefficient was used to determine co-linearity among the concentrations of pufM genes and environmental parameters using SPSS 13.0 software. Multivariate statistical analyses were performed using the Vegan package (v.1.15–1) in R (Oksanen, 2013). For community composition analysis, a dissimilarity

matrix (Bray–Curtis) was constructed based on the relative abundance (square root transformed) of each OTU and visualized using nMDS (Clarke 1993). Mantel tests were conducted to find correlations between this matrix and a matrix of environmental variables. The environmental parameters included in the analysis were fluorescence, salinity, temperature, Secchi depth, day length, light at the surface measured as solar radiation exposure, Chl*a* concentration and the concentration of phosphate, ammonium, nitrate and silicate. Chl*a* was not included in PHA statistical analyses due to missing values, and turbidity was not included in NSI and PHA analyses for the same reasons. To investigate which combination of environmental variables were best related to AAnPB community assemblages, we used the bioenv() procedure (Clarke and Ainsworth 1993), which finds the best subset of explanatory environmental variables. For visual interpretation of the resulting model in multi-dimensional space, we used distance based redundancy analysis (dbRDA) (Legendre and Andersson 1999), performed with the capscale function in Vegan, to investigate the relationship between station, depth and environmental variables. To test the significance of individual variables to the total AAnPB community we performed permutational multivariate ANOVA (perMANOVA). We tested for significant variation in OTU composition among microhabitats using the adonis() function in vegan (Oksanen *et al.*, 2013), which performs an analysis of variance with distance matrices using permutations. In an adonis, distance matrices are partitioned among sources of variation; in this case stations. In each adonis() analysis, the Bray-Curtis distance matrix of OTU composition was the response variable and station the

independent variable. The number of permutations was set at 999; all other arguments used the default values set in the function. The community matrices were transformed with the fourth-root transformation and then with the Hellinger transformation (Legendre and Gallagher, 2001).

Supplementary figures

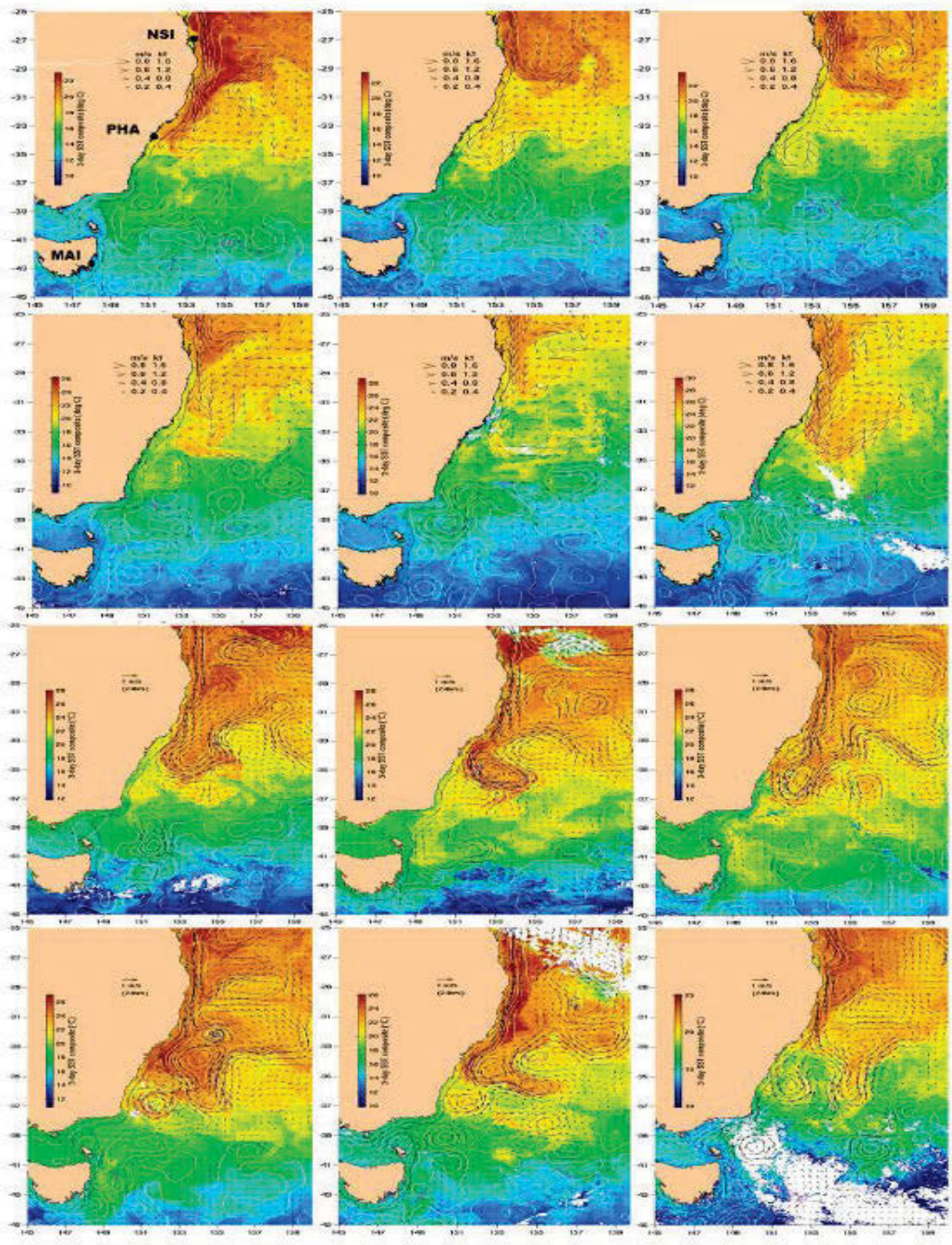

Figure S1: Sea Surface Temperature maps highlight the complex oceanography of the eastern Australian coastline where our samples were collected. Each image was taken the 15th day of the month, beginning with 15-Jul-2012 in the upper left-hand corner and continuing to the right with 15-Jun-2013 in the bottom right-hand corner. The East Australian Current (EAC) can be seen travelling south, indicated by the warm sea surface temperature, and separating into eddies near the Port Hacking region. Images source: IMOS (http://oceancurrent.imos.org.au/). North Stradbroke Island station (NSI), Port Hacking station (PHA) and Maria Island station (MAI).

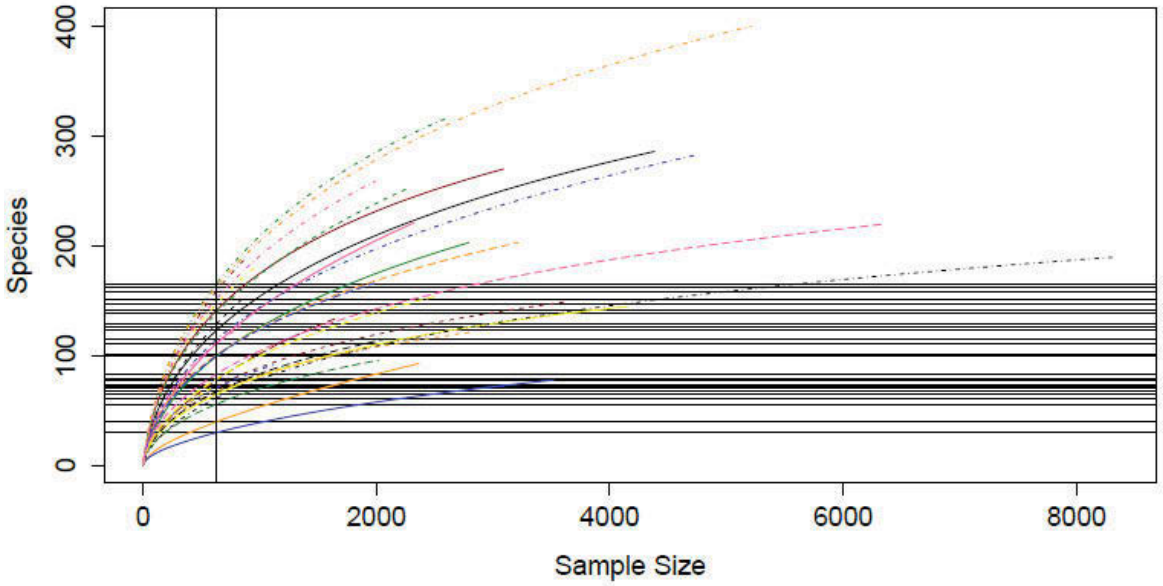

Figure S2: Rarefaction curve for all samples at all stations. The number of sequences per sample was homogenized via resampling to 629 with the statistical program R (http://www. Rproject.org/, v. 3.0.1) with the library vegan: Community Ecology Package (v. 2.0–8).

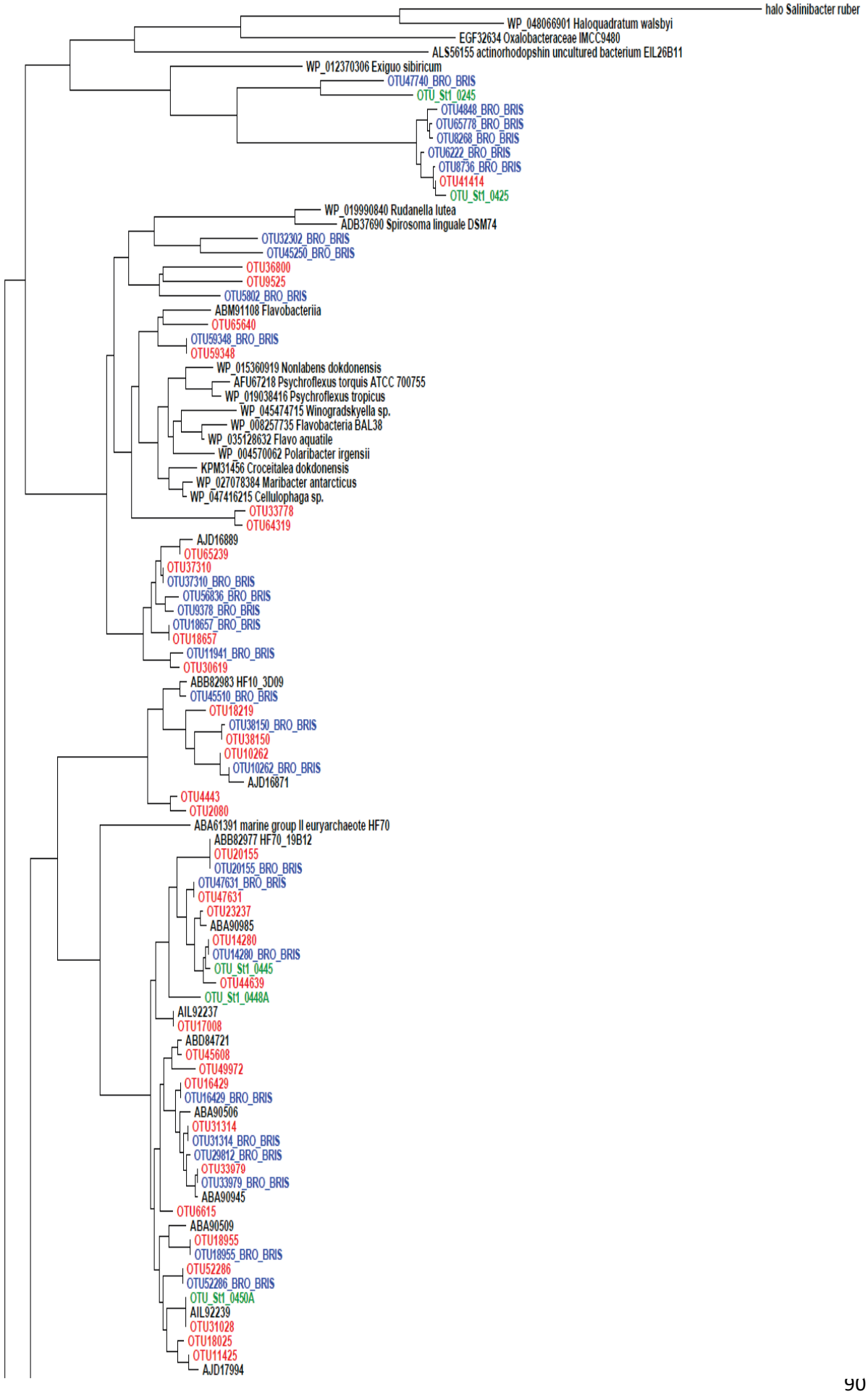
halo Salinibacter ruber
WP_048066901 Haloquadratum walsbyi
EGF32634 Oxalobacteraceae IMCC9480
ALS56155 actinorhodopshin uncultured bacterium EIL26B11
WP_012370306 Exiguo sibiricum
OTU47740_BRO_BRIS
OTU_St1_0245
OTU4848_BRO_BRIS
OTU65778_BRO_BRIS
OTU8268_BRO_BRIS
OTU6222_BRO_BRIS
OTU8736_BRO_BRIS
OTU41414
OTU_St1_0425
WP_019990840 Rudanella lutea
ADB37690 Spirosoma linguale DSM74
OTU32302_BRO_BRIS
OTU45250_BRO_BRIS
OTU36800
OTU9525
OTU5802_BRO_BRIS
ABM91108 Flavobacteriia
OTU65640
OTU59348_BRO_BRIS
OTU59348
WP_015360919 Nonlabens dokdonensis
AFU67218 Psychroflexus torquis ATCC 700755
WP_019038416 Psychroflexus tropicus
WP_045474715 Winogradskyella sp.
WP_008257735 Flavobacteria BAL38
WP_035128632 Flavo aquatile
WP_004570062 Polaribacter irgensii
KPM31456 Croceitalea dokdonensis
WP_027078384 Maribacter antarcticus
WP_047416215 Cellulophaga sp.
OTU33778
OTU64319
AJD16889
OTU65239
OTU37310
OTU37310_BRO_BRIS
OTU56836_BRO_BRIS
OTU9378_BRO_BRIS
OTU18657_BRO_BRIS
OTU18657
OTU11941_BRO_BRIS
OTU30619
ABB82983 HF10_3D09
OTU45510_BRO_BRIS
OTU18219
OTU38150_BRO_BRIS
OTU38150
OTU10262
OTU10262_BRO_BRIS
AJD16871
OTU4443
OTU2080
ABA61391 marine group II euryarchaeote HF70
ABB82977 HF70_19B12
OTU20155
OTU20155_BRO_BRIS
OTU47631_BRO_BRIS
OTU47631
OTU23237
ABA90985
OTU14280
OTU14280_BRO_BRIS
OTU_St1_0445
OTU44639
OTU_St1_0448A
AIL92237
OTU17008
ABD84721
OTU45608
OTU49972
OTU16429
OTU16429_BRO_BRIS
ABA90506
OTU31314
OTU31314_BRO_BRIS
OTU29812_BRO_BRIS
OTU33979
OTU33979_BRO_BRIS
ABA90945
OTU6615
ABA90509
OTU18955
OTU18955_BRO_BRIS
OTU52286
OTU52286_BRO_BRIS
OTU_St1_0450A
AIL92239
OTU31028
OTU18025
OTU11425
AJD17994

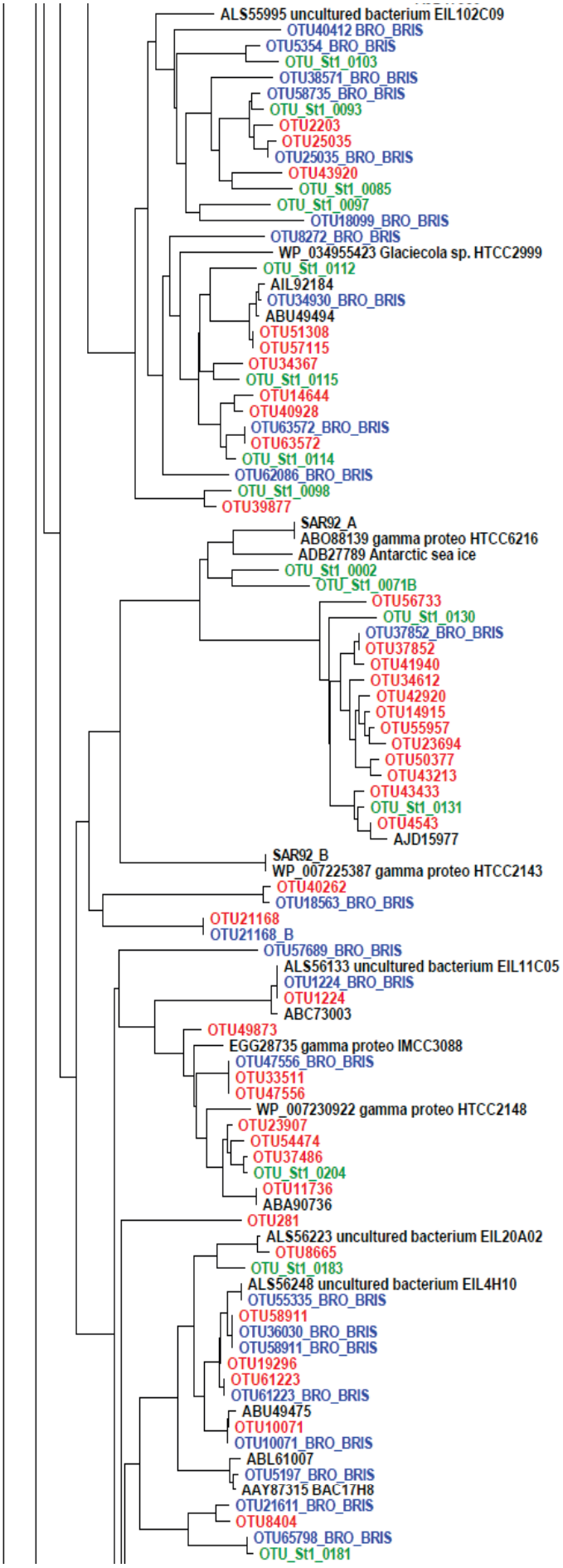
ALS55995 uncultured bacterium EIL102C09
OTU40412 BRO_BRIS
OTU5354_BRO_BRIS
OTU_St1_0103
OTU38571_BRO_BRIS
OTU58735_BRO_BRIS
OTU_St1_0093
OTU2203
OTU25035
OTU25035_BRO_BRIS
OTU43920
OTU_St1_0085
OTU_St1_0097
OTU18099_BRO_BRIS
OTU8272_BRO_BRIS
WP_034955423 Glaciecola sp. HTCC2999
OTU_St1_0112
AIL92184
OTU34930_BRO_BRIS
ABU49494
OTU51308
OTU57115
OTU34367
OTU_St1_0115
OTU14644
OTU40928
OTU63572_BRO_BRIS
OTU63572
OTU_St1_0114
OTU62086_BRO_BRIS
OTU_St1_0098
OTU39877
SAR92_A
ABO88139 gamma proteo HTCC6216
ADB27789 Antarctic sea ice
OTU_St1_0002
OTU_St1_0071B
OTU56733
OTU_St1_0130
OTU37852_BRO_BRIS
OTU37852
OTU41940
OTU34612
OTU42920
OTU14915
OTU55957
OTU23694
OTU50377
OTU43213
OTU43433
OTU_St1_0131
OTU4543
AJD15977
SAR92_B
WP_007225387 gamma proteo HTCC2143
OTU40262
OTU18563_BRO_BRIS
OTU21168
OTU21168_B
OTU57689_BRO_BRIS
ALS56133 uncultured bacterium EIL11C05
OTU1224_BRO_BRIS
OTU1224
ABC73003
OTU49873
EGG28735 gamma proteo IMCC3088
OTU47556_BRO_BRIS
OTU33511
OTU47556
WP_007230922 gamma proteo HTCC2148
OTU23907
OTU54474
OTU37486
OTU_St1_0204
OTU11736
ABA90736
OTU281
ALS56223 uncultured bacterium EIL20A02
OTU8665
OTU_St1_0183
ALS56248 uncultured bacterium EIL4H10
OTU55335_BRO_BRIS
OTU58911
OTU36030_BRO_BRIS
OTU58911_BRO_BRIS
OTU19296
OTU61223
OTU61223_BRO_BRIS
ABU49475
OTU10071
OTU10071_BRO_BRIS
ABL61007
OTU5197_BRO_BRIS
AAY87315 BAC17H8
OTU21611_BRO_BRIS
OTU8404
OTU65798_BRO_BRIS
OTU_St1_0181

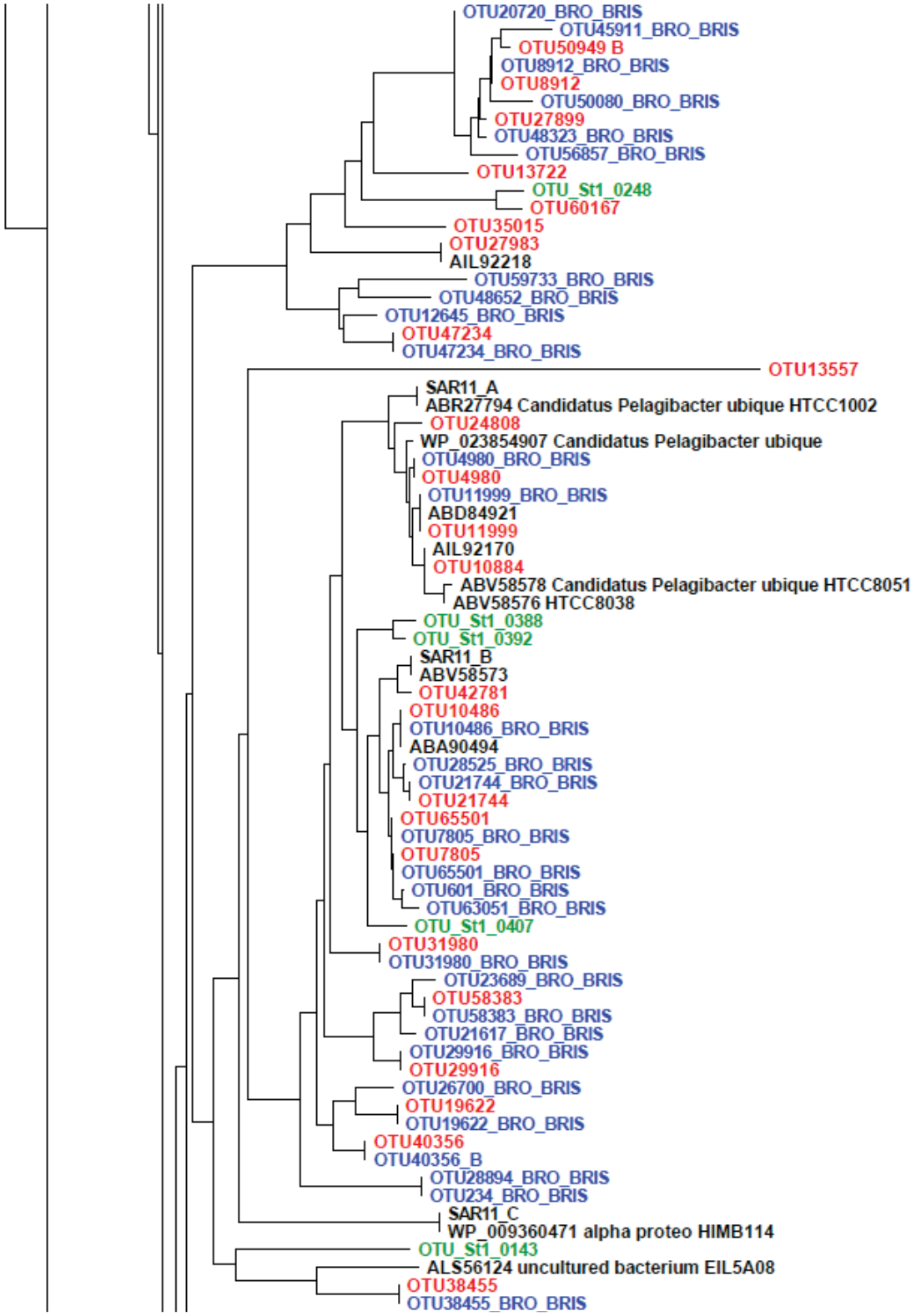
OTU20720_BRO_BRIS
OTU45911_BRO_BRIS
OTU50949 B
OTU8912_BRO_BRIS
OTU8912
OTU50080_BRO_BRIS
OTU27899
OTU48323_BRO_BRIS
OTU56857_BRO_BRIS
OTU13722
OTU_St1_0248
OTU60167
OTU35015
OTU27983
AIL92218
OTU59733_BRO_BRIS
OTU48652_BRO_BRIS
OTU12645_BRO_BRIS
OTU47234
OTU47234_BRO_BRIS
OTU13557
SAR11_A
ABR27794 Candidatus Pelagibacter ubique HTCC1002
OTU24808
WP_023854907 Candidatus Pelagibacter ubique
OTU4980_BRO_BRIS
OTU4980
OTU11999_BRO_BRIS
ABD84921
OTU11999
AIL92170
OTU10884
ABV58578 Candidatus Pelagibacter ubique HTCC8051
ABV58576 HTCC8038
OTU_St1_0388
OTU_St1_0392
SAR11_B
ABV58573
OTU42781
OTU10486
OTU10486_BRO_BRIS
ABA90494
OTU28525_BRO_BRIS
OTU21744_BRO_BRIS
OTU21744
OTU65501
OTU7805_BRO_BRIS
OTU7805
OTU65501_BRO_BRIS
OTU601_BRO_BRIS
OTU63051_BRO_BRIS
OTU_St1_0407
OTU31980
OTU31980_BRO_BRIS
OTU23689_BRO_BRIS
OTU58383
OTU58383_BRO_BRIS
OTU21617_BRO_BRIS
OTU29916_BRO_BRIS
OTU29916
OTU26700_BRO_BRIS
OTU19622
OTU19622_BRO_BRIS
OTU40356
OTU40356_B
OTU28894_BRO_BRIS
OTU234_BRO_BRIS
SAR11_C
WP_009360471 alpha proteo HIMB114
OTU_St1_0143
ALS56124 uncultured bacterium EIL5A08
OTU38455
OTU38455_BRO_BRIS

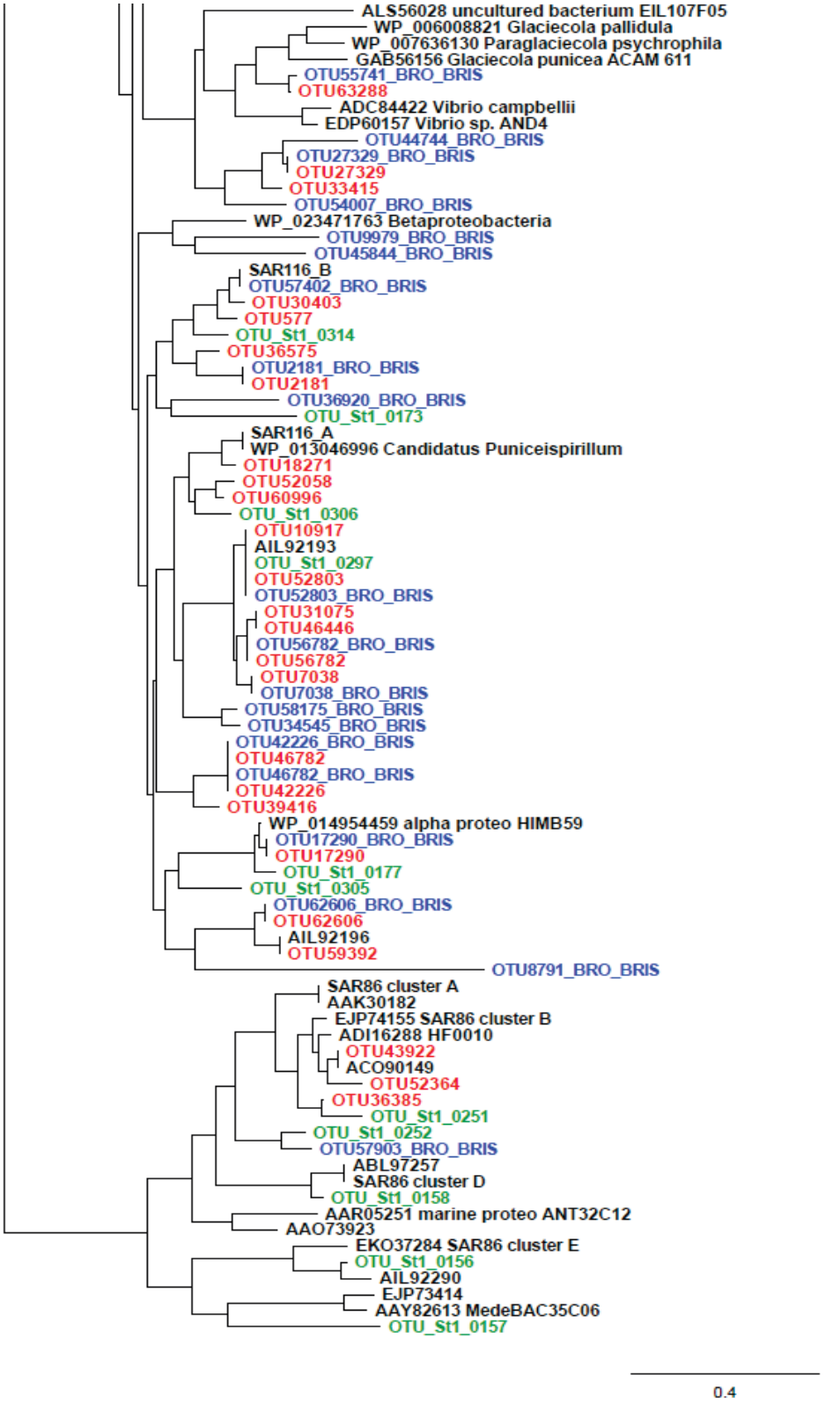

Figure S3: Phylogenetic tree showing the relationships between proteorhodopsin amino acid gene sequences from this study (red), clone sequences from previous study at Maria Island (2011-2012) (green), sequences from a recent research voyage in north coastal waters of Australia (blue) and nearest relatives from major taxonomic extracted from GenBank are including in the tree (Bold). Representative sequences of each OTU and short PR gene environmental sequences were aligned as above and added to the consensus Bayesian tree using the ADD_BY_PARSIMONY algorithm implemented in ARB. Phylogenetic trees were plotted using FigTree software (Rambaut, 2014).

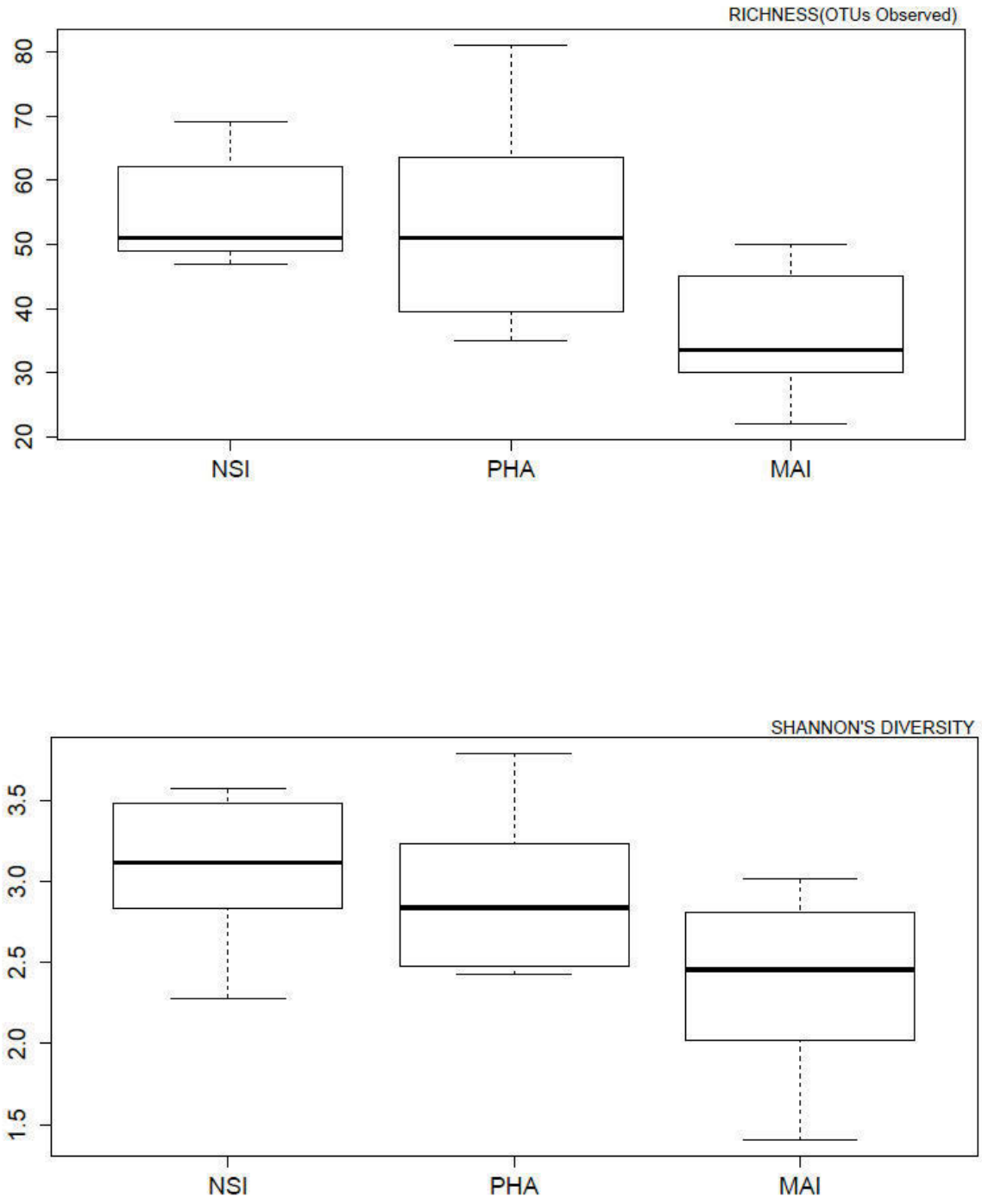

Figure S4: Box and whiskers representation of indices used to describe bacterial community richness (top) and Shannon's diversity index at three mooring stations. The box indicates median and quartile values, and the whiskers indicate the range (minima and maxima).

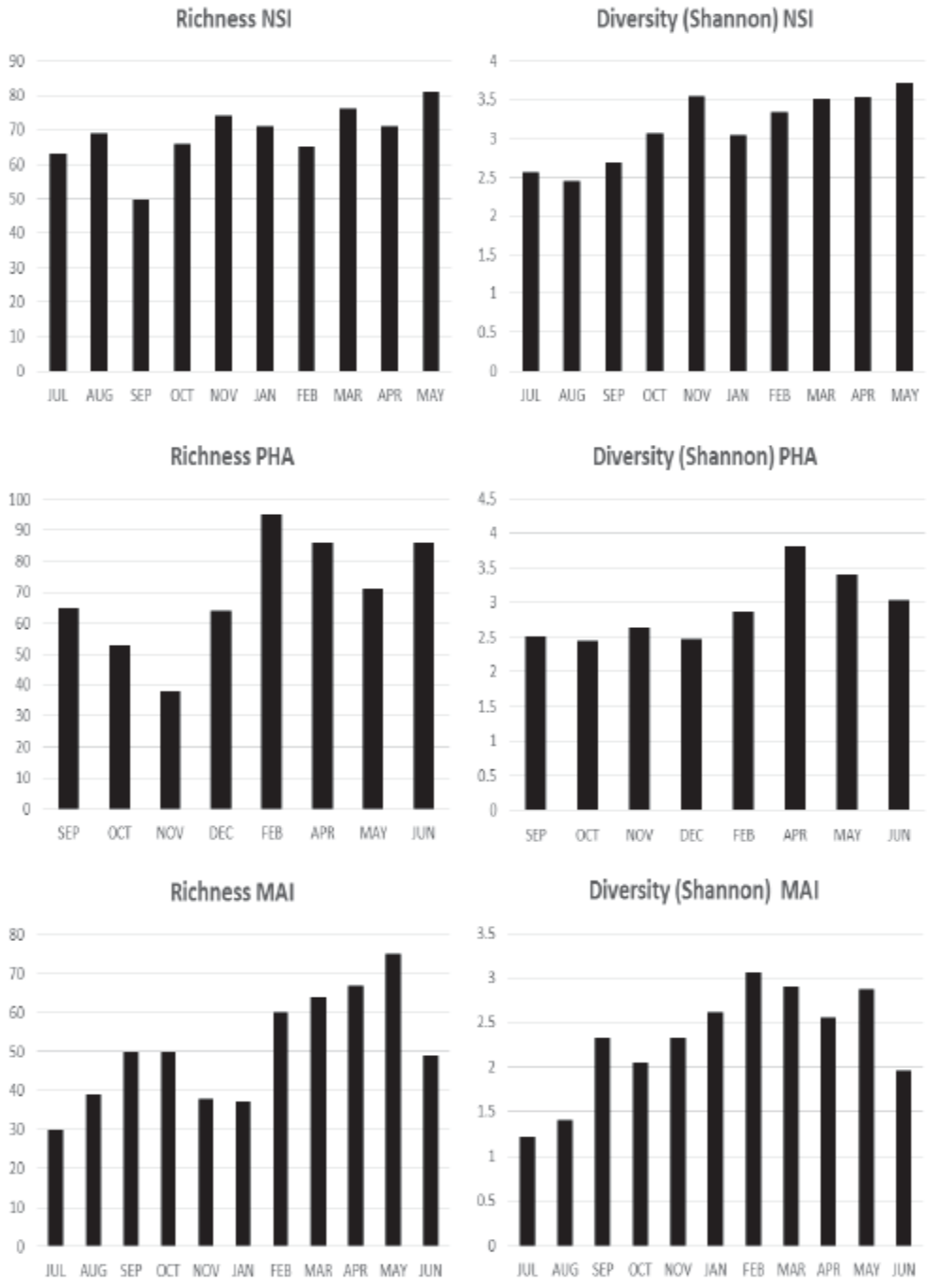

Figure S5: Bar graphs showing seasonal changes in richness (observed OTUs) and Shannon's diversity index at three mooring stations.

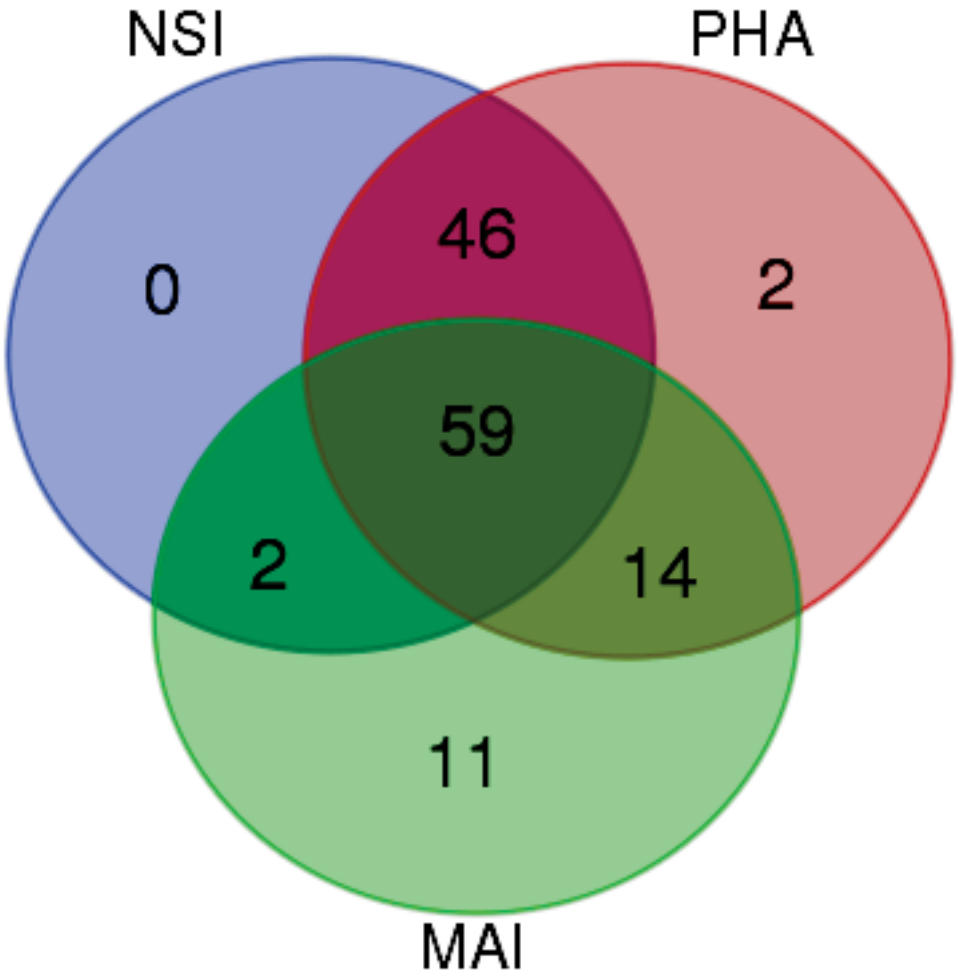

Figure S6: Shared and site-specific OTUs. Venn diagram representing the distribution of OTUs (and corresponding number of reads) in the three sampling sites, calculated both considering all the OTUs, and considering only the non-singletons.

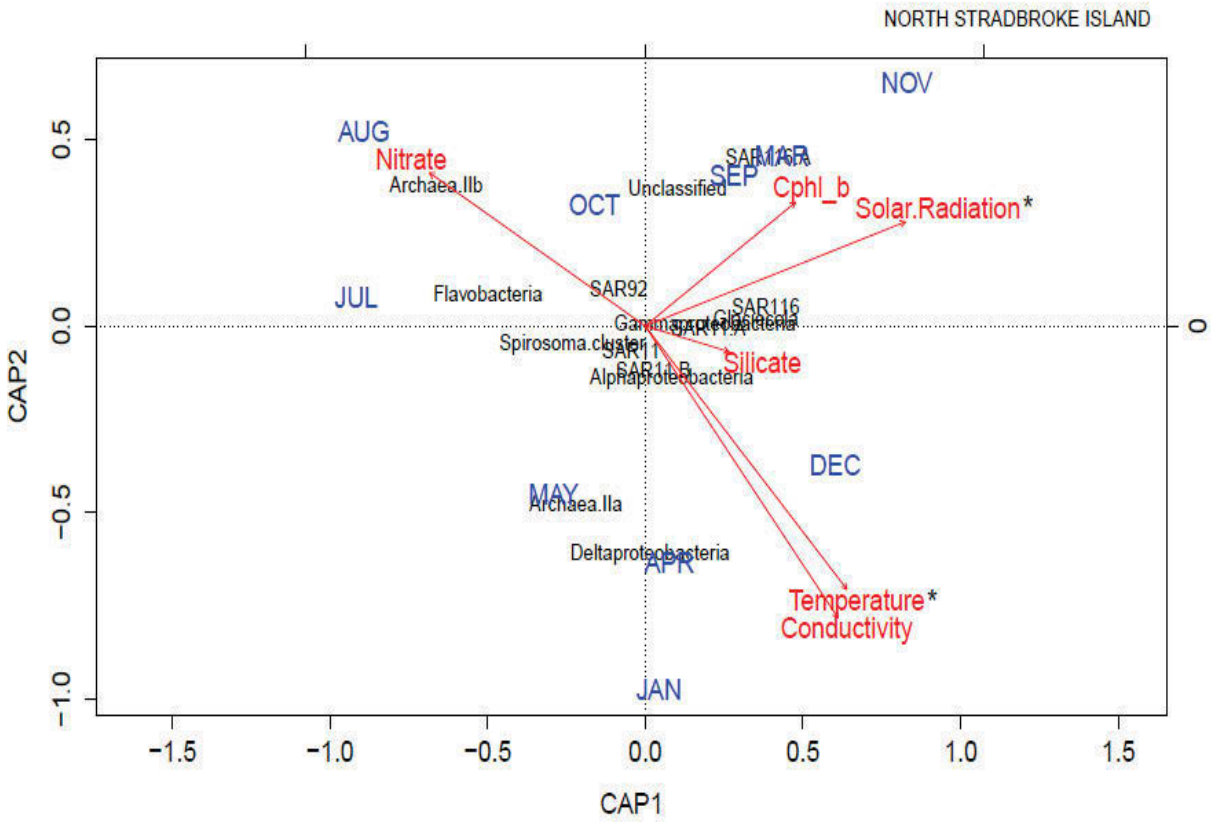
NORTH STRADBROKE ISLAND
NOV
AUG
Nitrate
Archaea.IIb
SEP
Cphl_b
Solar.Radiation*
OCT
Unclassified
JUL
Flavobacteria
SAR92
SAR116
Spirosoma.cluster
SAR11
Alphaproteobacteria
Silicate
DEC
MAY
Archaea.IIa
Deltaproteobacteria
APR
Temperature*
Conductivity
JAN
CAP2
CAP1
0.5
0.0
−0.5
−1.0
−1.5
−1.0
−0.5
0.0
0.5
1.0
1.5

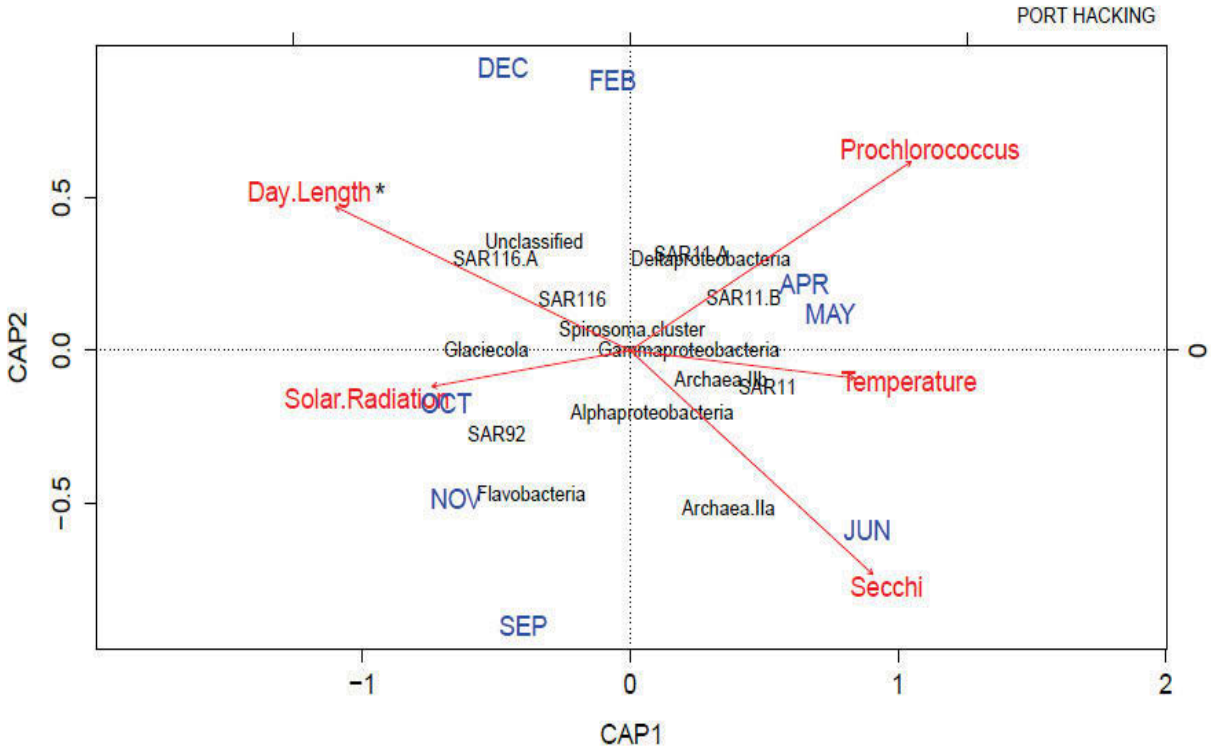
PORT HACKING
DEC
FEB
Prochlorococcus
Day.Length*
Unclassified
SAR116.A
Deltaproteobacteria
APR
SAR116
SAR11.B
MAY
Spirosoma.cluster
Glaciecola
Gammaproteobacteria
Archaea.IIb
SAR11
Temperature
Solar.Radiation
OCT
Alphaproteobacteria
SAR92
NOV
Flavobacteria
Archaea.IIa
JUN
Secchi
SEP
CAP2
CAP1
0.5
0.0
−0.5
−1
0
1
2

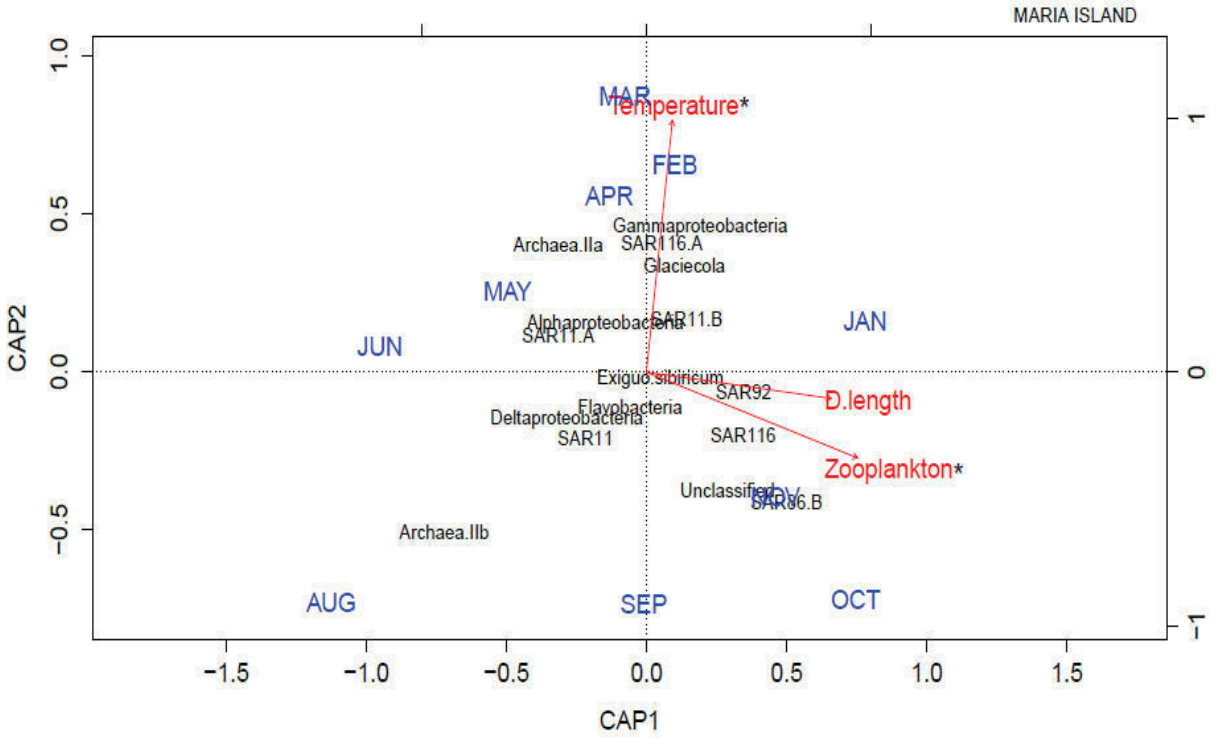

Figure S7: Relationship of PRBA community structure to environmental variables determined using a distance-based Redundancy Analysis at NSI (top), PHA (middle) and MAI (bottom). The length and direction of each vector indicates the strength and sign of the relationship between the given variable and the dbRDA axes. Only those significant ($P \leq 0.05$) are displayed with *.

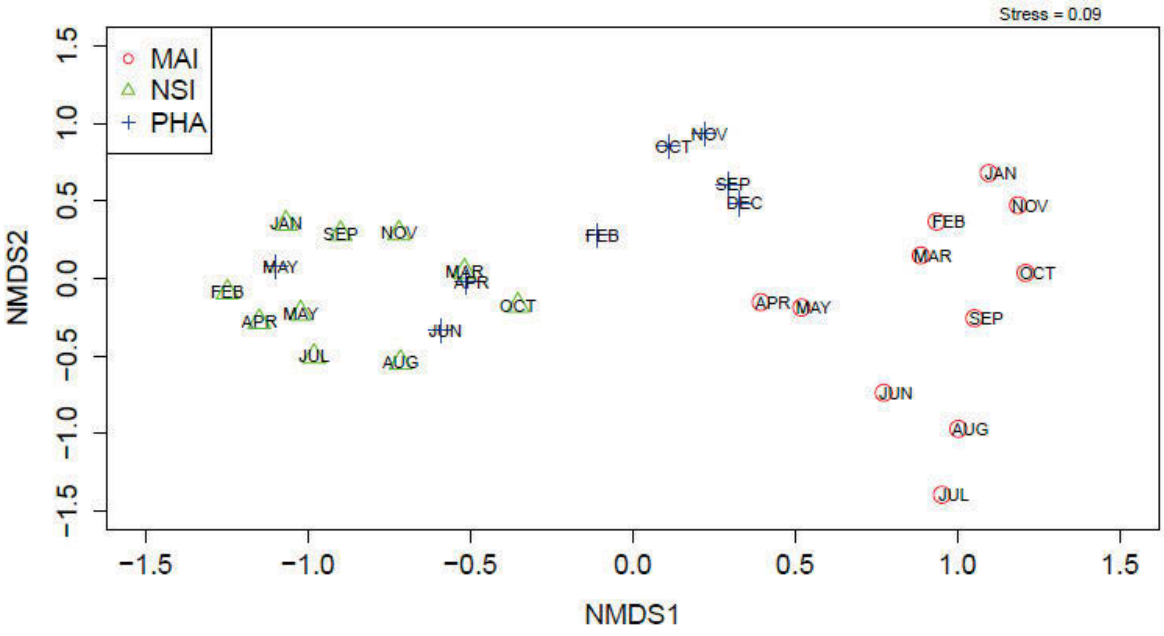

Figure S8: nMDS ordination of the dissimilarity in PRBA assemblages (nMDS stress = 0.09). Different colours indicates samples collected at the different station. The ordination is based on Bray-Curtis similarities calculated from square-root transformed PRBA relative abundances (134 OTUs).

Chapter 4

Shifts in the abundance and diversity of photoheterotrophic microbes across two oceanographic provinces in tropical northern Australia

Shifts in the abundance and diversity of photoheterotrophic microbes across two oceanographic provinces in tropical northern Australia

Jaime Bibiloni-Isaksson[1], Mark Brown[2], Justin Seymour[1]

.

Conceived and designed the experiments: JBI, JS, MVB. Performed the experiments: JBI. Analysed the data: JBI, JS, MVB. Wrote the paper: JBI, JS, MVB.

1. Plant Functional Biology and Climate Change Cluster, University of Technology, Sydney

2. School of Biotechnology and Biomolecular Science, UNSW Australia, Sydney, Australia 2052

Running title: Photoheterotrophs in tropical coastal waters

Abstract

Photoheterotrophic bacteria, including populations of aerobic anoxygenic phototrophic bacteria (AAnPB), and proteorhodopsin-containing Bacteria and Archaea (PRBA) play important trophic roles within marine ecosystems, but little is known about how the abundance and diversity of these important functional groups shifts across oceanographic boundaries. We examined patterns in both the AAnPB and PRBA communities across two distinct oceanic provinces spanning northern Australian waters - the oligotrophic Coral Sea and the more productive Arafura Timor Sea (ATS). Photoheterotrophic bacterial diversity and abundance were examined using Miseq Illumina sequencing and quantitative PCR (qPCR) approaches. Total bacterial abundance was higher in ATS waters, which was reflected by higher AAnPB abundance in this region, whereas the major proteorhodopsin containing clade, SAR11, displayed the opposite trend, with higher abundances in the Coral Sea. Among the AAnPB, the Gammaproteobacterial phylogroup K dominated the community in both regions, with relatively stable composition of AAnPB across regions. Conversely, the PRBA community displayed clear differences between the two regions, with the ATS dominated by SAR11-like and Betaproteobacterial sequences, while the Coral Sea was dominated by Archaea group IIb and members of SAR11 clade A and B. Our data indicate a transition in the abundance and diversity of key photoheterotrophic bacterial groups between northern Australian oceanographic regions, indicating that shifts in physical and biotic characteristics

across water masses can lead to sharp changes in the dynamics of these important marine microbial assemblages.

Introduction

Photoheterotrophic bacteria are a diverse and ecologically significant group of microbes that have the capacity to simultaneously harvest light energy and utilize dissolved organic compounds as carbon and energy sources (Beja and Suzuki, 2008). Two distinct groups of photoheterotrophic prokaryotes are currently known in the marine environment. These include the aerobic anoxygenic phototrophic bacteria (AAnPB), which utilize a form of chlorophyll, known as bacteriochlorophyll *a* (Bchl*a*), and proteorhodopsin containing Bacteria and Archaea (PRBA), which contain a transmembrane light-driven proton pump that produces ATP (Kolber *et al.,* 2001; Martinez *et al.,* 2007). Neither group is able to fix CO_2, so are not considered fully photosynthetic organisms. Within marine habitats photoheterotrophic bacteria can make up between 5-75% of total prokaryotic biomass and are believed to play important roles in carbon cycling in photic regions of the global ocean (Koblížek, 2011; Kirchman and Hanson, 2013; Karl, 2014).

There is evidence that the abundance and distribution of PRBA and AAnPB differs substantially between oceanographic provinces, indicating a possible niche separation driven by different chemical and physical parameters (Cottrell *et al.,* 2006, Mašín *et al.,* 2006, Sieracki *et al.,* 2006, Yutin *et al.,* 2007, Campbell *et al.,* 2008; Cotrell and Kirchman, 2009; Riedel *et al.,* 2010; Lehours *et al.,* 2010; Ritchie and Johnson, 2012; Giovanonni,

2013; Bibiloni-Isaksson *et al.,* 2016). With some exceptions (Lami *et al.,* 2007), AAnPB are typically more abundant in shelf and coastal waters than the open ocean (Schwalbach and Fuhrman 2005, Sieracki *et al.,* 2006, Ritchie and Johnson, 2012), while PRBA are more abundant in oligotrophic or ultra-oligotrophic environments, consistent with the abundance of the dominant proteorhodopsin containing clade, SAR11, which prefers oligotrophic conditions (Giovannoni, 2013; Church and Karl, 2014). In photic open ocean waters, the relative abundance of AAnPB ranges between 0.5 and 6% of the total bacterial community, while they can compose more than 16% of the community in estuaries and coastal waters (Cottrell *et al.,* 2006, Sieracki *et al.,* 2006, Jiao *et al.,* 2007; Waidner and Kirchman 2007, Cottrell *et al.,* 2010, Stegman *et al.,* 2014; Schwalbach and Fuhrman 2005; Sieracki *et al.,* 2006, Ritchie and Johnson, 2012; Bibiloni-Isaksson *et al.,* 2016). On the other hand, PRBA have been shown to compose up to 70% of total bacteria in oligotrophic Sargasso Sea waters, while in more productive waters of the North Atlantic their incidence was only 4 to 15% of the total bacterial community (Venter *et al.,* 2007; Campbell *et al.,* 2008; Riedel *et al.,* 2010).

Beyond these community-level patterns in total AAnPB and PRBA abundance, there is growing evidence that these two important groups of marine microbes are highly diverse, with different clades or phylogroups displaying distinct biogeographical patterns that are regulated by different environmental factors (Venter *et al.,* 2004; Yutin *et al.,* 2007). For instance, among the AAnPB, alphaproteobacteria, Roseobacter-like and betaproteobacterial sequences are particularly dominant in estuaries and

coastal waters (Beja *et al.* 2002; Yutin *et al.* 2007; Lehours *et al.* 2010;Waidner and Kirchman 2008; Salka *et al.* 2011; Boeuf *et al.* 2013), while open ocean waters are dominated by Gammaproteobacteria sequences (Bibiloni-Isaksson *et al.,* 2016). Among the PRBA, key members of this assemblage, such as the SAR11 clade, exhibit distinct vertical distributions throughout the water column (Carlson *et al.,* 2008), and spatio-temporal heterogeneity driven by various physicochemical factors (Eiler *et al.,* 2009; Morris *et al.,* 2005; Lami *et al.,* 2009).

In both AAnPB and PRBA there is evidence for shifts in population structure according to seasonal cycles (Cottrell and Kirchman, 2009; Bibiloni-Isaksson *et al.,* 2016) and across broad region scales (Ritchie and Johnson, 2012;Riedel *et al.,* 2010; Bibiloni-Isaksson *et al.,* 2016), but few studies have examined how the composition and diversity of these groups changes across oceanographic boundaries, meaning we currently lack insight into how spatially dynamic the composition of these photoheterotrophic communities are.

To examine patterns in the diversity and distributional dynamics of AAnPB and PRBA across discrete oceanographic provinces we conducted a study along a transect crossing the northern waters of the Australian continent (Fig.1). Two distinct oceanographic provinces were targeted, the Arafura and Timor Sea (ATS) and the Coral Sea, both of which play important roles in regional climate and ocean circulation (Tomczak and Godfrey, 2003). The ATS is characterised by high levels of productivity

(McKinnon *et al.*, 2011), while the Coral Sea is considered more oligotrophic (Condie and Dunn, 2006). Recently, we demonstrated that the diazotrophic community exhibited high levels of heterogeneity across these regions, with the community partitioned clearly according to these two provinces (Messer *et al.*, 2016). Here we tracked the spatial patterns in abundance and diversity of AAnPB and PRBA in this region to develop a better picture of the role of the marine environment in governing the dynamics of these key marine prokaryotic groups.

Methods

Sampling, nucleic acid collection and extraction

Sampling was performed during a voyage on-board of the Australian Commonwealth Scientific and Industrial Research Organisation (CSIRO) research vessel, *Southern Surveyor*, during the Austral winter (July- August) 2013 (Fig. 1). The voyage consisted of a ~5500 km transect from Broome (17.96° S, 122.23° E) to Brisbane (27.47° S, 153.03° E), with surface (5m) and, when discernible, chlorophyll maximum (DCM) seawater samples collected daily at both dawn and mid-afternoon during the 15 day voyage. Temperature and salinity profiles were obtained on the downward casts of a rosette equipped with a conductivity, temperature,

depth (CTD) profiler with a sensor for photosynthetically active radiation (PAR). Further data were obtained from water samples collected in Niskin bottles at various depths during each CTD cast. Parameters measured included temperature, fluorescence, salinity, dissolved oxygen, phosphate, nitrate, silicate, nitrite and pigments (Table S1 as Appendix IV). Nutrient samples were collected directly from the Niskin bottles and concentrations of nitrate, nitrite, silicate, ammonia and phosphate and were determined on board. Photosynthetic pigment data was obtained as described previously (Messer *et al.* 2016).

At each station, which were separated by between 1-2° longitude, 5-8 L of seawater was filtered through 0.22 μm Sterivex filter units (EMD Millipore, Billerica, MA, USA). Filters were immediately frozen in liquid nitrogen and stored at -80°C. Post-voyage, microbial community DNA was extracted using the PowerWater DNA Extraction Kit (MoBio Laboratories, Carlsbad, CA, USA) according to the manufacturer's instructions. The quality and quantity of DNA was assessed using a NanoDrop™ 8000 Spectrophotometer (Thermo Scientific™) and DNA stored at -80 °C prior to further analysis.

Quantitative PCR of aerobic anoxygenic phototrophic bacteria

Quantitative PCR (qPCR) was performed to quantify AAnPB abundance by targeting the *pufM* gene, which encodes the M subunit of bacterial chlorophyll *a* photosynthetic

reaction center (Yutin and Beja, 2005; Waidner and Kirchman, 2007). Each 20 µl reaction mixture contained 0.8 pmol of each of the primers (*pufM*-557F and *pufM*-WAWR) (Yutin and Beja, 2005; Waidner and Kirchman, 2007), 10 µl of ABI SYBR Select Master Mix (Life Technologies) and 10 ng of template DNA. qPCR was performed as described by Bibiloni-Isaksson *et al.* (2016) (Table S2). Similarly, to quantify the abundance of 16S rRNA genes, as a proxy measure for total bacterial abundance, each 20 µl reaction mixture contained 0.8 pmol of each of the primers (BACT-1369F CGG TGA ATA CGT TCY CGG PROK-1543R AAG GAG GTG ATC CR GCC GCA, Suzuki *et al.*, 2001), 10 µl of ABI SYBR Select Master Mix (Life Technologies) and 10 ng of template DNA. The temperature profile used to quantify targeted genes was performed as described in Suzuki et al. (2001) (Table S2). *pufM* copy numbers were subsequently normalised to the abundance of 16S rRNA genes (Suzuki et al., 2001). Standards for qPCR analysis of 16S rRNA and *pufM* gene abundance were generated using M13 vector PCR from clones obtained from this study. Briefly, PCR amplicons were ligated into a TOPO TA cloning vector and ligation products were transformed into *Escherichia coli* One Shot TOP10 cells (Invitrogen). Clones were amplified by PCR with vector-specific primers (M13). Positive clones containing the target gene insert were sequenced, and the most abundant of these was used for plasmid DNA extraction. After measuring the DNA concentration with a Qubit Fluorometer, the purified plasmid DNA was serially diluted according to known copies of PCR fragments of the respective gene and subjected to real-time PCR in triplicate to generate an external standard curve. Amplification efficiencies were between 92 and

103%. All amplification products were checked for quality by examination of melt curves and by gel electrophoresis to ensure products corresponded to the correct size, and to ensure the absence of non-specific products. The specificity of the primers used in this study has previously been established (Campbell *et al.,* 2008; Riedel *et al.,* 2010; Ritchie and Johnson, 2012).

Characterisation of aerobic anoxygenic phototrophic bacteria community structure abundance

Amplification of the *pufM* gene was performed in 25 μl PCR reaction mixture comprising 12.5 μl ImmoMix (Bioline, NSW, Australia), 10 pmol of each primer (*pufM*-557F TAC GGS AAC CTG TWC TAC; *pufM*-WAWR AYN GCR AAC CAC CAN GCC CA) (Yutin and Beja, 2005; Waidner and Kirchman, 2007), 9.5 μl of dH_2O, and 1 μl of template DNA (10 ng final concentration). Amplification proceeded under the following thermocycling conditions: an initial denaturation step at 95 °C for 10 minutes, followed by 40 cycles of denaturation at 95 °C for 10 seconds, annealing at 56 °C for 30 seconds, and extension at 72 °C for 45 seconds. *pufM* amplicons were purified using ISOLATE II PCR and Gel Kit (Bioline, Australia), and quantified using a Qubit fluorometer (Invitrogen). PCR products from all samples were normalized in equimolar amounts before sequencing.

pufM amplicon sequencing was performed using the Illumina MiSeq platform (Molecular Research LP, Shallowater, TX) according to the manufacturer's directions. Resultant sequence data were processed using the Quantitative Insights Into Microbial Ecology (QIIME) 1.8.0-dev pipeline (Caporaso *et al.,* 2010;

http://www.qiime.org/) using default parameters unless otherwise noted. Briefly, forward and reverse sequences were merged by overlapping paired-end reads. Sequences were quality trimmed, and assigned to samples based on unique 8-bp barcodes. Low quality fragments were removed before chimera detection and removal using U-Chime (Edgar *et al.,* 2011). Numbers of *pufM* reads ranged from 792 to 156997 per sample. Data were randomly resampled to 10148 sequences, resulting in 2 samples being removed due to a low number of reads. Sequences were binned into operational taxonomic units (OTUs) using de-novo Uclust (Edgar, 2010) with a 94% identity threshold (Lehours *et al.,* 2010; Ferrera *et al.,* 2014; Zheng *et al.,* 2015) and the most abundant sequence from each OTU was selected as a representative sequence for that OTU. OTUs with representative sequences that did not return a *pufM* gene as top hit in Blast search against NCBI NR database were removed.

Phylogenetic analysis of *pufM* communities was performed using the ARB software package (Ludwig *et al.,* 2004). Representative sequences from each OTU were imported and aligned to a curated in-house ARB database containing a custom reference collection of 297 *pufM* sequences compiled from cultured or otherwise well-characterized species in Genbank, supplemented with sequences reported from environmental surveys including from a recent study in eastern Australian waters (Bibiloni-Isaksson *et al.,* 2016). A guide tree of ~200bp length sequences was calculated using the ARB neighbour-joining method, and shorter sequences were added to the tree using the parsimony method. Each representative sequence was assigned to

previously defined AAnPB taxonomic groups (Yutin *et al.,* 2007; Lehours *et al.,* 2010; Boeuf *et al.,* 2013; Ferrera *et al.,* 2014). The resultant tree was exported and visualised using FigTree version. 1.4.2 (Rambaut, 2014).

Characterisation of proteorhodopsin bacteria community structure

In order to detect genes encoding proteorhodopsin (PR), a set of degenerate multiplex PCR primers was used. PCR reactions were performed in a 25 μl reaction mixture containing 12.5 μl ImmoMix (Bioline, NSW, Australia), 10 pmol of each primer (PR1 MGN TAY ATH GAY TGG YT; PR2 WWN MGN TAY GTN GAY TGG; PR3 GGR TAD ATN GCC CAN CC, Sabehi *et al.,* 2005) and template DNA (10 ng final concentration). Amplification proceeded under the following thermal cycling conditions: an initial denaturation step at 95°C for 10 minutes, followed by 34 cycles of denaturation at 95°C for 10 seconds, annealing at 47°C for 30 seconds, extension at 72°C for 1 minute, and a final extension at 72°C for 2 minutes.

As with *pufM* analysis, amplicon sequencing was performed using the Illumina MiSeq platform (Molecular Research LP, Shallowater, TX) according to the manufacturer's directions. Resultant sequence data were processed using the Quantitative Insights Into Microbial Ecology (QIIME) 1.8.0-dev pipeline (Caporaso *et al.,* 2010; http://www.qiime.org/) using default parameters unless otherwise noted. Single read sequences were quality trimmed, and assigned to samples based on unique 8-bp barcodes. Low quality fragments were removed before chimera detection and removal

using U-Chime (Edgar *et al.,* 2011). Numbers of proteorhodopsin reads ranged from 20 to 294933. Samples were randomly resampled to 629 sequences, resulting in 3 samples being removed due to low number of reads. Sequences were binned into OTUs using de-novo uclust (Edgar, 2010) with a 97% identity threshold (Philosof and Béjà, 2013; Sabehi *et al.,* 2003), and the most abundant sequence from each OTU was selected as a representative sequence for that OTU.

Phylogenetic analysis for PRBA communities was performed using the ARB software package (Ludwig *et al.,* 2004). OTU sequences that were binned at a 97% similarity cut-off, which comprised 99.99 % of all subsampled sequences (a total of 1078 sequences), were used for analysis. Translated protein sequences were blasted against a curated database for the analysis of microbial rhodopsin diversity and evolution (MicRhoDE) (Boeuf *et al.* 2015). The database currently covers 7857 aligned sequences. Representative sequences from each OTU were imported and aligned to a curated in-house database containing a custom reference collection of proteorhodopsin amino acid sequences compiled from cultured or otherwise well-characterized species in Genbank, supplemented with sequences reported from two previous environmental surveys within Australian waters, including studies performed in coastal waters of Tasmania (Bibiloni-Isaksson *et al.,* unpublished) and the east coast of Australia (Bibiloni-Isaksson *et al.,* unpublished). Sequences were aligned with muscle and manually revised in ARB. The resultant tree was exported and visualised using FigTree version. 1.4.2 (Rambaut, 2014).

Quantitative PCR of proteorhodopsin containing SAR11

Due to the high relative abundance of SAR11 sequences in the PR amplicon sequencing analysis (average: 34% and 20% of PR sequences at ATS and Coral Sea, respectively) we employed qPCR to quantify patterns in SAR11 abundance relative to the abundance of 16S rRNA genes (Suzuki *et al.,* 2001). Each 20 μl reaction mixture contained 0.8 pmol of each of the primers (SARPR-125F HG GWG GAT AYT TAG GWG AAG C; SARPR-288R CCC AAC CWA YWG TWA CRA TCA TTC T; Campbell *et al.* 2008), 10 μl of ABI SYBR Select Master Mix (Life Technologies) and 10 ng of template DNA. Primers used for qPCR analyses and cycling conditions used to quantify targeted genes follow the methods of Suzuki *et al.* (2001) (Table S2). Standards for qPCR were created and analysed as described above for *pufM* standards. Each 20 μl qPCR reaction mixture contained 0.8 pmol of each of the primers (BACT-1369F CGG TGA ATA CGT TCY CGG PROK-1543R AAG GAG GTG ATC CR GCC GCA), 10 μl of ABI SYBR Select Master Mix (Life Technologies) and 10 ng of template DNA.

Statistical analyses

Rarefied sequence data were square-root transformed and a resemblance matrix generated using Bray-Curtis similarity. Multivariate statistical analyses were all carried out using PRIMER 6.0 (PRIMER-E, Plymouth, UK; Clarke *et al.,* 2005). Environmental parameters (Table S1) were normalised using the normalisation function in PRIMER 6.0 and a resemblance matrix generated using Euclidean distance

(Clarke and Warwick, 2001). Statistical analyses including analysis of similarities (ANOSIM; Clarke 1993) to test similarities among depth and region, distance based linear modelling (DistLM) to calculate correlations of community composition to environmental factors and distance-based redundancy analysis (dbRDA) to visualise these correlations (Legendre and Anderson, 1999; McArdle and Anderson, 2001) were performed in the PRIMER + PERMANOVA software package (Clarke *et al.,* 2005).

In order to identify associations between individual phylogroups, OTUs and environmental parameters, we employed a network analysis approach (Steele *et al.,* 2011; Zhou *et al.,* 2011). We calculated the maximal information coefficient (MIC) between all variable (n=14878) pairs from all samples (n=27) using the MINE statistics package (Reshef *et al.,* 2011). A multiple test correction was performed according to the False Discovery rate (FDR) procedure (Benjamini and Hochberg, 1995). Only correlations which yielded a p-value ≤0.05 and q-value<0.05 were considered significant and plotted as a network using Cytoscape v 2.8 (Saito *et al.,* 2012).

Nucleotide sequence accession numbers

The sequences obtained in this study have been submitted to the European Nucleotide Archive (ENA) database under the study PRJEB14603.

Results

Physicochemical characteristics of the ATS and Coral Sea

ATS waters were warmer, exhibited lower salinities and had higher nutrient concentrations and phytoplankton abundances than Coral Sea waters (Table S1 as Appendix IV). Mean sea surface temperature (SST) in the ATS was 26.4 °C, compared to 24.3 °C in the Coral Sea. Salinity increased from 33.5 to > 35 PSU at a longitude of approximately 143 °E, reflecting the transition from the shelf region of the ATS to the open ocean conditions of the Coral Sea (Table S1). Nutrient concentrations (nitrate, phosphate and silicate) varied across the two regions, but were highest in the ATS (Table S1 as Appendix IV).

Abundance of total bacterioplankton across the two regions

The 16S rRNA gene abundance, as estimated by qPCR, ranged between 1.38×10^5 - 1.54×10^6 (average 8.71×10^5 copies mL^{-1}) within the ATS, and 1.03×10^5 to 1.25×10^6 (average 4.38×10^5 copies mL^{-1}) in the Coral Sea and were significantly higher in the ATS than the Coral Sea ($P<0.05$, Student's t-test) (Fig. S1). The WS13 station, which represented the transition point between the two regions, was the only sample in the Coral Sea where 16S rRNA gene abundance exceeded 10^6 copies mL^{-1}. Strong positive correlations (Pearson's) were observed between 16S rRNA gene copy abundance and temperature ($R=0.569$, $p=0.003$), while negative correlations between 16S rRNA gene abundance and salinity ($R=-0.565$, $p=0.003$), ammonia ($R=-0.425$, $p=0.034$) and Divinyl Chla ($R=-0.576$, $p=0.003$) were observed.

Spatial patterns in abundance of AAnPB across the ATS and Coral Sea

qPCR results indicated that *pufM* genes were always present, but were variable across the two regions and with depth (Table S3). The relative proportion of the bacterial community comprised of AAnPB was defined by the *pufM*: 16S rRNA ratio. Significant differences ($P<0.05$, Student's t-test) in this ratio were observed in surface samples between the ATS (1.2 - 5.5; mean 3.1) and Coral Sea (0.7-5.7; mean 2.3), but DCM samples were not significantly different between regions ($P>0.05$, Student's t-test). Across the entire dataset, and also specifically within the ATS region, *pufM*:16S rRNA were found to be significantly correlated to phosphate concentrations (Pearson's $R=0.407$, $p=0.043$; $R=0.634$, $p=0.015$, respectively). No correlations between the *pufM*:16S rRNA ratio and any environmental parameters were observed in the Coral Sea.

Spatial patterns in AAnPB composition across ATS and Coral Sea

A total of 51 *pufM* OTUs, which comprised 99.99% of all subsampled sequences, were identified. Neither AAnPB richness (chao1) nor Shannon's Diversity was significantly different between depths ($p=0.472$; 0.9), or oceanic region ($p=0.0571$; 0.72) (Table S3; Fig. S2). However, AAnPB community composition displayed clear

Table S3: Average, standard deviation (in brackets), maximum and minimum values for copy genes per mL, ratio of genes and richness and diversity values.

	ATS Surface	ATS DCM	Coral Sea Surface	Coral Sea DCM
pufM	2.72E+04(2.54E+04); 8.42E+04-3.79E+03	3.98E+04(4.18E+04); 1.02E+05- 1.42E+04	1.41E+04(1.75E+04); 4.79E+04-2.80E+02	8.84E+03(4.50E+03); 1.64E+04-3.46E+03
SAR11PR	2.16E+05(1.36E+05); 4.41E+05-7.36E+04	3.84E+05(4.12E+05); 9.99E+05-1.47E+05	1.40E+05(9.39E+04); 2.42E+05-4.61E+03	8.26E+04(5.21E+04); 1.71E+05-3.42E+04
16s rRNA	7.86E+05(4.41E+05); 1.54E+06-2.00E+05	2.25E+06(2.51E+06); 6.00E+06- 8.55E+05	5.39E+05(4.26E+05); 1.03E+06-1.25E+04	4.41E+05(3.69E+05); 9.18E+05-1.31E+05
***pufM*/16S genes**	3.11(1.30); 5.46-1.23	1.79(0.65); 2.61-1.14	2.28(1.63); 5.27-0.70	3.08(1.44); 4.62-1.46
SAR11PR/16S genes	27.79(9.5); 43.82-13.94	17.82(1.05); 18.92-16.64	31.82(8.01); 44.46-22.89	27.5(15.11); 44.50-4.98
chao1 (*pufM*)	189.89(61.91); 311-133.54	166.55(10.23); 178.07-151	207.73(38.83); 248.4-147.1	182.39(34.83); 228.15-140
chao1 (PR)	132.36(30.16); 167.2-70.55	134.64(20.94); 169.15-114.6	266.26(40.02); 310.81-232	268.49(40.04); 310.57-212.4
Margalef (*pufM*)	11.55(1.92); 15.05-9.26	11.34(1.86); 12.88-8.97	12.78(2.71); 16.35-9.40	12.71(2.45); 14.47-8.39
Margalef (PR)	11.92(2.03); 15.51-8.37	12.04(1.27); 13.19-9.93	24.28(3.85); 27.77-19.70	23.49(4.77); 28.24-16.29
Shannon (*pufM*)	3.60(0.34); 4.05-2.94	3.52(0.48); 4.10-2.84	3.50(0.46); 4.08-3.01	3.66(0.49); 4.13-3.07
Shannon (PR)	4.21(0.49); 4.894-3.29	4.41(0.16); 4.58-4.19	6.14(0.55); 6.61-5.38	6.01(0.61); 6.40-4.96

differences between regions (Fig. S3a) (ANOSIM R=0.854, P=0.001), but not between depths within regions (ANOSIM R=0.046, P= 0.199). Once we merged OTUs into phylogroups (Fig. S4) defined by Yutin *et al.* (2007), the majority of *pufM* OTUs belonged to Gammaproteobacteria (phylogroup K), accounting for 99% of sequences in the ATS, while in the Coral Sea alphaproteobacterial sequences, comprising mainly Roseobacter and Rhodobacterales related taxa, made up to 5% of the community (Fig. 2a). Notably, the three most abundant OTUs; OTU737, OTU2086 and OTU5000, comprised 26.3, 25.3 and 17.1% of total AAnPB sequences in the ATS, but in the Coral Sea the relative abundance of these OTUs shifted to 17.9, 45.6 and 1.2 respectively. Only 2 AAnPB OTUS were not affiliated with any Yutin *et al.* (2007) phylogroups.

Distance based redundancy analysis (dbRDA) (Fig. 3a) showed that ATS and Coral Sea samples formed distinct clusters. Distance based linear modelling (DistLM) revealed that 62.6 % of variability observed between AAnPB assemblages could be explained by 8 significant environmental variables; oxygen concentration ($p = 0.005$), fluorescence ($p = 0.002$) salinity, temperature, phosphate, silicate, Divinyl Chl*a* and Chl*a* (All $p = 0.005$).

Spatial patterns in PRBA composition across ATS and Coral Sea

PRBA community structure was characterised using 25 samples taken from surface (5m) and DCM samples. A total of 122 OTUs, representing 99.99 % of all subsampled sequences were used for analysis and these were associated with proteorhodopsin

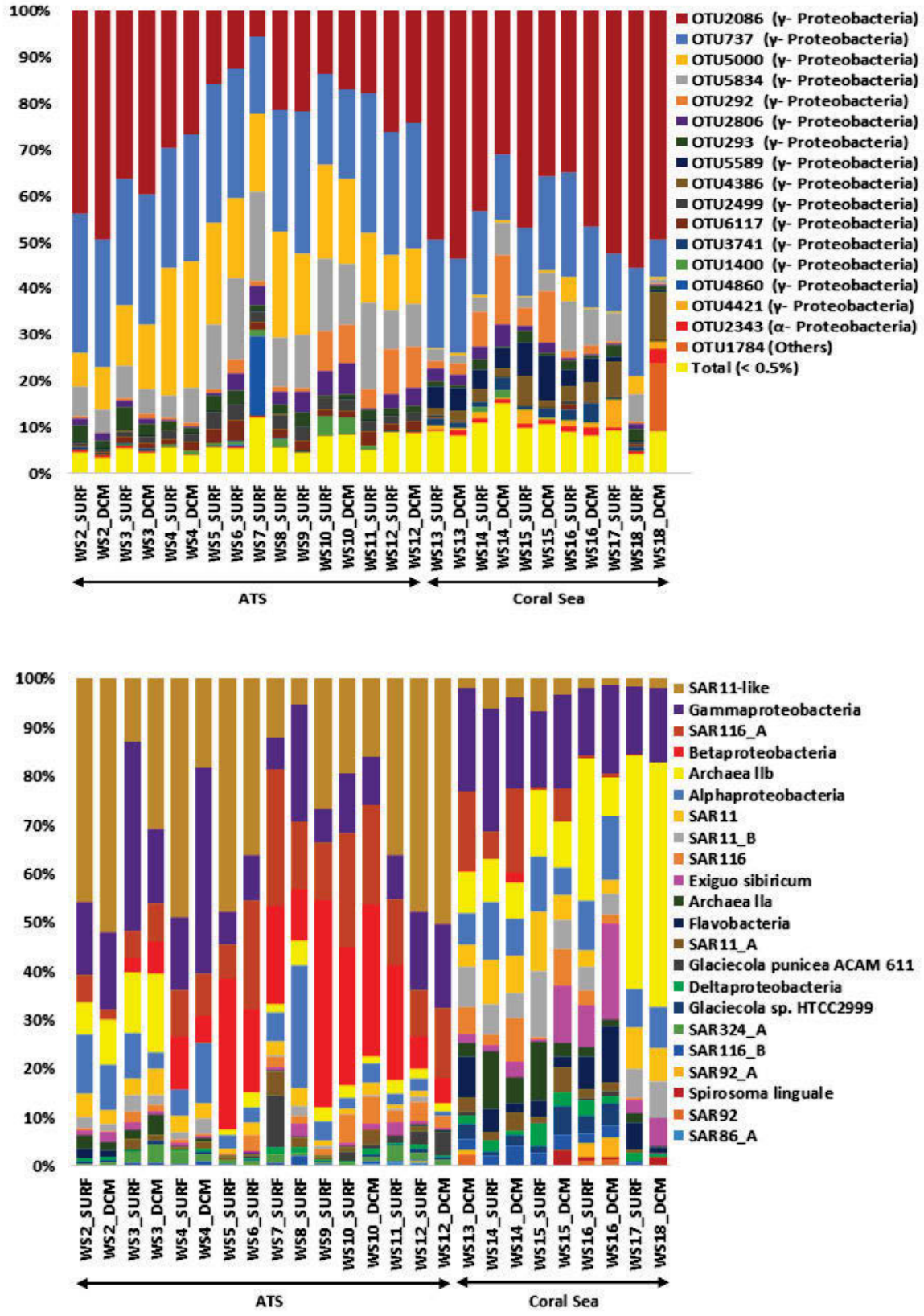

Figure 2: Relative composition of most abundant OTUs (> 0.5%) and affiliated AAnPB phylogroups (top) and relative composition of most PRBA phylogroups (bottom) at ATS and Coral Sea.

sequences from a wide range of marine clades (Fig. S5). PRBA richness (chao1) and Shannon's diversity was not significantly different between depths (both p=> 0.21), but were highly significantly different between the ATS and Coral Sea (both p=< 0.0001) (Table S3; Fig. S2). Both indices were positively correlated (Pearson's) with oxygen (richness R=0.468, p=0.018; Shannon's diversity R=0.453, p=0.023), salinity (R=0.854, p=0.000; R=0.837, p=0.000) and Divinyl Chl*a* (R=0.801, p=0.0000; R=0.771, p=0.0000), but negatively correlated to fluorescence (R=-0.637, p=0.001; R=-0.641, p=0.001), temperature (R=-0.701, p=0.001; R=-0.654, p=0.001), phosphate (R=-0.628, p=0.001; R=-0.717, p=0.000), silicate (R=-0.778, p=0.000; R=-0.739, p=0.000) and several pigments including fucoxanthin (R=-0.548, p=0.005; R=-0.584, p=0.002), Chl*b* (R=-0.543, p=0.005; R=-0.551, p=0.004) and Chl*a* (R=-0.547, p=0.005; R=-0.599, p=0.022).

PRBA community composition also displayed clear differences between the ATS and Coral Sea (Fig. 2b, Fig. S3b) (ANOSIM R=0.999, P=0.001), but not between depths within regions (ANOSIM R=0.001, P= 0.377). For instance, SAR11-like sequences accounted for 31.7% of PRBA within the ATS, but only 3.1% in the Coral Sea. This pattern in the sequence data was supported by the SAR11 qPCR (Table S3). Members of the *Betaproteobacteria* were the third most abundant phylogroup in the ATS, where they comprised 15% of the PRBA community, while within the Coral they only comprised 0.3%. On the other hand, proteorhodopsin containing members of the *Archaea* group IIb were the most abundant group of PRBA within the Coral Sea (21%) but made up a relatively small proportion in the

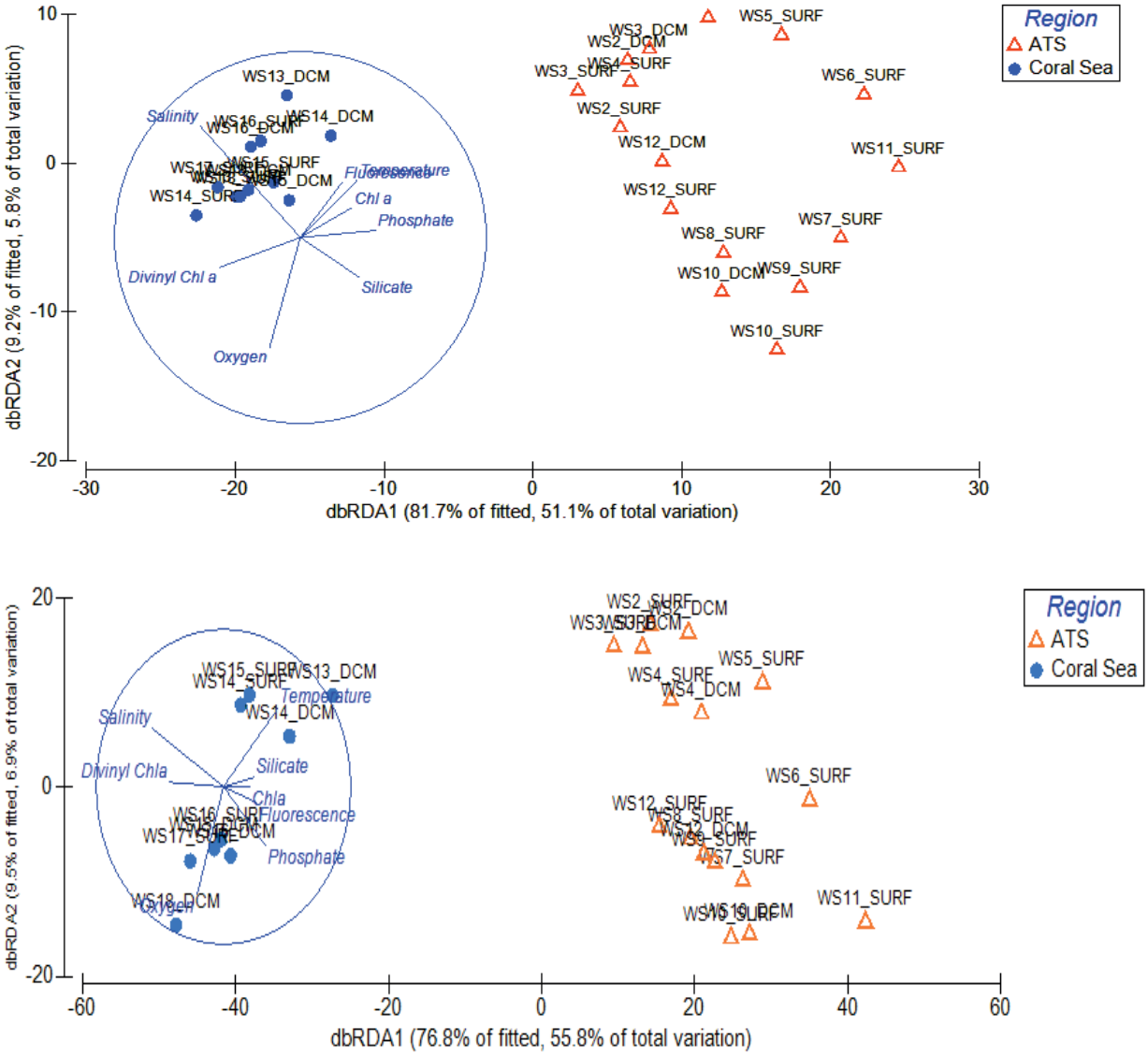

Figure 3: Distance-based redundancy analysis (dbRDA) plot of the DistLM based on the environmental parameters fitted to the variation in biogeochemical changes for AAnPB (top) and PRBA (bottom). Vectors indicate direction of the parameter effect in the ordination plot.

ATS (4.2%). Gammaproteobacteria, Deltaproteobacteria (including SAR324 A clade) and Alphaproteobacteria groups remained relatively constant across the two regions.

DistLM analysis revealed that 72.6 % of total variation was related to 8 significant environmental variables, including oxygen concentration and fluorescence ($p = 0.003$) salinity, temperature, phosphate, silicate, Divinyl Chl*a* (All $p = 0.001$) and Chla ($p = 0.002$). dbRDA (Fig. 3b) revealed clear separation in the PRBA communities between the ATS and Coral Sea. Further, the ATS the PRBA community changed with longitude, with samples collected from western stations (WS2-WS5) distinct from those collected from the eastern stations (WS6-WS18). Similarly, within the Coral Sea there was separation by latitude between the northern (WS13-WS15) and southern stations (WS16-WS18), correlated with changing salinity, temperature, chlorophyll and phosphate values.

We also analysed patterns in the distribution of proteorhodopsin spectral tuning variants defined on the basis of amino acid substitutions, including green light absorbing proteorhodopsin at 525 nm and 535 (GPR) (leucine and methionine substitutions respectively), and blue light absorbing proteorhodopsin at 490 nm (BPR) (glutamine) (Fig. 4). In the ATS, the predominance of SAR11-like OTUs meant that most proteorhodopsins were of the GPR-type (~68%), while in the Coral Sea the proportion of GPR decreased to 17% (Fig. 4). The shift towards a dominance of Archaeal OTUs in the Coral Sea PRBA community underpinned an increase in BPRs

(72% of all sequences). GPRs containing methionine were also more abundant in the Coral Sea (~6%) rather than ATS (~1.5%).

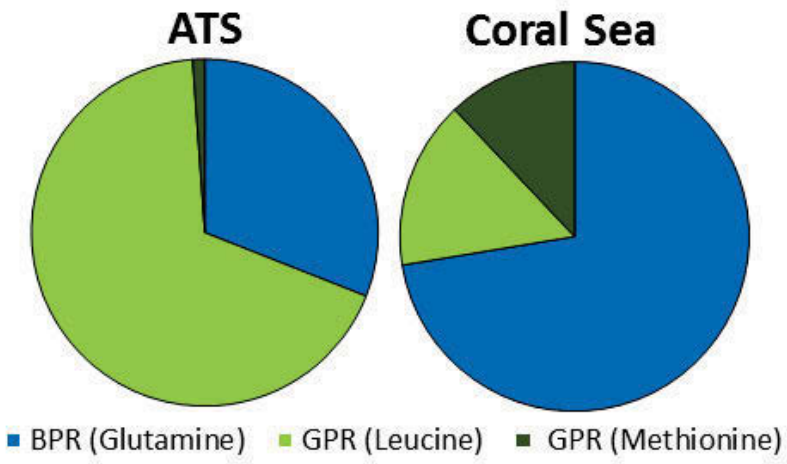

Figure 4: GPRs and BPRs distribution in the tropical north coast of Australia. Pie charts represent percentages of GPRs containing leucine (marked in green), BPRs containing glutamine (marked in blue) and GPRs containing methionine (marked in dark green) at ATS and Coral Sea.

Spatial patterns in Abundance of SAR11 *across ATS and Coral Sea*

We did not observed differences in SAR11PR:16S rRNA ratio between regions (P>0.05, Student's t-test) or between surface and DCM samples (P>0.05, Student's t-test). Across the two regions no correlations among SAR11PR:16S rRNA ratios and environmental parameters were recorded, however within ATS the SAR11PR:16S rRNA ratio was negatively correlated to fucoxanthin (R=-0.567, p=0.035), whereas in the Coral Sea it was positively correlated to fluorescence (R=0.805, p=0.003), fucoxanthin (R=0.656, p=0.028) and Chla (R=0.627, p=0.039),

Photoheterotrophic bacterial Network Analysis

Network analysis revealed many correlations between ecosystem variables and AAnPB and PRBA populations (Fig. 5a). The majority of correlations involved PRBA OTUs that formed highly interconnected clusters that responded similarly to their environment (Fig. 5a). We also observed instances of correlations between different taxonomic groups, including between archaeal and bacterial PRBA OTUs and between AAnPB and PRBA OTUs. For instance the abundance of Alphaproteobacteria proteorhodopsin OTU33492, was positively correlated with Archaea group IIb OTU20155 (Fig. 5b), and both interacted with temperature, whereby their abundances were zero above 25.3 C. Further, these PRBA OTUs were positively correlated to AAnPB Gammaproteobacteria OTU4386 which displayed a very similar negative relationship with temperature, (Fig. 5c), with abundances of zero at temperatures above 25.4 C. Two of the most abundant OTUs within the Archaea group IIb, OTU18955 and OT52286, displayed a classic co-occurrence relationship, whereby one OTU was only abundant when the other was also abundant (Fig. 5d). We identified a transition point between the ATS (station WS12) and Coral Sea stations (station WS13) where these OTUs started to become abundant, and their abundance continued to increase as the transect continued southward (Fig. 2b). Salinity was also observed to be correlated with several biotic parameters. For instance it was positively correlated with Archaea group II OTU20155, which only occurred in waters with a salinity > 35.2

and negatively correlated to pufM Gammaproteobacteria OTU4264 (Fig. 5e) which occurred at its highest abundance in the lowest salinity waters (33.2).

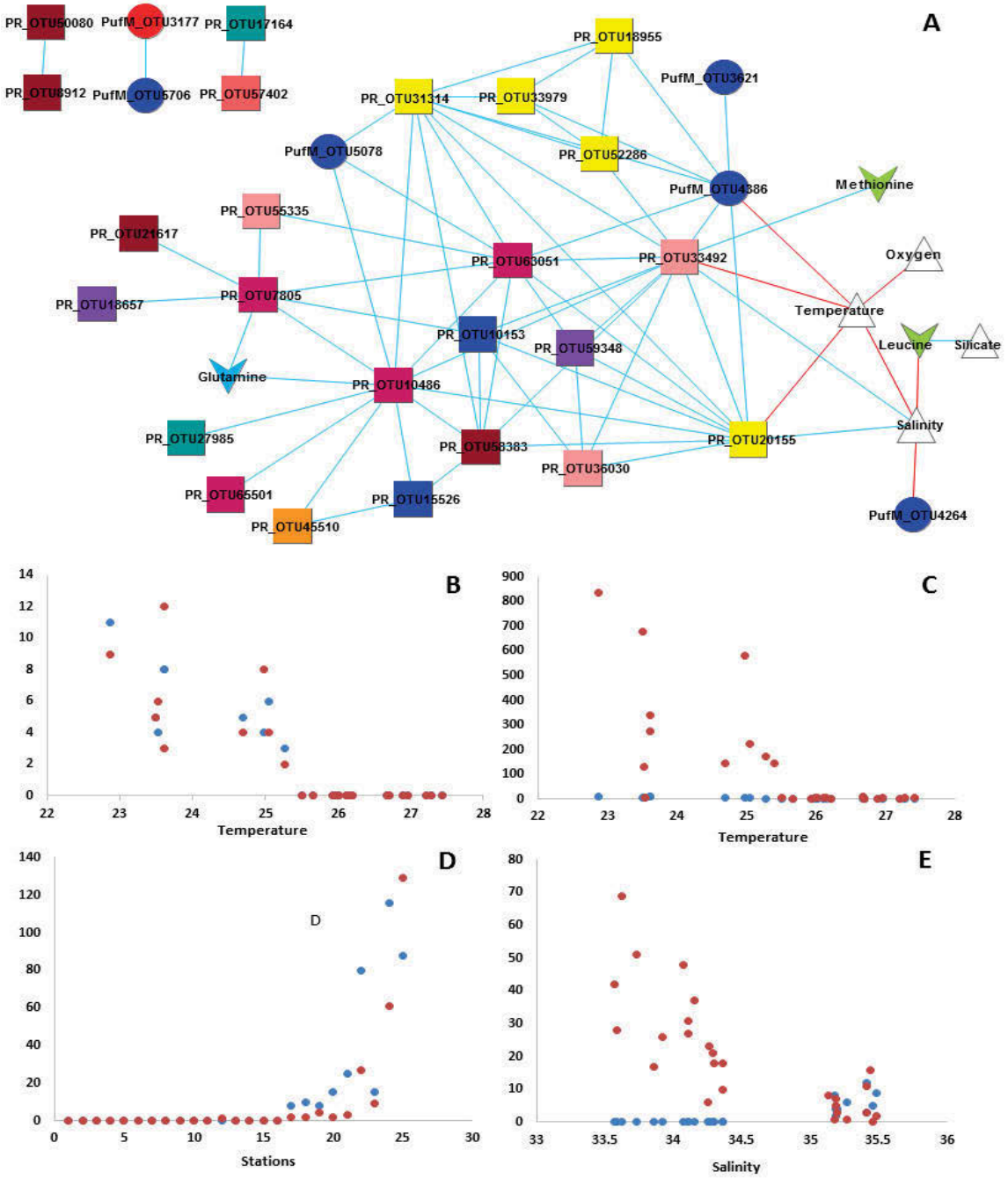

Figure 5: a) Visualisation of co-occurrence network generated from significant ($P < 0.05$) MIC relationships between AAnPB (circles) and PRBA (squares) and ecosystem components across the ATS and Coral Sea. Gammaproteobacteria = blue, Deltaproteobacteria = turquoise, Alphaproteobacteria = pink, Archaea group IIa = orange, Archaea group IIb = yellow, Flavobacteria=purple, Glaciecola HTCC2999=-blue-greenish, Roseobacter= Red, SAR11 and SAR11-like= dark red, SAR11 clade B= soft red, BPRs (Glutamine) =blue, GPRs (leucine and methionine) = green, physico-chemical variables = white triangles. Positive and negative linear regressions are denoted by blue and red solid lines, respectively. Edge width is positively related to MIC strength. b) Positive relationship between the relative abundance of OTU33492 (blue circles) and OTU20155 (red circles) and temperature. c) Differential relationships between OTU33492 (blue circles) and OTU4386 (red circles) and temperature. d) Relationship between OTU18955 (blue circles) and OTU52286 (red circles) e) Differential relationships between OTU20155 (blue circles) and OTU4264 (red circles) and salinity.

Discussion

The main objectives of this study were to examine spatial patterns of photoheterotrophic microbes in the low latitude region of the northern tropical coastal Australian waters and to assess changes in their abundance and diversity between two discrete oceanographic provinces, the ATS and Coral Sea. Differences in the physicochemical and biotic features of these two regions were expected to result in unique impacts on the diversity and abundance of photoheterotrophic microbes. Previous studies have demonstrated significant shifts in bacterioplankton community structure across physicochemical transition points (e.g. Alonso-Sáez et al., 2007; Baltar et al., 2007; Herlemann et al., 2011) and revealed that different water masses harbour specific microbial communities (e.g. Agogué et al., 2008; Galand *et al.,* 2010). We recently demonstrated significant shifts in the abundance, composition and activity of diazotrophic bacteria in this region, which were linked to intrinsic differences in physicochemical conditions between the two oceanographic provinces (Messer *et al.* 2015). Based on these previous results, and current knowledge of the environmental niche characteristics of AAnPB and PRBA (Suzuki and Beja, 2008; Koblížek, 2015), we hypothesized the existence of a pronounced change in photoheterotrophic community structure coinciding with the separation point between the ATS and Coral Sea.

Comparison of photoheterotrophic bacterial abundance at geographically different water masses

The distribution of temperature, nutrients and salinity across our transect reflects the different water masses, corresponding to the ATS and Coral Sea (Table S1). The climate in the ATS is tropical and the major oceanographic feature is the Indonesian Throughflow (ITF), a warm, low-salinity current flowing from the Pacific to the Indian Ocean, which crosses the north-western part of the ATS (Gordon & Fine 1996; Molcard et al. 2001; Gordon 2005). Upper ocean circulation is determined mainly by the onset of the northwest and southeast monsoon seasons with parameters such as water density, temperature, pH and salinity driven by large-scale variations in precipitation, river discharge and the nature of ocean currents (Gordon & Fine 1996; Gordon 2005). The major water mass of the Coral Sea is known as the Pacific North-West Tropical Warm Pool, and its major currents include the west ward flowing South Equatorial Current, which crosses the Coral Sea and then, at the east of the continental shelf, splits into the Coral Sea Coastal Current, also known Hiri Current, to the north and the EAC to the south (Lyne and Hayes 2005). This latter current brings warm, low-nutrient water and tropical species southward as a series of eddies. Productivity also changes seasonally and is higher in the dry season (the austral winter) than the summer wet season, especially in the northern Coral Sea (Lyne and Hayes 2005; Messie and Radenac, 2006). Additionally, there are subsurface layers rich in nutrients, at depths of between 50 and 140 m (Brewer et al. 2007). In this region, productivity is driven by

different organisms in these areas; for instance, diatoms are the primary producers in the EAC, whereas flagellates are more abundant offshore (Hobday *et al.* 2011).

Total AAnPB abundance was significantly higher in the ATS surface samples than in the Coral Sea and were in the same range as observed by several other studies including during summer periods in the Mediterranean Sea (0.6–11.1%, Hojerova *et al.* 2011) (0.1–4%, Lamy *et al.* 2011b), Baltic Sea (1.0–11.1%, Salka *et al.* 2008), Sargasso Sea (1.9–4.3%, Koblızek *et al.* 2007) and North Atlantic (1.5–12.9%, Michelou, Cottrell and Kirchman, 2007). We observed a positive correlation between *pufM*:16S rRNA ratios and phosphate concentrations. This is consistent with previous surveys of AAnPB abundance in aquatic environments that have shown a positive correlation between AAnPB abundance and nutrients and chlorophyll concentration (Jiao *et al.* 2007; Hojerova *et al.* 2011; Ritchie and Johnson 2012; Masın *et al,* 2012; Fauteux *et al.,* 2015).

Diversity analyses using targeting the *pufM* gene revealed that across both the ATS and Coral Sea, AAnPB diversity was significantly lower than has been reported in samples from the Mediterranean (Ferrara *et al.,* 2014), oligotrophic western Pacific Ocean (Zheng *et al.,* 2015) and East coast Australia (Bibiloni Isaksson *et al.,* 2016). A recent investigation of pufM dynamics along Australia's eastern seaboard highlighted a positive correlation between temperature and Gammaproteobacteria (phylogroup K) abundance, whereby this group was most abundant in water temperatures above 18 °C (Bibiloni-Isaksson *et al.,* 2016). Our study here was carried out in constantly warmer waters (23-27.4 °C) and, consistent with observations from other warm water

environments including the Mediterranean Sea and open ocean, oligotrophic regions of the Pacific Ocean (Lehours et al., 2010, Ritchie and Johnson 2012, Ferrera et al., 2014), Gammaproteobacteria were the dominant AAnPB phylogroup in both the ATS and Coral Sea.

Previous studies have shown shifts in AAnPB communities across spatial gradients, with some assemblages appearing more adapted to oligotrophic and others to eutrophic environments (Jiao *et al.*, 2007; Yutin *et al.*, 2007; Lehours *et al.*, 2010; Bibiloni-Isaksson *et al.*, 2016). In this study we found that although significant differences in community composition between regions were found, this reflected shifts in the relative abundance of taxa responding to gradients of oxygen, fluorescence, salinity, temperature, phosphate, silicate, Divinyl Chla and Chla, rather than a turnover of taxa. This highlights gammaproteobacterial AAnPB in northern Australian waters to inhabit quite diverse tropical oceanic regions,

We also observed a marked switch in the abundance and composition of the PRBA community between ATS and Coral Sea waters, and unlike the AAnPB, this shift was characterised by community turnover For instance SAR11-like, SAR116 clade A and Betaproteobacteria related sequences were mainly observed in the ATS. On the other hand, members of the Archaea group IIb, SAR11 clade, SAR116 clade B and *Flavobacteria* were more abundant in the Coral Sea,

These differences in cause of biogeographic patterns in the different photoheterotrophic bacteria suggest alternative ecological mechanisms driving

AAnPB and PRBA distributions in northern Australian waters. AAnPB taxa appear capable of inhabiting a wide range of environmental variables and their distributions may be governed by neutral facots, wheras the high turnover of PRBA taxa between the ATS and Coral Sea suggest niche factors control the dynamics of this group. This is supported by the differences in PRBA observed with latitude (between the north western and southern stations) and longitude (western and eastern stations), which clustered separately according to gradients in salinity, temperature, Chl*a* and phosphate.

We observed a dominance of Betaproteobacteria related sequences in the ATS, while in the Coral Sea they were generally absent. The Betaproteobacteria are a large and cosmopolitan class with a range of ecological roles in the global ocean (reviewed in Kirchman, 2008). The OM43 clade of Betaproteobacteria is associated with coastal phytoplankton blooms (Morris et al., 2006). In our study, Betaproteobacteria sequences were related to a cultured proteorhodopsin-containing representative (Strain MOLA814, 79% amino acid identity), commonly observed in the Ocean.

An interesting observation was the predominance of SAR11 PRBA in the ATS, while in the Coral Sea Archaea sequences dominated the community. It is perhaps surprising that SAR11, given its typical oligotrophic lifestyle, genome streamlining and potentially reduced capacity to respond to changing conditions, was equally sensitive to changes in Chl*a* as other heterotrophic groups (e.g., Gammaproteobacteria). Marine group IIb Archaea were the dominant taxonomic

group in the Coral Sea which resulted in the predominance of BPRs. The observation of abundant MGIIb in the oligotrophic Coral Sea is inconsistent with some other recent studies. For instance, archaeal seasonal variability was reported in the east coast of Australia (Bibiloni-Isaksson *et al.,* 2016, unpublished), where MG IIb were more abundant during periods of winter mixing when nutrients concentrations were high, and MG IIa became predominant in summer when nutrients were depleted. Similarly, summer peaks in the abundance and activity of MG IIa in surface waters were observed in the Mediterranean Sea, and were apparently linked to the enhanced phototrophy in response to greater irradiance (Hugoni *et al.,* 2013). It is possible that salinity and temperature are the most important drivers of transitions between Archaea IIa and IIb (Iverson *et al.,* 2012; Deschamps *et al.,* 2014),or that other factors not measured in these studies are responsible.

We observed a transition away from green light absorbing proteorhodopsins to blue light absorbing proteorhodopsins as we moved from the ATS to Coral Sea, which is consistent with the different water properties of these two regions. The semi-enclosed Arafura and Timor Seas (ATS) is relatively shallow and exhibits high productivity, whereas the Coral Sea is characterise by deep blue, nutrient-poor waters. During this transition from ATS to Coral the BPR containing taxa *Archaea* Group IIb, *Glaciecola* and SAR11 B became more abundant, while GPR containing taxa, including SAR11 like sequences, SAR116 clade A and *Betaproteobacteria* became less abundant. However, among the GPR groups, those containing methionine became more abundant in the

Coral Sea, mainly due to increases in the abundance of *Flavobacteria* related sequences. One of the few studies on seasonal adaptation and spectral tuning in marine proteorhodopsin (Sabehi *et al.,* 2007) found that in the Sargasso Sea all PRs were BPR, while in the Mediterranean Sea most were GPR at the surface and BPR in deeper waters. Recently we demonstrated that seasonality in proteorhodopsin spectral tuning occurs, with high diversity in proteorhodopsin types despite similar physical water column properties such as particles and light availability. All of these observations suggest that differential exploitation of the light spectrum via the use of variants of proteorhodopsin underpin a separation of the proteorhodopsin community across different water column properties. Therefore as stated by Stomp *et al*. (2007) utilisation of different features of the light spectrum could provide opportunities for niche differentiation and allows coexistence of PRBA species absorbing different wavelength of the light.

Conclusion

We show that the separation of different oceanic regions serve as clear transition zones in the composition and diversity of photoheterotrophic microbes in the ocean. Understanding the factors controlling the distribution of marine microbes is crucial if we are to reveal how marine ecosystems will respond to climate change. We suggest that boundaries of oceanic regions can act as key features, similar to ecotones. Lefort and Gasol (2013) demonstrated that salinity is a major barrier to microbial aquatic

communities, showing a strong global-scale distributions of marine surface bacterioplankton groups along gradients of salinity, temperature, and chlorophyll. Recently, Baltar *et al.* (2016) demonstrated strong shifts in bacterioplankton community composition across the subtropical frontal zone off New Zealand. In these studies transitions between water masses resulted in a clear modification of the dominant taxa and a significant increase in community dissimilarity. Our study shows differences in the response to oceanic transition zones in different photoheterotrophic groups. AAnPB populations responded by shifting the relative abundance of predominantly the same taxa, while PRBA displayed near complete taxonomic turnover from the eutrophic conditions of the ATS to the oligotrophic conditions of the Coral Sea, revealing potentially different ecological strategies in these groups.

Acknowledgements

We gratefully thank the scientific crew, captain and scientists on-board the *R/V Southern Surveyor* for assistance with sampling and nutrient analyses. This research was supported by the Australian Research Council Discovery Grant Scheme (DP120102764 to JS and MB, FT130100218 to JS, and DP0988002 to MB).

Supplementary material

Table S1: Environmental variables from surface water (5m) and DCM during the s

winter 2013 voyage within Australia's tropical marine waters (as Appendix IV).

Table S2: PCR primers used for screening environmental DNA and for determining gene abundance using qPCR.

Primer name	**Sequence (5′→3′)**	***Ta*[a] (°C)**	**Product size (bp)**	**Application**	**Reference**
pufM-557F	TAC GGS AAC CTG TWC TAC	56	~240	*pufM* Miseq Illumina sequencing and Q-PCR	Yutin *et al.* (2007); Ritchie and Johnson (2012)
*pufM*_WAWR	AYN GCR AAC CAC CAN GCC CA				
PR1	MGN TAY ATH GAY TGG YT	47	~312	Proteorhodopsin Miseq Illumina sequencing	Sabehi *et al.* (2005)
PR2	WWN MGN TAY GTN GAY TGG				
PR3	GGR TAD ATN GCC CAN CC				
SARPR_125F	HG GWG GAT AYT TAG GWG AAG C	54	~163	SAR11 proteorhodopsin Q-PCR	Riedel *et al.* 2010; Campbell *et al.* (2008)
SARPR_288R	CCC AAC CWA YWG TWA CRA TCA TTC T				
BACT1369F	CGG TGA ATA CGT TCY CGG	58	~174	Total bacterial rRNA gene Q-PCR	Suzuki *et al.* (2001)
PROK1543R	AAG GAG GTG ATC CR GCC GCA				

[a] *Ta*, annealing temperature.

Table 1: Average, standard deviation, maximum and minimum values for ratio of genes and richness and diversity values.

	ATS Surface	ATS DCM	Coral Sea Surface	Coral Sea DCM
***pufM*/16S genes**	3.11(1.30); 5.46-1.23	1.79(0.65); 2.61-1.14	2.28(1.63); 5.27-0.70	3.08(1.44); 4.62-1.46
SAR11PR/16S genes	27.79(9.5); 43.82-13.94	17.82(1.05); 18.92-16.64	31.82(8.01); 44.46-22.89	27.5(15.11); 44.50-4.98
chao1 (*pufM*)	189.89(61.91); 311-133.54	166.55(10.23); 178.07-151	207.73(38.83); 248.4-147.1	182.39(34.83); 228.15-140
chao1 (PR)	132.36(30.16); 167.2-70.55	134.64(20.94); 169.15-114.6	266.26(40.02); 310.81-232	268.49(40.04); 310.57-212.4
Margalef (*pufM*)	11.55(1.92); 15.05-9.26	11.34(1.86); 12.88-8.97	12.78(2.71); 16.35-9.40	12.71(2.45); 14.47-8.39
Margalef (PR)	11.92(2.03); 15.51-8.37	12.04(1.27); 13.19-9.93	24.28(3.85); 27.77-19.70	23.49(4.77); 28.24-16.29
Shannon (*pufM*)	3.60(0.34); 4.05-2.94	3.52(0.48); 4.10-2.84	3.50(0.46); 4.08-3.01	3.66(0.49); 4.13-3.07
Shannon (PR)	4.21(0.49); 4.894-3.29	4.41(0.16); 4.58-4.19	6.14(0.55); 6.61-5.38	6.01(0.61); 6.40-4.96
Simpson (*pufM*)	0.84(0.03); 0.89-0.78	0.82(0.06); 0.89-0.72	0.78(0.05); 0.87-0.73	0.82(0.06); 0.87-0.70
Simpson (PR)	0.88(0.04); 0.92-0.79	0.90(0.02); 0.92-0.88	0.96(0.01); 0.98-0.93	0.96(0.02); 0.97-0.92

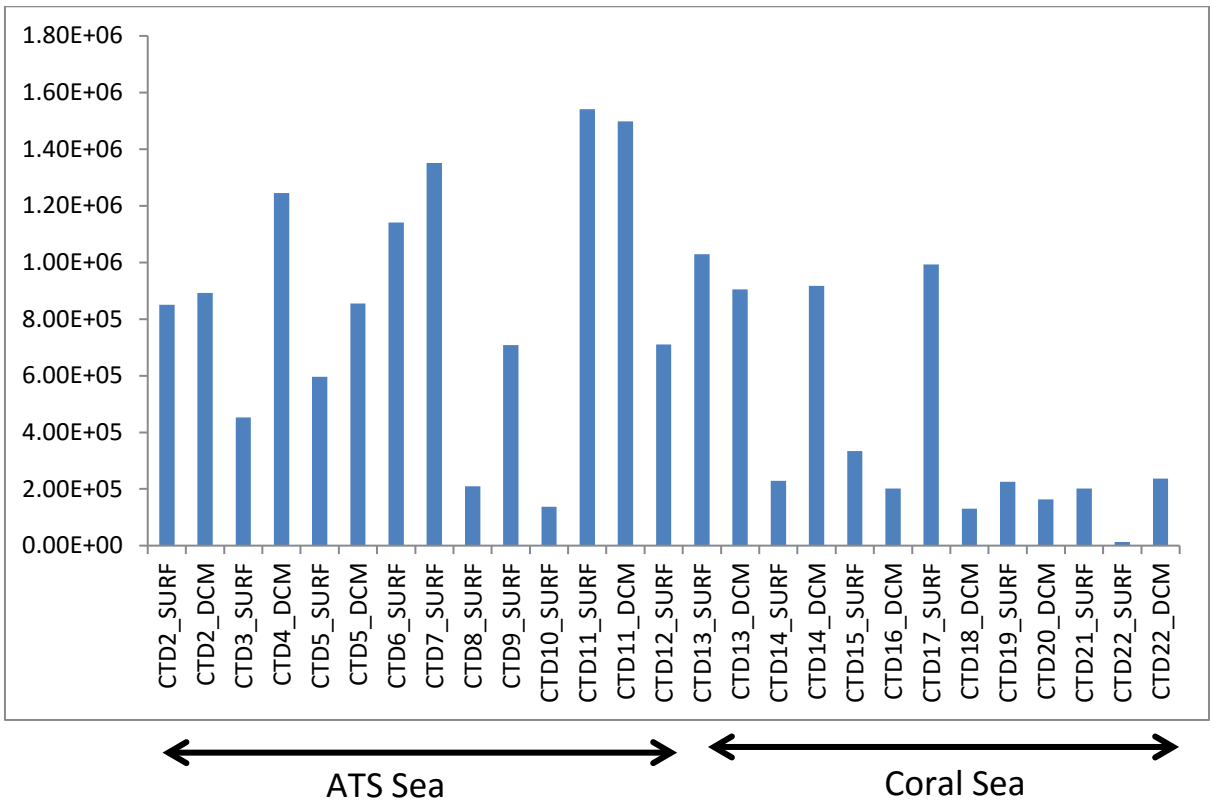

Figure S1: Total 16S rRNA abundance across both regions and surface and DCM

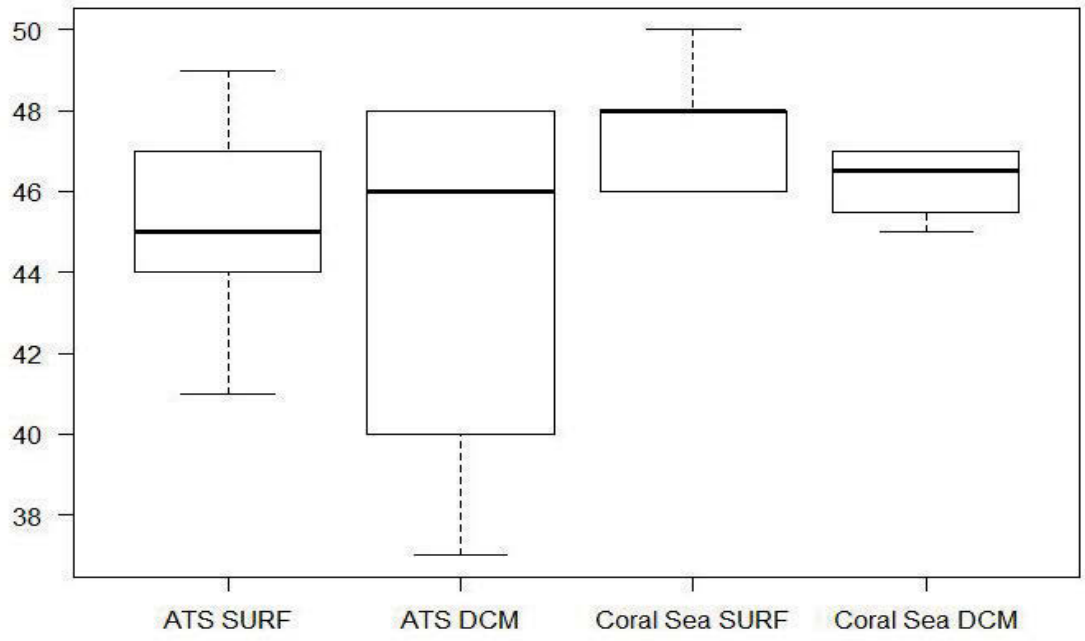
50
48
46
44
42
40
38
ATS SURF
ATS DCM
Coral Sea SURF
Coral Sea DCM

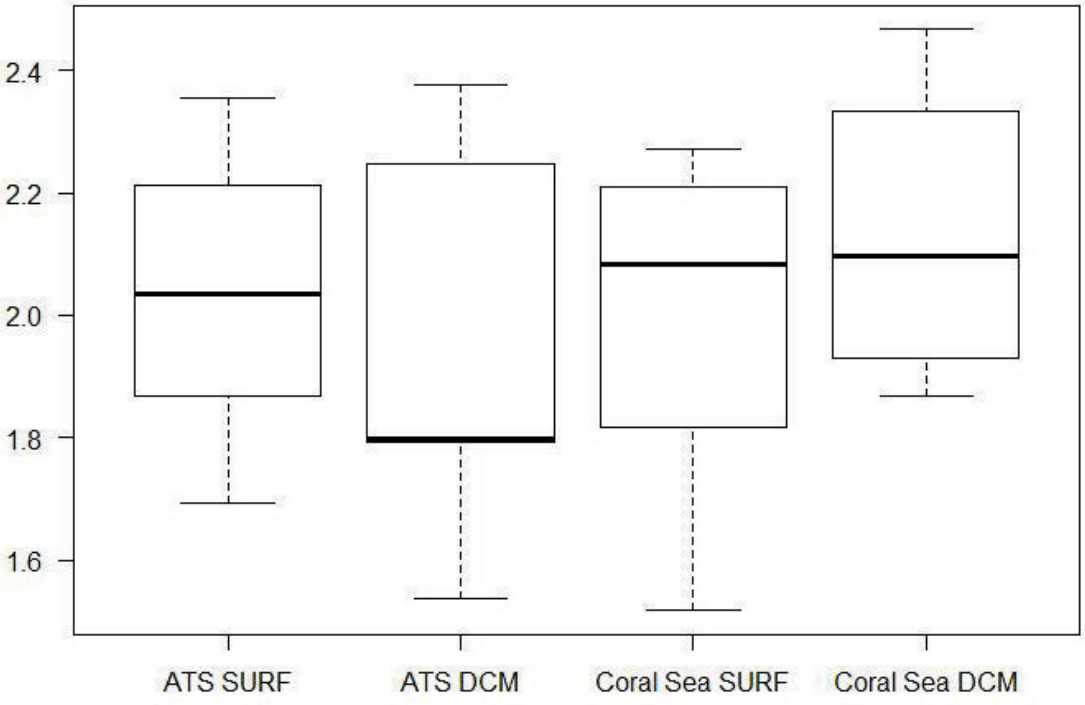
2.4
2.2
2.0
1.8
1.6
ATS SURF
ATS DCM
Coral Sea SURF
Coral Sea DCM

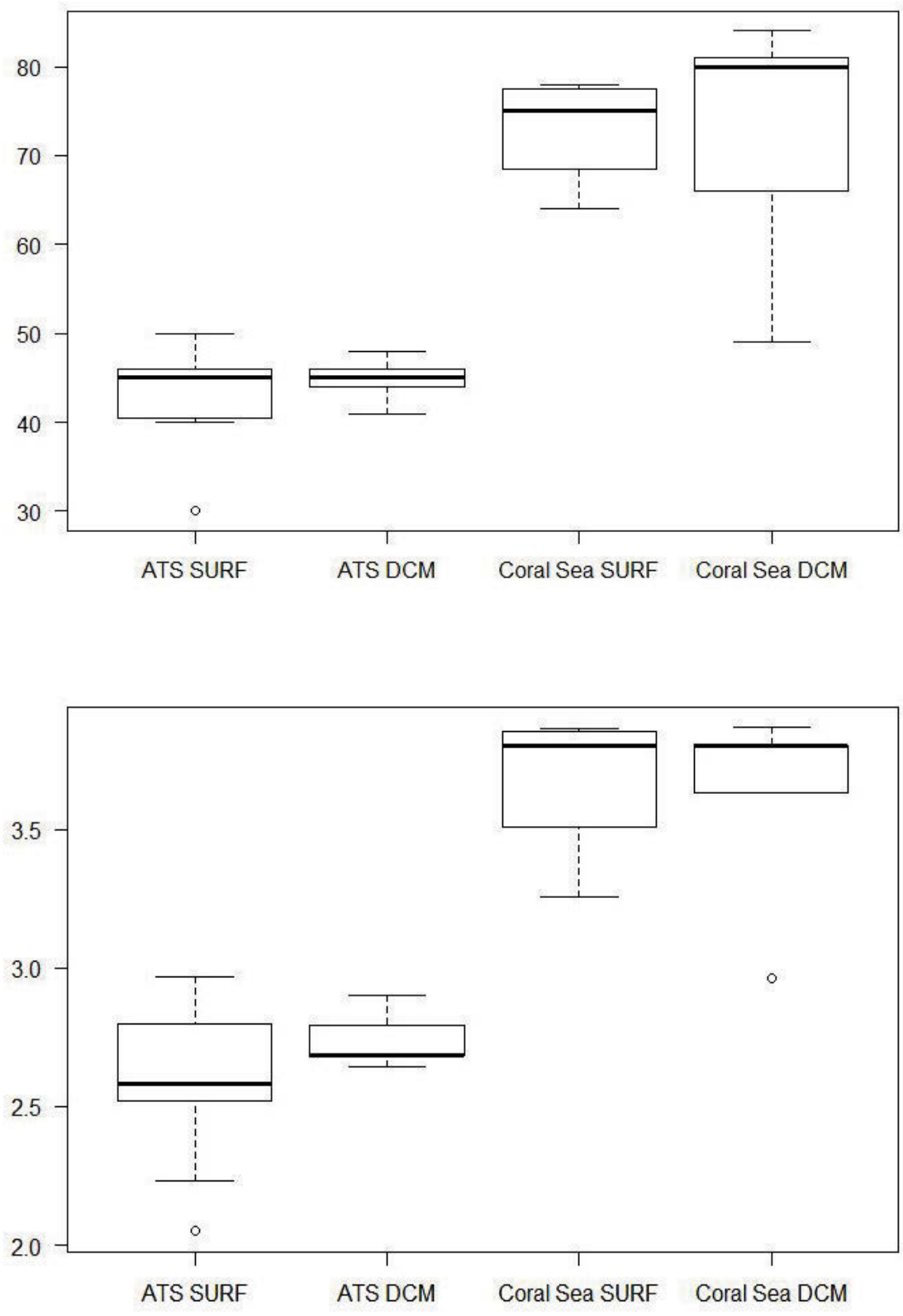

Figure S2: Box and whiskers representation of indices used to describe bacterial community richness and Shannon's diversity index at ATS (a, b) and Coral (c, d). The box indicates median and quartile values, and the whiskers indicate the range (minima and maxima).

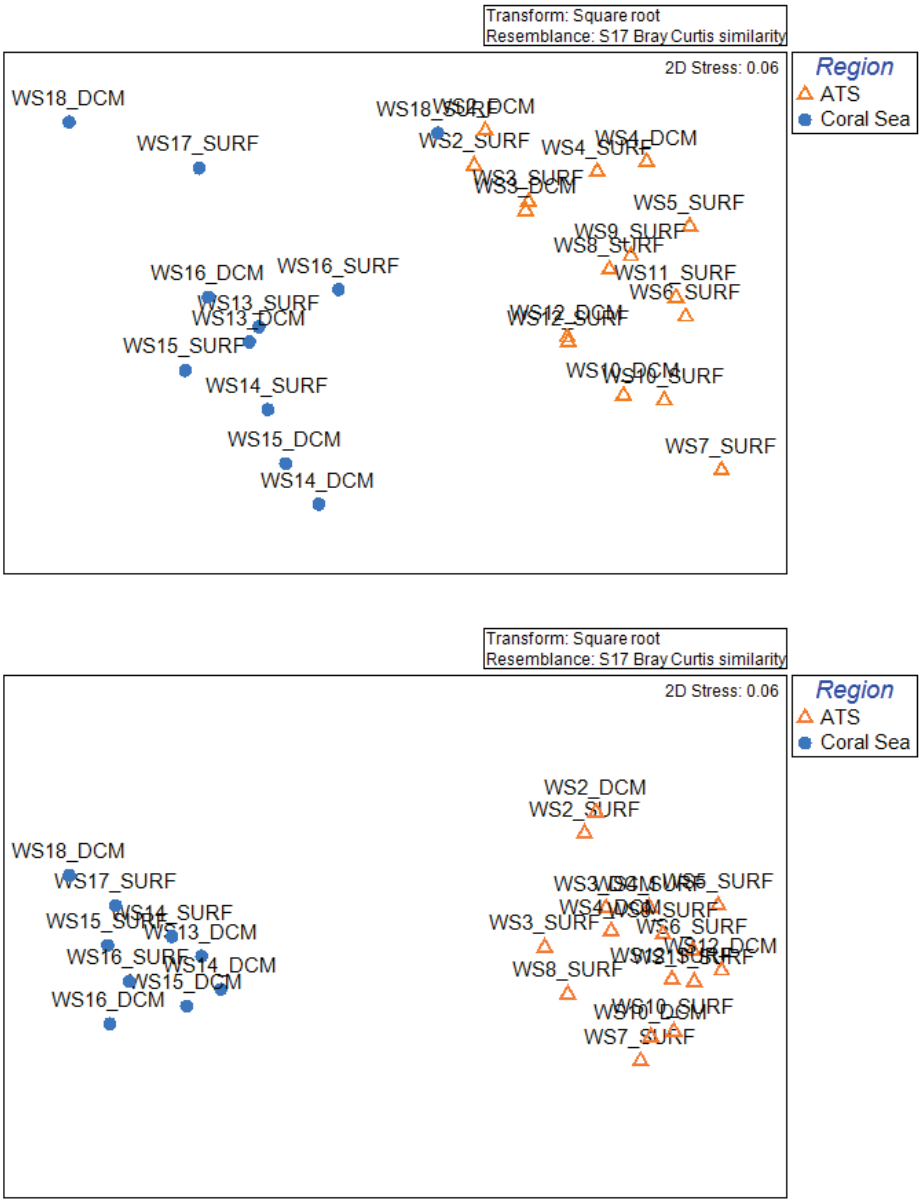

Figure S3: nMDS ordination of the dissimilarity in AAnPB (top) and PRBA(bottom) assemblages (both nMDS stress = 0.06). The ordination is based on Bray-Curtis similarities calculated from square-root transformed AAnPB abundances (51 OTUs) and PRBA (122 OTUs).

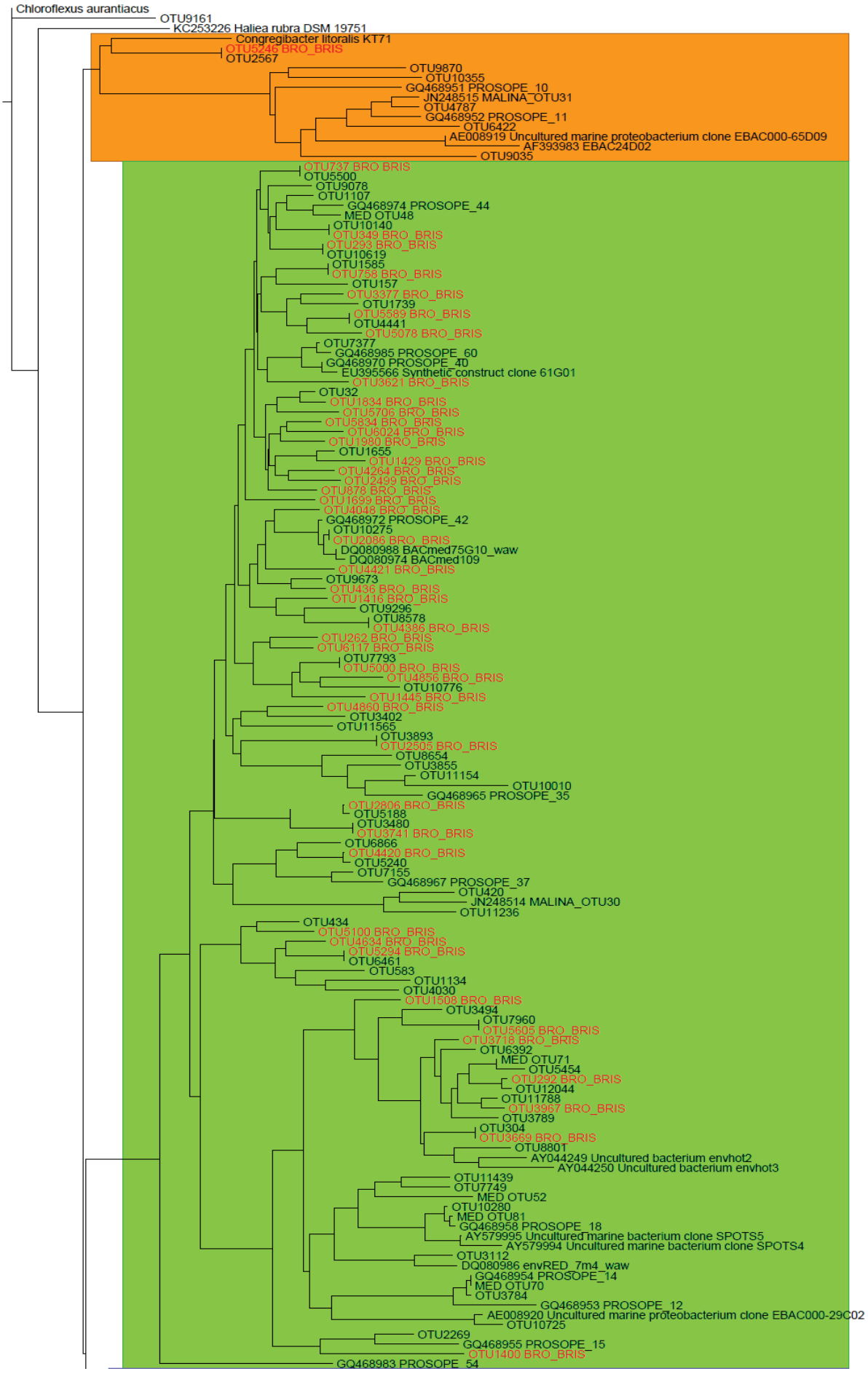
Chloroflexus aurantiacus
OTU9161
KC253226 Haliea rubra DSM 19751
Congregibacter litoralis KT71
OTU5246 BRO_BRIS
OTU2567
OTU9870
OTU10355
GQ468951 PROSOPE_10
JN248515 MALINA_OTU31
OTU4787
GQ468952 PROSOPE_11
OTU6422
AE008919 Uncultured marine proteobacterium clone EBAC000-65D09
AF393983 EBAC24D02
OTU9035
OTU737 BRO_BRIS
OTU5500
OTU9078
OTU1107
GQ468974 PROSOPE_44
MED OTU48
OTU10140
OTU349 BRO_BRIS
OTU293 BRO_BRIS
OTU10619
OTU1585
OTU758 BRO_BRIS
OTU157
OTU3377 BRO_BRIS
OTU1739
OTU5589 BRO_BRIS
OTU4441
OTU5078 BRO_BRIS
OTU7377
GQ468985 PROSOPE_60
GQ468970 PROSOPE_40
EU395566 Synthetic construct clone 61G01
OTU3621 BRO_BRIS
OTU32
OTU1834 BRO_BRIS
OTU5706 BRO_BRIS
OTU5834 BRO_BRIS
OTU6024 BRO_BRIS
OTU1980 BRO_BRIS
OTU1655
OTU1429 BRO_BRIS
OTU4264 BRO_BRIS
OTU2499 BRO_BRIS
OTU878 BRO_BRIS
OTU1699 BRO_BRIS
OTU4048 BRO_BRIS
GQ468972 PROSOPE_42
OTU10275
OTU2086 BRO_BRIS
DQ080988 BACmed75G10_waw
DQ080974 BACmed109
OTU4421 BRO_BRIS
OTU9673
OTU436 BRO_BRIS
OTU1416 BRO_BRIS
OTU9296
OTU8578
OTU4386 BRO_BRIS
OTU262 BRO_BRIS
OTU6117 BRO_BRIS
OTU7793
OTU5000 BRO_BRIS
OTU4856 BRO_BRIS
OTU10776
OTU1445 BRO_BRIS
OTU4860 BRO_BRIS
OTU3402
OTU11565
OTU3893
OTU2505 BRO_BRIS
OTU8654
OTU3855
OTU11154
OTU10010
GQ468965 PROSOPE_35
OTU2806 BRO_BRIS
OTU5188
OTU3480
OTU3741 BRO_BRIS
OTU6866
OTU4426 BRO_BRIS
OTU5240
OTU7155
GQ468967 PROSOPE_37
OTU420
JN248514 MALINA_OTU30
OTU11236
OTU434
OTU5100 BRO_BRIS
OTU4634 BRO_BRIS
OTU5294 BRO_BRIS
OTU6461
OTU583
OTU1134
OTU4030
OTU1508 BRO_BRIS
OTU3494
OTU7960
OTU5605 BRO_BRIS
OTU3718 BRO_BRIS
OTU6392
MED OTU71
OTU5454
OTU292 BRO_BRIS
OTU12044
OTU11788
OTU3967 BRO_BRIS
OTU3789
OTU304
OTU3689 BRO_BRIS
OTU880T
AY044249 Uncultured bacterium envhot2
AY044250 Uncultured bacterium envhot3
OTU11439
OTU7749
MED OTU52
OTU10280
MED OTU81
GQ468958 PROSOPE_18
AY579995 Uncultured marine bacterium clone SPOTS5
AY579994 Uncultured marine bacterium clone SPOTS4
OTU3112
DQ080986 envRED_7m4_waw
GQ468954 PROSOPE_14
MED OTU70
OTU3784
GQ468953 PROSOPE_12
AE008920 Uncultured marine proteobacterium clone EBAC000-29C02
OTU10725
OTU2269
GQ468955 PROSOPE_15
OTU1400 BRO_BRIS
GQ468983 PROSOPE_54


OTU1633
DS999405 gamma proteobacterium NOR5-3
OTU6312
OTU1290
EU196298 Arctic spring bacterium CP26
OTU1877
OTU7605
DQ484037 Erythrobacter JL475
AY326260 Erythrobacter sp. NAP1
AY326265 Erythrobacter sp. BA13
AY326261 Erythrobacter sp. COL13
AY326264 Erythrobacter sp. NJ3Y
AB010981 Erythrobacter litoralis
AB020599 Porphyrobacter tepidarius MBIC3363
EU564436 Erythromicrobium B04
JN248476 MALINA_OTU11
AB031016 Sphingomonas ursincola
OTU9548
JN248488 MALINA_OTU15
JN248516 MALINA_OTU32
JN248466 MALINA_OTU02
HM003578 Sphingomonas humi PB323
AY853585 Sphingomonas PB229
AY853584 Sphingomonas PB180
JN248467 MALINA_OTU03
JN248508 MALINA_OTU27
CP002292 Rhodomicrobium vannielii
DQ080991 Citromicrobium CV44
DQ915719 Roseivivax halotolerans NBRC16686
HQ663708 Gamma proteobacterium SCGC AAA027-D16
FR852762 Thalassobaculum RCC 1910
MED OTU54
JN248473 MALINA_OTU08
AF182374 Bradyrhizobium ORS278
DQ017875 Bradyrhizobium denitrificans
DQ017854 Blastobacter denitrificans strain
AY390602 Rhodospirillum rubrum
HE565696 Rhodospirillum
J03731 R.rubrum
FM208080 Roseospira visakhapatnamensis
D50681 Rhodospirillum photometricum
AY242845 Roseospirillum parvum
AM773547 Roseateles terrae
AM773546 Roseateles depolymerans
D85518 Thermochromatium tepidum
AB543090 Thermochromatium tepidum
EU910949 Chromatiaceae bacterium
EU910948 Thermochromatium tepidum ATCC 43061
EU910946 Chromatiaceae bacterium G8
D50647 Chromatium vinosum
FJ812042 Allochromatium vinosum DSM 180
FN257131 Allochromatium vinosum
FJ812046 Allochromatium renukae strain DSM 18713
FN257155 Allochromatium MT6010
EU910945 Thiocapsa imhoffii
EU910952 Chromatiaceae bacterium GVC4
EU921780 Uncultured bacterium clone C1
AJ544223 Thiocapsa roseopersicina
EU910951 Thiocapsa roseopersicina strain DSM 217
FN257146 Thiocapsa roseopersicina
FN257140 Thiocapsa marina
FN257149 Thiocystis violacea
CP000463 Rhodopseudomonas palustris BisA53
CP001096 Rhodopseudomonas palustris
BX572597 Rhodopseudomonas palustris
AB241418 Rhodopseudomonas oryzae
KC465430 Rhodopseudomonas W2
FR846226 Rhodopseudomonas JA576
FR846223 Rhodopseudomonas JA575
GU080287 Proteobacterium G11
AB498859 Rhodopseudomonas palustris
FN821502 Marichromatium JA553
FJ376396 Marichromatium purpuratum
HQ663707 Gamma proteobacterium SCGC AAA024-O13
CP001280 Methylocella silvestris BL2
OTU2005
AB013379 Acidiphilium acidophilum
AB005220 Acidiphilium cryptum
AB005219 Acidiphilium angustum
AB005218 Acidiphilium rubrum
AB034704 Rubrivivax gelatinosus
D16822 Rubrivivax gelatinosus
AY234384 Rubrivivax gelatinos
AJ010302 Rhodobacter sphaeroides
AB062783 Rhodobacter azotoformans
KC465420 Rhodobacter W1
CP001312 Rhodobacter capsulatus SB 1003
Z11165 R.capsulatus
AB189946 Rhodobacter blasticus
D50649 Rhodobacter blasticus
AB062784 Rhodobacter veldkampii
EU196353 Loktanella NP29
EU196352 Alkalibacterium NP13
GQ468950 PROSOPE 9
JQ995753 Roseicitreum antarcticum strain ZS2-28
CP000264 Jannaschia CCS1
DQ915720 Roseovarius tolerans NBRC16695
DQ915724 Thalassobacter stenotrophicus CECT529
OTU2343 BRO_BRIS
CP000830 Dinoroseobacter shibae
KM669766 Rhodobacteraceae bacterium TS-T30
EU009365 Roseobacter B09
FR852763 Marivita RCC 1921
EU026123 Roseobacter WM2
DQ915721 Roseobacter denitrificans NBRC15277
CP002624 Roseobacter litoralis Och 149
AB016990 Roseobacter litoralis
NZ_ABIG01000015 Roseobacter litoralis
OTU7468
CP004372 Roseibacterium elongatum DSM 1949
AY177986 Uncultured proteobacterium clone LFc17
GQ468981 PROSOPE_51
OTU3177 BRO_BRIS
OTU9180
FN984739 Rhodovulum sp. MTCH3IM048
AB088687 Rhodovulum strictum
AB020784 Rhodovulum sulfidophilum
OTU9971
OTU163
OTU8372
OTU4227
OTU4212
OTU2352 BRO_BRIS
OTU10101
EU009366 Roseobacter B11
FR852764 Bacterium RCC 1922
AF393993 Alpha proteobacterium R2A163

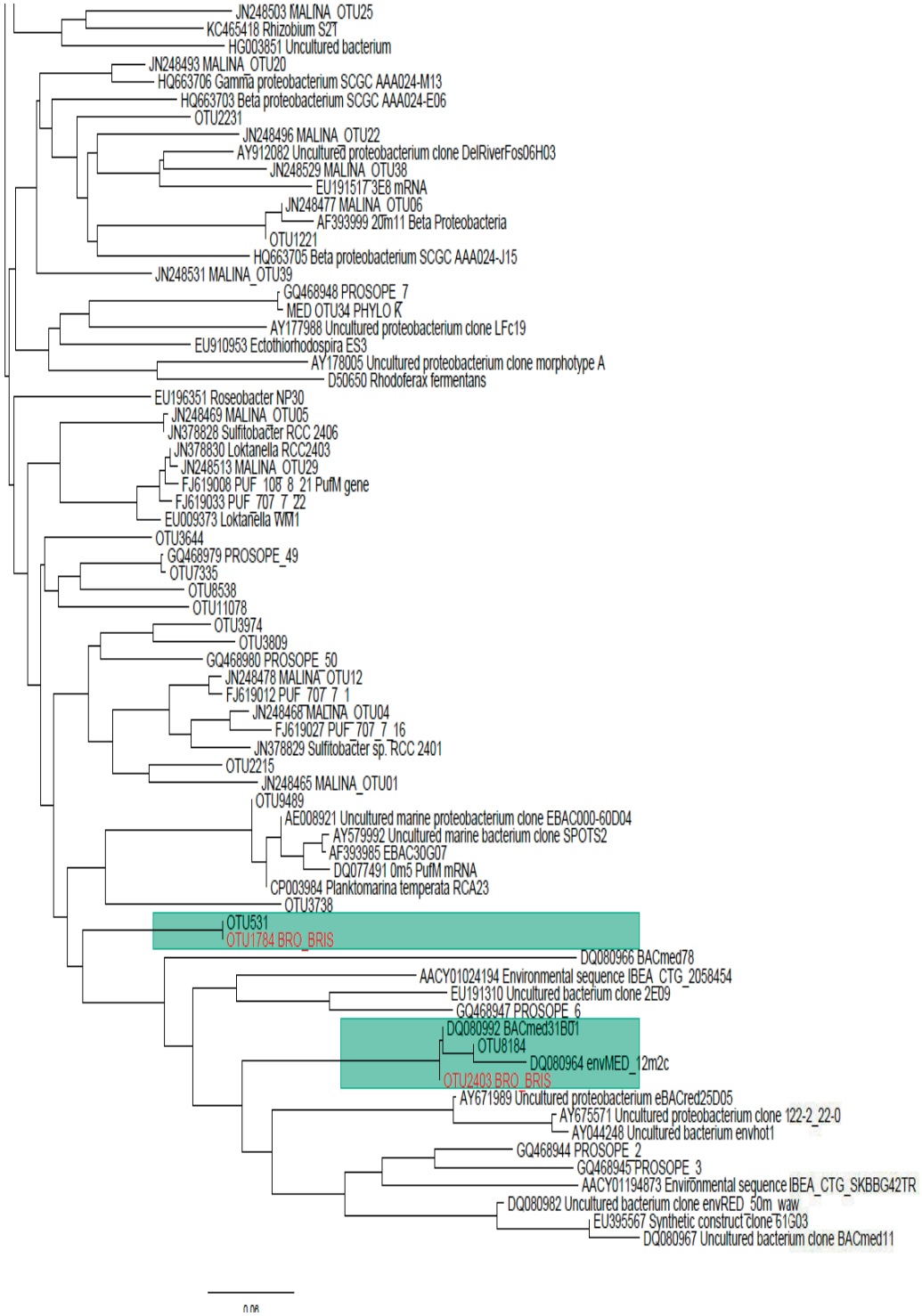

Figure S4: Phylogenetic tree showing the relationships between *pufM* gene sequences from this study and environmental samples and nearest relatives retrieved from GenBank. The tree is based on a Bayesian tree to which short sequences were added by ARB_PARSIMONY.

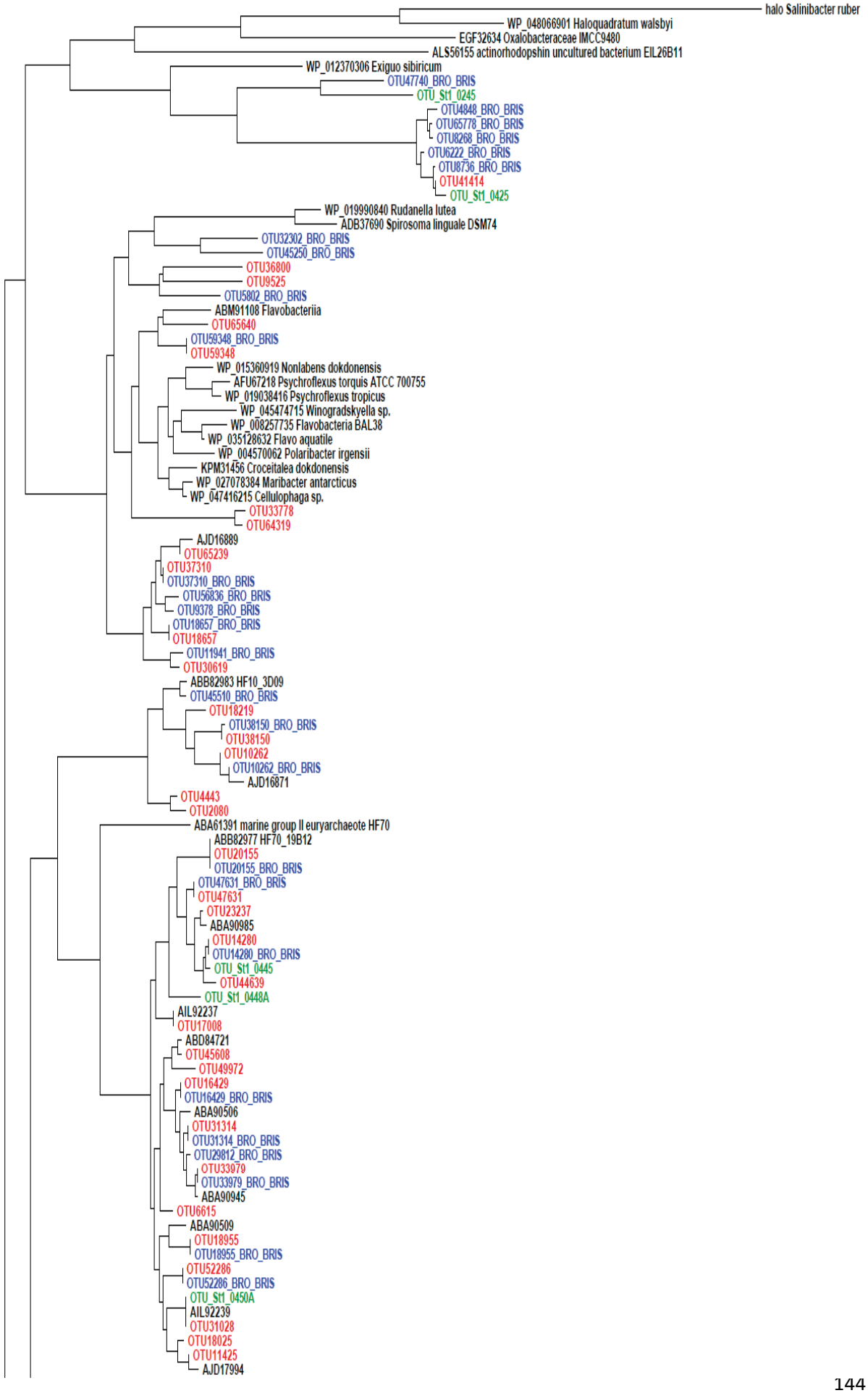
halo Salinibacter ruber
WP_048066901 Haloquadratum walsbyi
EGF32634 Oxalobacteraceae IMCC9480
ALS56155 actinorhodopshin uncultured bacterium EIL26B11
WP_012370306 Exiguo sibiricum
OTU47740_BRO_BRIS
OTU_St1_0245
OTU4848_BRO_BRIS
OTU65778_BRO_BRIS
OTU8268_BRO_BRIS
OTU6222_BRO_BRIS
OTU8736_BRO_BRIS
OTU41414
OTU_St1_0425
WP_019990840 Rudanella lutea
ADB37690 Spirosoma linguale DSM74
OTU32302_BRO_BRIS
OTU45250_BRO_BRIS
OTU36800
OTU9525
OTU5802_BRO_BRIS
ABM91108 Flavobacteriia
OTU65640
OTU59348_BRO_BRIS
OTU59348
WP_015360919 Nonlabens dokdonensis
AFU67218 Psychroflexus torquis ATCC 700755
WP_019038416 Psychroflexus tropicus
WP_045474715 Winogradskyella sp.
WP_008257735 Flavobacteria BAL38
WP_035128632 Flavo aquatile
WP_004570062 Polaribacter irgensii
KPM31456 Croceitalea dokdonensis
WP_027078384 Maribacter antarcticus
WP_047416215 Cellulophaga sp.
OTU33778
OTU64319
AJD16889
OTU65239
OTU37310
OTU37310_BRO_BRIS
OTU56836_BRO_BRIS
OTU9378_BRO_BRIS
OTU18657_BRO_BRIS
OTU18657
OTU11941_BRO_BRIS
OTU30619
ABB82983 HF10_3D09
OTU45510_BRO_BRIS
OTU18219
OTU38150_BRO_BRIS
OTU38150
OTU10262
OTU10262_BRO_BRIS
AJD16871
OTU4443
OTU2080
ABA61391 marine group II euryarchaeote HF70
ABB82977 HF70_19B12
OTU20155
OTU20155_BRO_BRIS
OTU47631_BRO_BRIS
OTU47631
OTU23237
ABA90985
OTU14280
OTU14280_BRO_BRIS
OTU_St1_0445
OTU44639
OTU_St1_0448A
AIL92237
OTU17008
ABD84721
OTU45608
OTU49972
OTU16429
OTU16429_BRO_BRIS
ABA90506
OTU31314
OTU31314_BRO_BRIS
OTU29812_BRO_BRIS
OTU33979
OTU33979_BRO_BRIS
ABA90945
OTU6615
ABA90509
OTU18955
OTU18955_BRO_BRIS
OTU52286
OTU52286_BRO_BRIS
OTU_St1_0450A
AIL92239
OTU31028
OTU18025
OTU11425
AJD17994

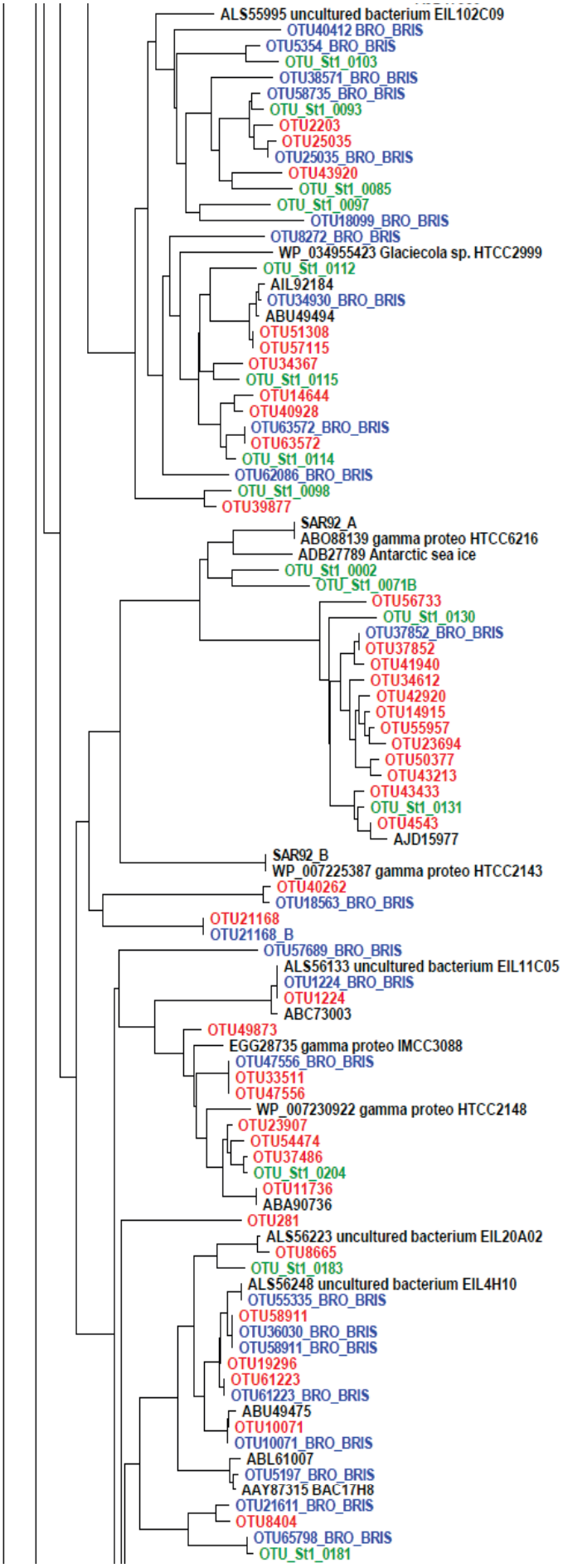
ALS55995 uncultured bacterium EIL102C09
OTU40412 BRO_BRIS
OTU5354_BRO_BRIS
OTU_St1_0103
OTU38571_BRO_BRIS
OTU58735_BRO_BRIS
OTU_St1_0093
OTU2203
OTU25035
OTU25035_BRO_BRIS
OTU43920
OTU_St1_0085
OTU_St1_0097
OTU18099_BRO_BRIS
OTU8272_BRO_BRIS
WP_034955423 Glaciecola sp. HTCC2999
OTU_St1_0112
AIL92184
OTU34930_BRO_BRIS
ABU49494
OTU51308
OTU57115
OTU34367
OTU_St1_0115
OTU14644
OTU40928
OTU63572_BRO_BRIS
OTU63572
OTU_St1_0114
OTU62086_BRO_BRIS
OTU_St1_0098
OTU39877
SAR92_A
ABO88139 gamma proteo HTCC6216
ADB27789 Antarctic sea ice
OTU_St1_0002
OTU_St1_0071B
OTU56733
OTU_St1_0130
OTU37852_BRO_BRIS
OTU37852
OTU41940
OTU34612
OTU42920
OTU14915
OTU55957
OTU23694
OTU50377
OTU43213
OTU43433
OTU_St1_0131
OTU4543
AJD15977
SAR92_B
WP_007225387 gamma proteo HTCC2143
OTU40262
OTU18563_BRO_BRIS
OTU21168
OTU21168_B
OTU57689_BRO_BRIS
ALS56133 uncultured bacterium EIL11C05
OTU1224_BRO_BRIS
OTU1224
ABC73003
OTU49873
EGG28735 gamma proteo IMCC3088
OTU47556_BRO_BRIS
OTU33511
OTU47556
WP_007230922 gamma proteo HTCC2148
OTU23907
OTU54474
OTU37486
OTU_St1_0204
OTU11736
ABA90736
OTU281
ALS56223 uncultured bacterium EIL20A02
OTU8665
OTU_St1_0183
ALS56248 uncultured bacterium EIL4H10
OTU55335_BRO_BRIS
OTU58911
OTU36030_BRO_BRIS
OTU58911_BRO_BRIS
OTU19296
OTU61223
OTU61223_BRO_BRIS
ABU49475
OTU10071
OTU10071_BRO_BRIS
ABL61007
OTU5197_BRO_BRIS
AAY87315 BAC17H8
OTU21611_BRO_BRIS
OTU8404
OTU65798_BRO_BRIS
OTU_St1_0181

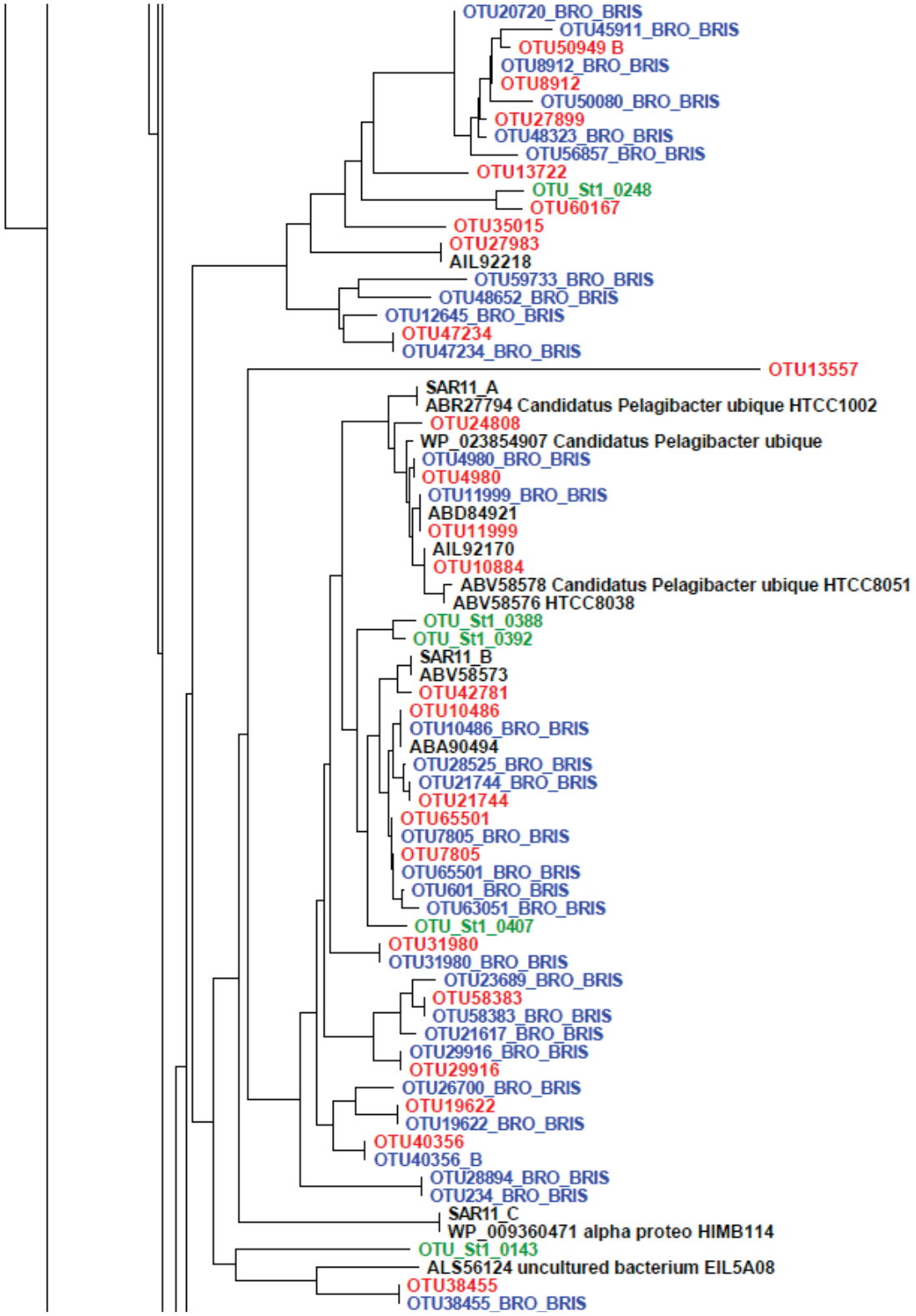
OTU20720_BRO_BRIS
OTU45911_BRO_BRIS
OTU50949 B
OTU8912_BRO_BRIS
OTU8912
OTU50080_BRO_BRIS
OTU27899
OTU48323_BRO_BRIS
OTU56857_BRO_BRIS
OTU13722
OTU_St1_0248
OTU60167
OTU35015
OTU27983
AIL92218
OTU59733_BRO_BRIS
OTU48652_BRO_BRIS
OTU12645_BRO_BRIS
OTU47234
OTU47234_BRO_BRIS
OTU13557
SAR11_A
ABR27794 Candidatus Pelagibacter ubique HTCC1002
OTU24808
WP_023854907 Candidatus Pelagibacter ubique
OTU4980_BRO_BRIS
OTU4980
OTU11999_BRO_BRIS
ABD84921
OTU11999
AIL92170
OTU10884
ABV58578 Candidatus Pelagibacter ubique HTCC8051
ABV58576 HTCC8038
OTU_St1_0388
OTU_St1_0392
SAR11_B
ABV58573
OTU42781
OTU10486
OTU10486_BRO_BRIS
ABA90494
OTU28525_BRO_BRIS
OTU21744_BRO_BRIS
OTU21744
OTU65501
OTU7805_BRO_BRIS
OTU7805
OTU65501_BRO_BRIS
OTU601_BRO_BRIS
OTU63051_BRO_BRIS
OTU_St1_0407
OTU31980
OTU31980_BRO_BRIS
OTU23689_BRO_BRIS
OTU58383
OTU58383_BRO_BRIS
OTU21617_BRO_BRIS
OTU29916_BRO_BRIS
OTU29916
OTU26700_BRO_BRIS
OTU19622
OTU19622_BRO_BRIS
OTU40356
OTU40356_B
OTU28894_BRO_BRIS
OTU234_BRO_BRIS
SAR11_C
WP_009360471 alpha proteo HIMB114
OTU_St1_0143
ALS56124 uncultured bacterium EIL5A08
OTU38455
OTU38455_BRO_BRIS

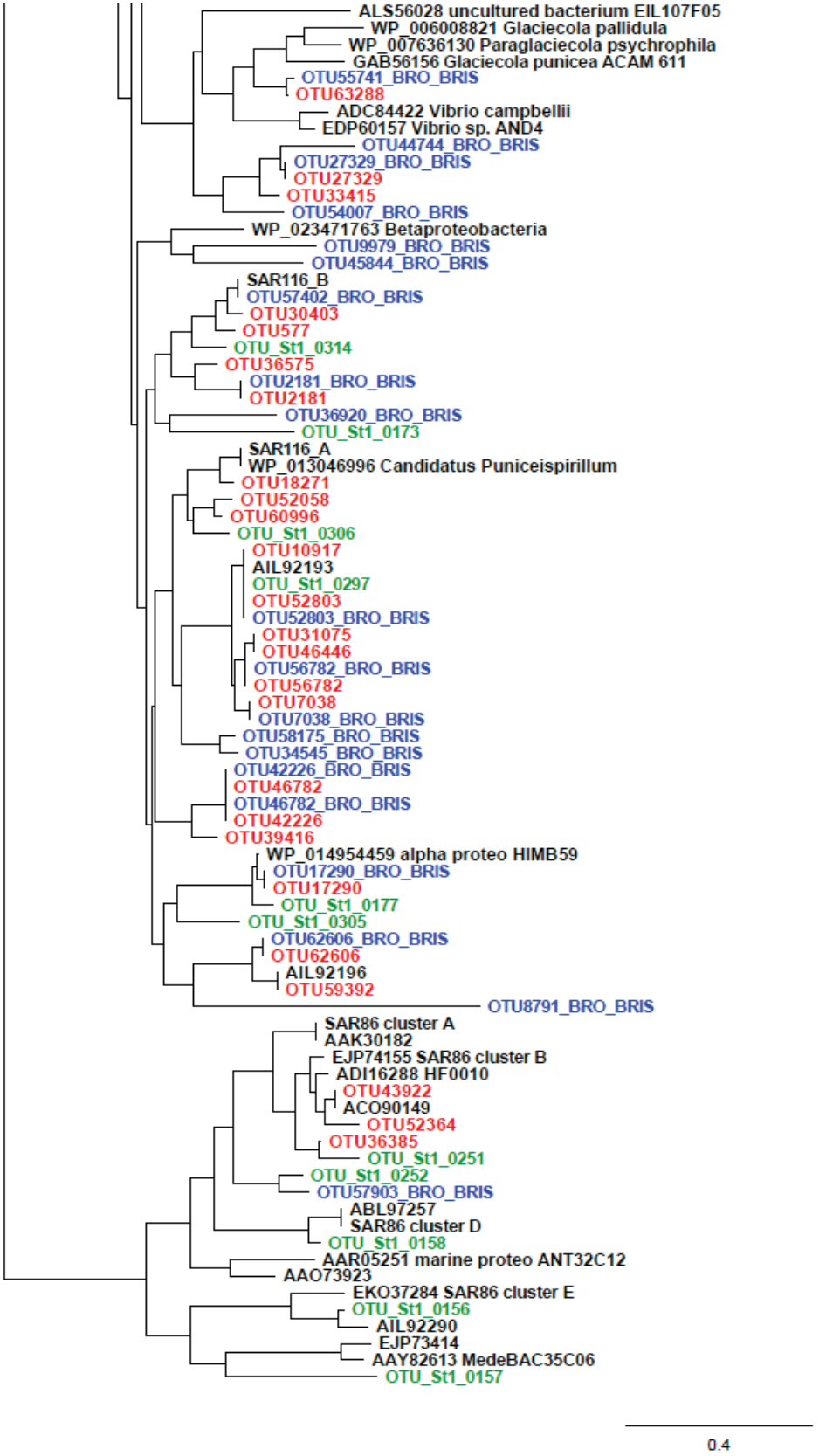

Figure S5: Phylogenetic tree showing the relationships between proteorhodopsin gene sequences from this study and environmental samples and nearest relatives retrieved from GenBank. The tree is based on a Bayesian tree to which short sequences were added by ARB_PARSIMONY.

GENERAL DISCUSSION

The marine environment has immense social and economic value to Australia, but marine habitats are already experiencing changes due to over-exploitation of fisheries, environmental degradation and climate change (e.g. Johnson *et al.,* 2011). Therefore, there is an urgent need to understand the processes that maintain the on-going health of oceanic ecosystems. Microorganisms are key indicators of marine health as they form the foundation of ocean's food web and control the flux of energy and biologically important chemical elements in the ocean (Falkowski *et al.,* 2008). However, marine microbial communities are not currently well characterized in Australian waters and only a few studies have investigated spatiotemporal patterns in community structure.

Revealing the ecological role that proteorhodopsin (PR) and bacteriochlorophyll a play in the marine environment is a key challenge in modern marine microbiology (Karl, 2014). Although knowledge of photoheterotrophic organisms globally has expanded significantly in the recent years, our understanding of the role photoheterotrophs play in the Australian marine environment is scarce. Studying the abundance and distribution of important marine microbial functional groups and revealing the factors influencing these dynamics is a crucial step towards understanding ecosystem functioning and predicting response to environmental change.

Pelagic microbial communities are highly diverse and their biogeography appears to be controlled by specific sets of habitat conditions (Fuhrman *et al.,* 2006, Hewson *et al.,* 2007). To date it appears there are no common rules forecasting the composition, abundance or distribution of bacterial communities in the ocean, rather interactions between biotic and abiotic factors define bacterial communities in individual habitats (Fuhrman *et al.,* 2006). The principle goal of this research was to define the environmental variables influencing the dynamics of a functionally important group of marine microbes. Within this final chapter, the results from each experimental chapter will be addressed within the context of the 3 specific questions and thesis objectives detail in Chapter 1.

Do photoheterotrophic microbes constitute a significant element in Australian ocean waters?

Investigations of changes in the growth and abundance of key marine microbial groups, or functional guilds, over time can contribute significantly to an understanding of what controls microbial function and activity. This can be achieved by examining the abundance of genes related to specific compartments of the microbial community. An example of this involves the calculation of abundance of genes associated with photoheterotrophy (PR and *pufM*) over space and time and characterising the ratio of these genes to total bacterial 16S rRNA. This provides the means to determine how environmental parameters may affect the abundance of different bacterial taxa and relate this to a functional aspect.

Most of the studies of AAnPB in marine ecosystems indicate a positive correlation between AAnPB cell numbers and chlorophyll (Jiao *et al.* 2007; Hojerova *et al.* 2011; Ritchie and Johnson 2012). Remarkably, one the most interesting factors is the effects on light in the ecology of AAnPB. In laboratory experiments light has shown to have a different effects on AAnPB, however in marine communities its effects still remains unclear. In samples from the North Pacific Ocean (Van Mooy, Devol and Keil 2004) showed a strong influence of light over a large part of the marine bacterial community, however samples from the San Pedro Channel in California showed no effect on microbial community structure (Schwalbach, Brown and Fuhrman 2005). Studies on AAnPB indicate a potential effect on different bacterial processes. Studies in Chesapeake Bay showed a higher leucine incorporation in comparison to average bacteria, however no effect was observed between light and dark (Stegman, Cottrell and Kirchman 2014). AAnPB are typically observed in the euphotic zones of the oceans and below the euphotic zone is mainly undetected. Ferrera *et al.* (2014) observed a positive effect of light from seasonal studies in coastal waters of the Mediterranean. These result indicate that light may have an effect on AAnPB in long term. In addition it has been suggested that light may improve survival AAnPB while nutrient are scarce (Shiba 1984; Soora and Cypionka 2013). Consequently, in long term light may represent a competitive advantage over heterotrophic bacteria increasing AAnPB fitness. Another environmental parameter that clearly shows that influences AAnPB numbers is temperature. Seasonal studies indicate a positive effect of temperature on AAnPB (Masın *et al.* 2006; Zhang and Jiao 2007; Lamy *et al.* 2011;

Ferrera *et al.,* 2014). Yet, correlations among temperature and AAnPB numbers are still inconclusive as temperature may overlap with other environmental parameters. As shown by Ferrera *et al.* (2014) temperature of water it may be just an indication of the amount of solar radiation during any particular season, and also could be an indication of positive relationship of light on autochthonous DOC by phytoplankton and photoheterotrophic microbes.

In chapters 2 and 4, quantitative PCR was used to estimate the abundance of aerobic anoxygenic phototrophic bacteria (AAnPB) (by targeting *pufM* genes), proteorhodopsin containing SAR11 clade organisms (by targeting SAR11 specific PR), and the total bacterial assemblage (by targeting bacterial 16s ribosomal RNA genes). In chapter 2 we revealed that *pufM* genes were always present and sometimes very abundant at all three National Reference Station study sites along Australia's east coast; North Stradbroke Island (NSI), Port Hacking (PH) and Maria Island (MAI). The strongest correlations between *pufM* copy number and environmental parameters were with day length and solar radiation exposure, revealing these light-associated factors as overarching seasonal structuring parameters. However, the timing of peak AAnPB abundance differed between the stations revealing AAnPB populations also responded to local environmental fluctuations. The degree of seasonality in day length and solar exposure parameters may not have been sufficient to drive significant shifts in community structure at NSI or PHA as no significant correlations between *pufM* copy number and any of the measured environmental parameters were observed at

these sites. However at MAI, where day lengths varied the most, we observed that *pufM* copy numbers were positively and significantly correlated with day length and Chla, and negatively correlated with Secchi depth, suggesting AAnPB here are also related to water column productivity.

Using community sequencing approaches we identified some common drivers of photoheterotrophs community structure as well. For instance both AAnPB richness (chapter 2) and PRBA richness (chapter 3) were higher at NSI and PHA than at MAI, with both positively correlated with temperature across the three NRS sites, which displayed temperatures ranging from 12 – 27 °C. However, in the chapter 4 study focusing on contrasting tropical northern Australian waters of the Arafura and Timor Seas region (ATS) and the Coral Sea, AAnPB richness was not significantly linked to any environmental variable, while PRBA richness was negatively correlated to temperature. It is likely that over the wide temperature range experienced in chapters 2 and 3, photoheterotrophic diversity increases, while the temperature range for the chapter 4 study (23 - 27 °C) was insufficient to drive differences in diversity. Taken together these data suggest a temperature related increase in diversity of photoheterotrophs peaking at temperatures ~23 °C, and that studies that only sample in very warm waters miss this temperature related affect.

Just a few studies have examined PR gene abundance in the oceans. Unlike other prokaryotic phototrophs (e.g. cyanobacteria and aerobic anoxygenic phototrophic bacteria), PR-containing microbes cannot be quantified using direct methods such as

microscopy or flow cytometry (Schwalbach and Fuhrman, 2005; Cottrell *et al.,* 2006; Michelou *et al.,* 2007). In addition creating a set of primers to calculate all PR groups is a daunting task due to the high gene nucleotide variability. In order to estimate the abundance of different PR genes groups compared to the abundance of bacterial 16S rRNA genes a real-time qPCR-based approach is most appropriate. Indeed in chapter 4, we were able to calculate the ratio of *pufM* and SAR11PR to total bacteria using qPCR and these results indicated considerable variation in functional gene abundances across environments. Throughout the entire dataset pufM:16sRNA ratios were correlated with phosphate concentrations while no correlations among SAR11PR:16sRNA ratios and environmental parameters were identified, possibly an indication of SAR11 being dominant across both regions. However within the ATS the SAR11PR:16sRNA ratio was negatively correlate to fucoxanthin, whereas in the Coral Sea it was positively correlated to primary production (i.e. fluorescence, fucoxanthin and Chla), which may indicate that local rather than regional processes may influence SAR11 abundance.

Overall, using a complementary quantitative PCR (qPCR)-based approach of measuring abundance of photoheterotrophic groups in the coastal waters of Australia, we have demonstrated that AAnPB and PRBA are often numerically important members of the marine microbial assemblage and that their relative abundance is governed by a suite of environmental factors linked to seasonal and geographic shifts in water temperature, light regimes and productivity.

What environmental factors influence photoheterotrophic community composition and diversity?

Since the discovery of a rhodopsin gene in a *Gammaproteobacteria* SAR86 genomic fragment near Monterey, California (Beja *et al.* 2000), has increased the interest in the investigation of rhodopsin gene diversity and fuction in a range of aquatics ecosystems marine habitats accelerated (See review by Pinhassi *et al.,* 2016). Many of the studies are from the Northern Hemisphere, while in the Southern Hemisphere are more scarce. Different approaches to quantitative estimates of the ratio of PRBA indicate a 15% to up to 70% (Venter *et al*., 2004; Rusch *et al*., 2007; Campbell *et al*., 2008; Riedel 2010; Sabehi *et al*., 2003), in comparison to AAnPB which is to up 30% of total bacteria (Koblizec, 2015). Recently, Finkel *et al.* (2013) reported that on average 60% of total bacteria contain rhodopsin genes, while around 20% contain bacteriochlorophyll *a*. So far, we can confirm that the majority of bacteria contain rhodopsin genes. Nevertheless, the variability of the results of these studies can probably be associated to both in differences in approaches for quantification and a range of environmental factors.

In chapters 2 and 3, both seasonal and local environmental factors were identified as drivers of AAnPB and PRBA photoheterotrophic assemblages, while in chapter 4 we identified clear differences in AAnPB and PRBA across two tropical but disparate oceanic regions. These studies demonstrated that specific photoheterotrophic bacterial groups respond to specific environmental conditions, characteristic of niche

diversification, and that the composition of AAnPB and PRBA assemblages is sometimes predictable from environmental factors.

Degenerate PR primers were first applied in samples collected in the Mediterranean and Red Sea and revealed a large phylogenetic rhodopsin diversity (Sabehi *et al.*, 2003), with some rhodopsin sequences observed at both seas and others found only in one of the seas. Later, Venter *et al.* (2004) first report on new 782 rhodopsin genes on metagenome shotgun sequencing of microbial DNA from the Sargasso Sea and significantly extended the range of phylogenetic diversity of PRs that can be found at a single geographic location. In a similar study by Rusch *et al.* (2007) observed that in several SAR11 PR clades, similar PR sequences were found in the Pacific and Atlantic Oceans. Further, Campbell *et al.* (2008) using clone library construction by degenerate PR gene primers (Sabehi *et al.,* 2003) and quantitative PCR (qPCR) astudied the distribution of PR genes in the North Atlantic Ocean. They first characterized PR gene diversity in a sample from the Sargasso Sea. Among the total of 27 PR gene clusters recorded, four distinct clusters of PRs including three alphaproteobacterial (SAR11 and HOT2C01 PRs were particularly abundant) and one Flavobacterial, estimated that 50% of bacteria in the Sargasso Sea contained rhodopsin genes., while further northeast in the Atlantic were much less abundant. Remarkably, there was an overall negative correlation between PR gene abundance and chlorophyll a concentrations (but not light) and inorganic nutrients in the surface samples and also in the depth profiles (Campbell *et al.,* 2008). Zhao *et al.* (2009) used similar approach to study

Flavobacterial PRs in the eastern and southern China Sea. Results indicated that PRs were structured essentially according to clone library sampling site. Additionally, qPCR showed a higher abundance of these PR genes in offshore waters than in coastal waters, and represented up to 1.6% of total bacteria, similar results observed in the Sargasso Sea (Campbell *et al.*, 2008). Different spatial distributions of PRs have also been observed from the Arctic compared to samples from lower latitudes (Cottrell *et al.*, 2009) and Arctic PRs from Antarctica (Béjà *et al.*, 2001). Furthermore, Cottrell *et al.* (2009) using qPCR analyses reported that the abundance of PR gene-containing bacteria largely changed in relation to total bacterial abundance from summer to winter, and the proportion of PR- and bacteriochlorophyll-containing bacteria continued stable across these seasons, despite extreme differences in day length. In a similar study Nguyen *et al.* (2015) reported a relatively stable abundance of PR genes during dark winter months in the Arctic, with visible changes in *Bacteroidetes* and *Alphaproteobacteria*, while *Gammaproteobacteria.* Overall, very few studies have comprehensively investigated spatial and temporal variability in PR diversity and prevalence distributions.

In chapter 2, we observed a dominance of Gammaproteobacterial (phylogroup K) AAnPB at all NRS, and a clear seasonal transition between phylogroups occurring at the southern-most site Maria Island, where phylogroup E was dominant in the winter months while phylogroup K was dominant during the spring/summer. Temperature, salinity, phosphate, and day length were all correlated with AAnPB community

structure. Likewise, in chapter 3, we demonstrated that shifts in the taxonomic composition of the PRBA assemblage were best explained by temperature and day length. In this chapter we observed a characteristic winter proteorhodopsin assemblage at all stations, dominated by Archaeal taxa, and transitions away from this assemblage beginning in the austral spring. These taxonomic shifts were paralleled by a transition in proteorhodopsin spectral tuning. In general green tuned proteorhodopsin genes (GPR) were most abundant during spring through to summer and blue proteorhodopsin genes (BPR) most abundant in autumn and winter. Interestingly, we observed that the timing of changes in AAnPB and PRBA at the Port Hacking site coincided with the penetration of warm EAC waters into the near-coastal region (as observed by SST and in line with known seasonal dynamics of the EAC in this region) suggesting this current has an influence in driving microbial assembly in these temperate waters.

In chapter 4, AAnPB and PRBA community composition displayed clear differences between the ATS and Coral Sea but not between depths within regions. The majority of AAnPB OTUs belonged to the Gammaproteobacteria (phylogroup K), which accounted for 99% of sequences in the ATS, suggesting these taxa, which were also most abundant in the temperate sites during summer (chapter 2), are prevalent in warm water conditions of the lower latitudes.

We also observed a clear biogeographic pattern when considering PRBA. For instance, SAR11-like sequences and Betaproteobacteria were higher within the ATS than the

Coral Sea, while members of the Archaea group IIb, and Flavobacteria were abundant within the Coral Sea, but comprised only a low proportion of the proteorhodopsin containing community in the ATS. Interestingly, consistent with the dynamics of Gammaproteobacterial AAnPB, the relative abundance of proteorhodopsin containing members of the Gammaproteobacteria remained relatively constant across the two regions, and the same was observed for the Deltaproteobacterial (including SAR324 A clade) and Alphaproteobacterial groups.

In addition to the regional difference between the ATS and Coral Sea, the ATS community differed with longitude, with samples collected from western stations (WS2-WS5) distinct from those collected from the eastern stations (WS6-WS18). Similarly, with the Coral Sea there was separation by latitude, with differences in the PR community between the northern (WS13-WS15) and southern stations (WS16-WS18), which clustered separately according to salinity, temperature, Chl*a* and phosphate values.

Overall, our findings of divergent photoheterotrophic bacterial communities across different oceanographic coastal waters of Australia underline the presence of biogeographical patterns among important groups of marine bacteria (Lefort and Gasol, 2013) and highlight the influence of a combination of environmental parameters on bacterial distributions.

Do distinct photoheterotrophic microbes fill specific niches within ocean environments?

Beyond community level analyses, the importance of studying the dynamics of individual OTUs and their individual interactions is rapidly becoming apparent (Barberán *et al.,* 2011; Ma *et al.,* 2016). Previous studies of marine microbial diversity have revealed that species abundance distributions are characterised by a majority of taxa occurring in low relative abundances (also known by some authors "rare"), with only a few "abundant" taxa present (Kirchman et al 2012; Pedros-Alio, 2006). Statistical approaches reveal that removing data on low-abundance taxa can result in better correlations between community composition and environmental parameters (Gobet *et al.*, 2010). Rare taxa are generally considered to have less impact or activity within their environment, and are thought to act as a seed bank. Meanwhile some of the abundant microorganisms are often considered the keystone species, acting as ecosystem engineers that have a strong influence in the environment (Falkowski *et al.,* 2008). While conceptually this paradigm is appealing, abundance is not always a proxy for influence and some research proposes that low abundance microbes may be significant for the response of aquatic environments to turbulences (Montoya *et al.,* 2004; Jones and Lennon, 2010.).

Network analysis has recently been applied in microbial ecology to examine spatial and temporal associations between discrete microbial operational taxonomic units (OTUs) and their environment (Steele *et al.,* 2011; Zhou *et al.,* 2011). Using this approach, I have identified correlations within and between photoheterotrophic OTUs and several biotic and abiotic parameters, revealing the existence of specific niches for

some photoheterotrophic bacteria in Australian coastal waters. In chapter 2, I identified linear and non-linear correlations between ecosystem variables and AAnPB populations. The majority of correlations occurred within, rather than between AAnPB phylogroups, particularly within phylogroup K (Gammaproteobacteria), which formed several highly interconnected clusters of OTUs that responded similarly to their environment. Total phylogroup K abundance was negatively correlated with phylogroup G abundance and both interacted with phosphate levels in different ways. In addition, total phylogroup E abundance had a negative relationship with temperature (displaying near zero abundances at temperatures > 18 °C) and a positive relationship with Chl*a*. On the other hand, total phylogroup K abundance was positively correlated with temperature and we observed consistently high abundance of this group at water temperatures > 18 °C. However, when considering individual phylogroup K OTU dynamics we observed that the most abundant OTUs, OTU10275 and OTU3893, displayed a classic non-co-occurrence relationship, whereby one OTU was only abundant when the other was essentially absent, with a transition between the two occurring at ~17 °C. These OTUs were closely related, with both occurring on one of the major branches of the phylogroup K lineage, but their clearly distinct dynamics, including their relationships to solar radiation and Chla, suggest they act as distinct ecotypes.

In chapter 4, network analysis indicated that the majority of correlations involved PRBA OTUs that formed highly interconnected clusters that responded similarly to

their environment. In addition, we observed examples of correlations between different taxonomic groups, including between archaeal and bacterial PRBA OTUs and between AAnPB and PRBA OTUs. For instance the abundance of the proteorhodopsin-containing Alphaproteobacteria OTU33492, was positively correlated with that of Archaea group IIb OTU20155, with both interacting with temperature, whereby their abundances were zero above 25.3 C. Further, These PRBA OTUs were positively correlated to pufM Gammaproteobacteria OTU4386, which displayed a very similar negative relationship with temperature, with abundances of zero at temperatures above 25.4 C. Two of the most abundant OTUs within the Archaea group IIb, OTU18955 and OT52286, displayed a classic co-occurrence relationship, whereby one OTU was only abundant when the other was also abundant. We identified a transition point between the ATS (WS12) and Coral Sea stations (WS14) where these OTUs started to become abundant, and their abundance continued to increase as the transect continued southward. Salinity was observed to be correlated with several biotic parameters. For instance it was positively correlated with Archaea group II OTU20155, which only occurred in waters with a salinity > 35.2 and negatively correlated to *pufM* Gammaproteobacteria OTU4264 which occurred at its highest abundance in the lowest salinity waters (33.2).

Rhodopsins role as a light energy-absorbing protein, and different spectral tuning to wavelength and light intensity play a key role in their ecological distribution. First studies in oceanic surface water indicate that Gammaproteobacteria SAR86 PR had an

absorbance maximum in the green light range (520 nm) (Beja *et al.*, 2000). Later, similar studies reported a divergence of PRs with absorption maxima in the range from blue (around 490 nm) mainly dominant in deeper waters and green (around 540 nm in shallow waters (Béjà *et al.* 2001). All these discoveries generated research to determine the biochemical and genetic foundation for PR spectral tuning, allowing to interpret the ecological distributions' patterns of different PRs. Further, studies in the Eastern Mediterranean Sea, Sabehi *et al.* (2003) observed during summer under stratified waters, GPRs dominated the surface, whereas BPRs mainly dominated at the 55-m depth. On the other hand, on winter GPRs and BPRs distribution throughout the mixed layer were relatively similar. In contrast, studies in the Sargasso Sea, the majority were BPRs along the year and depth (Sabehi *et al.*, 2007). Further Rusch *et al.* (2007) examined the diversity and spatial distribution of rhodopsins across the northwest Atlantic to the Pacific and observed GPRs more abundant in temperate coastal waters, whereas BPRs dominated in warmer open ocean water. This indicate that the spatial distribution of rhodopsin tuning variants might reflect changing spectral properties of the light along the coastal-open ocean transition, similar to was observed by depth (Sabehi *et al.*, 2003). In addition, studies at the North Sea nearly all PRs (96%) were GPRs and associated to Bacteriodetes and Proteobacteria (Riedel *et al.*, 2010), while in surface waters of the Red Sea a majority (70%) were BPRs related to bacterial and Archaeal rhodopsins (Philosof and Béjà, 2013).

In addition to network analysis, diverse statistical tools unravel other specific niches of PRBA population. In chapter 3, GPRs particularly those containing leucine, were strongly positively correlated to day length and solar radiation along with indicators of water body productivity including picoeukaryotes and zooplankton abundances. Conversely, Secchi depth, was positively correlated to BPRs which is consistent with the previously demonstrated preferences of this group for clear water, low productivity, and oligotrophic conditions (Sabehi *et al.*, 2007). In chapter 4, we observed a transition away from green light absorbing proteorhodopsins to blue light absorbing proteorhodopsins as we moved from the ATS to Coral Sea, which is again consistent with the different water properties of these two regions. The semi-enclosed Arafura and Timor Seas (ATS) is relatively shallow and exhibits high productivity, whereas Coral Sea is characterised by deep blue, nutrient-poor waters. During this transition from ATS to the Coral Sea, the BPR containing taxa Archaea Group IIb, Glaciecola and SAR11 B became more abundant, while GPR containing taxa, including SAR11 like sequences, SAR116 clade A and Betaproteobacteria became less abundant. However, among the GPR groups, those containing methionine became more abundant in the Coral Sea, mainly due to increases in the abundance of Flavobacteria related sequences. One of the few studies on seasonal adaptation and spectral tuning in marine proteorhodopsin (Sabehi *et al.*, 2007) found that in the Sargasso Sea all PRs were BPR, while in the Mediterranean Sea most were GPR at the surface and BPR in deeper waters. All of these observations suggest that differential exploitation of the light spectrum via the use of variants of proteorhodopsin underpin a separation of the

proteorhodopsin community across different seasons, positions in the water column or different regions of the ocean. Thus the ecological significance of spectral tuning may be considered within the context of classical niche theory, whereby utilisation of different features of the light spectrum provide opportunities for niche differentiation and allows coexistence of PRBA species absorbing different colours of light (Stomp *et al.,* 2007).

FUTURE DIRECTIONS

Aerobic anoxygenic phototrophic bacteria (Koblizec, 2015) are photoheterotrophs that despite their low abundances have been hypothesized to play an ecologically and biogeochemically important role in aquatic systems. Characterizing this role requires a better understanding of the in situ dynamics and activity of AAnPB. Approaches such single-cell activity of freshwater AAnPB and their contribution to total bacterial production across lakes (Garcia-Chaves *et al.*, 2016) and estuary (Stegman *et al.*, 2014) and exploring the role of light in regulating AAnPB activity have provided new insights of the potential role of AAnPB in aquatics systems. Garcia-Chaves *et al.*, 2016 reported that the proportion of cells that were active in leucine incorporation and the level of activity per cell were consistently higher for AAnPB than for the bulk bacteria across lakes. Thus, AAnPB contributed excessively more towards total bacterial production than to total bacterial abundance. Remarkably, although environmentally driven patterns in activity did not differ mostly between AAnPB and bulk bacteria, light showed to had an effect in increasing the proportion of active AAnPB with no

clear effect on their cell-specific activity. This result may indicate that light may play a key role in the activation of AAnPB, allowing to contribute more to the carbon cycle rather by their abundance.

Similarly, Stegman *et al.* (2014) explored the activity of AAnPB in estuary and coastal waters using a new approach that combines infrared epifluorescence microscopy and microautoradiography to examined AAnPB single-cell 3H-leucine incorporation. Results showed that the percent of active AAnPB was up to twofold higher than the percentage of active cells in the rest of the bacterial community in the estuary, with higher rates of leucine consumption by AAnPB. Moreover, the cell size of AAnPB was 50% bigger than the size of other bacteria, about the same difference on average as measured for activity. AAnPB abundance was negatively correlated and their activity positively correlated with light, although light did not affect ^{3}H-leucine incorporation in light and dark experiments. These results are in accordance with studies by Garcia-Chaves *et al.* (2016) that suggest that AAnPB are bigger and more active than other bacteria, and likely contribute more to organic carbon fluxes than indicated by their abundance. Futures studies should follow similar approaches to elucidate if similar results are found in AAnPB and PRBA in marine ecosystems.

One of the most important effects of increasing sea temperatures is an increase in surface stratification, which retains phytoplankton at the surface but reduces access to nutrients from underneath. It also causes a strengthened link between primary and secondary producers by increasing DOC production and bacterial respiration. As a

result, Ducklow *et al.*, (2010) hypothesise that microbial community structure and activity will change depending on the type and abundance of resources (e.g. DOC). Some microorganisms have the potential to dominate, and become the more abundant taxa (Sogin *et al.*, 2006), especially those that play a major role of a key nutrient cycling and activity (Malmstrom *et al.*, 2005). On the other hand, it could also lead to an augmentation of rarer species. These species are often dormant and have slow growth rates (Jones and Lennon, 2010), and are known to play an essential role in oligotrophic marine ecosystem (Montoya *et al.*, 2004). Such changes could alter the functional complexity and diversity of the microbial community, which could result in some bacterial species shifting from specialists to generalists (Mou *et al.*, 2008). Moreover, some currently less abundant microbes may in the future have new but essential roles to play, including being keystone species, acting as reservoir of genetic and functional diversity, or acting as a buffer against changes within an ecosystem in the event of species lost or climate change i.e. via functional redundancy (Brown *et al.* 2009). However the relationship between bacterial abundance and activity is still not well understood.

Other potential effects of increased temperature on the microbial loop include increases in bacterial abundance, and growth and respiration rates that would lead to compensatory bacteriophage control and lysis and thus a positive feedback, resulting in additional DOC top-down control (Weinbauer and Rassoulzadegan, 2004; Suttle, 2007). As such DOC is assimilated by bacteria and released via bacterial lysis and

metabolized by other bacteria, enhancing upper ocean respiration (Furhman, 1999). Thus further studies should be focus on in situ or temperature simulated experiments on photoheterotrophic bacteria to understand possible effects of predicted higher temperatures in the ocean.

One of the crucial questions remains how and to what extend photohetetrophic bacteria actually benefit from light under natural conditions. An intriguing question is if these organisms have the capacity to fix CO_2. The phototrophic competence of AAnPB and PRBA, and the way they use light as an energy source, still remains to elucidate. These organisms that contain photochemically active reaction centres are not able to grow photoautotrophically, as they require a supply of organic carbon (Kolber *et al.*, 2001; Yurkov and Csotonyi, 2009; Gonzalez *et al.*, 2008). Currently no studies have shown that AAnPB are able to fix CO_2. Experiments with Erythrobacter sp. NAP1 and Dokdonia sp. MED134 revealed light-enhanced CO2 incorporation, however the activity was only weak, likely rejecting enhanced anaplerotic carboxylation activity (Kolber *et al.,* 2001; Gomez-Cosarnau *et al.,* 2007). Recently it was suggested that PR-bearing marine bacteria bacterium Polaribacter sp. MED 152 (Flavobacteria) may be able to fix CO_2 anaplerotically (via incorporation into Krebs cycle intermediates) (Gonzalez *et al.,* 2011). It was showed that the amount of bicarbonate fixed through anaplerotic enzymes is larger in the light than in the dark. These results suggest that MED152 may allow using more efficiently use organic matter for biosynthesis in the light. It is clear that the capacity to generate energy is

beneficial in many different habitats. However, many questions remain still to answer. New approaches to isolate pure cultures of photohetetrophic bacteria (Rappe, 2013; Durham et al 2014), will help to have a better understanding of the role of these microorganism in the ocean.

Finally, future studies should be focus in determining the dynamics of AAnPB and PRBA communities in relation to bchl*a* and rhodopsin gene expression patterns over different spatiotemporal regions. These results may help to answer questions if expression of bchl*a* and rhodopsin genes is giving ecological advantages which determine the seasonal dynamics and activity of particular photohetetrophic bacterial communities.

CONCLUSIONS AND PERSPECTIVES

The results reported in this thesis provide evidence for distinct niche differentiation and substantial population level responses to environmental variability among both of the major photoheterotrophic bacterial groups, the AAnPB and the PRBA. Furthermore, this work provides insights into how regional oceanographic processes influence the dynamics and distribution of these abundant bacterioplankton in the ocean. These results confirm that rather than being single functional entities, both the AAnPB and PRBA communities are comprised of multiple discrete compartments that dynamically shift in relative importance according to environmental niche preferences. This thesis emphasizes the critical importance of connecting analysis of photoheterotrophic bacterial population dynamics with examination of

environmental factors in order to improve our understanding of processes that regulate their distribution and activity.

This work indicates that Seasonality and spatial variation in environmental conditions significantly shape the abundance and structure of marine photoheterotrophic bacterioplankton communities. This thesis has begun to identify the environmental niches of key photoheterotrophic microbes and provides a framework for potentially using some of these organisms as bio-indicators of environmental condition. Measurements of indicator populations over long periods of time (years to decades) will potentially provide a new capacity to monitor changes in the biotic status of the sea.

Forecast future changes in the marine environment will include, among others, increased sea surface temperatures and shifts in nutrient regimes. This thesis has revealed the environmental preferences of different components of photoheterotrophic marine microbial assemblages and highlight examples where anticipated changes in ocean physics and chemistry will likely be advantageous to some of these populations (e.g. those with preferences for warmer waters), while disadvantageous to others (e.g. those with preferences for eutrophic rather than oligotrophic conditions). I argue that in order to fully understand and predict future climate change effects, photoheterotrophic bacteria should be integrated into food-web and biogeochemical models.

The distribution of microorganism in the ocean has previously been predicted to be devoid of physical barriers (Rusch *et al.*, 2007). While dispersal of microbial populations across the ocean may well be widespread, this thesis also provides evidence for regionality and in some cases endemism among photoheterotrophic populations. Therefore, as commonly accepted in terrestrial microbial ecology, the establishment of local sites by bacterial populations from a regional pool could be an important mechanism for regulating the genomic potential among photoheterotrophic bacterial populations.

Finally, this thesis comprises the most detailed investigations of photoheterotrophic bacterial communities in Australian coastal waters and the outcome of this thesis significantly broadens our knowledge and understanding of photoheterotrophs in southern hemisphere waters. The insights gained by these investigations are crucial for our understanding of ecological process and future impacts due to climate change in our coastal areas. We believe that the insights provided by this work assist predictions regarding the impact of environmental changes in the Australian coastal waters.

BIBLIOGRAPHY

Agogue, H., M. Brink, J. Dinasquet, and G. J. Herndl. 2008. Major gradients in putatively nitrifying and non-nitrifying Archaea in the deep North Atlantic. Nature **456**:788-791.

Ajani, P., R. Lee, T. Pritchard, and M. Krogh. 2001. Phytoplankton Dynamics at a Long-term Coastal Station off Sydney, Australia. Journal of Coastal Research:60-73.

Atlas RM, Bartha R (1993) Microbial ecology. Fundamentals and applications. Benjamin/Cummings, Redwood City, CA

Baltar, F., K. Currie, E. Stuck, S. Roosa, and S. E. Morales. 2016. Oceanic fronts: transition zones for bacterioplankton community composition. Environ Microbiol Rep **8**:132-138.

Beja, O., L. Aravind, E. V. Koonin, M. T. Suzuki, A. Hadd, L. P. Nguyen, S. B. Jovanovich, C. M. Gates, R. A. Feldman, J. L. Spudich, E. N. Spudich, and E. F. DeLong. 2000. Bacterial rhodopsin: Evidence for a new type of phototrophy in the sea. Science **289**:1902-1906.

Béja, O., E. N. Spudich, J. L. Spudich, M. Leclerc, and E. F. DeLong. 2001. Proteorhodopsin phototrophy in the ocean. Nature **411**:786-789.

Béjà, O., and M. T. Suzuki. 2008. Photoheterotrophic Marine Prokaryotes. Pages 131-157 Microbial Ecology of the Oceans. John Wiley & Sons, Inc.

Beja, O., M. T. Suzuki, J. F. Heidelberg, W. C. Nelson, C. M. Preston, T. Hamada, J. A. Eisen, C. M. Fraser, and E. F. DeLong. 2002. Unsuspected diversity among marine aerobic anoxygenic phototrophs. Nature **415**:630-633.

Benjamini, Y., and Y. Hochberg. 1995. Controlling the False Discovery Rate: A Practical and Powerful Approach to Multiple Testing. Journal of the Royal Statistical Society. Series B (Methodological) **57**:289-300.

Bergo, V., J. J. Amsden, E. N. Spudich, J. L. Spudich, and K. J. Rothschild. 2004. Structural changes in the photoactive site of proteorhodopsin during the primary photoreaction. Biochemistry **43**:9075-9083.

Bibiloni-Isaksson, J., J. R. Seymour, T. Ingleton, J. van de Kamp, L. Bodrossy, and M. V. Brown. 2016. Spatial and temporal variability of aerobic anoxygenic photoheterotrophic bacteria along the east coast of Australia. Environ Microbiol:n/a-n/a.

Bielawski, J. P., K. A. Dunn, G. Sabehi, and O. Béjà. 2004. Darwinian adaptation of proteorhodopsin to different light intensities in the marine environment. Proc Natl Acad Sci U S A **101**:14824-14829.

Boeuf, D., M. T. Cottrell, D. L. Kirchman, P. Lebaron, and C. Jeanthon. 2013. Summer community structure of aerobic anoxygenic phototrophic bacteria in the western Arctic Ocean. FEMS Microbiol Ecol **85**:417-432.

Brinkhoff, T., H. A. Giebel, and M. Simon. 2008. Diversity, ecology, and genomics of the Roseobacter clade: A short overview. Arch Microbiol **189**:531-539.

Brown, M. V., M. S. Schwalbach, I. Hewson, and J. A. Fuhrman. 2005a. Coupling 16S-ITS rDNA clone libraries and automated ribosomal intergenic spacer analysis to show marine microbial diversity: development and application to a time series. Environ Microbiol **7**:1466-1479.

Brown, M. V., M. S. Schwalbach, I. Hewson, and J. A. Fuhrman. 2005b. Coupling 16S-ITS rDNA clone libraries and automated ribosomal intergenic spacer analysis to show marine microbial diversity: development and application to a time series. Environ Microbiol **7**:1466-1479.

Bulleri, F., J. F. Bruno, B. R. Silliman, and J. J. Stachowicz. 2016. Facilitation and the niche: implications for coexistence, range shifts and ecosystem functioning. Functional Ecology **30**:70-78.

Campbell, B. J., L. A. Waidner, M. T. Cottrell, and D. L. Kirchman. 2008. Abundant proteorhodopsin genes in the North Atlantic Ocean. Environ Microbiol **10**:99-109.

Caporaso, J. G., J. Kuczynski, J. Stombaugh, K. Bittinger, F. D. Bushman, E. K. Costello, N. Fierer, A. G. Pena, J. K. Goodrich, J. I. Gordon, G. A. Huttley, S. T. Kelley, D. Knights, J. E. Koenig, R. E. Ley, C. A. Lozupone, D. McDonald, B. D. Muegge, M. Pirrung, J. Reeder, J. R. Sevinsky, P. J. Turnbaugh, W. A. Walters, J. Widmann, T. Yatsunenko, J. Zaneveld, and R. Knight. 2010. QIIME allows analysis of high-throughput community sequencing data. Nat Methods **7**:335-336.

Cho, J. C., M. D. Stapels, R. M. Morris, K. L. Vergin, M. S. Schwalbach, S. A. Givan, D. F. Barofsky, and S. J. Giovannoni. 2007. Polyphyletic photosynthetic reaction centre genes in oligotrophic marine Gammaproteobacteria. Environ Microbiol **9**:1456-1463.

Choi, D. H., K.-T. Park, S. M. An, K. Lee, J.-C. Cho, J.-H. Lee, D. Kim, D. Jeon, and J. H. Noh. 2015. Pyrosequencing Revealed SAR116 Clade as Dominant dddP-Containing Bacteria in Oligotrophic NW Pacific Ocean. PLoS ONE **10**:e0116271.

Chow, C.-E. T., R. Sachdeva, J. A. Cram, J. A. Steele, D. M. Needham, A. Patel, A. E. Parada, and J. A. Fuhrman. 2013. Temporal variability and coherence of euphotic zone bacterial communities over a decade in the Southern California Bight. ISME J **7**:2259-2273.

Clarke, K. R. 1993. Non-parametric multivariate analyses of changes in community structure. Australian Journal of Ecology **18**:117-143.

Cottrell, M. T., and D. L. Kirchman. 2009. Photoheterotrophic microbes in the arctic ocean in summer and winter. Applied and Environmental Microbiology **75**:4958-4966.

Cottrell, M. T., A. Mannino, and D. L. Kirchman. 2006. Aerobic anoxygenic phototrophic bacteria in the Mid-Atlantic Bight and the North Pacific Gyre. Appl Environ Microbiol **72**:557-564.

Cottrell, M. T., J. Ras, and D. L. Kirchman. 2010. Bacteriochlorophyll and community structure of aerobic anoxygenic phototrophic bacteria in a particle-rich estuary. ISME J **4**:945-954.

Cram, J. A., C.-E. T. Chow, R. Sachdeva, D. M. Needham, A. E. Parada, J. A. Steele, and J. A. Fuhrman. 2015. Seasonal and interannual variability of the marine bacterioplankton community throughout the water column over ten years. ISME J **9**:563-580.

Csotonyi, J. T., J. Swiderski, E. Stackebrandt, and V. Yurkov. 2010. A new extreme environment for aerobic anoxygenic phototrophs: biological soil crusts. Adv Exp Med Biol **675**:3-14.

De la Torre, J. R., L. M. Christianson, O. Béjà, M. T. Suzuki, D. M. Karl, J. Heidelberg, and E. F. DeLong. 2003. Proteorhodopsin genes are distributed among divergent marine bacterial taxa. Proceedings of the National Academy of Sciences of the United States of America **100**:12830-12835.

del Giorgio, P. A., and C. M. Duarte. 2002. Respiration in the open ocean. Nature **420**:379-384.

del Giorgio, P.A., and P.J.leB. Williams. 2005. The global significance of respiration in aquatic ecosystems: From single cells to the biosphere. Pp. 267–303 in Respiration in Aquatic Ecosystems. P.A. del Giorgio and P.J.leB. Williams. eds, Oxford University Press, New York.

Deschamps, P., Y. Zivanovic, D. Moreira, F. Rodriguez-Valera, and P. López-García. 2014. Pangenome Evidence for Extensive Interdomain Horizontal Transfer Affecting Lineage Core and Shell Genes in Uncultured Planktonic Thaumarchaeota and Euryarchaeota. Genome Biol Evol **6**:1549-1563.

Dioumaev, A. K., J. M. Wang, Z. Bálint, G. Váró, and J. K. Lanyi. 2003. Proton Transport by Proteorhodopsin Requires that the Retinal Schiff Base Counterion Asp-97 Be Anionic. Biochemistry **42**:6582-6587.

Edgar, R. C., B. J. Haas, J. C. Clemente, C. Quince, and R. Knight. 2011. UCHIME improves sensitivity and speed of chimera detection. Bioinformatics **27**:2194-2200.

Eiler, A. 2006. Evidence for the ubiquity of mixotrophic bacteria in the upper ocean: Implications and consequences. Appl Environ Microbiol **72**:7431-7437.

Eiler, A., D. H. Hayakawa, and M. S. Rappé. 2011. Non-Random Assembly of Bacterioplankton Communities in the Subtropical North Pacific Ocean. Front Microbiol **2**:140.

Evans, C., P. R. Gómez-Pereira, A. P. Martin, D. J. Scanlan, and M. V. Zubkov. 2015. Photoheterotrophy of bacterioplankton is ubiquitous in the surface oligotrophic ocean. Progress in Oceanography **135**:139-145.

Fabricius, K. E., and D. W. Klumpp. 1995. Widespread mixotrophy in reef-inhabiting soft corals: the influence of depth, and colony expansion and contraction on photosynthesis. Marine Ecology Progress Series **125**:195-204.

Feng, S., S. M. Powell, R. Wilson, and J. P. Bowman. 2013. Light-stimulated growth of proteorhodopsin-bearing sea-ice psychrophile Psychroflexus torquis is salinity dependent. ISME Journal **7**:2206-2213.

Ferrera, I., C. M. Borrego, G. Salazar, and J. M. Gasol. 2014. Marked seasonality of aerobic anoxygenic phototrophic bacteria in the coastal NW Mediterranean Sea as revealed by cell abundance, pigment concentration and pyrosequencing of pufM gene. Environ Microbiol **16**:2953-2965.

Finkel, O. M., O. Béjà, and S. Belkin. 2013. Global abundance of microbial rhodopsins. ISME Journal **7**:448-451.

Frigaard, N. U., A. Martinez, T. J. Mincer, and E. F. DeLong. 2006. Proteorhodopsin lateral gene transfer between marine planktonic Bacteria and Archaea. Nature **439**:847-850.

Fuchs, B. M., S. Spring, H. Teeling, C. Quast, J. Wulf, M. Schattenhofer, S. Yan, S. Ferriera, J. Johnson, F. O. Glockner, and R. Amann. 2007a. Characterization of a marine gammaproteobacterium capable of aerobic anoxygenic photosynthesis. Proc Natl Acad Sci U S A **104**:2891-2896.

Fuchs, B. M., S. Spring, H. Teeling, C. Quast, J. Wulf, M. Schattenhofer, S. Yan, S. Ferriera, J. Johnson, F. O. Glöckner, and R. Amann. 2007b. Characterization of a marine gammaproteobacterium capable of aerobic anoxygenic photosynthesis. Proc Natl Acad Sci U S A **104**:2891-2896.

Fuhrman, J. A., J. A. Steele, I. Hewson, M. S. Schwalbach, M. V. Brown, J. L. Green, and J. H. Brown. 2008. A latitudinal diversity gradient in planktonic marine bacteria. Proceedings of the National Academy of Sciences **105**:7774-7778.

Galand, P. E., C. Gutiérrez-Provecho, R. Massana, J. M. Gasol, and E. O. Casamayor. 2010a. Inter-annual recurrence of archaeal assemblages in the coastal NW Mediterranean Sea (Blanes Bay Microbial Observatory). Limnology and Oceanography **55**:2117-2125.

Galand, P. E., M. Potvin, E. O. Casamayor, and C. Lovejoy. 2010b. Hydrography shapes bacterial biogeography of the deep Arctic Ocean. ISME J **4**:564-576.

Giebel, H. A., D. Kalhoefer, A. Lemke, S. Thole, R. Gahl-Janssen, M. Simon, and T. Brinkhoff. 2011. Distribution of Roseobacter RCA and SAR11 lineages in the North Sea and characteristics of an abundant RCA isolate. ISME J **5**:8-19.

Gilbert, J. A., J. A. Steele, J. G. Caporaso, L. Steinbrück, J. Reeder, B. Temperton, S. Huse, A. C. McHardy, R. Knight, I. Joint, P. Somerfield, J. A. Fuhrman, and D. Field. 2012. Defining seasonal marine microbial community dynamics. ISME J **6**:298-308.

Giovannoni, S. J., L. Bibbs, J. C. Cho, M. D. Stapels, R. Desiderio, K. L. Vergin, M. S. Rappé, S. Laney, L. J. Wilhelm, H. J. Tripp, E. J. Mathur, and D. F. Barofsky. 2005. Proteorhodopsin in the ubiquitous marine bacterium SAR11. Nature **438**:82-85.

Gómez-Consarnau, L., N. Akram, K. Lindell, A. Pedersen, R. Neutze, D. L. Milton, J. M. González, and J. Pinhassi. 2010. Proteorhodopsin phototrophy promotes survival of marine bacteria during starvation. PLoS Biology **8**.

Gomez-Consarnau, L., J. M. Gonzalez, T. Riedel, S. Jaenicke, I. Wagner-Dobler, S. A. Sanudo-Wilhelmy, and J. A. Fuhrman. 2016. Proteorhodopsin light-enhanced growth linked to vitamin-B1 acquisition in marine Flavobacteria. ISME J **10**:1102-1112.

Gomez-Pereira, P. R., M. Hartmann, C. Grob, G. A. Tarran, A. P. Martin, B. M. Fuchs, D. J. Scanlan, and M. V. Zubkov. 2013. Comparable light stimulation of organic nutrient uptake by SAR11 and Prochlorococcus in the North Atlantic subtropical gyre. ISME J **7**:603-614.

González, J. M., R. Simó, R. Massana, J. S. Covert, E. O. Casamayor, C. Pedrós-Alió, and M. A. Moran. 2000. Bacterial Community Structure Associated with a Dimethylsulfoniopropionate-Producing North Atlantic Algal Bloom. Appl Environ Microbiol **66**:4237-4246.

Gordon, A. L., and R. A. Fine. 1996. Pathways of water between the Pacific and Indian oceans in the Indonesian seas. Nature **379**:146-149.

Hallegraeff, G. M. 1981. Seasonal study of phytoplankton pigments and species at a coastal station off Sydney: Importance of diatoms and the nanoplankton. Marine Biology **61**:107-118.

Harris, G., C. Nilsson, L. Clementson, and D. Thomas. 1987. The water masses of the east coast of Tasmania: Seasonal and interannual variability and the influence on phytoplankton biomass and productivity. Marine and Freshwater Research **38**:569-590.

Hauruseu, D., and M. Koblizek. 2012. Influence of light on carbon utilization in aerobic anoxygenic phototrophs. Appl Environ Microbiol **78**:7414-7419.

Herlemann, D. P. R., M. Labrenz, K. Jurgens, S. Bertilsson, J. J. Waniek, and A. F. Andersson. 2011. Transitions in bacterial communities along the 2000[thinsp]km salinity gradient of the Baltic Sea. ISME J **5**:1571-1579.

Hojerova, E., M. Masin, C. Brunet, I. Ferrera, J. M. Gasol, and M. Koblizek. 2011. Distribution and growth of aerobic anoxygenic phototrophs in the Mediterranean Sea. Environ Microbiol **13**:2717-2725.

Holbrook, N. J. 2005. Erratum: "Oscillatory and propagating modes of temperature variability at the 3-3.5- and 4-4.5-yr time scales in the Upper Southwest Pacific Ocean" (Journal of Climate vol. 18 (5) (719-736)). Journal of Climate **18**:1637-1639.

Holbrook, N. J., P. S. L. Chan, and S. A. Venegas. 2005. Oscillatory and propagating modes of temperature variability at the 3-3.5- and 4-4.5-yr. time scales in the upper southwest Pacific Ocean. Journal of Climate **18**:719-736.

Holbrook, N. J., and A. M. Maharaj. 2008. Southwest Pacific subtropical mode water: A climatology. Progress in Oceanography **77**:298-315.

Hu, Y., H. Du, N. Jiao, and Y. Zeng. 2006. Abundant presence of the γ-like Proteobacterial pufM gene in oxic seawater. FEMS Microbiology Letters **263**:200-206.

Hugoni, M., N. Taib, D. Debroas, I. Domaizon, I. Jouan Dufournel, G. Bronner, I. Salter, H. Agogué, I. Mary, and P. E. Galand. 2013. Structure of the rare archaeal biosphere and seasonal dynamics of active ecotypes in surface coastal waters. Proc Natl Acad Sci U S A **110**:6004-6009.

Iverson, V., R. M. Morris, C. D. Frazar, C. T. Berthiaume, R. L. Morales, and E. V. Armbrust. 2012. Untangling Genomes from Metagenomes: Revealing an Uncultured Class of Marine Euryarchaeota. Science **335**:587-590.

Jeanthon, C., D. Boeuf, O. Dahan, F. Le Gall, L. Garczarek, E. M. Bendif, and A. C. Lehours. 2011. Diversity of cultivated and metabolically active aerobic anoxygenic phototrophic bacteria along an oligotrophic gradient in the Mediterranean Sea. Biogeosciences **8**:1955-1970.

Jiang, H., H. Dong, B. Yu, G. Lv, S. Deng, Y. Wu, M. Dai, and N. Jiao. 2009. Abundance and diversity of aerobic anoxygenic phototrophic bacteria in saline lakes on the Tibetan plateau. FEMS Microbiol Ecol **67**:268-278.

Jiao, N., F. Zhang, and N. Hong. 2010. Significant roles of bacteriochlorophylla supplemental to chlorophylla in the ocean. ISME J **4**:595-597.

Jiao, N., Y. Zhang, Y. Zeng, N. Hong, R. Liu, F. Chen, and P. Wang. 2007. Distinct distribution pattern of abundance and diversity of aerobic anoxygenic phototrophic bacteria in the global ocean. Environmental Microbiology **9**:3091-3099.

Johnson, C. R., S. C. Banks, N. S. Barrett, F. Cazassus, P. K. Dunstan, G. J. Edgar, S. D. Frusher, C. Gardner, M. Haddon, F. Helidoniotis, K. L. Hill, N. J. Holbrook, G. W. Hosie, P. R. Last, S. D. Ling, J. Melbourne-Thomas, K. Miller, G. T. Pecl, A. J. Richardson, K. R. Ridgway, S. R. Rintoul, D. A. Ritz, D. J. Ross, J. C. Sanderson, S. A. Shepherd, A. Slotwinski, K. M. Swadling, and N. Taw. 2011. Climate change cascades: Shifts in oceanography, species' ranges and subtidal marine community dynamics in eastern Tasmania. Journal of Experimental Marine Biology and Ecology **400**:17-32.

Karl, D. M. Solar energy capture and transformation in the sea. Elementa http://dx.doi.org/10.12952/journal. elementa.000021 (2014).

Karl, D. M., and M. J. Church. 2014. Microbial oceanography and the Hawaii Ocean Time-series programme. Nat Rev Micro **12**:699-713.

Kip, N., B. E. Dutilh, Y. Pan, L. Bodrossy, K. Neveling, M. P. Kwint, M. S. M. Jetten, and H. J. M. Op den Camp. 2011. Ultra-deep pyrosequencing of pmoA amplicons confirms the prevalence of Methylomonas and Methylocystis in Sphagnum mosses from a Dutch peat bog. Environ Microbiol Rep **3**:667-673.

Kirchman, D. L., M. T. Cottrell, and C. Lovejoy. 2010. The structure of bacterial communities in the western Arctic Ocean as revealed by pyrosequencing of 16S rRNA genes. Environ Microbiol **12**:1132-1143.

Kirchman, D. L., and T. E. Hanson. 2013. Bioenergetics of photoheterotrophic bacteria in the oceans. Environ Microbiol Rep **5**:188-199.

Koblizek, M. 2015. Ecology of aerobic anoxygenic phototrophs in aquatic environments. FEMS Microbiol Rev.

Koblizek, M., O. Beja, R. R. Bidigare, S. Christensen, B. Benitez-Nelson, C. Vetriani, M. K. Kolber, P. G. Falkowski, and Z. S. Kolber. 2003. Isolation and characterization of Erythrobacter sp. strains from the upper ocean. Arch Microbiol **180**:327-338.

Koh EY, Atamna-Ismaeel N, Martin A, Cowie RO, Beja O, Davy SK, et al. Proteorhodopsin-bearing bacteria in Antarctic sea ice. Appl Environ Microbiol. **2010**:76:5918–5925

Kolber, Z. S., F. G. Plumley, A. S. Lang, J. T. Beatty, R. E. Blankenship, C. L. VanDover, C. Vetriani, M. Koblizek, C. Rathgeber, and P. G. Falkowski. 2001. Contribution of aerobic photoheterotrophic bacteria to the carbon cycle in the ocean. Science **292**:2492-2495.

Kolber, Z. S., C. L. Van Dover, R. A. Niederman, and P. G. Falkowski. 2000. Bacterial photosynthesis in surface waters of the open ocean. Nature **407**:177-179.

Lami, R., M. T. Cottrell, J. Ras, O. Ulloa, I. Obernosterer, H. Claustre, D. L. Kirchman, and P. Lebaron. 2007. High abundances of aerobic anoxygenic photosynthetic bacteria in the South Pacific Ocean. Appl Environ Microbiol **73**:4198-4205.

Lami, R., and D. L. Kirchman. 2014. Diurnal expression of SAR11 proteorhodopsin and 16S rRNA genes in coastal North Atlantic waters. Aquatic Microbial Ecology **73**:185-194.

Legendre, P., and M. J. Anderson. 1999. Distance-based redundancy analysis: testing multispecies responses in multifactorial ecological experiments. Ecological Monographs **69**:1-24.

Lehours, A.-C., and C. Jeanthon. 2015. The hydrological context determines the beta-diversity of aerobic anoxygenic phototrophic bacteria in European Arctic seas but does not favor endemism. Frontiers in Microbiology **6**.

Lehours, A. C., M. T. Cottrell, O. Dahan, D. L. Kirchman, and C. Jeanthon. 2010. Summer distribution and diversity of aerobic anoxygenic phototrophic bacteria in the Mediterranean Sea in relation to environmental variables. FEMS Microbiol Ecol **74**:397-409.

Levine, J. M., and J. HilleRisLambers. 2009. The importance of niches for the maintenance of species diversity. Nature **461**:254-257.

Ludwig, W., O. Strunk, R. Westram, L. Richter, H. Meier, Yadhukumar, A. Buchner, T. Lai, S. Steppi, G. Jobb, W. Forster, I. Brettske, S. Gerber, A. W. Ginhart, O. Gross, S. Grumann, S. Hermann, R. Jost, A. Konig, T. Liss, R. Lussmann, M. May, B. Nonhoff, B. Reichel, R. Strehlow, A. Stamatakis, N. Stuckmann, A. Vilbig, M. Lenke, T. Ludwig, A. Bode, and K. H. Schleifer. 2004. ARB: a software environment for sequence data. Nucleic Acids Res **32**:1363-1371.

Madigan MT, Martinko JM, Stahl DA, Clark DP. 2011. Brock biology of microorganisms, 13th ed. Pearson Benjamin Cummings, San Francisco, CA.

Malmstrom, R. R., R. P. Kiene, and D. L. Kirchman. 2004. Identification and enumeration of bacteria assimilating dimethylsulfoniopropionate (DMSP) in the North Atlantic and Gulf of Mexico. Limnology and Oceanography **49**:597-606.

Man, D., W. Wang, G. Sabehi, L. Aravind, A. F. Post, R. Massana, E. N. Spudich, J. L. Spudich, and O. Béjà. 2003. Diversification and spectral tuning in marine proteorhodopsins. EMBO Journal **22**:1725-1731.

Martinez-Garcia, M., B. K. Swan, N. J. Poulton, M. L. Gomez, D. Masland, M. E. Sieracki, and R. Stepanauskas. 2012. High-throughput single-cell sequencing identifies photoheterotrophs and chemoautotrophs in freshwater bacterioplankton. ISME J **6**:113-123.

Martinez, A., A. S. Bradley, J. R. Waldbauer, R. E. Summons, and E. F. DeLong. 2007. Proteorhodopsin photosystem gene expression enables photophosphorylation in a heterologous host. Proceedings of the National Academy of Sciences of the United States of America **104**:5590-5595.

Masin, M., J. Nedoma, L. Pechar, and M. Koblizek. 2008. Distribution of aerobic anoxygenic phototrophs in temperate freshwater systems. Environ Microbiol **10**:1988-1996.

Mašín, M., A. Zdun, J. Stoń-Egiert, M. Nausch, M. Labrenz, V. Moulisová, and M. Koblížek. 2006. Seasonal changes and diversity of aerobic anoxygenic phototrophs in the Baltic Sea. Aquatic Microbial Ecology **45**:247-254.

McCarren, J., and E. F. DeLong. 2007. Proteorhodopsin photosystem gene clusters exhibit co-evolutionary trends and shared ancestry among diverse marine microbial phyla. Environmental Microbiology **9**:846-858.

Moran, M. A., and W. L. Miller. 2007. Resourceful heterotrophs make the most of light in the coastal ocean. Nature Reviews Microbiology **5**:792-800.

Morris, R. M., K. Longnecker, and S. J. Giovannoni. 2006. Pirellula and OM43 are among the dominant lineages identified in an Oregon coast diatom bloom. Environ Microbiol **8**:1361-1370.

Oh, H.-M., K. K. Kwon, I. Kang, S. G. Kang, J.-H. Lee, S.-J. Kim, and J.-C. Cho. 2010. Complete Genome Sequence of "Candidatus Puniceispirillum marinum" IMCC1322, a Representative of the SAR116 Clade in the Alphaproteobacteria. Journal of Bacteriology **192**:3240-3241.

Oesterhelt, D., and W. Stoeckenius. 1971. Rhodopsin-like protein from the purple membrane of Halobacterium halobium. Nature (London) New Biol. 233:149–152. [PubMed]

Palenik, B., B. Brahamsha, F. W. Larimer, M. Land, L. Hauser, P. Chain, J. Lamerdin, W. Regala, E. E. Allen, J. McCarren, I. Paulsen, A. Dufresne, F. Partensky, E. A. Webb, and J. Waterbury. 2003. The genome of a motile marine Synechococcus. Nature **424**:1037-1042.

Partensky, F., W. R. Hess, and D. Vaulot. 1999. Prochlorococcus, a marine photosynthetic prokaryote of global significance. Microbiol Mol Biol Rev **63**:106-127.

Philosof, A., and O. Béjà. 2013. Bacterial, archaeal and viral-like rhodopsins from the Red Sea. Environmental Microbiology Reports **5**:475-482.

Pomeroy, L. R. 1974. The Ocean's Food Web, A Changing Paradigm. BioScience **24**:499-504.

Pushkarev, A., and O. Beja. 2016. Functional metagenomic screen reveals new and diverse microbial rhodopsins. ISME J.

Rappe, M. S., S. A. Connon, K. L. Vergin, and S. J. Giovannoni. 2002. Cultivation of the ubiquitous SAR11 marine bacterioplankton clade. Nature **418**:630-633.

Rathgeber, C., J. T. Beatty, and V. Yurkov. 2004. Aerobic Phototrophic Bacteria: New Evidence for the Diversity, Ecological Importance and Applied Potential of this Previously Overlooked Group. Springer Science & Business Media, Dordrecht.

Reshef, D. N., Y. A. Reshef, H. K. Finucane, S. R. Grossman, G. McVean, P. J. Turnbaugh, E. S. Lander, M. Mitzenmacher, and P. C. Sabeti. 2011. Detecting Novel Associations in Large Data Sets. Science **334**:1518-1524.

Ridgway, K. R. 2007. Seasonal circulation around Tasmania: An interface between eastern and western boundary dynamics. Journal of Geophysical Research: Oceans **112**:n/a-n/a.

Ridgway, K. R., and J. R. Dunn. 2003. Mesoscale structure of the mean East Australian Current System and its relationship with topography. Progress in Oceanography **56**:189-222.

Riedel, T., J. Tomasch, I. Buchholz, J. Jacobs, M. Kollenberg, G. Gerdts, A. Wicheis, T. Brinkhoff, H. Cypionka, and I. Wagner-Döbler. 2010. Constitutive expression of the proteorhodopsin gene by a flavobacterium strain representative of the proteorhodopsin-producing microbial community in the North Sea. Applied and Environmental Microbiology **76**:3187-3197.

Ritchie, A. E., and Z. I. Johnson. 2012. Abundance and genetic diversity of aerobic anoxygenic phototrophic bacteria of coastal regions of the pacific ocean. Appl Environ Microbiol **78**:2858-2866.

Rocap, G., F. W. Larimer, J. Lamerdin, S. Malfatti, P. Chain, N. A. Ahlgren, A. Arellano, M. Coleman, L. Hauser, W. R. Hess, Z. I. Johnson, M. Land, D. Lindell, A. F. Post, W. Regala, M. Shah, S. L. Shaw, C. Steglich, M. B. Sullivan, C. S. Ting, A. Tolonen, E. A. Webb, E. R. Zinser, and S. W. Chisholm. 2003. Genome divergence in two Prochlorococcus ecotypes reflects oceanic niche differentiation. Nature **424**:1042-1047.

Rossi, V., A. Schaeffer, J. Wood, G. Galibert, B. Morris, J. Sudre, M. Roughan, and A. M. Waite. 2014. Seasonality of sporadic physical processes driving temperature and nutrient high-frequency variability in the coastal ocean off southeast Australia. Journal of Geophysical Research: Oceans **119**:445-460.

Roughan, M., and J. H. Middleton. 2004. On the East Australian Current: Variability, encroachment, and upwelling. Journal of Geophysical Research C: Oceans **109**:C07003 07001-07016.

Ruiz-González, C., R. Simó, R. Sommaruga, and J. M. Gasol. 2013. Away from darkness: a review on the effects of solar radiation on heterotrophic bacterioplankton activity. Front Microbiol **4**:131.

Rusch, D. B., A. L. Halpern, G. Sutton, K. B. Heidelberg, S. Williamson, S. Yooseph, D. Wu, J. A. Eisen, J. M. Hoffman, K. Remington, K. Beeson, B. Tran, H. Smith, H. Baden-Tillson, C. Stewart, J. Thorpe, J. Freeman, C. Andrews-Pfannkoch, J. E. Venter, K. Li, S. Kravitz, J. F. Heidelberg, T. Utterback, Y. H. Rogers, L. I. Falcón, V. Souza, G. Bonilla-Rosso, L. E. Eguiarte, D. M. Karl, S. Sathyendranath, T. Platt, E. Bermingham, V. Gallardo, G. Tamayo-Castillo, M. R. Ferrari, R. L. Strausberg, K. Nealson, R. Friedman, M. Frazier, and J. C. Venter. 2007. The Sorcerer II Global Ocean Sampling expedition: northwest Atlantic through eastern tropical Pacific. PLoS Biology **5**.

Sabehi, G., O. Béjà, M. T. Suzuki, C. M. Preston, and E. F. DeLong. 2004. Different SAR86 subgroups harbour divergent proteorhodopsins. Environmental Microbiology **6**:903-910.

Sabehi, G., B. C. Kirkup, M. Rozenberg, N. Stambler, M. F. Polz, and O. Béjá. 2007. Adaptation and spectral tuning in divergent marine proteorhodopsins from the eastern Mediterranean and the Sargasso Seas. ISME Journal **1**:48-55.

Sabehi, G., A. Loy, K. H. Jung, R. Partha, J. L. Spudich, T. Isaacson, J. Hirschberg, M. Wagner, and O. Béjà. 2005. New insights into metabolic properties of marine bacteria encoding proteorhodopsins. PLoS Biology **3**.

Sabehi, G., R. Massana, J. P. Bielawski, M. Rosenberg, E. F. Delong, and O. Béjà. 2003. Novel proteorhodopsin variants from the Mediterranean and Red Seas. Environ Microbiol **5**:842-849.

Saito, R., M. E. Smoot, K. Ono, J. Ruscheinski, P.-L. Wang, S. Lotia, A. R. Pico, G. D. Bader, and T. Ideker. 2012. A travel guide to Cytoscape plugins. Nat Meth **9**:1069-1076.

Salka, I., V. Moulisova, M. Koblizek, G. Jost, K. Jurgens, and M. Labrenz. 2008a. Abundance, depth distribution, and composition of aerobic bacteriochlorophyll a-producing bacteria in four basins of the central Baltic Sea. Appl Environ Microbiol **74**:4398-4404.

Salter, I., P. E. Galand, S. K. Fagervold, P. Lebaron, I. Obernosterer, M. J. Oliver, M. T. Suzuki, and C. Tricoire. 2015. Seasonal dynamics of active SAR11 ecotypes in the oligotrophic Northwest Mediterranean Sea. ISME J **9**:347-360.

Schwalbach, M. S., and J. A. Fuhrman. 2005. Wide-ranging abundances of aerobic anoxygenic phototrophic bacteria in the world ocean revealed by epifluorescence microscopy and quantitative PCR. Limnology and Oceanography **50**:620-628.

Selje, N., M. Simon, and T. Brinkhoff. 2004. A newly discovered Roseobacter cluster in temperate and polar oceans. Nature **427**:445-448.

Seymour, J. R., M. A. Doblin, T. C. Jeffries, M. V. Brown, K. Newton, P. J. Ralph, M. Baird, and J. G. Mitchell. 2012. Contrasting microbial assemblages in adjacent water masses associated with the East Australian Current. Environ Microbiol Rep **4**:548-555.

Sherr, E., and B. Sherr. 1988. Role of microbes in pelagic food webs: A revised concept. Limnology and Oceanography **33**:1225-1227.

Shiba, T., U. Simidu, and N. Taga. 1979. Distribution of aerobic bacteria which contain bacteriochlorophyll a. Appl Environ Microbiol **38**:43-45.

Sieracki, M. E., I. C. Gilg, E. C. Thier, N. J. Poulton, and R. Goericke. 2006. Distribution of planktonic aerobic anoxygenic photoheterotrophic bacteria in the northwest Atlantic. Limnology and Oceanography **51**:38-46.

Sogin, M. L., H. G. Morrison, J. A. Huber, D. M. Welch, S. M. Huse, P. R. Neal, J. M. Arrieta, and G. J. Herndl. 2006. Microbial diversity in the deep sea and the underexplored "rare biosphere". Proceedings of the National Academy of Sciences **103**:12115-12120.

Spring, S., and T. Riedel. 2013a. Mixotrophic growth of bacteriochlorophyll a-containing members of the OM60/NOR5 clade of marine gammaproteobacteria is carbon-starvation independent and correlates with the type of carbon source and oxygen availability. BMC Microbiol **13**:117-117.

Spring, S., and T. Riedel. 2013b. Mixotrophic growth of bacteriochlorophyll a-containing members of the OM60/NOR5 clade of marine gammaproteobacteria is carbon-starvation independent and correlates with the type of carbon source and oxygen availability. BMC Microbiol **13**:1-11.

Spring, S., T. Riedel, C. Spröer, S. Yan, J. Harder, and B. M. Fuchs. 2013. Taxonomy and evolution of bacteriochlorophyll a-containing members of the OM60/NOR5 clade of marine gammaproteobacteria: description of Luminiphilus syltensis gen. nov., sp. nov., reclassification of Haliea rubra as Pseudohaliea rubra gen. nov., comb. nov., and emendation of Chromatocurvus halotolerans. BMC Microbiol **13**:118-118.

Stegman, M. R., M. T. Cottrell, and D. L. Kirchman. 2014. Leucine incorporation by aerobic anoxygenic phototrophic bacteria in the Delaware estuary. ISME J **8**:2339-2348.

Stingl, U., R. A. Desiderio, J. C. Cho, K. L. Vergin, and S. J. Giovannoni. 2007. The SAR92 clade: An abundant coastal clade of culturable marine bacteria possessing proteorhodopsin. Applied and Environmental Microbiology **73**:2290-2296.

Stoecker, D. K., A. E. Michaels, and L. H. Davis. 1987. Large proportion of marine planktonic ciliates found to contain functional chloroplasts. Nature **326**:790-792.

Suthers, I. M., J. W. Young, M. E. Baird, M. Roughan, J. D. Everett, G. B. Brassington, M. Byrne, S. A. Condie, J. R. Hartog, C. S. Hassler, A. J. Hobday, N. J. Holbrook, H. A. Malcolm, P. R. Oke, P. A. Thompson, and K. Ridgway. 2011. The strengthening East Australian Current, its eddies and biological effects — an introduction and overview. Deep Sea Research Part II: Topical Studies in Oceanography **58**:538-546.

Suzuki, M. T., C. M. Preston, F. P. Chavez, and E. F. DeLong. 2001. Quantitative mapping of bacterioplankton populations in seawater: field tests across an upwelling plume in Monterey Bay. Aquatic Microbial Ecology **24**:117-127.

Thiel, V., M. Tank, S. C. Neulinger, L. Gehrmann, C. Dorador, and J. F. Imhoff. 2010. Unique communities of anoxygenic phototrophic bacteria in saline lakes of Salar de Atacama (Chile): evidence for a new phylogenetic lineage of phototrophic Gammaproteobacteria from pufLM gene analyses. FEMS Microbiol Ecol **74**:510-522.

Thompson, P. A., P. Bonham, A. M. Waite, L. A. Clementson, N. Cherukuru, C. Hassler, and M. A. Doblin. 2011. Contrasting oceanographic conditions and phytoplankton communities on the east and west coasts of Australia. Deep Sea Research Part II: Topical Studies in Oceanography **58**:645-663.

Tomczak, Matthias & J Stuart Godfrey: Regional Oceanography: an Introduction 2nd edn (2003).

Venter, J. C., K. Remington, J. F. Heidelberg, A. L. Halpern, D. Rusch, J. A. Eisen, D. Wu, I. Paulsen, K. E. Nelson, W. Nelson, D. E. Fouts, S. Levy, A. H. Knap, M. W. Lomas, K. Nealson, O. White, J. Peterson, J. Hoffman, R. Parsons, H. Baden-Tillson, C. Pfannkoch, Y. H. Rogers, and H. O. Smith. 2004. Environmental Genome Shotgun Sequencing of the Sargasso Sea. Science **304**:66-74.

Waidner, L. A., and D. L. Kirchman. 2007. Aerobic anoxygenic phototrophic bacteria attached to particles in turbid waters of the Delaware and Chesapeake estuaries. Appl Environ Microbiol **73**:3936-3944.

Whitman, W. B., D. C. Coleman, and W. J. Wiebe. 1998. Prokaryotes: The unseen majority. Proceedings of the National Academy of Sciences **95**:6578-6583.

Wu, L., W. Cai, L. Zhang, H. Nakamura, A. Timmermann, T. Joyce, M. J. McPhaden, M. Alexander, B. Qiu, M. Visbeck, P. Chang, and B. Giese. 2012. Enhanced warming over the global subtropical western boundary currents. Nature Clim. Change **2**:161-166.

Yan, S., B. M. Fuchs, S. Lenk, J. Harder, J. Wulf, N. Z. Jiao, and R. Amann. 2009. Biogeography and phylogeny of the NOR5/OM60 clade of Gammaproteobacteria. Syst Appl Microbiol **32**:124-139.

Yoshizawa, S., A. Kawanabe, H. Ito, H. Kandori, and K. Kogure. 2012. Diversity and functional analysis of proteorhodopsin in marine Flavobacteria. Environmental Microbiology **14**:1240-1248.

Yurkov, V., and J. T. Beatty. 1998a. Isolation of aerobic anoxygenic photosynthetic bacteria from black smoker plume waters of the juan de fuca ridge in the pacific ocean. Appl Environ Microbiol **64**:337-341.

Yurkov, V. V., and J. T. Beatty. 1998b. Aerobic anoxygenic phototrophic bacteria. Microbiol Mol Biol Rev **62**:695-724.

Yutin, N., and O. Beja. 2005. Putative novel photosynthetic reaction centre organizations in marine aerobic anoxygenic photosynthetic bacteria: insights from metagenomics and environmental genomics. Environ Microbiol **7**:2027-2033.

Yutin, N., M. T. Suzuki, and O. Béjà. 2005. Novel primers reveal wider diversity among marine aerobic anoxygenic phototrophs. Applied and Environmental Microbiology **71**:8958-8962.

Yutin, N., M. T. Suzuki, H. Teeling, M. Weber, J. C. Venter, D. B. Rusch, and O. Beja. 2007a. Assessing diversity and biogeography of aerobic anoxygenic phototrophic bacteria in surface waters of the Atlantic and Pacific Oceans using the Global Ocean Sampling expedition metagenomes. Environ Microbiol **9**:1464-1475.

Zeng, Y. H., X. H. Chen, and N. Z. Jiao. 2007. Genetic diversity assessment of anoxygenic photosynthetic bacteria by distance-based grouping analysis of pufM sequences. Lett Appl Microbiol **45**:639-645.

Zhang, Y., and N. Jiao. 2007. Dynamics of aerobic anoxygenic phototrophic bacteria in the East China Sea. FEMS Microbiol Ecol **61**:459-469.

Zhao, M., F. Chen, and N. Jiao. 2009. Genetic diversity and abundance of flavobacterial proteorhodopsin in China seas. Applied and Environmental Microbiology **75**:529-533.

Zheng, Q., Y. Liu, L. Steindler, and N. Jiao. 2015. Pyrosequencing analysis of aerobic anoxygenic phototrophic bacterial community structure in the oligotrophic western Pacific Ocean. FEMS Microbiol Lett **362**:fnv034.

Zubkov, M. V. 2009. Photoheterotrophy in marine prokaryotes. Journal of Plankton Research **31**:933-938.

APPENDIX I

Table S1: Environmental parameters recorded at all stations.

Parameters available at all Stations														
Month	**Station**	**Ammo**	**D.Length**	**Nitr**	**Phos**	**Picoeuk**	**Proc**	**Sali**	**Secchi**	**Sili**	**Sol.exp**	**Syne**	**Temp**	**Zoo**
JUL	NSI	0.17	658	0.05	0.10	3801	23227	35.47	22	0.26	17.40	18638	20.85	7.72
AUG	NSI	0.15	678	0.31	0.11	2069	17158	35.53	19	0.39	14.30	15267	21.07	14.00
SEP	NSI	0.06	711	0.05	0.13	1276	2032	35.52	21	0.01	19.30	8836	21.03	19.02
OCT	NSI	0.80	767	0.00	0.16	10086	6169	35.51	13	0.70	28.60	57194	21.59	21.72
DEC	NSI	0.07	822	0.00	0.11	12404	38994	35.57	14	1.07	30.20	29870	25.82	14.47
JAN	NSI	0.04	811	0.00	0.09	4221	59010	35.43	22	0.71	16.10	28771	27.28	11.32
MAR	NSI	0.10	718	0.00	0.08	6332	14102	34.45	13	1.92	22.20	41034	25.55	8.81
APR	NSI	0.00	683	0.00	0.10	1203	28917	35.26	34	0.37	19.00	12280	25.38	8.73
MAY	NSI	0.15	643	0.00	0.12	2502	26072	35.27	17	0.42	14.90	15459	23.56	11.21
JUL	PHA	0.08	608	1.34	0.11	4022	79	35.46	13	2.33	3.10	3702	17.58	4.24
SEP	PHA	0.58	718	3.92	0.37	6122	218	35.45	17	1.45	4.80	2943	17.54	54.32
OCT	PHA	0.38	764	0.54	0.23	8222	357	35.52	10	0.88	7.00	2184	17.49	9.88
NOV	PHA	0.18	842	0.01	0.12	2269	330	35.49	12	0.00	7.60	2416	18.89	31.18
DEC	PHA	0.44	865	0.00	0.19	19630	4389	35.47	9	0.75	6.30	43675	18.79	2.48
FEB	PHA	0.52	771	7.54	0.72	2195	1969	35.40	11	3.71	1.00	4521	17.26	1.80
APR	PHA	0.42	679	0.78	0.18	4521	10726	35.32	17	0.54	4.90	18155	18.81	1.26
MAY	PHA	0.52	622	0.86	0.26	5350	14307	35.36	15	1.24	3.40	31479	20.36	0.73
JUN	PHA	1.44	595	1.40	0.36	5025	6332	35.60	17	0.78	0.90	15299	19.66	0.04
AUG	MAI	0.12	639	3.11	0.28	2578	1654	35.29	15	0.76	2.60	6148	12.18	1.95
SEP	MAI	0.29	755	4.74	0.44	2762	2559	35.07	15	1.09	3.80	5193	11.98	11.35
OCT	MAI	0.26	800	1.98	0.33	24256	1628	35.03	13	0.01	2.70	97871	12.19	22.72
NOV	MAI	0.12	866	0.59	0.26	23064	2710	35.04	10	0.87	7.00	31726	13.29	17.11
JAN	MAI	0.29	863	0.00	0.21	2184	1492	35.12	10	0.44	7.80	23174	16.13	18.96

FEB	MAI	0.33	826	0.06	0.28	14995	15425	23.15	18	0.42	4.30	21499	16.80	9.89
MAR	MAI	0.06	747	0.00	0.20	2694	4374	35.26	15	0.51	5.60	10894	17.48	4.52
APR	MAI	0.30	634	1.15	0.22	4695	116	35.37	15	0.30	1.30	5623	16.49	8.32
MAY	MAI	0.01	564	2.42	0.31	3235	208	35.40	19	0.54	1.70	4489	15.08	5.65
JUN	MAI	0.13	550	2.29	0.31	1775	300	35.35	21	0.42	1.30	3356	14.50	2.99

North Stradbroke Island

Month	Temp	Cond	Fluore	Sali	Sili	Ni	Phos	Ammo	Zoo	Proc	Syne	Picoeuk	Fuco	Neo
JUL	20.85	4.94	0.28	35.47	0.26	0.05	0.10	0.17	7.72	23227	18638	3801	0.06	0.00
AUG	21.07	4.96	0.39	35.53	0.39	0.31	0.11	0.15	14.00	17158	15267	2069	0.07	0.00
SEP	21.03	4.96	0.26	35.52	0.01	0.05	0.13	0.06	19.02	2032	8836	1276	0.03	0.00
OCT	21.59	5.02	0.25	35.51	0.70	0.00	0.16	0.80	21.72	6169	57194	10086	0.05	0.02
DEC	25.82	5.47	0.29	35.57	1.07	0.00	0.11	0.07	14.47	38994	29870	12404	0.01	0.01
JAN	27.28	5.61	0.19	35.43	0.71	0.00	0.09	0.04	11.32	59010	28771	4221	0.03	0.01
MAR	25.55	5.29	0.30	34.45	1.92	0.00	0.08	0.10	8.81	14102	41034	6332	0.05	0.01
APR	25.38	5.38	0.14	35.26	0.37	0.00	0.10	0.00	8.73	28917	12280	1203	0.01	0.00
MAY	23.56	5.19	0.29	35.27	0.42	0.00	0.12	0.15	11.21	26072	15459	2502	0.05	0.01

Month	Anth	Allo	Diato	Zea	Dv_Cphl_B	Cphl_B	Dv_Cphl_A	Cphl_A	ABC	Sol.exp	D.Length	Secchi
JUL	0.00	0.00	0.00	0.03	0.00	0.02	0.02	0.28	0.01	17.40	658	22
AUG	0.00	0.00	0.00	0.02	0.00	0.03	0.02	0.29	0.01	14.30	678	19
SEP	0.00	0.00	0.00	0.00	0.00	0.01	0.00	0.09	0.00	19.30	711	21
OCT	0.00	0.00	0.00	0.04	0.00	0.08	0.00	0.32	0.01	28.60	767	13
DEC	0.00	0.00	0.00	0.08	0.00	0.05	0.06	0.22	0.02	30.20	822	14
JAN	0.00	0.00	0.00	0.06	0.01	0.04	0.07	0.23	0.02	16.10	811	22
MAR	0.00	0.00	0.00	0.05	0.00	0.04	0.01	0.28	0.01	22.20	718	13
APR	0.00	0.00	0.00	0.03	0.00	0.01	0.04	0.08	0.01	19.00	683	34
MAY	0.00	0.00	0.00	0.04	0.00	0.04	0.03	0.33	0.02	14.90	643	17

Port Hacking

Month	Sali	Sili	Nitr	Phos	Ammo	Temp	Proc	Syne	Pico	Zoo	Sol.exp	D.Lenght	Secc
JUL	35.46	2.33	1.34	0.11	0.08	17.58	79	3702	4022	4.24	6.00	608	12.50
SEP	35.45	1.45	3.92	0.37	0.58	17.54	218	2943	6122	54.32	17.10	718	16.50
OCT	35.52	0.88	0.54	0.23	0.38	17.49	357	2184	8222	9.88	25.50	764	10.00
NOV	35.49	0.00	0.01	0.12	0.18	18.89	330	2416	2269	31.18	24.20	842	12.00
DEC	35.47	0.75	0.00	0.19	0.44	18.79	4389	43675	19630	2.48	21.50	865	9.00
FEB	35.40	3.71	7.54	0.72	0.52	17.26	1969	4521	2195	1.80	3.90	771	11.00
APR	35.32	0.54	0.78	0.18	0.42	18.81	10726	18155	4521	1.26	17.80	679	17.00
MAY	35.36	1.24	0.86	0.26	0.52	20.36	14307	31479	5350	0.73	12.50	622	15.00
JUN	35.60	0.78	1.40	0.36	1.44	19.66	6332	15299	5025	0.04	3.10	595	17.00

Maria Island

Month	Temp	Cond	Fluo	Turb	Inor	Orga	Zoo	Proc	Syne	Pico	Sali	Sili	Nitr	Phos
AUG	12.18	4.05	0.16	0.23	0.15	0.25	1.95	1654	6148	2578	35.29	0.76	3.11	0.28
SEP	11.98	4.00	0.27	0.19	0.05	0.30	11.35	2559	5193	2762	35.07	1.09	4.74	0.44
OCT	12.19	4.02	0.67	0.23	0.25	0.35	22.72	1628	97871	24256	35.03	0.01	1.98	0.33
NOV	13.29	4.13	0.41	0.27	0.15	0.40	17.11	2710	31726	23064	35.04	0.87	0.59	0.26
JAN	16.13	4.42	0.59	0.25	0.20	0.40	18.96	1492	23174	2184	35.12	0.44	0.00	0.21
FEB	16.80	4.49	0.47	0.22	0.20	0.25	9.89	15425	21499	14995	23.15	0.42	0.06	0.28
MAR	17.48	4.57	0.34	0.20	0.65	0.50	4.52	4374	10894	2694	35.26	0.51	0.00	0.20
APR	16.49	4.48	0.18	0.21	0.25	0.25	8.32	116	5623	4695	35.37	0.30	1.15	0.22
MAY	15.08	4.34	0.20	0.23	0.50	0.35	5.65	208	4489	3235	35.40	0.54	2.42	0.31
JUN	14.50	4.28	0.22	0.19	0.30	0.30	2.99	300	3356	1775	35.35	0.42	2.29	0.31

Month	Ammo	Sol.exp	D.Length	Secc	Cphl_C3	Cphl_C2	Fuco	Neo	Hex_Fuco	Anth	Allo	Zea	Cphl_B	Cphl_A	ABC
AUG	0.12	9.50	639	15	0.03	0.05	0.05	0.01	0.05	0.00	0.01	0.01	0.11	0.44	0.01
SEP	0.29	13.60	755	15	0.03	0.05	0.10	0.01	0.04	0.00	0.01	0.00	0.05	0.39	0.01
OCT	0.26	13.00	800	13	0.09	0.21	0.41	0.01	0.06	0.00	0.01	0.01	0.13	1.32	0.03
NOV	0.12	29.00	866	10	0.06	0.15	0.16	0.05	0.03	0.01	0.08	0.06	0.41	1.25	0.05
JAN	0.29	28.20	863	10	0.26	0.26	0.20	0.03	0.40	0.01	0.07	0.02	0.27	1.62	0.05

FEB	0.33	24.80	826	18	0.05	0.06	0.04	0.01	0.10	0.00	0.01	0.01	0.06	0.40	0.01
MAR	0.06	20.20	747	15	0.05	0.07	0.04	0.01	0.09	0.00	0.02	0.01	0.08	0.45	0.02
APR	0.30	4.50	634	15	0.04	0.07	0.04	0.01	0.08	0.00	0.03	0.01	0.11	0.50	0.02
MAY	0.01	6.10	564	19	0.06	0.07	0.06	0.01	0.09	0.00	0.02	0.01	0.10	0.46	0.01
JUN	0.13	4.60	550	21	0.03	0.04	0.03	0.00	0.04	0.00	0.01	0.00	0.04	0.18	0.01

APPENDIX II

Table S1: Environmental parameters recorded at all stations. **Abbreviations**: **Temp**= Temperature (ºC), **Cond**= Conductivity (µS cm^{-1}), **Fluo**= Fluoresence (FUs), **Turb**= Turbidity (NTU), **Inor**= Inorganic Fraction (mg L^{-1}), **Orga**= Organic Fraction (mg L^{-1}), **Zoo**= Zooplankton (mg m^{-3}), **Proc**= Prochlorococcus (cells per ml), **Syne**= Synechococcus (cells per ml), **Pico**= Picoeukaryotes (cells per ml), **Sali**= Salinity (PSU), **Sili**=Silica (µmol L^{-1}), **Nitr**= Nitrate/Nitrite (µmol L^{-1}), **Phos**= Phosphorous (µmol L^{-1}), **Ammo**= Ammonium (µmol L^{-1}), **Sol.exp**= Solar radiation exposure (MJ m^{-2}), **D.Length**= Day length (minutes), **Secc**= Secchi depth (meters), **Cphl_C3**= Chlorophyll c3 (mg m^{-3}), **Cphl_C2**= Chlorophyll c2 (mg m^{-3}), **Fuco**= Fucoxanthin (mg m^{-3}), **Neo**= Neoxanthin (mg m^{-3}), **Diato**= Diatoxanthin (mg m^{-3}), **Hex_Fuco**= 19'-hexanoyloxyfucoxanthin (mg m^{-3}), **Anth**= Anthocyanin (mg m^{-3}), **Allo**= Alloxanthin (mg m^{-3}), **Zea**= Zeaxanthin (mg m^{-3}), **Cphl_B**= Chlorophyll b (mg m^{-3}), **Cphl_A**= Chlorophyll a (mg m^{-3}), **ABC**= α-β carotene (mg m^{-3}), **Dv_Cphl_B**= Divinyl Chlorophyll b (mg m^{-3}), **Dv_Cphl_A**= Divinyl Chlorophyll a (mg m^{-3}).

Parameters available at all Stations														
Month	**Station**	**Ammo**	**D.Length**	**Nitr**	**Phos**	**Picoeuk**	**Proc**	**Sali**	**Secchi**	**Sili**	**Sol.exp**	**Syne**	**Temp**	**Zoo**
JUL	NSI	0.17	658	0.05	0.10	3801	23227	35.47	22	0.26	17.40	18638	20.85	7.72
AUG	NSI	0.15	678	0.31	0.11	2069	17158	35.53	19	0.39	14.30	15267	21.07	14.00
SEP	NSI	0.06	711	0.05	0.13	1276	2032	35.52	21	0.01	19.30	8836	21.03	19.02
OCT	NSI	0.80	767	0.00	0.16	10086	6169	35.51	13	0.70	28.60	57194	21.59	21.72
DEC	NSI	0.07	822	0.00	0.11	12404	38994	35.57	14	1.07	30.20	29870	25.82	14.47
JAN	NSI	0.04	811	0.00	0.09	4221	59010	35.43	22	0.71	16.10	28771	27.28	11.32
MAR	NSI	0.10	718	0.00	0.08	6332	14102	34.45	13	1.92	22.20	41034	25.55	8.81
APR	NSI	0.00	683	0.00	0.10	1203	28917	35.26	34	0.37	19.00	12280	25.38	8.73
MAY	NSI	0.15	643	0.00	0.12	2502	26072	35.27	17	0.42	14.90	15459	23.56	11.21
JUL	PHA	0.08	608	1.34	0.11	4022	79	35.46	13	2.33	3.10	3702	17.58	4.24
SEP	PHA	0.58	718	3.92	0.37	6122	218	35.45	17	1.45	4.80	2943	17.54	54.32
OCT	PHA	0.38	764	0.54	0.23	8222	357	35.52	10	0.88	7.00	2184	17.49	9.88
NOV	PHA	0.18	842	0.01	0.12	2269	330	35.49	12	0.00	7.60	2416	18.89	31.18
DEC	PHA	0.44	865	0.00	0.19	19630	4389	35.47	9	0.75	6.30	43675	18.79	2.48

FEB	PHA	0.52	771	7.54	0.72	2195	1969	35.40	11	3.71	1.00	4521	17.26	1.80
APR	PHA	0.42	679	0.78	0.18	4521	10726	35.32	17	0.54	4.90	18155	18.81	1.26
MAY	PHA	0.52	622	0.86	0.26	5350	14307	35.36	15	1.24	3.40	31479	20.36	0.73
JUN	PHA	1.44	595	1.40	0.36	5025	6332	35.60	17	0.78	0.90	15299	19.66	0.04
AUG	MAI	0.12	639	3.11	0.28	2578	1654	35.29	15	0.76	2.60	6148	12.18	1.95
SEP	MAI	0.29	755	4.74	0.44	2762	2559	35.07	15	1.09	3.80	5193	11.98	11.35
OCT	MAI	0.26	800	1.98	0.33	24256	1628	35.03	13	0.01	2.70	97871	12.19	22.72
NOV	MAI	0.12	866	0.59	0.26	23064	2710	35.04	10	0.87	7.00	31726	13.29	17.11
JAN	MAI	0.29	863	0.00	0.21	2184	1492	35.12	10	0.44	7.80	23174	16.13	18.96
FEB	MAI	0.33	826	0.06	0.28	14995	15425	23.15	18	0.42	4.30	21499	16.80	9.89
MAR	MAI	0.06	747	0.00	0.20	2694	4374	35.26	15	0.51	5.60	10894	17.48	4.52
APR	MAI	0.30	634	1.15	0.22	4695	116	35.37	15	0.30	1.30	5623	16.49	8.32
MAY	MAI	0.01	564	2.42	0.31	3235	208	35.40	19	0.54	1.70	4489	15.08	5.65
JUN	MAI	0.13	550	2.29	0.31	1775	300	35.35	21	0.42	1.30	3356	14.50	2.99

North Stradbroke Island

Month	**Temp**	**Cond**	**Fluore**	**Sali**	**Sili**	**Nitr**	**Phos**	**Ammo**	**Zoo**	**Proc**	**Syne**	**Picoeuk**	**Fuco**	**Neo**
JUL	20.85	4.94	0.28	35.47	0.26	0.05	0.10	0.17	7.72	23227	18638	3801	0.06	0.00
AUG	21.07	4.96	0.39	35.53	0.39	0.31	0.11	0.15	14.00	17158	15267	2069	0.07	0.00
SEP	21.03	4.96	0.26	35.52	0.01	0.05	0.13	0.06	19.02	2032	8836	1276	0.03	0.00
OCT	21.59	5.02	0.25	35.51	0.70	0.00	0.16	0.80	21.72	6169	57194	10086	0.05	0.02
DEC	25.82	5.47	0.29	35.57	1.07	0.00	0.11	0.07	14.47	38994	29870	12404	0.01	0.01
JAN	27.28	5.61	0.19	35.43	0.71	0.00	0.09	0.04	11.32	59010	28771	4221	0.03	0.01
MAR	25.55	5.29	0.30	34.45	1.92	0.00	0.08	0.10	8.81	14102	41034	6332	0.05	0.01
APR	25.38	5.38	0.14	35.26	0.37	0.00	0.10	0.00	8.73	28917	12280	1203	0.01	0.00
MAY	23.56	5.19	0.29	35.27	0.42	0.00	0.12	0.15	11.21	26072	15459	2502	0.05	0.01
Month	**Anth**	**Allo**	**Diato**	**Zea**	**Dv_Cphl_B**	**Cphl_B**	**Dv_Cphl_A**	**Cphl_A**	**ABC**	**Sol.exp**	**D.Length**	**Secchi**		
JUL	0.00	0.00	0.00	0.03	0.00	0.02	0.02	0.28	0.01	17.40	658	22		
AUG	0.00	0.00	0.00	0.02	0.00	0.03	0.02	0.29	0.01	14.30	678	19		
SEP	0.00	0.00	0.00	0.00	0.00	0.01	0.00	0.09	0.00	19.30	711	21		
OCT	0.00	0.00	0.00	0.04	0.00	0.08	0.00	0.32	0.01	28.60	767	13		

DEC	0.00	0.00	0.00	0.08	0.00	0.05	0.06	0.22	0.02	30.20	822	14
JAN	0.00	0.00	0.00	0.06	0.01	0.04	0.07	0.23	0.02	16.10	811	22
MAR	0.00	0.00	0.00	0.05	0.00	0.04	0.01	0.28	0.01	22.20	718	13
APR	0.00	0.00	0.00	0.03	0.00	0.01	0.04	0.08	0.01	19.00	683	34
MAY	0.00	0.00	0.00	0.04	0.00	0.04	0.03	0.33	0.02	14.90	643	17

Port Hacking

Month	Sali	Sili	Nitr	Phos	Ammo	Temp	Proc	Syne	Pico	Zoo	Sol.exp	D.Lenght	Secc
JUL	35.46	2.33	1.34	0.11	0.08	17.58	79	3702	4022	4.24	6.00	608	12.50
SEP	35.45	1.45	3.92	0.37	0.58	17.54	218	2943	6122	54.32	17.10	718	16.50
OCT	35.52	0.88	0.54	0.23	0.38	17.49	357	2184	8222	9.88	25.50	764	10.00
NOV	35.49	0.00	0.01	0.12	0.18	18.89	330	2416	2269	31.18	24.20	842	12.00
DEC	35.47	0.75	0.00	0.19	0.44	18.79	4389	43675	19630	2.48	21.50	865	9.00
FEB	35.40	3.71	7.54	0.72	0.52	17.26	1969	4521	2195	1.80	3.90	771	11.00
APR	35.32	0.54	0.78	0.18	0.42	18.81	10726	18155	4521	1.26	17.80	679	17.00
MAY	35.36	1.24	0.86	0.26	0.52	20.36	14307	31479	5350	0.73	12.50	622	15.00
JUN	35.60	0.78	1.40	0.36	1.44	19.66	6332	15299	5025	0.04	3.10	595	17.00

Maria Island

Month	Temp	Cond	Fluo	Turb	Inor	Orga	Zoo	Proc	Syne	Pico	Sali	Sili	Nitr	Phos
AUG	12.18	4.05	0.16	0.23	0.15	0.25	1.95	1654	6148	2578	35.29	0.76	3.11	0.28
SEP	11.98	4.00	0.27	0.19	0.05	0.30	11.35	2559	5193	2762	35.07	1.09	4.74	0.44
OCT	12.19	4.02	0.67	0.23	0.25	0.35	22.72	1628	97871	24256	35.03	0.01	1.98	0.33
NOV	13.29	4.13	0.41	0.27	0.15	0.40	17.11	2710	31726	23064	35.04	0.87	0.59	0.26
JAN	16.13	4.42	0.59	0.25	0.20	0.40	18.96	1492	23174	2184	35.12	0.44	0.00	0.21
FEB	16.80	4.49	0.47	0.22	0.20	0.25	9.89	15425	21499	14995	23.15	0.42	0.06	0.28
MAR	17.48	4.57	0.34	0.20	0.65	0.50	4.52	4374	10894	2694	35.26	0.51	0.00	0.20
APR	16.49	4.48	0.18	0.21	0.25	0.25	8.32	116	5623	4695	35.37	0.30	1.15	0.22
MAY	15.08	4.34	0.20	0.23	0.50	0.35	5.65	208	4489	3235	35.40	0.54	2.42	0.31
JUN	14.50	4.28	0.22	0.19	0.30	0.30	2.99	300	3356	1775	35.35	0.42	2.29	0.31

Month	Ammo	Sol.exp	D.Length	Secc	Cphl_C3	Cphl_C2	Fuco	Neo	Hex_Fuco	Anth	Allo	Zea	Cphl_B	Cphl_A	ABC
AUG	0.12	9.50	639	15	0.03	0.05	0.05	0.01	0.05	0.00	0.01	0.01	0.11	0.44	0.01
SEP	0.29	13.60	755	15	0.03	0.05	0.10	0.01	0.04	0.00	0.01	0.00	0.05	0.39	0.01
OCT	0.26	13.00	800	13	0.09	0.21	0.41	0.01	0.06	0.00	0.01	0.01	0.13	1.32	0.03
NOV	0.12	29.00	866	10	0.06	0.15	0.16	0.05	0.03	0.01	0.08	0.06	0.41	1.25	0.05
JAN	0.29	28.20	863	10	0.26	0.26	0.20	0.03	0.40	0.01	0.07	0.02	0.27	1.62	0.05
FEB	0.33	24.80	826	18	0.05	0.06	0.04	0.01	0.10	0.00	0.01	0.01	0.06	0.40	0.01
MAR	0.06	20.20	747	15	0.05	0.07	0.04	0.01	0.09	0.00	0.02	0.01	0.08	0.45	0.02
APR	0.30	4.50	634	15	0.04	0.07	0.04	0.01	0.08	0.00	0.03	0.01	0.11	0.50	0.02
MAY	0.01	6.10	564	19	0.06	0.07	0.06	0.01	0.09	0.00	0.02	0.01	0.10	0.46	0.01
JUN	0.13	4.60	550	21	0.03	0.04	0.03	0.00	0.04	0.00	0.01	0.00	0.04	0.18	0.01

APPENDIX III

Table S2: Pearson correlations of species richness, Shannon's diversity and spectral tunning types with environmental variables

All stations

		chao1	observed_species	shannon	margalef	simpson	NH4	Daylength	NO2NO3	PO4	Picoeukaryotes
chao1	Pearson Correlation	1	.809**	.734**	.809**	.599**	.251	-.289	-.072	-.143	-.330
	Sig. (2-tailed)		.000	.000	.000	.001	.197	.135	.716	.468	.086
	N	28	28	28	28	28	28	28	28	28	28
observed_species	Pearson Correlation	.809**	1	.941**	1.000**	.767**	.044	-.254	-.291	-.385*	-.298
	Sig. (2-tailed)	.000		.000	0.000	.000	.825	.193	.132	.043	.124
	N	28	28	28	28	28	28	28	28	28	28
shannon	Pearson Correlation	.734**	.941**	1	.941**	.922**	.050	-.094	-.341	-.361	-.244
	Sig. (2-tailed)	.000	.000		.000	.000	.801	.634	.076	.059	.211
	N	28	28	28	28	28	28	28	28	28	28
margalef	Pearson Correlation	.809**	1.000**	.941**	1	.767**	.044	-.254	-.291	-.385*	-.298
	Sig. (2-tailed)	.000	0.000	.000		.000	.825	.193	.132	.043	.124
	N	28	28	28	28	28	28	28	28	28	28
simpson	Pearson Correlation	.599**	.767**	.922**	.767**	1	.052	.042	-.346	-.315	-.244
	Sig. (2-tailed)	.001	.000	.000	.000		.791	.832	.071	.102	.210
	N	28	28	28	28	28	28	28	28	28	28
NH4	Pearson Correlation	.251	.044	.050	.044	.052	1	-.040	.180	.386*	.133
	Sig. (2-tailed)	.197	.825	.801	.825	.791		.840	.358	.043	.499
	N	28	28	28	28	28	28	28	28	28	28
Daylength	Pearson Correlation	-.289	-.254	-.094	-.254	.042	-.040	1	-.171	-.018	.497**
	Sig. (2-tailed)	.135	.193	.634	.193	.832	.840		.383	.929	.007
	N	28	28	28	28	28	28	28	28	28	28
NO2NO3	Pearson Correlation	-.072	-.291	-.341	-.291	-.346	.180	-.171	1	.898**	-.122

	Sig. (2-tailed)	.716	.132	.076	.132	.071	.358	.383		.000	.535
	N	28	28	28	28	28	28	28	28	28	28
PO4	Pearson Correlation	-.143	-.385*	-.361	-.385*	-.315	.386*	-.018	.898**	1	.095
	Sig. (2-tailed)	.468	.043	.059	.043	.102	.043	.929	.000		.632
	N	28	28	28	28	28	28	28	28	28	28
Picoeukaryotes	Pearson Correlation	-.330	-.298	-.244	-.298	-.244	.133	.497**	-.122	.095	1
	Sig. (2-tailed)	.086	.124	.211	.124	.210	.499	.007	.535	.632	
	N	28	28	28	28	28	28	28	28	28	28
Prochlorococcus	Pearson Correlation	.347	.550**	.485**	.550**	.370	-.203	.065	-.372	-.439*	-.154
	Sig. (2-tailed)	.071	.002	.009	.002	.053	.301	.742	.051	.019	.435
	N	28	28	28	28	28	28	28	28	28	28
Salinity	Pearson Correlation	.064	.053	-.096	.053	-.158	.010	-.236	.121	-.072	-.290
	Sig. (2-tailed)	.747	.790	.627	.790	.421	.961	.227	.538	.715	.134
	N	28	28	28	28	28	28	28	28	28	28
Secchi	Pearson Correlation	.300	.379*	.271	.379*	.181	-.257	-.422*	-.165	-.281	-.413*
	Sig. (2-tailed)	.121	.047	.163	.047	.356	.187	.025	.402	.148	.029
	N	28	28	28	28	28	28	28	28	28	28
Silicate	Pearson Correlation	.053	.150	.150	.150	.110	.172	-.062	.645**	.553**	-.077
	Sig. (2-tailed)	.787	.445	.447	.445	.577	.381	.754	.000	.002	.697
	N	28	28	28	28	28	28	28	28	28	28
Solarradiation	Pearson Correlation	-.074	-.007	.137	-.007	.262	-.126	.743**	-.571**	-.453*	.297
	Sig. (2-tailed)	.708	.970	.488	.970	.179	.523	.000	.001	.016	.125
	N	28	28	28	28	28	28	28	28	28	28
Synechococcus	Pearson Correlation	-.054	.051	-.012	.051	-.137	.137	.359	-.233	-.098	.725**
	Sig. (2-tailed)	.786	.797	.951	.797	.486	.487	.061	.234	.621	.000
	N	28	28	28	28	28	28	28	28	28	28
Temperature	Pearson Correlation	.458*	.759**	.723**	.759**	.641**	-.024	.022	-.509**	-.587**	-.323
	Sig. (2-tailed)	.014	.000	.000	.000	.000	.905	.913	.006	.001	.094
	N	28	28	28	28	28	28	28	28	28	28
Zooplankton	Pearson Correlation	-.290	-.241	-.146	-.241	.025	.008	.389*	-.003	-.068	.125

	Sig. (2-tailed)	.134	.217	.459	.217	.899	.966	.041	.989	.732	.525
	N	28	28	28	28	28	28	28	28	28	28
BPRGlutamine	Pearson Correlation	.221	.142	-.079	.142	-.272	.021	-.763**	.058	-.097	-.402*
	Sig. (2-tailed)	.258	.472	.689	.472	.161	.915	.000	.770	.625	.034
	N	28	28	28	28	28	28	28	28	28	28
GPRLeucine	Pearson Correlation	-.350	-.332	-.139	-.332	.034	.046	.745**	.001	.176	.444*
	Sig. (2-tailed)	.068	.085	.481	.085	.862	.817	.000	.998	.371	.018
	N	28	28	28	28	28	28	28	28	28	28
GPRMethionine	Pearson Correlation	-.113	-.253	-.132	-.253	.122	-.090	.134	.211	.188	-.021
	Sig. (2-tailed)	.566	.194	.504	.194	.537	.647	.497	.282	.337	.916
	N	28	28	28	28	28	28	28	28	28	28

		Prochlorococcus	Salinity	Secchi	Silicate	Solarradiation	Synechococcus	Temperature	Zooplankton	BPRGlutamine	GPRLeucine	GPRMethionine
chao1	Pearson Correlation	.347	.064	.300	.053	-.074	-.054	.458*	-.290	.221	-.350	-.113
	Sig. (2-tailed)	.071	.747	.121	.787	.708	.786	.014	.134	.258	.068	.566
	N	28	28	28	28	28	28	28	28	28	28	28
observed_species	Pearson Correlation	.550**	.053	.379*	.150	-.007	.051	.759**	-.241	.142	-.332	-.253
	Sig. (2-tailed)	.002	.790	.047	.445	.970	.797	.000	.217	.472	.085	.194
	N	28	28	28	28	28	28	28	28	28	28	28
shannon	Pearson Correlation	.485**	-.096	.271	.150	.137	-.012	.723**	-.146	-.079	-.139	-.132
	Sig. (2-tailed)	.009	.627	.163	.447	.488	.951	.000	.459	.689	.481	.504
	N	28	28	28	28	28	28	28	28	28	28	28
margalef	Pearson Correlation	.550**	.053	.379*	.150	-.007	.051	.759**	-.241	.142	-.332	-.253
	Sig. (2-tailed)	.002	.790	.047	.445	.970	.797	.000	.217	.472	.085	.194

	N	28	28	28	28	28	28	28	28	28	28	28
simpson	Pearson Correlation	.370	-.158	.181	.110	.262	-.137	.641**	.025	-.272	.034	.122
	Sig. (2-tailed)	.053	.421	.356	.577	.179	.486	.000	.899	.161	.862	.537
	N	28	28	28	28	28	28	28	28	28	28	28
NH4	Pearson Correlation	-.203	.010	-.257	.172	-.126	.137	-.024	.008	.021	.046	-.090
	Sig. (2-tailed)	.301	.961	.187	.381	.523	.487	.905	.966	.915	.817	.647
	N	28	28	28	28	28	28	28	28	28	28	28
Daylength	Pearson Correlation	.065	-.236	-.422*	-.062	.743**	.359	.022	.389*	-.763**	.745**	.134
	Sig. (2-tailed)	.742	.227	.025	.754	.000	.061	.913	.041	.000	.000	.497
	N	28	28	28	28	28	28	28	28	28	28	28
NO2NO3	Pearson Correlation	-.372	.121	-.165	.645**	-.571**	-.233	-.509**	-.003	.058	.001	.211
	Sig. (2-tailed)	.051	.538	.402	.000	.001	.234	.006	.989	.770	.998	.282
	N	28	28	28	28	28	28	28	28	28	28	28
PO4	Pearson Correlation	-.439*	-.072	-.281	.553**	-.453*	-.098	-.587**	-.068	-.097	.176	.188
	Sig. (2-tailed)	.019	.715	.148	.002	.016	.621	.001	.732	.625	.371	.337
	N	28	28	28	28	28	28	28	28	28	28	28
Picoeukaryotes	Pearson Correlation	-.154	-.290	-.413*	-.077	.297	.725**	-.323	.125	-.402*	.444*	-.021
	Sig. (2-tailed)	.435	.134	.029	.697	.125	.000	.094	.525	.034	.018	.916
	N	28	28	28	28	28	28	28	28	28	28	28
Prochlorococcus	Pearson Correlation	1	-.090	.553**	-.150	.130	.109	.732**	-.116	.151	-.262	-.259
	Sig. (2-tailed)		.651	.002	.447	.509	.582	.000	.558	.444	.178	.183

	N	28	28	28	28	28	28	28	28	28	28	28
Salinity	Pearson Correlation	-.090	1	-.059	.073	-.208	-.057	.097	.036	.050	.015	-.072
	Sig. (2-tailed)	.651		.764	.714	.288	.772	.622	.854	.800	.941	.717
	N	28	28	28	28	28	28	28	28	28	28	28
Secchi	Pearson Correlation	.553**	-.059	1	-.333	-.183	-.216	.422*	-.078	.385*	-.422*	-.160
	Sig. (2-tailed)	.002	.764		.084	.351	.270	.025	.691	.043	.025	.417
	N	28	28	28	28	28	28	28	28	28	28	28
Silicate	Pearson Correlation	-.150	.073	-.333	1	-.337	-.147	-.059	-.181	-.055	-.014	.111
	Sig. (2-tailed)	.447	.714	.084		.080	.456	.764	.357	.782	.944	.573
	N	28	28	28	28	28	28	28	28	28	28	28
Solarradiation	Pearson Correlation	.130	-.208	-.183	-.337	1	.241	.282	.417*	-.589**	.505**	.157
	Sig. (2-tailed)	.509	.288	.351	.080		.217	.146	.027	.001	.006	.426
	N	28	28	28	28	28	28	28	28	28	28	28
Synechococcus	Pearson Correlation	.109	-.057	-.216	-.147	.241	1	.002	.087	-.247	.262	-.262
	Sig. (2-tailed)	.582	.772	.270	.456	.217		.992	.660	.205	.178	.178
	N	28	28	28	28	28	28	28	28	28	28	28
Temperature	Pearson Correlation	.732**	.097	.422*	-.059	.282	.002	1	.019	.029	-.153	-.318
	Sig. (2-tailed)	.000	.622	.025	.764	.146	.992		.922	.884	.436	.099
	N	28	28	28	28	28	28	28	28	28	28	28
Zooplankton	Pearson Correlation	-.116	.036	-.078	-.181	.417*	.087	.019	1	-.440*	.402*	.338
	Sig. (2-tailed)	.558	.854	.691	.357	.027	.660	.922		.019	.034	.079

	N	28	28	28	28	28	28	28	28	28	28	28
BPRGlutamine	Pearson Correlation	.151	.050	.385*	-.055	-.589**	-.247	.029	-.440*	1	-.938**	-.262
	Sig. (2-tailed)	.444	.800	.043	.782	.001	.205	.884	.019		.000	.178
	N	28	28	28	28	28	28	28	28	28	28	28
GPRLeucine	Pearson Correlation	-.262	.015	-.422*	-.014	.505**	.262	-.153	.402*	-.938**	1	.060
	Sig. (2-tailed)	.178	.941	.025	.944	.006	.178	.436	.034	.000		.763
	N	28	28	28	28	28	28	28	28	28	28	28
GPRMethionine	Pearson Correlation	-.259	-.072	-.160	.111	.157	-.262	-.318	.338	-.262	.060	1
	Sig. (2-tailed)	.183	.717	.417	.573	.426	.178	.099	.079	.178	.763	
	N	28	28	28	28	28	28	28	28	28	28	28

		RatioBPR_GPR	RatioBPR_methi	Ratio_GRP_methio
chao1	Pearson Correlation	-.512**	-.360	.035
	Sig. (2-tailed)	.005	.060	.860
	N	28	28	28
observed_species	Pearson Correlation	-.476*	-.473*	.038
	Sig. (2-tailed)	.011	.011	.848
	N	28	28	28
shannon	Pearson Correlation	-.296	-.293	.029
	Sig. (2-tailed)	.126	.131	.883
	N	28	28	28
margalef	Pearson Correlation	-.476*	-.473*	.038
	Sig. (2-tailed)	.011	.011	.848
	N	28	28	28

simpson	Pearson Correlation	-.121	.012	-.079
	Sig. (2-tailed)	.540	.951	.688
	N	28	28	28
NH4	Pearson Correlation	.007	-.001	.139
	Sig. (2-tailed)	.971	.994	.479
	N	28	28	28
Daylength	Pearson Correlation	.660**	.367	.329
	Sig. (2-tailed)	.000	.055	.088
	N	28	28	28
NO2NO3	Pearson Correlation	-.112	.134	.104
	Sig. (2-tailed)	.570	.497	.597
	N	28	28	28
PO4	Pearson Correlation	.071	.197	.207
	Sig. (2-tailed)	.720	.314	.291
	N	28	28	28
Picoeukaryotes	Pearson Correlation	.348	.145	.333
	Sig. (2-tailed)	.069	.463	.084
	N	28	28	28
Prochlorococcus	Pearson Correlation	-.307	-.348	-.021
	Sig. (2-tailed)	.112	.069	.914
	N	28	28	28
Salinity	Pearson Correlation	.066	-.005	.120
	Sig. (2-tailed)	.738	.981	.542
	N	28	28	28
Secchi	Pearson Correlation	-.479**	-.356	-.063
	Sig. (2-tailed)	.010	.063	.749
	N	28	28	28
Silicate	Pearson Correlation	-.090	.082	-.065
	Sig. (2-tailed)	.650	.680	.742

	N	28	28	28
Solarradiation	Pearson Correlation	.511**	.376*	.012
	Sig. (2-tailed)	.005	.049	.954
	N	28	28	28
Synechococcus	Pearson Correlation	.200	-.221	.511**
	Sig. (2-tailed)	.308	.259	.005
	N	28	28	28
Temperature	Pearson Correlation	-.235	-.352	.005
	Sig. (2-tailed)	.229	.067	.981
	N	28	28	28
Zooplankton	Pearson Correlation	.321	.456*	.032
	Sig. (2-tailed)	.096	.015	.870
	N	28	28	28

****. Correlation is significant at the 0.01 level (2-tailed). *. Correlation is significant at the 0.05 level (2-tailed).**

North Stradbroke Island

		chao1	observed_species	shannon	margalef	simpson	NH4	Daylength	NO2NO3	PO4	Picoeukaryotes	Prochlorococcus
chao1	Pearson Correlation	1	.567	.500	.567	.497	.396	.173	-.171	.207	.072	-.068
	Sig. (2-tailed)		.087	.141	.087	.144	.258	.632	.637	.565	.843	.851
	N	10	10	10	10	10	10	10	10	10	10	10
observed_species	Pearson Correlation	.567	1	.960**	1.000**	.930**	-.120	-.140	.077	-.200	.049	.089
	Sig. (2-tailed)	.087		.000	0.000	.000	.741	.699	.832	.579	.892	.808
	N	10	10	10	10	10	10	10	10	10	10	10
shannon	Pearson Correlation	.500	.960**	1	.960**	.992**	-.161	-.032	.144	-.143	.011	.049
	Sig. (2-tailed)	.141	.000		.000	.000	.656	.930	.691	.692	.975	.892
	N	10	10	10	10	10	10	10	10	10	10	10
margalef	Pearson Correlation	.567	1.000**	.960**	1	.930**	-.120	-.140	.077	-.200	.049	.089

	Sig. (2-tailed)	.087	0.000	.000		.000	.741	.699	.832	.579	.892	.808
	N	10	10	10	10	10	10	10	10	10	10	10
simpson	Pearson Correlation	.497	.930**	.992**	.930**	1	-.175	.045	.148	-.156	.001	.057
	Sig. (2-tailed)	.144	.000	.000	.000		.629	.901	.683	.667	.997	.877
	N	10	10	10	10	10	10	10	10	10	10	10
NH4	Pearson Correlation	.396	-.120	-.161	-.120	-.175	1	.346	-.182	.724*	.783**	-.316
	Sig. (2-tailed)	.258	.741	.656	.741	.629		.327	.616	.018	.007	.374
	N	10	10	10	10	10	10	10	10	10	10	10
Daylength	Pearson Correlation	.173	-.140	-.032	-.140	.045	.346	1	-.565	.060	.298	.396
	Sig. (2-tailed)	.632	.699	.930	.699	.901	.327		.089	.869	.404	.258
	N	10	10	10	10	10	10	10	10	10	10	10
NO2NO3	Pearson Correlation	-.171	.077	.144	.077	.148	-.182	-.565	1	.050	-.035	-.423
	Sig. (2-tailed)	.637	.832	.691	.832	.683	.616	.089		.891	.923	.223
	N	10	10	10	10	10	10	10	10	10	10	10
PO4	Pearson Correlation	.207	-.200	-.143	-.200	-.156	.724*	.060	.050	1	.351	-.532
	Sig. (2-tailed)	.565	.579	.692	.579	.667	.018	.869	.891		.320	.114
	N	10	10	10	10	10	10	10	10	10	10	10
Picoeukaryotes	Pearson Correlation	.072	.049	.011	.049	.001	.783**	.298	-.035	.351	1	-.163
	Sig. (2-tailed)	.843	.892	.975	.892	.997	.007	.404	.923	.320		.653
	N	10	10	10	10	10	10	10	10	10	10	10
Prochlorococcus	Pearson Correlation	-.068	.089	.049	.089	.057	-.316	.396	-.423	-.532	-.163	1
	Sig. (2-tailed)	.851	.808	.892	.808	.877	.374	.258	.223	.114	.653	
	N	10	10	10	10	10	10	10	10	10	10	10
Salinity	Pearson Correlation	-.028	-.489	-.431	-.489	-.437	.218	.011	.201	.528	-.219	-.015
	Sig. (2-tailed)	.939	.151	.214	.151	.207	.544	.975	.577	.116	.543	.968
	N	10	10	10	10	10	10	10	10	10	10	10
Secchi	Pearson Correlation	-.086	-.028	-.111	-.028	-.116	-.458	-.022	-.349	-.323	-.586	.475
	Sig. (2-tailed)	.814	.939	.760	.939	.749	.183	.952	.323	.362	.075	.166
	N	10	10	10	10	10	10	10	10	10	10	10
Silicate	Pearson Correlation	-.186	.379	.396	.379	.402	-.101	-.335	.677*	-.220	.409	-.250

	Sig. (2-tailed)	.607	.280	.258	.280	.250	.782	.344	.032	.542	.240	.487
	N	10	10	10	10	10	10	10	10	10	10	10
Solarradiation	Pearson Correlation	.494	.006	.011	.006	.042	.598	.735*	-.694*	.260	.367	-.055
	Sig. (2-tailed)	.147	.987	.976	.987	.909	.068	.015	.026	.468	.296	.881
	N	10	10	10	10	10	10	10	10	10	10	10
Synechococcus	Pearson Correlation	.021	-.032	-.107	-.032	-.109	.689*	.437	-.403	.233	.895**	.069
	Sig. (2-tailed)	.953	.931	.769	.931	.764	.028	.207	.248	.517	.000	.849
	N	10	10	10	10	10	10	10	10	10	10	10
Temperature	Pearson Correlation	.292	.334	.330	.334	.374	-.152	.680*	-.699*	-.457	-.052	.713*
	Sig. (2-tailed)	.413	.345	.351	.345	.287	.675	.030	.024	.184	.886	.021
	N	10	10	10	10	10	10	10	10	10	10	10
Zooplankton	Pearson Correlation	.292	-.371	-.279	-.371	-.234	.635*	.644*	-.491	.680*	.214	-.207
	Sig. (2-tailed)	.412	.291	.434	.291	.515	.049	.044	.150	.030	.552	.566
	N	10	10	10	10	10	10	10	10	10	10	10
BPRGlutamine	Pearson Correlation	-.076	-.190	-.390	-.190	-.446	-.028	-.506	.181	-.316	.053	.097
	Sig. (2-tailed)	.835	.600	.265	.600	.197	.939	.136	.617	.374	.885	.789
	N	10	10	10	10	10	10	10	10	10	10	10
GPRLeucine	Pearson Correlation	.048	-.051	.141	-.051	.207	.093	.579	-.245	.377	-.106	-.093
	Sig. (2-tailed)	.896	.889	.699	.889	.565	.799	.079	.495	.283	.771	.798
	N	10	10	10	10	10	10	10	10	10	10	10
GPRMethionine	Pearson Correlation	-.226	-.116	-.167	-.116	-.217	.316	-.549	.709*	.252	.480	-.493
	Sig. (2-tailed)	.530	.751	.644	.751	.547	.374	.100	.022	.483	.160	.148
	N	10	10	10	10	10	10	10	10	10	10	10

		Salinity	Secchi	Silicate	Solarradiation	Synechococcus	Temperature	Zooplankton	BPRGlutamine	GPRLeucine	GPRMethionine
chao1	Pearson Correlation	-.028	-.086	-.186	.494	.021	.292	.292	-.076	.048	-.226
	Sig. (2-tailed)	.939	.814	.607	.147	.953	.413	.412	.835	.896	.530
	N	10	10	10	10	10	10	10	10	10	10
observed_species	Pearson Correlation	-.489	-.028	.379	.006	-.032	.334	-.371	-.190	-.051	-.116
	Sig. (2-tailed)	.151	.939	.280	.987	.931	.345	.291	.600	.889	.751

	N	10	10	10	10	10	10	10	10	10	10
shannon	Pearson Correlation	-.431	-.111	.396	.011	-.107	.330	-.279	-.390	.141	-.167
	Sig. (2-tailed)	.214	.760	.258	.976	.769	.351	.434	.265	.699	.644
	N	10	10	10	10	10	10	10	10	10	10
margalef	Pearson Correlation	-.489	-.028	.379	.006	-.032	.334	-.371	-.190	-.051	-.116
	Sig. (2-tailed)	.151	.939	.280	.987	.931	.345	.291	.600	.889	.751
	N	10	10	10	10	10	10	10	10	10	10
simpson	Pearson Correlation	-.437	-.116	.402	.042	-.109	.374	-.234	-.446	.207	-.217
	Sig. (2-tailed)	.207	.749	.250	.909	.764	.287	.515	.197	.565	.547
	N	10	10	10	10	10	10	10	10	10	10
NH4	Pearson Correlation	.218	-.458	-.101	.598	.689*	-.152	.635*	-.028	.093	.316
	Sig. (2-tailed)	.544	.183	.782	.068	.028	.675	.049	.939	.799	.374
	N	10	10	10	10	10	10	10	10	10	10
Daylength	Pearson Correlation	.011	-.022	-.335	.735*	.437	.680*	.644*	-.506	.579	-.549
	Sig. (2-tailed)	.975	.952	.344	.015	.207	.030	.044	.136	.079	.100
	N	10	10	10	10	10	10	10	10	10	10
NO2NO3	Pearson Correlation	.201	-.349	.677*	-.694*	-.403	-.699*	-.491	.181	-.245	.709*
	Sig. (2-tailed)	.577	.323	.032	.026	.248	.024	.150	.617	.495	.022
	N	10	10	10	10	10	10	10	10	10	10
PO4	Pearson Correlation	.528	-.323	-.220	.260	.233	-.457	.680*	-.316	.377	.252
	Sig. (2-tailed)	.116	.362	.542	.468	.517	.184	.030	.374	.283	.483
	N	10	10	10	10	10	10	10	10	10	10
Picoeukaryotes	Pearson Correlation	-.219	-.586	.409	.367	.895**	-.052	.214	.053	-.106	.480
	Sig. (2-tailed)	.543	.075	.240	.296	.000	.886	.552	.885	.771	.160
	N	10	10	10	10	10	10	10	10	10	10
Prochlorococcus	Pearson Correlation	-.015	.475	-.250	-.055	.069	.713*	-.207	.097	-.093	-.493
	Sig. (2-tailed)	.968	.166	.487	.881	.849	.021	.566	.789	.798	.148
	N	10	10	10	10	10	10	10	10	10	10
Salinity	Pearson Correlation	1	.172	-.497	-.133	-.344	-.423	.333	-.043	.227	.137
	Sig. (2-tailed)		.634	.144	.714	.330	.224	.347	.905	.529	.705

	N	10	10	10	10	10	10	10	10	10	10
Secchi	Pearson Correlation	.172	1	-.510	-.062	-.332	.334	-.167	-.097	.205	-.542
	Sig. (2-tailed)	.634		.132	.864	.348	.346	.644	.791	.570	.106
	N	10	10	10	10	10	10	10	10	10	10
Silicate	Pearson Correlation	-.497	-.510	1	-.442	.175	-.267	-.589	.164	-.353	.611
	Sig. (2-tailed)	.144	.132		.201	.628	.457	.073	.650	.317	.061
	N	10	10	10	10	10	10	10	10	10	10
Solarradiation	Pearson Correlation	-.133	-.062	-.442	1	.489	.490	.748*	-.411	.481	-.446
	Sig. (2-tailed)	.714	.864	.201		.152	.151	.013	.237	.159	.196
	N	10	10	10	10	10	10	10	10	10	10
Synechococcus	Pearson Correlation	-.344	-.332	.175	.489	1	.237	.308	.044	-.062	.154
	Sig. (2-tailed)	.330	.348	.628	.152		.509	.386	.905	.866	.670
	N	10	10	10	10	10	10	10	10	10	10
Temperature	Pearson Correlation	-.423	.334	-.267	.490	.237	1	.140	-.292	.255	-.812**
	Sig. (2-tailed)	.224	.346	.457	.151	.509		.700	.413	.478	.004
	N	10	10	10	10	10	10	10	10	10	10
Zooplankton	Pearson Correlation	.333	-.167	-.589	.748*	.308	.140	1	-.476	.616	-.347
	Sig. (2-tailed)	.347	.644	.073	.013	.386	.700		.164	.058	.326
	N	10	10	10	10	10	10	10	10	10	10
BPRGlutamine	Pearson Correlation	-.043	-.097	.164	-.411	.044	-.292	-.476	1	-.954**	.498
	Sig. (2-tailed)	.905	.791	.650	.237	.905	.413	.164		.000	.143
	N	10	10	10	10	10	10	10	10	10	10
GPRLeucine	Pearson Correlation	.227	.205	-.353	.481	-.062	.255	.616	-.954**	1	-.533
	Sig. (2-tailed)	.529	.570	.317	.159	.866	.478	.058	.000		.113
	N	10	10	10	10	10	10	10	10	10	10
GPRMethionine	Pearson Correlation	.137	-.542	.611	-.446	.154	-.812**	-.347	.498	-.533	1
	Sig. (2-tailed)	.705	.106	.061	.196	.670	.004	.326	.143	.113	
	N	10	10	10	10	10	10	10	10	10	10

**. Correlation is significant at the 0.01 level (2-tailed). *. Correlation is significant at the 0.05 level (2-tailed).

Port Hacking

		chao1	observed_species	shannon	margalef	simpson	NH4	Daylength	NO2NO3	PO4	Picoeukaryotes
chao1	Pearson Correlation	1	.949**	.962**	.949**	.792*	.293	-.694	-.075	-.034	-.306
	Sig. (2-tailed)		.000	.000	.000	.019	.481	.056	.859	.936	.461
	N	8	8	8	8	8	8	8	8	8	8
observed_species	Pearson Correlation	.949**	1	.983**	1.000**	.755*	.293	-.698	.024	.091	-.321
	Sig. (2-tailed)	.000		.000	0.000	.030	.481	.054	.955	.831	.439
	N	8	8	8	8	8	8	8	8	8	8
shannon	Pearson Correlation	.962**	.983**	1	.983**	.859**	.222	-.692	-.042	-.005	-.422
	Sig. (2-tailed)	.000	.000		.000	.006	.597	.057	.921	.990	.298
	N	8	8	8	8	8	8	8	8	8	8
margalef	Pearson Correlation	.949**	1.000**	.983**	1	.755*	.293	-.698	.024	.091	-.321
	Sig. (2-tailed)	.000	0.000	.000		.030	.481	.054	.955	.831	.439
	N	8	8	8	8	8	8	8	8	8	8
simpson	Pearson Correlation	.792*	.755*	.859**	.755*	1	.001	-.629	-.210	-.260	-.621
	Sig. (2-tailed)	.019	.030	.006	.030		.999	.095	.617	.535	.100
	N	8	8	8	8	8	8	8	8	8	8
NH4	Pearson Correlation	.293	.293	.222	.293	.001	1	-.682	.103	.298	-.073
	Sig. (2-tailed)	.481	.481	.597	.481	.999		.063	.808	.474	.864
	N	8	8	8	8	8	8	8	8	8	8
Daylength	Pearson Correlation	-.694	-.698	-.692	-.698	-.629	-.682	1	-.039	-.149	.422
	Sig. (2-tailed)	.056	.054	.057	.054	.095	.063		.926	.724	.298
	N	8	8	8	8	8	8	8	8	8	8
NO2NO3	Pearson Correlation	-.075	.024	-.042	.024	-.210	.103	-.039	1	.955**	-.393
	Sig. (2-tailed)	.859	.955	.921	.955	.617	.808	.926		.000	.335
	N	8	8	8	8	8	8	8	8	8	8

PO4	Pearson Correlation	-.034	.091	-.005	.091	-.260	.298	-.149	.955**	1	-.331
	Sig. (2-tailed)	.936	.831	.990	.831	.535	.474	.724	.000		.423
	N	8	8	8	8	8	8	8	8	8	8
Picoeukaryotes	Pearson Correlation	-.306	-.321	-.422	-.321	-.621	-.073	.422	-.393	-.331	1
	Sig. (2-tailed)	.461	.439	.298	.439	.100	.864	.298	.335	.423	
	N	8	8	8	8	8	8	8	8	8	8
Prochlorococcus	Pearson Correlation	.856**	.912**	.885**	.912**	.687	.199	-.639	-.282	-.192	-.025
	Sig. (2-tailed)	.007	.002	.003	.002	.060	.637	.088	.499	.649	.953
	N	8	8	8	8	8	8	8	8	8	8
Salinity	Pearson Correlation	-.552	-.580	-.595	-.580	-.533	.525	.068	-.164	-.025	.151
	Sig. (2-tailed)	.156	.132	.120	.132	.174	.182	.874	.698	.952	.720
	N	8	8	8	8	8	8	8	8	8	8
Secchi	Pearson Correlation	.673	.596	.648	.596	.708*	.510	-.819*	.014	-.024	-.485
	Sig. (2-tailed)	.068	.119	.082	.119	.049	.197	.013	.973	.956	.223
	N	8	8	8	8	8	8	8	8	8	8
Silicate	Pearson Correlation	-.052	.095	-.006	.095	-.263	.057	-.024	.940**	.956**	-.236
	Sig. (2-tailed)	.903	.823	.989	.823	.529	.893	.954	.001	.000	.573
	N	8	8	8	8	8	8	8	8	8	8
Solarradiation	Pearson Correlation	-.430	-.553	-.458	-.553	-.119	-.725*	.600	-.618	-.756*	.373
	Sig. (2-tailed)	.288	.155	.253	.155	.779	.042	.116	.102	.030	.363
	N	8	8	8	8	8	8	8	8	8	8
Synechococcus	Pearson Correlation	.307	.390	.283	.390	-.051	.077	-.023	-.416	-.307	.711*
	Sig. (2-tailed)	.460	.340	.497	.340	.905	.856	.957	.306	.460	.048
	N	8	8	8	8	8	8	8	8	8	8
Temperature	Pearson Correlation	.547	.638	.633	.638	.534	.327	-.486	-.581	-.455	.035
	Sig. (2-tailed)	.160	.089	.092	.089	.173	.430	.222	.131	.258	.935
	N	8	8	8	8	8	8	8	8	8	8

Zooplankton	Pearson Correlation	-.516	-.554	-.474	-.554	-.114	-.254	.240	.118	-.103	-.169
	Sig. (2-tailed)	.190	.155	.235	.155	.787	.543	.567	.781	.808	.689
	N	8	8	8	8	8	8	8	8	8	8
BPRGlutamine	Pearson Correlation	.725*	.690	.678	.690	.495	.832*	-.808*	-.004	.133	-.347
	Sig. (2-tailed)	.042	.058	.065	.058	.212	.010	.015	.992	.753	.400
	N	8	8	8	8	8	8	8	8	8	8
GPRLeucine	Pearson Correlation	-.726*	-.715*	-.707*	-.715*	-.576	-.804*	.907**	-.019	-.128	.391
	Sig. (2-tailed)	.041	.046	.050	.046	.135	.016	.002	.964	.763	.338
	N	8	8	8	8	8	8	8	8	8	8
GPRMethionine	Pearson Correlation	-.597	-.660	-.606	-.660	-.253	-.251	.183	.100	-.072	.004
	Sig. (2-tailed)	.118	.075	.111	.075	.545	.548	.664	.814	.866	.992
	N	8	8	8	8	8	8	8	8	8	8

		Prochlorococcus	Salinity	Secchi	Silicate	Solarradiation	Synechococcus	Temperature	Zooplankton	BPRGlutamine	GPRLeucine	GPRMethionine
chao1	Pearson Correlation	.856**	-.552	.673	-.052	-.430	.307	.547	-.516	.725*	-.726*	-.597
	Sig. (2-tailed)	.007	.156	.068	.903	.288	.460	.160	.190	.042	.041	.118
	N	8	8	8	8	8	8	8	8	8	8	8
observed_species	Pearson Correlation	.912**	-.580	.596	.095	-.553	.390	.638	-.554	.690	-.715*	-.660
	Sig. (2-tailed)	.002	.132	.119	.823	.155	.340	.089	.155	.058	.046	.075
	N	8	8	8	8	8	8	8	8	8	8	8
shannon	Pearson Correlation	.885**	-.595	.648	-.006	-.458	.283	.633	-.474	.678	-.707*	-.606
	Sig. (2-tailed)	.003	.120	.082	.989	.253	.497	.092	.235	.065	.050	.111
	N	8	8	8	8	8	8	8	8	8	8	8

margalef	Pearson Correlation	.912**	-.580	.596	.095	-.553	.390	.638	-.554	.690	-.715*	-.660
	Sig. (2-tailed)	.002	.132	.119	.823	.155	.340	.089	.155	.058	.046	.075
	N	8	8	8	8	8	8	8	8	8	8	8
simpson	Pearson Correlation	.687	-.533	.708*	-.263	-.119	-.051	.534	-.114	.495	-.576	-.253
	Sig. (2-tailed)	.060	.174	.049	.529	.779	.905	.173	.787	.212	.135	.545
	N	8	8	8	8	8	8	8	8	8	8	8
NH4	Pearson Correlation	.199	.525	.510	.057	-.725*	.077	.327	-.254	.832*	-.804*	-.251
	Sig. (2-tailed)	.637	.182	.197	.893	.042	.856	.430	.543	.010	.016	.548
	N	8	8	8	8	8	8	8	8	8	8	8
Daylength	Pearson Correlation	-.639	.068	-.819*	-.024	.600	-.023	-.486	.240	-.808*	.907**	.183
	Sig. (2-tailed)	.088	.874	.013	.954	.116	.957	.222	.567	.015	.002	.664
	N	8	8	8	8	8	8	8	8	8	8	8
NO2NO3	Pearson Correlation	-.282	-.164	.014	.940**	-.618	-.416	-.581	.118	-.004	-.019	.100
	Sig. (2-tailed)	.499	.698	.973	.001	.102	.306	.131	.781	.992	.964	.814
	N	8	8	8	8	8	8	8	8	8	8	8
PO4	Pearson Correlation	-.192	-.025	-.024	.956**	-.756*	-.307	-.455	-.103	.133	-.128	-.072
	Sig. (2-tailed)	.649	.952	.956	.000	.030	.460	.258	.808	.753	.763	.866
	N	8	8	8	8	8	8	8	8	8	8	8
Picoeukaryotes	Pearson Correlation	-.025	.151	-.485	-.236	.373	.711*	.035	-.169	-.347	.391	.004
	Sig. (2-tailed)	.953	.720	.223	.573	.363	.048	.935	.689	.400	.338	.992
	N	8	8	8	8	8	8	8	8	8	8	8

Prochlorococcus	Pearson Correlation	1	-.551	.471	-.133	-.296	.630	.777*	-.581	.532	-.585	-.588
	Sig. (2-tailed)		.157	.239	.754	.477	.094	.023	.131	.175	.127	.125
	N	8	8	8	8	8	8	8	8	8	8	8
Salinity	Pearson Correlation	-.551	1	-.167	-.233	-.033	-.245	-.069	.145	.122	-.043	.186
	Sig. (2-tailed)	.157		.693	.578	.938	.559	.872	.731	.773	.920	.659
	N	8	8	8	8	8	8	8	8	8	8	8
Secchi	Pearson Correlation	.471	-.167	1	-.168	-.407	-.107	.384	.170	.750*	-.862**	.035
	Sig. (2-tailed)	.239	.693		.692	.317	.801	.348	.687	.032	.006	.934
	N	8	8	8	8	8	8	8	8	8	8	8
Silicate	Pearson Correlation	-.133	-.233	-.168	1	-.616	-.203	-.491	-.136	-.074	.061	-.062
	Sig. (2-tailed)	.754	.578	.692		.104	.629	.217	.748	.862	.886	.884
	N	8	8	8	8	8	8	8	8	8	8	8
Solarradiation	Pearson Correlation	-.296	-.033	-.407	-.616	1	-.010	-.173	.362	-.710*	.694	.450
	Sig. (2-tailed)	.477	.938	.317	.104		.981	.682	.378	.048	.056	.263
	N	8	8	8	8	8	8	8	8	8	8	8
Synechococcus	Pearson Correlation	.630	-.245	-.107	-.203	-.010	1	.608	-.519	.106	-.088	-.499
	Sig. (2-tailed)	.094	.559	.801	.629	.981		.110	.187	.804	.836	.209
	N	8	8	8	8	8	8	8	8	8	8	8
Temperature	Pearson Correlation	.777*	-.069	.384	-.491	-.173	.608	1	-.392	.552	-.573	-.546
	Sig. (2-tailed)	.023	.872	.348	.217	.682	.110		.336	.156	.137	.162
	N	8	8	8	8	8	8	8	8	8	8	8

Zooplankton	Pearson Correlation	-.581	.145	.170	-.136	.362	-.519	-.392	1	-.376	.236	.877**
	Sig. (2-tailed)	.131	.731	.687	.748	.378	.187	.336		.359	.573	.004
	N	8	8	8	8	8	8	8	8	8	8	8
BPRGlutamine	Pearson Correlation	.532	.122	.750*	-.074	-.710*	.106	.552	-.376	1	-.965**	-.507
	Sig. (2-tailed)	.175	.773	.032	.862	.048	.804	.156	.359		.000	.200
	N	8	8	8	8	8	8	8	8	8	8	8
GPRLeucine	Pearson Correlation	-.585	-.043	-.862**	.061	.694	-.088	-.573	.236	-.965**	1	.347
	Sig. (2-tailed)	.127	.920	.006	.886	.056	.836	.137	.573	.000		.400
	N	8	8	8	8	8	8	8	8	8	8	8
GPRMethionine	Pearson Correlation	-.588	.186	.035	-.062	.450	-.499	-.546	.877**	-.507	.347	1
	Sig. (2-tailed)	.125	.659	.934	.884	.263	.209	.162	.004	.200	.400	
	N	8	8	8	8	8	8	8	8	8	8	8

**. Correlation is significant at the 0.01 level (2-tailed). *. Correlation is significant at the 0.05 level (2-tailed).

Maria Island

		chao1	observed_species	shannon	margalef	simpson	NH4	Daylength	NO2NO3	PO4	Picoeukaryotes
chao1	Pearson Correlation	1	.644*	.421	.644*	.454	.250	-.068	.473	.547	-.307
	Sig. (2-tailed)		.044	.226	.044	.188	.486	.851	.167	.102	.387
	N	10	10	10	10	10	10	10	10	10	10
observed_species	Pearson Correlation	.644*	1	.877**	1.000**	.841**	.120	.076	-.253	-.034	-.048
	Sig. (2-tailed)	.044		.001	0.000	.002	.742	.835	.481	.927	.896
	N	10	10	10	10	10	10	10	10	10	10
shannon	Pearson Correlation	.421	.877**	1	.877**	.984**	.162	.340	-.506	-.171	.055
	Sig. (2-tailed)	.226	.001		.001	.000	.655	.336	.136	.636	.880
	N	10	10	10	10	10	10	10	10	10	10
margalef	Pearson Correlation	.644*	1.000**	.877**	1	.841**	.120	.076	-.253	-.034	-.048
	Sig. (2-tailed)	.044	0.000	.001		.002	.742	.835	.481	.927	.896
	N	10	10	10	10	10	10	10	10	10	10
simpson	Pearson Correlation	.454	.841**	.984**	.841**	1	.147	.313	-.447	-.126	-.032
	Sig. (2-tailed)	.188	.002	.000	.002		.685	.378	.196	.729	.930
	N	10	10	10	10	10	10	10	10	10	10
NH4	Pearson Correlation	.250	.120	.162	.120	.147	1	.485	-.057	.139	.209
	Sig. (2-tailed)	.486	.742	.655	.742	.685		.156	.875	.701	.563
	N	10	10	10	10	10	10	10	10	10	10
Daylength	Pearson Correlation	-.068	.076	.340	.076	.313	.485	1	-.458	-.145	.578
	Sig. (2-tailed)	.851	.835	.336	.835	.378	.156		.183	.690	.080
	N	10	10	10	10	10	10	10	10	10	10
NO2NO3	Pearson Correlation	.473	-.253	-.506	-.253	-.447	-.057	-.458	1	.851**	-.263
	Sig. (2-tailed)	.167	.481	.136	.481	.196	.875	.183		.002	.462
	N	10	10	10	10	10	10	10	10	10	10

PO4	Pearson Correlation	.547	-.034	-.171	-.034	-.126	.139	-.145	.851**	1	.055
	Sig. (2-tailed)	.102	.927	.636	.927	.729	.701	.690	.002		.880
	N	10	10	10	10	10	10	10	10	10	10
Picoeukaryotes	Pearson Correlation	-.307	-.048	.055	-.048	-.032	.209	.578	-.263	.055	1
	Sig. (2-tailed)	.387	.896	.880	.896	.930	.563	.080	.462	.880	
	N	10	10	10	10	10	10	10	10	10	10
Prochlorococcus	Pearson Correlation	.162	.407	.557	.407	.459	.354	.455	-.396	-.046	.301
	Sig. (2-tailed)	.655	.243	.094	.243	.182	.316	.187	.257	.900	.398
	N	10	10	10	10	10	10	10	10	10	10
Salinity	Pearson Correlation	-.111	-.344	-.507	-.344	-.415	-.424	-.330	.352	.006	-.287
	Sig. (2-tailed)	.760	.331	.135	.331	.233	.222	.352	.318	.987	.421
	N	10	10	10	10	10	10	10	10	10	10
Secchi	Pearson Correlation	.234	.246	.067	.246	.052	-.273	-.764*	.298	.297	-.395
	Sig. (2-tailed)	.515	.493	.855	.493	.886	.446	.010	.403	.405	.259
	N	10	10	10	10	10	10	10	10	10	10
Silicate	Pearson Correlation	.449	-.125	-.087	-.125	-.001	-.198	.063	.449	.385	-.255
	Sig. (2-tailed)	.193	.731	.812	.731	.998	.584	.863	.193	.272	.477
	N	10	10	10	10	10	10	10	10	10	10
Solarradiation	Pearson Correlation	-.184	.050	.413	.050	.404	.227	.912**	-.606	-.316	.413
	Sig. (2-tailed)	.610	.891	.235	.891	.246	.527	.000	.063	.375	.236
	N	10	10	10	10	10	10	10	10	10	10
Synechococcus	Pearson Correlation	-.360	-.121	-.096	-.121	-.174	.283	.497	-.150	.078	.798**
	Sig. (2-tailed)	.307	.738	.793	.738	.632	.429	.143	.680	.830	.006
	N	10	10	10	10	10	10	10	10	10	10
Temperature	Pearson Correlation	-.009	.604	.705*	.604	.679*	.007	.013	-.759*	-.704*	-.286
	Sig. (2-tailed)	.980	.065	.023	.065	.031	.984	.971	.011	.023	.423
	N	10	10	10	10	10	10	10	10	10	10

Zooplankton	Pearson Correlation	-.191	-.075	.126	-.075	.128	.515	.766**	-.232	.053	.683*
	Sig. (2-tailed)	.597	.837	.729	.837	.725	.127	.010	.519	.885	.029
	N	10	10	10	10	10	10	10	10	10	10
BPRGlutamine	Pearson Correlation	-.025	-.256	-.510	-.256	-.522	-.328	-.858**	.386	.036	-.530
	Sig. (2-tailed)	.946	.476	.132	.476	.122	.354	.002	.271	.922	.115
	N	10	10	10	10	10	10	10	10	10	10
GPRLeucine	Pearson Correlation	-.247	-.017	.267	-.017	.280	.367	.799**	-.399	-.121	.600
	Sig. (2-tailed)	.491	.962	.455	.962	.434	.296	.006	.253	.739	.067
	N	10	10	10	10	10	10	10	10	10	10
GPRMethionine	Pearson Correlation	.735*	.637*	.554	.637*	.584	-.186	.189	.142	.265	-.205
	Sig. (2-tailed)	.015	.047	.096	.047	.077	.606	.601	.695	.459	.569
	N	10	10	10	10	10	10	10	10	10	10

		Prochlorococcus	Salinity	Secchi	Silicate	Solarradiation	Synechococcus	Temperature	Zooplankton	BPRGlutamine	GPRLeucine	GPRMethionine
chao1	Pearson Correlation	.162	-.111	.234	.449	-.184	-.360	-.009	-.191	-.025	-.247	.735*
	Sig. (2-tailed)	.655	.760	.515	.193	.610	.307	.980	.597	.946	.491	.015
	N	10	10	10	10	10	10	10	10	10	10	10
observed_species	Pearson Correlation	.407	-.344	.246	-.125	.050	-.121	.604	-.075	-.256	-.017	.637*
	Sig. (2-tailed)	.243	.331	.493	.731	.891	.738	.065	.837	.476	.962	.047
	N	10	10	10	10	10	10	10	10	10	10	10
shannon	Pearson Correlation	.557	-.507	.067	-.087	.413	-.096	.705*	.126	-.510	.267	.554
	Sig. (2-tailed)	.094	.135	.855	.812	.235	.793	.023	.729	.132	.455	.096
	N	10	10	10	10	10	10	10	10	10	10	10

margalef	Pearson Correlation	.407	-.344	.246	-.125	.050	-.121	.604	-.075	-.256	-.017	.637*
	Sig. (2-tailed)	.243	.331	.493	.731	.891	.738	.065	.837	.476	.962	.047
	N	10	10	10	10	10	10	10	10	10	10	10
simpson	Pearson Correlation	.459	-.415	.052	-.001	.404	-.174	.679*	.128	-.522	.280	.584
	Sig. (2-tailed)	.182	.233	.886	.998	.246	.632	.031	.725	.122	.434	.077
	N	10	10	10	10	10	10	10	10	10	10	10
NH4	Pearson Correlation	.354	-.424	-.273	-.198	.227	.283	.007	.515	-.328	.367	-.186
	Sig. (2-tailed)	.316	.222	.446	.584	.527	.429	.984	.127	.354	.296	.606
	N	10	10	10	10	10	10	10	10	10	10	10
Daylength	Pearson Correlation	.455	-.330	-.764*	.063	.912**	.497	.013	.766**	-.858**	.799**	.189
	Sig. (2-tailed)	.187	.352	.010	.863	.000	.143	.971	.010	.002	.006	.601
	N	10	10	10	10	10	10	10	10	10	10	10
NO2NO3	Pearson Correlation	-.396	.352	.298	.449	-.606	-.150	-.759*	-.232	.386	-.399	.142
	Sig. (2-tailed)	.257	.318	.403	.193	.063	.680	.011	.519	.271	.253	.695
	N	10	10	10	10	10	10	10	10	10	10	10
PO4	Pearson Correlation	-.046	.006	.297	.385	-.316	.078	-.704*	.053	.036	-.121	.265
	Sig. (2-tailed)	.900	.987	.405	.272	.375	.830	.023	.885	.922	.739	.459
	N	10	10	10	10	10	10	10	10	10	10	10
Picoeukaryotes	Pearson Correlation	.301	-.287	-.395	-.255	.413	.798**	-.286	.683*	-.530	.600	-.205
	Sig. (2-tailed)	.398	.421	.259	.477	.236	.006	.423	.029	.115	.067	.569
	N	10	10	10	10	10	10	10	10	10	10	10

Prochlorococcus	Pearson Correlation	1	-.962**	.148	-.021	.507	.039	.357	.014	-.205	.035	.202
	Sig. (2-tailed)		.000	.684	.954	.135	.915	.311	.969	.570	.924	.576
	N	10	10	10	10	10	10	10	10	10	10	10
Salinity	Pearson Correlation	-.962**	1	-.258	.126	-.370	-.030	-.350	-.008	.112	-.006	-.008
	Sig. (2-tailed)	.000		.471	.728	.292	.935	.322	.982	.757	.987	.981
	N	10	10	10	10	10	10	10	10	10	10	10
Secchi	Pearson Correlation	.148	-.258	1	-.120	-.652*	-.421	.172	-.722*	.687*	-.766**	.003
	Sig. (2-tailed)	.684	.471		.742	.041	.226	.634	.018	.028	.010	.992
	N	10	10	10	10	10	10	10	10	10	10	10
Silicate	Pearson Correlation	-.021	.126	-.120	1	.185	-.552	-.357	-.250	.038	-.204	.552
	Sig. (2-tailed)	.954	.728	.742		.609	.098	.311	.486	.918	.572	.098
	N	10	10	10	10	10	10	10	10	10	10	10
Solarradiation	Pearson Correlation	.507	-.370	-.652*	.185	1	.232	.205	.541	-.760*	.673*	.237
	Sig. (2-tailed)	.135	.292	.041	.609		.520	.570	.106	.011	.033	.509
	N	10	10	10	10	10	10	10	10	10	10	10
Synechococcus	Pearson Correlation	.039	-.030	-.421	-.552	.232	1	-.335	.785**	-.545	.669*	-.287
	Sig. (2-tailed)	.915	.935	.226	.098	.520		.344	.007	.103	.034	.421
	N	10	10	10	10	10	10	10	10	10	10	10
Temperature	Pearson Correlation	.357	-.350	.172	-.357	.205	-.335	1	-.230	-.052	-.048	.119
	Sig. (2-tailed)	.311	.322	.634	.311	.570	.344		.523	.886	.894	.743
	N	10	10	10	10	10	10	10	10	10	10	10

Zooplankton	Pearson Correlation	.014	-.008	-.722*	-.250	.541	.785**	-.230	1	-.858**	.955**	-.138
	Sig. (2-tailed)	.969	.982	.018	.486	.106	.007	.523		.002	.000	.703
	N	10	10	10	10	10	10	10	10	10	10	10
BPRGlutamine	Pearson Correlation	-.205	.112	.687*	.038	-.760*	-.545	-.052	-.858**	1	-.930**	-.303
	Sig. (2-tailed)	.570	.757	.028	.918	.011	.103	.886	.002		.000	.396
	N	10	10	10	10	10	10	10	10	10	10	10
GPRLeucine	Pearson Correlation	.035	-.006	-.766**	-.204	.673*	.669*	-.048	.955**	-.930**	1	-.048
	Sig. (2-tailed)	.924	.987	.010	.572	.033	.034	.894	.000	.000		.895
	N	10	10	10	10	10	10	10	10	10	10	10
GPRMethionine	Pearson Correlation	.202	-.008	.003	.552	.237	-.287	.119	-.138	-.303	-.048	1
	Sig. (2-tailed)	.576	.981	.992	.098	.509	.421	.743	.703	.396	.895	
	N	10	10	10	10	10	10	10	10	10	10	10

**. Correlation is significant at the 0.01 level (2-tailed). *. Correlation is significant at the 0.05 level (2-tailed).

APPENDIX IV

Table S1: Environmental variables from surface water (5m) and DCM during the s winter 2013 voyage within Australia's tropical marine waters.

Station	Fluoresence	Oxygen	PAR	Salinity	Temperature	Nitrate	Phosphate	Silicate
WS2_SURF	23.50041	204.2319	410.5179	34.26043	27.4275	0	0.09	3.52
WS2_DCM	27.98232	202.2397	19.24053	34.25314	27.27638	0.06	0.1	3.54
WS3_SURF	28.45571	200.1987	29.79042	34.28803	26.68153	0.26	0.11	2.96
WS3_SURF	28.23905	200.9887	52.55527	34.29638	26.70256	0.28	0.1	2.93
WS4_SURF	26.82807	206.5384	268.0921	34.3629	26.96625	0.02	0.1	2.37
WS4_DCM	30.22883	203.6669	38.01017	34.36469	26.69062	0.37	0.16	2.99
WS5_SURF	27.77602	200.5529	25.51017	34.15245	27.20908	0.6	0.23	4.46
WS6_SURF	31.93975	206.8042	53.96758	34.07142	26.88997	0.1	0.24	5.16
WS7_SURF	27.68159	208.7866	5.020279	33.86007	25.97829	0.37	0.24	5.7
WS8_SURF	23.37352	209.1779	285.95	33.91997	26.1507	0	0.16	3.52
WS9_SURF	23.59655	207.3177	11.79265	33.72753	25.92756	0	0.22	5.2
WS10_SURF	26.90016	212.4953	214.2484	33.57352	25.66202	0	0.11	3.32
WS10_DCM	30.09517	210.4606	29.87178	33.58969	25.4995	0	0.11	3.44
WS11_SURF	26.42724	206.2934	6.057131	33.62218	26.20768	0.01	0.26	1.83
WS12_SURF	20.131	208.8321	178.9464	34.10873	26.11487	0	0.17	1.96
WS12_DCM	24.74318	209.0062	86.53651	34.10971	26.01556	0	0.17	2.01
WS13_DCM	24.30817	208.4306	1.186507	35.1872	25.26839	0.12	0.05	1.08
WS14_SURF	19.9221	209.4646	7.083249	35.19608	25.04446	0	0.06	1.4
WS14_DCM	20.69817	209.9633	2.064183	35.1867	24.68979	0.15	0.07	1.6
WS15_SURF	15.21618	208.9963	8.484778	35.18142	24.97475	0	0.07	1.16
WS15_DCM	25.09901	212.1557	2.887248	35.26748	23.52187	0.14	0.1	1.57
WS16_SURF	22.25414	213.509	6.243384	35.41511	23.60541	0.03	0.09	0.96
WS16_DCM	24.12892	214.2494	14.54746	35.41572	23.60787	0.06	0.09	0.95

WS17_SURF	23.49372	214.4425	14.71635	35.45407	23.49805	0.03	0.1	0.97
WS18_DCM	24.22759	216.3356	0.960317	35.48299	22.86954	0.09	0.11	0.85

Station	Ammonia	Fucoxanthin	Zeaxanthin	Chlb	Divinyl Chla	Chla
WS2_SURF	0	0.03	0.1	0.04	0	0.42
WS2_DCM	0	0.05	0.03	0.05	0	0.39
WS3_SURF	0	0.08	0.05	0.04	0.03	0.49
WS3_SURF	0	0.13	0.01	0.05	0	0.62
WS4_SURF	0	0.07	0.14	0.06	0	0.57
WS4_DCM	0.02	0.14	0.06	0.07	0	0.71
WS5_SURF	0	0.1	0.03	0.05	0	0.5
WS6_SURF	0.01	0.2	0.03	0.09	0	0.84
WS7_SURF	0.01	0.18	0.02	0.07	0	0.56
WS8_SURF	0	0.04	0.11	0.04	0	0.4
WS9_SURF	0.28	0.07	0.02	0.03	0	0.32
WS10_SURF	0	0.12	0.09	0.05	0	0.64
WS10_DCM	0	0.06	0.05	0.04	0	0.32
WS11_SURF	0.02	0.19	0.02	0.04	0	0.61
WS12_SURF	0	0.03	0.11	0.02	0	0.28
WS12_DCM	0	0.02	0.09	0.02	0	0.21
WS13_DCM	0	0.06	0.03	0.02	0.04	0.3
WS14_SURF	0.01	0.01	0.03	0.01	0.07	0.11
WS14_DCM	0.03	0.01	0.03	0.01	0.02	0.27
WS15_SURF	0	0	0.02	0	0.03	0.06
WS15_DCM	0.07	0.04	0.05	0.07	0.06	0.49
WS16_SURF	0.01	0.02	0.02	0.02	0.03	0.19
WS16_DCM	0.01	0.03	0.03	0.01	0.04	0.24
WS17_SURF	0.02	0.03	0.04	0.01	0.06	0.28
WS18_DCM	0.07	0.035	0.04	0.04	0.05	0.365